Università degli Studi di Padova

Dipartimento di Scienze Chimiche

SCUOLA DI DOTTORATO DI RICERCA IN SCIENZE MOLECOLARI

CURRICOLO SCIENZE CHIMICHE

CICLO XXIX

Aminotriphenolate Complexes for Effective Epoxide Activation

Coordinatore: Ch.mo Prof. Antonino Polimeno

Supervisore: Ch.ma Prof.ssa Giulia Marina Licini

Dottoranda : Claudia Miceli

Contents

Abstract

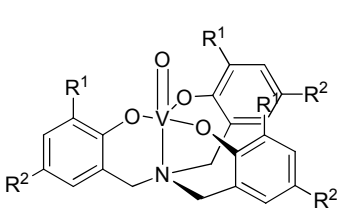

VO(L^{d}): $R^1 = R^2 = Cl$
VO(L^{h}): $R^1 = H$, $R^2 = t$Bu

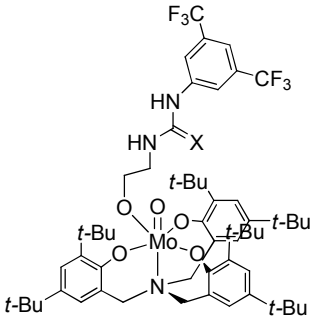

MoO(L^{c})(TU): X = S
MoO(L^{c})(U): X = O

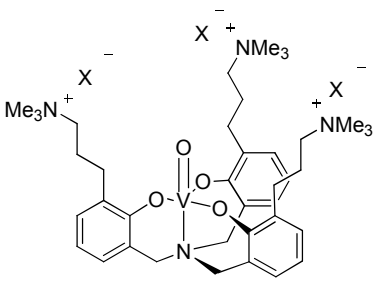

VO(L^{q}) X = I
VO(L^{r}) X = Cl

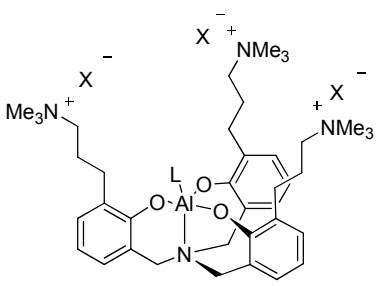

Al(L^{q})(DMF) X = I
Al(L^{r})(DMF) X = Cl

L = DMF

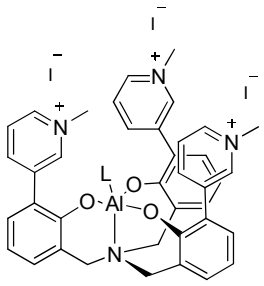

Al(L^{s})(DMF)

This thesis focuses on the synthesis of vanadium(V) and molybdnenum(VI) aminotriphenolate complexes **VO(L^{d,h,q,r})**, **MoO(L^{c})(TU)**, **MoO(L^{c})(U)**, **Al(L^{q,r,s})(DMF)** and their use in activation of epoxides in ring opening reactions by amines and CO_2 cycloadditions. Triphenolamines have been chosen as ligands because of their high versatility in metal complexation and the possibility of functionalization. Indeed, it will be pointed out that according to the metal employed and the different ligand substitutions, aminotriphenolate complexes exert a preferential activity towards a specific reaction or substrate. Moreover, the strong Lewis acidity of many aminotriphenolate complexes makes these catalysts a first choice for epoxide activation.

Tert-butyl substituted vanadium(V)aminotriphenolate complex **VO(L^{h})** gave the best performance in catalyzing ring opening of epoxides by amines, reaching complete conversion of 1,2-epoxyhexane (taken as a reference substrate) in 30 minutes, using dibutylamine as nucleophile, with 1mol% of catalyst. A wide amine and substrate scope, covering all the principal classes of amines and epoxides, has been conducted, showing excellent conversions in most cases.

Chloro-substituted vanadium(V) aminotriphenolate complex **VO(L^d)** is the catalyst of choice for CO_2 cycloaddition reactions to epoxides, demonstrating to be a highly active catalyst for coupling of both internal and terminal epoxides. High yields of cyclic carbonates have been afforded using 0.5 mol% of catalyst at 85°C in 16 hours, with a CO_2 pressure of 10 bar. Interestingly, some insights into the nature of the active species involved in the catalytic cycle could be inferred from the X-ray of an unusual structure of propylene oxide coordinated to **VO(L^d)**.

The aminotriphenolate functionalization can also be designed specifically to link another catalytic moiety to the complex, in order to build a bifunctional catalyst. This is the case of complex **MoO(L^c)(TU)**, **MoO(L^c)(U)**, which have been synthesized and tested as bifunctional catalysts for olefin epoxidation - epoxide ring opening tandem reactions. These systems are composed by a Molybdenum centre, effective catalyst for olefin epoxidations, and a (thio)urea moiety, a well-known organocatalyst able to activate epoxides via hydrogen bonds towards nucleophilic attack.

Decorating aminotriphenolate ligands with three ammonium or pyridinium salts – with halide anions as counterions – led to the synthesis of bifunctional catalysts **VO($L^{q,r}$) and Al($L^{q,r,s}$)(DMF)**, which have been tested for the synthesis of cyclic carbonates starting from epoxides and CO_2. In these systems, the metal catalyst and the halide salts used as co-catalysts are linked together, exploiting the proximity effect to get higher catalytic activities in respect to the binary systems.

Riassunto

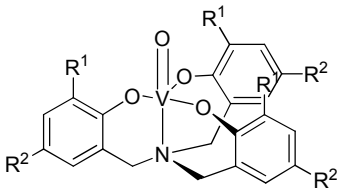

VO(L^{d}): $R^1 = R^2 = Cl$
VO(L^{h}): $R^1 = H$, $R^2 = t$Bu

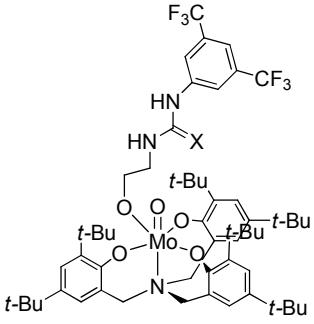

MoO(L^{c})(TU): X = S
MoO(L^{c})(U): X = O

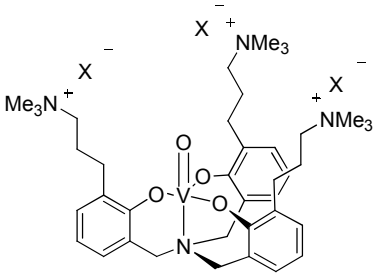

VO(L^{q}) X = I
VO(L^{r}) X = Cl

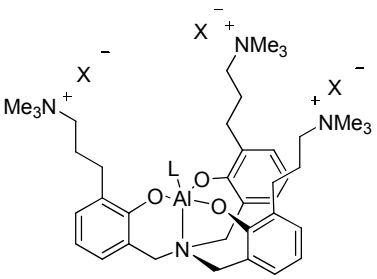

Al(L^{q})(DMF) X = I
Al(L^{r})(DMF) X = Cl

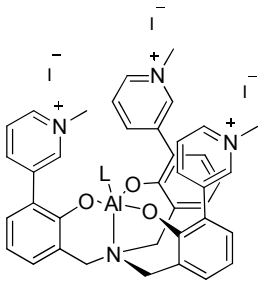

Al(L^{s})(DMF)

In questo lavoro di tesi, sono stati progettati e sintetizzati i complessi amminotrifenolati di vanadio alluminio e molibdeno **VO(L^{d,h,q,r})**, **MoO(L^{c})(TU)**, **MoO(L^{c})(U)**, **Al(L^{q,r,s})(DMF)**, da utilizzarsi come acidi di Lewis per l'attivazione di epossidi, nella catalisi di reazioni di apertura dell'anello epossidico e di cicloaddizioni di CO_2.

Particolare riguardo è stato dedicato alla scelta della funzionalizzazione dei leganti trifenolamici: la possibilità di avere diversi tipi di sostituenti agli anelli aromatici permette di creare una libreria di complessi con caratteristiche anche molto diverse. La stabilità, solubilità e reattività dei complessi può variare anche di molto a seconda della sostituzione degli anelli aromatici. Nello specifico, mi sono occupata di funzionalizzare i complessi con degli altri gruppi aventi attività catalitica, per lo sviluppo di catalizzatori bifunzionali per attività cooperativa o reazioni tandem. I vari complessi sono poi stati testati nelle reazioni di apertura dell'anello epossidico o di cicloaddizione di CO_2, come descritto in seguito.

Nel *Capitolo 2*, viene descritta la sintesi, caratterizzazione e attività in catalisi dei due catalizzatori bifunzionali **MoO(L^{c})(TU)** e **MoO(L^{c})(U)**. In questi sistemi, un derivato (tio)ureico è stato legato al metallo in modo da ottere un catalizzatore bifunzionale per reazioni tandem. Infatti, complessi trifenolati di molibdeno sono dei catalizzatori efficaci per le reazioni di epossidazione di olefine, mentre i derivati della (tio)urea sono organocatalizzatori ampiamente utilizzati nelle reazioni di apertura degli epossidi da parte di ammine.

Il lavoro di tesi è stato poi focalizzato sulla sola reazione di apertura nucleofila dell'anello epossidico, in quanto dei complessi amminotrifenolati di molibdeno e vanadio si sono dimostrati essere particolarmente efficaci per questa catalisi. Il *Capitolo 3* descrive quindi l'attività in catalisi di vari complessi amminotrifenolati nella reazione di apertura di epossidi da parte di ammine. In particolare, lo studio viene focalizzato sul complesso di vanadio **VO(L^{h})**, che mostra l'attività catalitica più elevata per questa reazione.

L'attività di complessi di vanadio nelle reazioni di cicloaddizione di CO_2 agli epossidi è il tema del *Capitolo 4*. I due complessi di vanadio **VO(L^{d})** e **VO(L^{h})**, nei quali gli anelli aromatici del legante sono sostituiti con cloro o terz-butile, sono stati sperimentati utilizzando epossidi terminali o interni come substrati. Mi sono soffermata in particolare sugli epossidi interni, dato che sono i meno reattivi e dunque più difficili da reagire. Inoltre, è stato effettuato uno studio sulla modalità di coordinazione degli epossidi al metallo, utilizzando titolazioni ^{51}V-NMR.

Nel *Capitolo 5* viene affrontata la sintesi di catalizzatori bifunzionali a base dei complessi trifenolati di alluminio e vanadio **Al(L^{q,r,s})(DMF)** e **VO(L^{q,r})**, per reazioni di cicloaddizione di CO_2 a epossidi. In questi sistemi, il legante è stato funzionalizzato con dei sali di ammonio o piridinio con cloruro o ioduro come controioni. Sali di ammonio sono infatti comunemente utilizzati come co-catalizzatori in queste reazioni, insieme a complessi metallici acidi di Lewis. È stato riservata particolare attenzione al confronto tra questi nuovi catalizzatori bifunzionali e i rispettivi sistemi binari, in modo da chiarire l'importanza nell'avere le due funzionalità catalitiche parte di uno stesso sistema.

Chapter 1

General Introduction

1.1 Triphenolamines

Triphenolamines (TPA, LH_3) are highly modular tetradentate ligands (*Figure 1*) able to coordinate to a wide variety of transition metals (Ti(IV),[1] Zr(IV),[2] In(III),[3] Ga(III),3Fe(III),[4] Ta(V),[5] Al(III),[6] V(V),[7] Co(II) and Co(III),[8] Mo(VI)[9]) and main groups elements(Si(IV),[10] P(V)[11]).

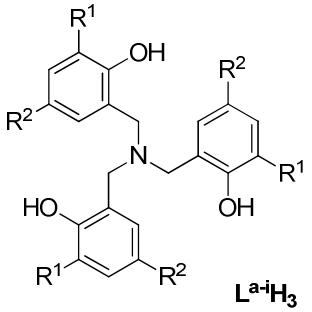

a $R^1 = R^2 = H$
b $R^1 = R^2 = Me$
c $R^1 = R^2 = t$Bu
d $R^1 = R^2 = Cl$
e $R^1 = t$Bu, $R^2 = Me$
f $R^1 = Me$ $R^2 = t$Bu
g $R^1 = Me$ $R^2 = H$
h $R^1 = t$Bu, $R^2 = H$
i $R^1 = Ph$, $R^2 = H$

Figure 1 Structures of triphenolamines $\mathbf{L^{a\text{-}i}H_3}$.

These $(ArO)_3N$ chelating agents combine a multidentate coordination ability with relative ease for variation of the ligand through synthetic modulations. Two main advantages of multidentate ligands

[1] a) Bull, S. D.; Davidson, M. G.; Johnson, A. L.; Robinson, D. E. J. E.; Mahon, M. F. *Chem. Commun*. **2003** 1750; b) Kol, M.; Shamis, M.; Goldberg, I.; Goldschmidt, Z.; Alfi, S.; Hayut-Salant, E. *Inorg. Chem. Commun*. **2001** (4), 177; c) Michalczyk, L.; De Gala, S.; Bruno, J. W. *Organometallics* **2001** (20), 5547; d) Kim, Y.; Verkade, J. G. *Organometallics* **2002** (21), 2395; e) Kim, Y.; Jnaneshwara, G. K.; Verkade, J. G. *Inorg. Chem*. **2003** (42), 1437; f) Wang, W.; Fujiki, M.; Nomura, K. Macromol. *Rapid Commun*. **2004** (25), 504; g) Ugrinova, V.; Ellis, G. A.; Brown, S. N. *Chem. Commun*. **2004**, 468; h) Fortner, K. C.; Bigi, J. P.; Brown, S. N. *Inorg. Chem*. **2005** (44), 2803; i) Kim, Y.; Verkade, J. G. Phosphorus, *Sulfur Silicon Relat. Elem*. **2004** (179), 729; j) Mba, M; Prins, L. J.; Zonta, C.; Cametti, M.; Valonen, A.; Rissanen, K.; Licini, G. Dalton Trans **2010** (39), 7384; k) Bernardinelli, G.; Seidel, T. M.; Kündig, E. P.; Prins, L. J., Kolarovic, A.; Mba, M.; Pontini, M.; Licini, G. *Dalton Trans*. **2007**, 1573; Zonta, C.; Cazzola, E.; Mba, M.; Licini, G. *Adv. Synth. Catal*. **2008** (350), 2503.

[2]Davidson, M. G.; Doherty, C. L.; Johnson, A. L.; Mahon, M. F. *Chem. Commun*. **2003**, 1832.

[3] Motekaitis, R.; Martell, A. E.; Koch, S. A.; Hwang, J.; Quarless, D. A., Jr.; Welch, M. J. *Inorg. Chem*. **1998** (37), 5902.

[4]a) Hwang, J.; Govindaswamy, K.; Koch, S. A. *Chem. Commun*. **1998**, 1667; b) Whiteoak, C. J.; Gjoka, B.; Martin, E.; Mart, M.; Escudero-ada, E. C.; Zonta, C.; Licini, G.; Kleij, A. W. *Inorg. Chem*. **2012** (51), 10639.

[5] a) Groysman, S.; Segal, S.; Goldberg, I.; Kol, M.; Goldschmidt, Z. Inorg. *Chem. Commun*. **2004** (7), 938. b) Groysman, S.; Segal, S.; Shamis, M.; Goldberg, I.; Kol, M.; Goldschmidt, Z.; Hayut-Salant, E. J. Chem. Soc.- Dalton Trans. **2002** 3425; c) Kim, Y. J.; Kapoor, P. N.; Verkade, J. G. *Inorg. Chem*. **2002** (41), 4834.

[6]a) Kim, Y.; Verkade, J. G. *Inorg. Chem*. **2003**, 42, 4804; b) Whiteoak, C. J.; Kielland, N.; Laserna, V.; Escudero-Adán, E. C.; Martin, E.; Kleij, A. W. *J. Am. Chem. Soc*. **2013** (135), 1228.

[7]a) Groysman, S.; Goldberg, I.; Goldschmidt, Z.; Kol, M. *Inorg. Chem.* **2005** (44), 5073; b) Mba, M.; Pontini, M.; Lovat, S.; Zonta, C.; Bernardinelli, G.; Kündig, P. E.; Licini, G. *Inorg. Chem.* **2008** (47), 8616.

[8]Martín, C.; Whiteoak, C. J.; Martin, E.; Escudero-Adán, E. C.; Galán-Mascarós, J. R.; Kleij, A. *Inorg. Chem*. **2014** (53), 11675.

[9] Romano, F.; Linden, A.; Mba, M.; Zonta, C.; Licini, G. *Adv. Synth. Cat*. **2010** (352), 2937.

[10]a) Timosheva, N. V.; Chandrasekaran, A.; Day, R. O.; Holmes, R. R. *Organometallics* **2001** (20), 2331; b) Chandrasekaran, A.; Day, R. O.; Holmes, R. R. *J. Am. Chem. Soc*. **2000** (122), 1066;c) Timosheva, N. V.; Chandrasekaran, A.; Day, R. O.; Holmes, R. R. *Organometallics* **2000** (19), 5614.

[11] Timosheva, N. V.; Chandrasekaran, A.; Day, R. O.; Holmes, R. R. *J. Am. Chem. Soc*. **2002** (124), 7035.

are the high thermodynamic stability of the resulting metal complexes, which allows low catalyst concentrations without loss of catalyst integrity, and the inhibited formation of multimeric metal species under turnover conditions. This is obtained by the nearly complete filling of all vacant sites of the metal by a single ligand. In addition, the presence of single mononuclear species facilitates mechanistic studies and catalyst optimization, especially in stereoselective processes.[12]

1.2 Synthesis of triphenolamines and related complexes

The first synthesis of triphenolamines dates back to 1922 when the natural product Salicin, a benzyl alcohol b-glycoside extracted from willow bark, was converted to the corresponding benzyl bromide and reacted with ammonia.[13]Later on, other three synthetic strategies for TPA synthesis have been developed.[14]The first is based upon the Mannich reaction of *ortho*, *para*-disubstituted phenols (*Scheme 1*).[15]

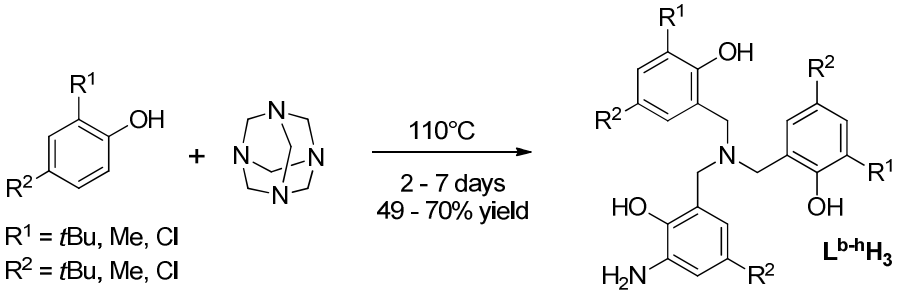

Scheme 1 Synthesis of triphenolamines $\mathbf{L^bH_3}$, $\mathbf{L^cH_3}$,$\mathbf{L^dH_3}$, $\mathbf{L^eH_3}$, $\mathbf{L^fH_3}$, $\mathbf{L^gH_3}$, $\mathbf{L^hH_3}$ via Mannich reaction.

The method can be used only with *ortho*, *para*-disubstituted phenols and it affords the products in 40–70% yields. Although the method is straightforward, requiring only one step from the phenol to the ligand, long reaction times, up to two weeks, and harsh reaction conditions are needed. To design a more easy triphenolamine synthesis, another synthetic procedure, based on the nucleophilic substitution of a 2-methoxybenzylamine with two equivalents of methoxybenzylbromide, has been developed.[16] This reaction, in order to afford reasonable yields, requires the phenolic functions to be protected.As example, it has been applied to the synthesis of the unsubstituted compound $\mathbf{L^aH_3}$

[12] Mba, M.; Prins, L. J.; Zonta, C.; Cametti, M.; Valkonen, A.; Licini, G. *Dalton Trans*. **2010** (39), 7384.
[13] a) Zemplén, G.; Kunz, A. *Chem. Ber*. **1922** (55), 979.
[14]K. Hultzsch, *Chem. Ber*. **1949** (82), 16.
[15]A. Chandrasekaran, R. O. Day and R. R. Holmes, *J. Am. Chem. Soc.* **2000** (122), 1066, and references therein.
[16]Hwang, J.; Govindaswamy, K.; Koch, S. A.*Chem. Commun.* **1998**, 1667.

(R^1,R^2=H), affording the product, after removal of the protecting groups with $AlCl_3$, in 56% overall yield (*Scheme 2*).

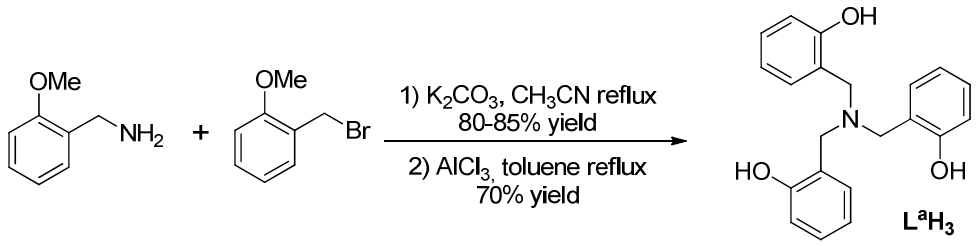

Scheme 2 Synthesis of triphenolamine $\mathbf{L^aH_3}$ via S_N1.

This reaction requires the synthesis of the two reaction partners independently, with the advantage of the possibility to prepare unsymmetric TPA. However, the method can be less practical for the synthesis of symmetric ligands. More recently, another strategy for the synthesis of *C*3 symmetric TPA was reported by our research group. The key step is a threefold reductive amination starting from *ortho*-sustituted salicyl aldehydes using NH_4AcO as nitrogen source, and $NaBH(AcO)_3$ as reducing agent (*Scheme 3*).[17]

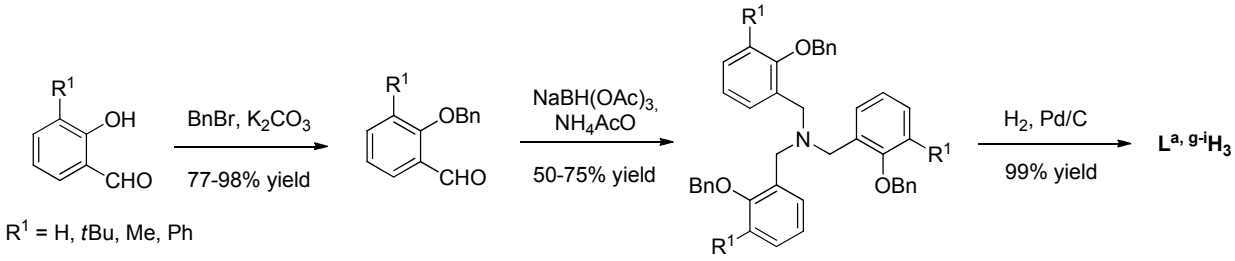

Scheme 3 Synthesis of triphenolamines $\mathbf{L^aH_3}$,$\mathbf{L^gH_3}$,$\mathbf{L^hH_3}$,$\mathbf{L^iH_3}$ via reductive amination.

Salicyl aldehydes, coming from commercial sources or prepared from the corresponding phenols, are protected as benzyl ethers, which are removed in the final step *via* hydrogenolysis, even in the presence of bulky *t*-Bu groups. Moreover, benzyl protecting groups facilitate the crystallization of the intermediates and consequently their purification. The large availability of starting materials combined with the ease of synthesis make this strategy effective for the preparation of *C*3 symmetric ligands in gram scale.

[17]Prins, L. J.; Blázquez, M. M.; Kolaróvic A.; Licini, G. *Tetrahedron Lett.* **2006** (47), 2735.

Numerous examples of amine triphenolate complexes can be found in literature for early transition metals (d^0, d^5) and main group elements (d^{10}). This large amount of data arises from the high stability of amine triphenolate complexes, for which the chelate effect coming from the polydentate TPA ligand is a direct responsible. In these complexes, TPA usually binds the metal as a tetradentate ligand: the three anionic oxygen atoms occupying equatorial positions and the tertiary amine occupying one of the axial positions (*Scheme 4*).

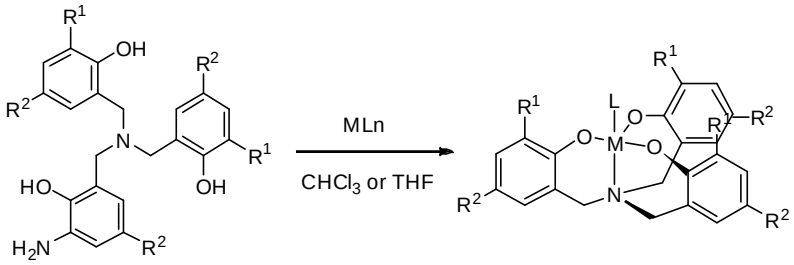

Scheme 4 Complexation reaction of TPA ligands and a generic metal ion.

In the vast majority of cases, mononuclear complexes are obtained with a 1:1 ligand/metal ratio. The most common geometries of the complexes are trigonal bypiramidal (TBP) or octahedral (OCT), while the trigonal monopyramidal (TMP) is less observed (*Figure 2*).

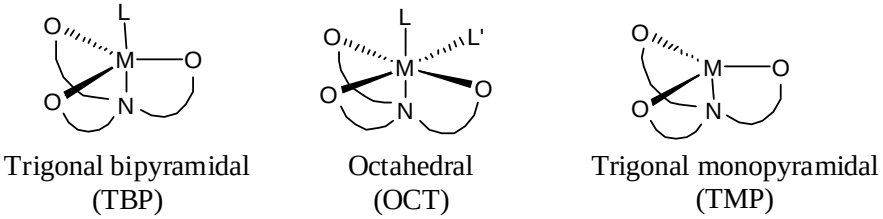

Figure 2 Principal geometry of aminotriphenolate complexes.

When the TPA complexes form, the ligands assume a propeller-like arrangement around the metal ion, when viewed along the metal-nitrogen axis. Consequently, the complexes are chiral with clockwise or counter-clockwise Δ/Λconfigurations, and they form as a racemic mixture, in which the two enantiomeric complexes rapidly interconvert at room temperature (*Figure 3*)[12].

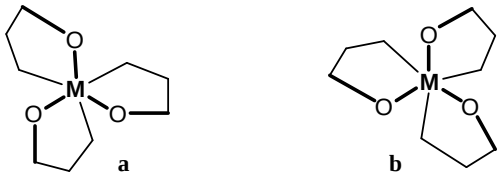

Figure 3 Clockwise (**b**) and counter-clockwise (**a**) enantiomeric configuration of TPA complexes.

1.3 Molybdenum(VI) aminetriphenolate complexes

Recently, our group has been involved in studying the reactivity of Mo(VI) amino triphenolate complexes as catalysts for sulfoxidation, epoxidation and haloperoxidation.[9] Complexes **MoO(L^h)Cl** and **MoO(L^h)(OMe)** were synthesized in good yields using MoO_2Cl_2 as metal source, as shown in *Scheme 5*. An octahedral coordination geometry can be established by symmetry considerations on the basis of ^{1}H-NMR spectra. At room temperature, **MoO(L^h)Cl** and **MoO(L^h)(OMe)** show a ^{1}H-NMR spectrum with three set of signals for the diastereotopic benzylic protons, consistent with a C_S average symmetry of the system caused by fluxional processes. At lower temperatures (-60°C) the benzylic proton resonances resolve into five sets of signals, consistent with a C_1symmetry of the complex.

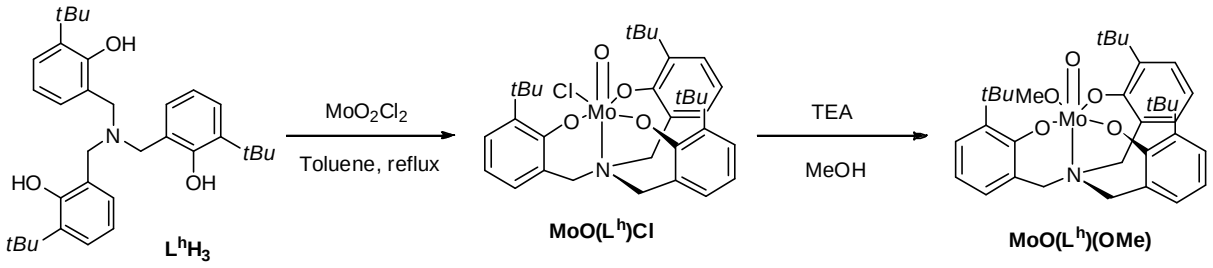

Scheme 5 Synthesis of Mo(VI) amino triphenolate complexes **MoO(L^h)Cl** and **MoO(L^h)(OMe)**.

The octahedral coordination geometry has been confirmed by the X-ray crystal structure of **MoO(L^h)Cl** (*Figure 4*). In the mononuclear complex, the nitrogen atom donor is located *trans* to the terminal oxo group.

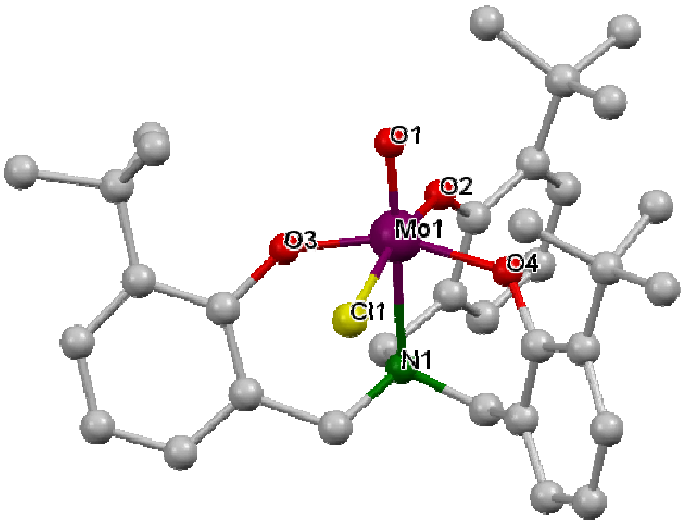

Figure 4 X-ray structure of complex **MoO(L^h)Cl**.Selected bond distances (Å) and angles (deg): Mo-O1 1.680(2), Mo-O2 1.903(2), Mo-O3 1.879(2), Mo-O4 1.916(2), Mo-N1 2.437(2), Mo-Cl1 2.3742(8); Cl1-Mo-O1 96.51(7), Cl1-Mo-O2 166.60(6), Cl1-Mo-O3 84.16(6), Cl1-Mo-O4 85.09(6), Cl1-Mo-N1 86.64(6), O1-Mo-O2 96.69(9), O1-Mo-O3 100.47(9), O1-Mo-O4 100.80(9), O1-Mo-N1 175.88(9), O2-Mo-O3 95.67(8), O2-Mo-O4 90.20(8), O2-Mo-N1 80.28(8), O3-Mo-O4 157.09(8), O3-Mo-N1 73.15(8), O4-Mo-N1 177.79(7).

Molybdenum(VI) amino triphenolate complexes **MoO(L^h)Cl** and **MoO(L^h)(OMe)** has proven to be activecatalysts in the oxidation of sulfides, olefins and halidesusing alkyl hydroperoxides or hydrogen peroxideas primary oxidants (*Scheme 6*).

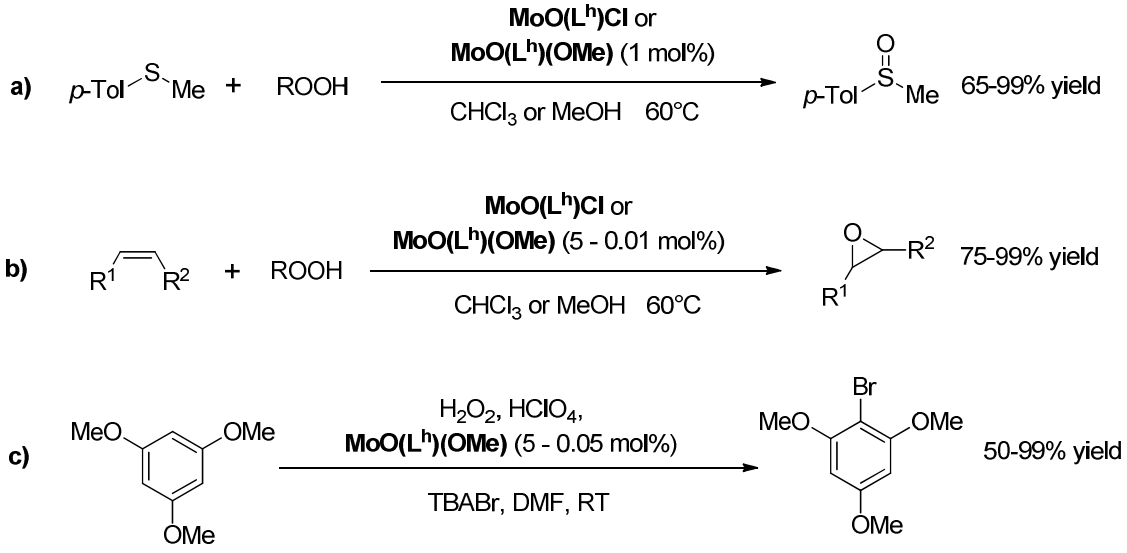

Scheme 6 Reaction catalyzed by Mo(VI) aminotriphenolate complexes **MoO(L^h)Cl** and **MoO(L^h)OMe**. R = tBu, H, PhCMe$_2$.

Sulfides can be oxidize to sulfoxides (*Scheme 6, a*) with good yields using both **MoO(L^h)Cl** and **MoO(L^h)(OMe)** as catalysts in no longer than 40-120 minutes. Using vanadium(V) aminotriphenolate complexes (see *Paragraph 1.4*) as catalysts, even better results can be obtained, especially considering reaction rates. Being the epoxidation of alkenes (*Scheme 6, b*) the major application of Mo(VI)-based catalysts is, complexes **MoO(L^h)Cl** and **MoO(L^h)(OMe)**have been tested for the oxidation of a wide range of epoxides, showing a good versatility in the substrate scope. For this transformation, the amount of catalyst can be lower to 0.01 mol% without affecting the yield of the reaction. Due to the remarkable stability shown by complexes **MoO(L^h)Cl** and **MoO(L^h)(OMe)** under turnover conditions, their catalytic performance was also tested in haloperoxidation reactions, where the catalyst requires to be stable under aqueous highly acidic conditions,[18] obtaining good yields.

1.4 Vanadium(V) aminotriphenolate complexes

The synthesis on vanadium(V) aminotriphenolate complexes was first reported by Kol and co-workers in 2005.[19] Before that, the chemistry of several V(IV) and V(V) complexes, including those with amino diphenolate[20] and triethanol amine ligands,[21] had been deeply investigated, inspired by the discovery of vanadium bioingorganic functions.[22]

For example, the finding of vanadate-dependant haloperoxidases in some seaweeds or terrestrial fungi had led to the design and synthesis of a series of model compounds that mimic the metal coordination sphere in the active site of the enzyme.[23] In the resting state, vanadium possesses a trigonal bipyramidal geometry, being surrounded by three equatorial oxygen donors and axial oxygen and nitrogen (histidine residue).[19]With its three phenolate moieties, the tetradentate TPA ligand provide a natural environment for vanadium, which emulate the active site of the enzymes.

[18]Podgoršek, A.; Zupan, M.; Iskra, J.*Angew. Chem. Int. Ed*. **2009** (48), 8424.
[19] Groysman, S.; Goldberg, I.; Goldschmidt, Z.; Kol, M. *Inorg. Chem.* **2005** (44), 5073.
[20]Crans, D.; Chen, H.; Anderson, O. P.; Miller, M. M. *J. Am. Chem. Soc.* **1993** (*115),* 6769
[21](a) Wolff, F.; Lorber, C.; Choukroun, R.; Donnadieu, B. *Inorg. Chem.* **2003**, *42*, 7839. (b) Wolff, F.; Lorber, C.; Choukroun, R.; Donnadieu, B. *Eur. J. Inorg. Chem*. **2004**, 2861.
[22]Crans, D. C.; Smee, J. J.; Gaidamauskas, E.; Yang, L. *Chem. Rev.* **2004** (104), 849.
[23] a) Rehder, D.; Santoni, G.; Licini, G. M.; Schulzke, C.; Meier, B. *Coord. Chem. Re*v. **2003** (237*),* 53;b) Ligtenbarg, A. G. J.; Hage, R.; Feringa, B. L. *Coord. Chem. Re*v. **2003** (237*),* 89. (6) Bolm, C. *Coord. Chem. Re*v. **2003** (237), 245.

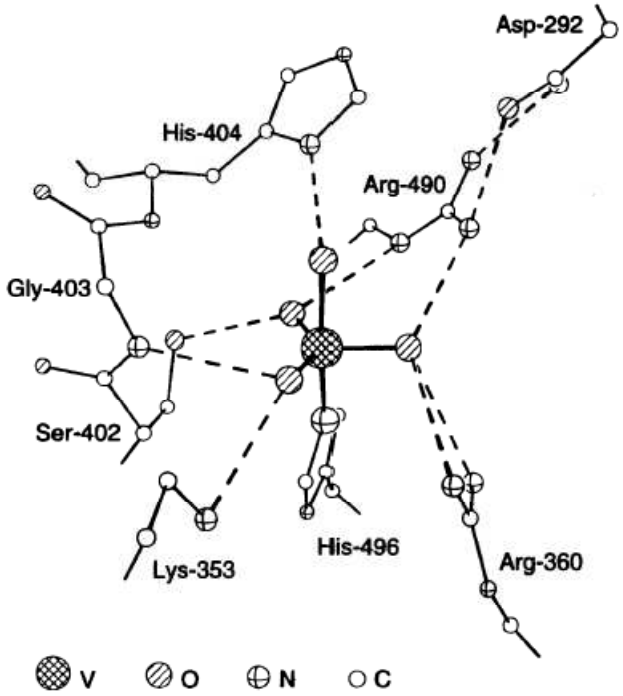

Figure 5 Structure of the active site of vanadium haloperoxidase from the fungus *C. inaequalis*. Adapted with permission from Crans, D. C.; Smee, J. J.; Gaidamauskas, E.; Yang, L. *Chem. Rev.* **2004** (104), 849. Copyright 2004 American Chemical Society.[22]

Scheme 7 shows the general synthesis of V(V) aminotriphenolate complexes reported by Kol and co-workers, which is the procedure that we are still using to synthesize these compounds.

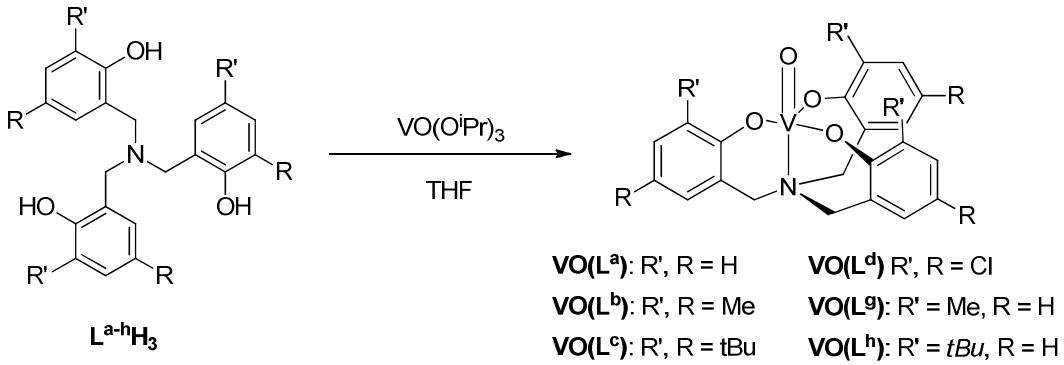

Scheme 7 General synthesis of V(V) amino triphenolate complexes.

X-ray structures of complexes **VO(L^h)** (R^1 = *t*Bu, R^2 = H)and **VO(L^b)** (R^1, R^2 = Me)showed that both of them assume a trigonal bypyramidal (TBP) geometry, with the oxo group occupying an axial position, *trans* to the nitrogen (*Figure 6*). Later on, our group reported a similar synthesis for complexes **VO(L^h)**, **VO(L^a)**(R^1, R^2 = H) and **VO(L^b)**.[24] C_3-symmetric mononuclear species were obtained in the case of complexes **VO(L^h)** and **VO(L^b)**. X-ray structure showed that complex **VO(L^h)** adopts a trigonal bipyramidal geometry, with the oxo function that occupies the axial position, *trans* to the central nitrogen. The vanadium centre is slightly above the plane defined by the phenolateoxygens.

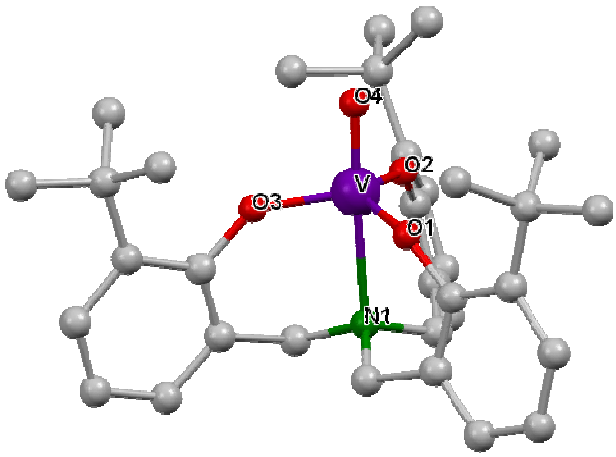

Figure 6 X-ray structure of complex **VO(L^h).** Selected bond distances (Å) and angles (deg): V-O1 1.809(1), V-O2 1.807(1), V-O3 1.807(1), V-O4 1.604(2), V-N1 2.416(2); O1-V-O2 122.51(6), O1-V-O3 117.42(6), O1-V-O4 97.75(7), O1-V-N1 81.36(6), O2-V-O3 114.18(6), O2-V-O4 97.68(7), O2-V-N1 81.16(6), O3-V-O4 98.98(7), O3-V-N1 83.22(6), O4-V-N1 177.79(7).

Also in this case, the coordination environment of vanadium in these complexes mimics that of vanadium centre in vanadate-dependent haloperoxidases, thus the possibility to use these complexes as model compounds of VHPOs has been tested, both in halide and sulfide oxidations. Complex **VO(L^h)**(R^1 = *t*Bu, R^2 = H) showed to be the most effective in catalyzing sulfide oxidations and halogenation of aromatic substrates (*Scheme 8*).

[24] Mba, M.; Pontini, M.; Lovat, S.; Zonta, C.; Bernardinelli, G.; Kündig, P. E.; Licini, G. *Inorg. Chem.* **2008** (47), 8616.

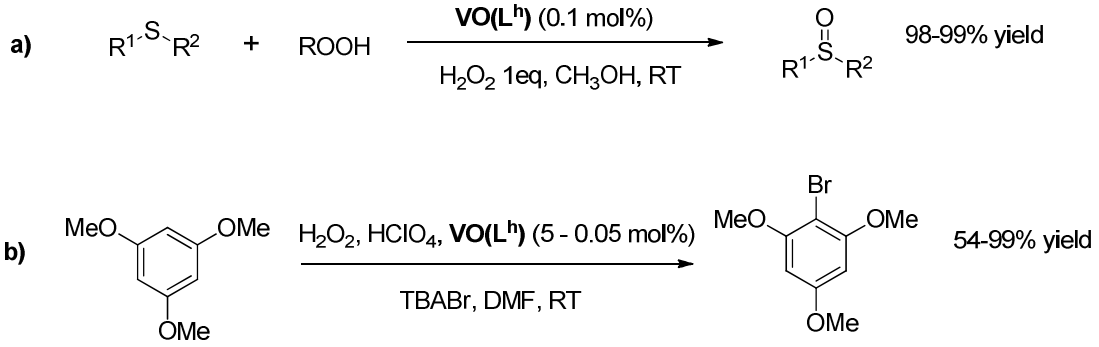

Scheme 8 Reactions catalyzed by vanadium(V) aminotriphenolate complex **VO(L^h)**.

The complex catalyzes efficiently sulfoxidations (*Scheme 8, a*) at room temperature using hydrogen peroxide as the terminal oxidant, yielding the corresponding sulfoxides in quantitative yields and high selectivities (catalyst loading down to 0.01%, TONs up to 9900, and TOFs up to 8000 h^{-1}). Also bromination of 1,3,5-trimethoxybenzene(*Scheme 8, b*) using **VO(L^h)** as catalysts gave excellent results with catalyst loading down to 0.05%, TONs up to 1260, and TOFs up to 220 h^{-1}.

1.5 Triphenolamines functionalization

The nature of substituents in *para* and *ortho* position respect to phenolate moieties (R^1 and R^2) play an important role both in the stability and reactivity of aminotriphenolate complexes. Bulky substituents in *ortho* position (*t*Bu, Ph) shield the metal centre preventing in this way aggregation events which lead to shorter complex life in turnover conditions. This '*ortho* effect' is quite pronounced for example in titanium(IV) aminotriphenolate complexes (*Figure 7*).[25]

Ti(IV) complexes **Ti(L^h)(O*i*Pr)** and **Ti(L^c)(O*i*Pr)**, functionalized with *t*Bu groups in ortho position, showed to be highly stable complexes, not prone to hydrolisis. On the other hand, complexes **Ti(L^a)(O*i*Pr)**,**Ti(L^b)(O*i*Pr)** and **Ti(L^g)(O*i*Pr)**, functionalized with methyl groups or a simple H, have a pronounced tendency to aggregate.

[25] a) Kol, M.; Shamis, M.; Goldberg, I.; Goldschmidt, Z.; Alfi, S.; Hayut-Salant E. *Inorg. Chem. Commun.* **2001** (4), 177; b) Mba, M.; Prins, L. J.; Licini, G. *Org. Lett.* **2007** (9), 21; (b) Zonta, C.; Cazzola, E.; Mba, M.; Licini, G. *Adv. Synth. Catal.* **2008** (*350)*, 2503.

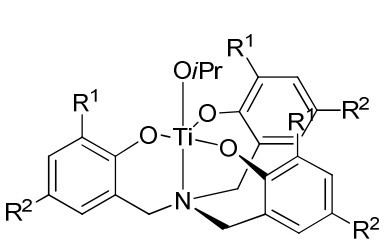

Ti(L^{c})(O*i*Pr) (R^1, R^2 = *t*Bu)
Ti(L^{h})(O*i*Pr) (R^1 = *t*Bu, R^2 = H)

stable to hydrolisis

Ti(L^{a})(O*i*Pr) (R^1, R^2 = H)
Ti(L^{b})(O*i*Pr) (R^1, R^2 = Me)
Ti(L^{g})(O*i*Pr) (R^1 = Me, R^2 = H)

tendency to aggregate/condense

Ti(L^{i})(O*i*Pr) (R^1 = Ph, R^2 = H)

formation of stable u-oxo dinuclear complexes

Figure 7'*Ortho effect*' on the stability of Ti(IV) aminotriphenolate complexes.

Moreover, these *ortho-para* ligand substitutions can be exploited to tune the electronic properties of the complex, with dramatic effect in the catalytic behavior. For example, electron-withdrawing groups (Cl, NO_2) decrease the electron density at the metal centre, thus increasing its Lewis acidity (*Figure 8*).

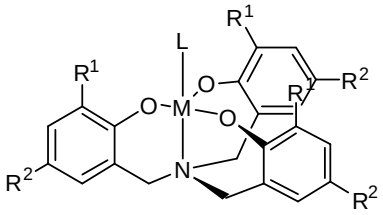

R^1 and/or R^2 = Me, tBu, Cl, NO_2

Lewis Acidity:

Me, tBu < Cl, NO_2

Figure 8 Effect of substituents on Lewis acidity of the metal centre.

The opportunity of choosing the proper R^1 and R^2 substituent for a certain catalyst or a certain reaction is the key feature that makes triphenolamines ligands of choice for the design of new omogeneous metal catalysts. Another advantageous possibility is to use *ortho* and *para* functionalizations to decorate the ligand with pendant groups in order to provide the catalyst with another competence (increased solubility, anchoring abilities, bifunctional catalytic behavior).For this reason, two different synthetic procedures have been set up in our group to decorate aminotriphenolate ligands with functional groups. Suzuki-Miyaura cross coupling reactions can be effectively exploited to decorate iodo- or bromo-functionalized aminotriphenolate ligands using substituted phenylboronic acids (*Scheme 9*).[26]

[26] Badetti, E.; Romano, F.; Lorenzo, D.; Veciana, J.; Cristiano, V.; Licini, G. *Eur. J. Inorg. Chem.* **2016**, 4968.

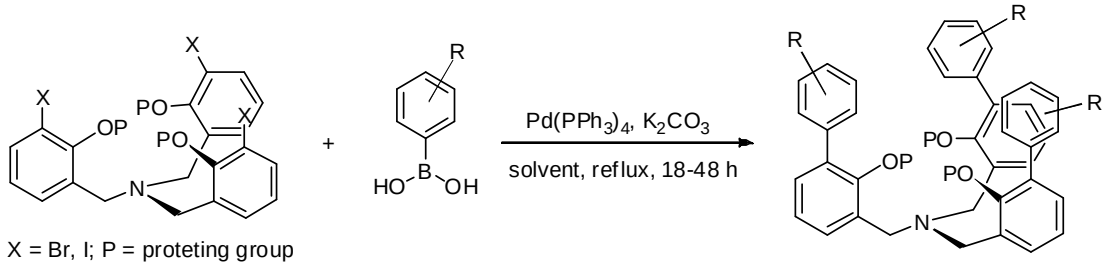

Scheme 9 General scheme for functionalization of triphenolamines using Suzuki-Miyaura cross-coupling reactions.

This procedure have been used to decorate tris(2-pyridylmethyl)amine ligands with one phenyl group functionalized with an aldehyde moiety, for the determination of amino acids enantiomeric excess *ee* (*Figure 9*).[27]

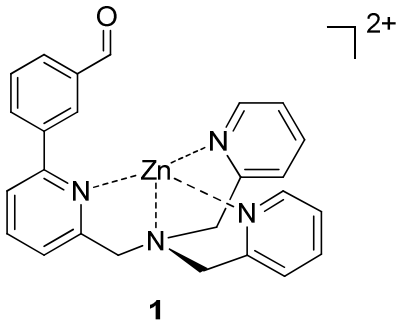

Figure 9 tris(2-pyridylmethyl)amine zinc(II) complex **1**functionalized using Suzuki-Miyaura cross coupling reaction.

Another functionalization strategy designed previously in our group takes advantage of the established 'click type' oxime bond formation.[28] Generally, formation of an oxime bond involves a condensation reaction between a carbonyl group, aldehyde or ketone, with an alkyl- or phenyloxyamine (*Scheme 10*).

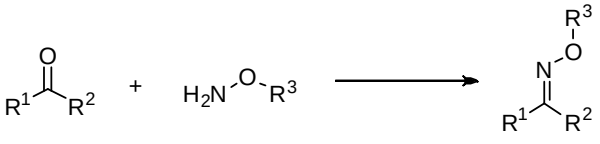

Scheme 10 General oxime bond formation.

[27] Badetti, E.; Wurst, K.; Licini, G.; Zonta, C. *Chem. - A Eur. J.* **2016** (22), 6515.
[28]Schlick, T.L.; Ding, Z.; Kovacs, E.W.; Francis, M.B. *J. Am. Chem. Soc.* **2005** (127), 3718

Triphenolamines must be functionalized with aldehydic groups to be the proper substrate for this transformation. Using Suzuki-Miyaura (see *Figure 9*) or Duff reactions, aminotriphenolate ligands $\mathbf{L^jH_3}$ and $\mathbf{L^kH_3}$ have been synthesized and further reacted with previously prepared alcoxyamine residues (*Scheme 11*). In this way, different decorated ligands have been prepared with new advantageous features.[29] Ligand $\mathbf{L^nH_3}$ was used to synthesize water soluble vanadium(V) aminotriphenolate complex and its catalytic activity has been tested in oxidative C-C cleavage reactions of diols in water, upon solubilization in micelles. Another vanadium(V) aminotriphenolate complex has been synthesized using ligand $\mathbf{L^mH_3}$, functionalized with organogelator moieties to obtain new metallogels to be tested in sulfoxiation reactions. Functionalization of triphenolamine with pyrene moieties ($\mathbf{L^lH_3}$) has been used to prepare μ-oxo Ti(IV) aminotriphenolate complexes, which have been found to be interesting receptors for fullerene.

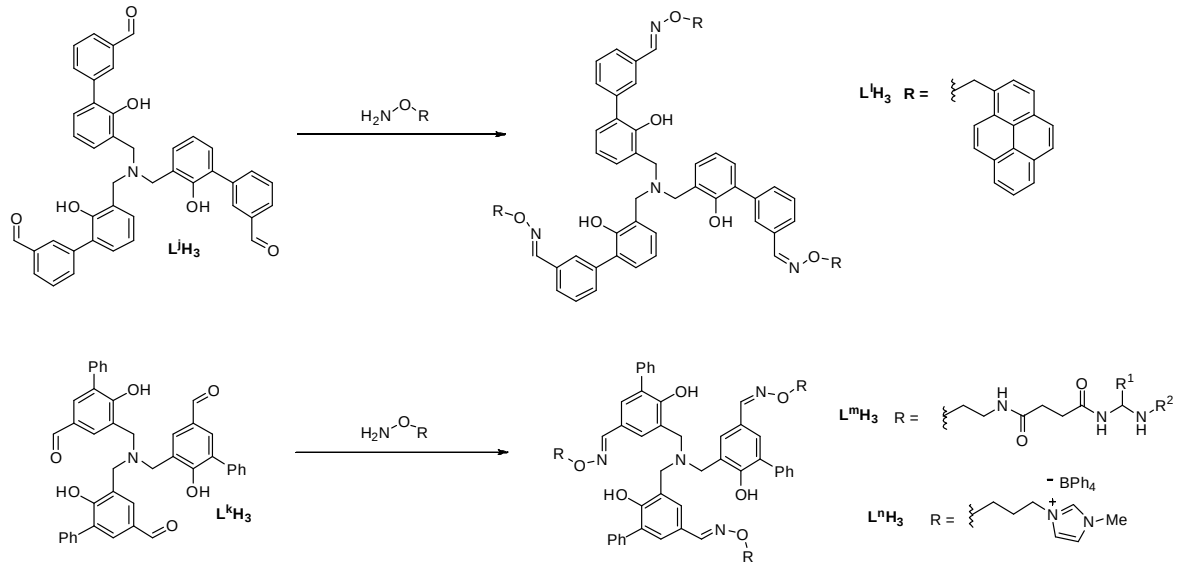

Scheme 11 Synthetic scheme of highly functionalized triphenolamines $\mathbf{L^lH_3}$, $\mathbf{L^mH_3}$ and $\mathbf{L^nH_3}$.

These selected examples clearly demonstrate the high versatility of triphenolamines towards functionalization in terms both of nature and position of anchoring groups. In particular, the possibility to choose between an *ortho* or *para* substitution is highly important as they provide very different spatial arrangements. When talking about catalysis, decorations in *ortho* position will result in pending groups close to the metal, possibly interacting with it (*Figure 10*, **b**). This type of functionalization is particularly useful when a cooperative interaction is needed between the metal

[29] Di Lorenzo, R. PhD Thesis.

and the attached functional group. On the other hand, *para* substitution leads to pending group far from the metal centre (*Figure 10*, **a**). When the action of the inserting group is not related to the metal catalytic centre (e.g. for solubility enhancement in ligand $\mathbf{L^nH_3}$) the *para* position is usually preferred for the functionalization in order not to disturb catalysis.

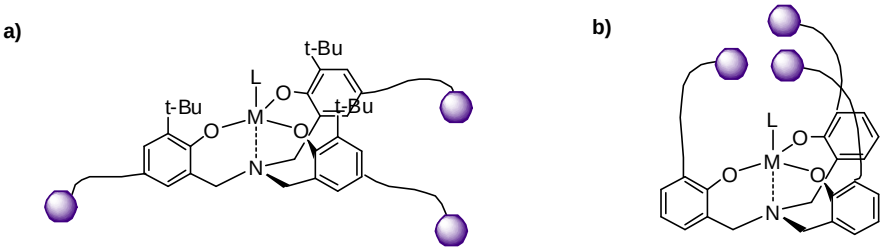

Figure 10 Generic representation of different spatial arrangements of pending groups inserted in *ortho* or *para* position respect to the phenolate moieties.

1.6 Epoxide ring opening reactions

Epoxides are among the most important classes of building blocks in organic chemistry thanks to their facile synthesis from olefins and the broad range of high-valuable 1,2-difunctionalized products that can result from the ring opening reactions by nucleophiles (*Scheme 14*).[30]

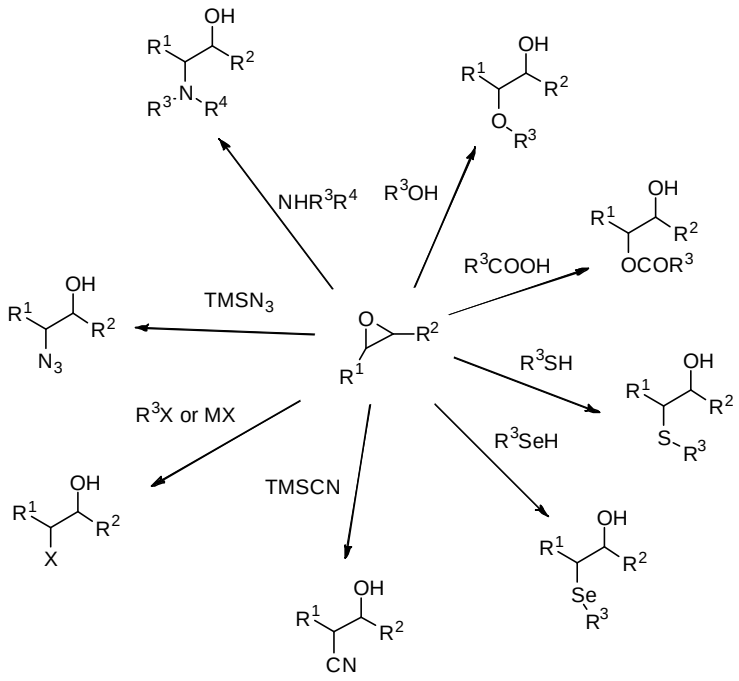

Scheme 12 Examples of 1,2-difunctionalized substrates products of epoxide ring opening reactions by different nucleophiles, namely amines, alcohols, carboxylic acids, thiols, selenols, cyanides, halogens and azides.

[30] Schneider, C. *Synthesis* **2006**, 3919.

Starting from the requisite alkenes, a diverse set of differently substituted epoxides is synthetically available through oxidation reactions,[31] generating a pool of substrates easily accessible for subsequent transformations. Many different nucleophiles are commonly employed to convert oxiranes into appealing 1,2-disubstituted products, as depicted in *Scheme 12*. As examples, epoxide ring opening by amines or alcohols generates substituted 1,2-aminoalcohols (see *Chapter 3*) or 1,2-hydroxyethers, which are wide-spread constituents of both natural occurring and synthetic molecules.[32] Also, ring opening by an amine is a step in the catalytic mechanism of the cyclic carbonate synthesis starting from epoxides and CO_2 (see *Chapter 4* and *5*).

Due to their strain ring (having a high thermodynamic driving force, usually greater than 20 kcal/mol), epoxides are considered reactive compounds. However, their reactivity can be enhanced by using a Lewis acid catalyst coordinating the oxygen atom.[33] Indeed, reaction times are in many cases too long if the epoxide ring opening is run without a catalyst, or harsh reaction conditions have to be used. In the general catalytic mechanism (depicted in *Scheme 13*), the catalyst coordinates to the oxygen atom of the epoxide thus enhancing the electrophilic character of the ring.[31,31]

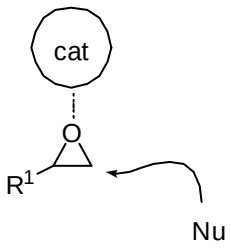

Scheme 13 Schematic representation of the catalytic activation of epoxides towards nucleophilic attack. An electron-poor group of the catalyst (which can be a Lewis/Brønsted acid or an organocatalyst) coordinates to the oxygen atom of the epoxide enhancing the electrophilic character of carbon atoms of the epoxidic ring.

Several Lewisand Brønsted acids have been reported as catalysts for the activation of epoxides to nucleophilic attack, including metal and lanthanide halides[34,35], perchlorates[36], triflates[37] together with porphyrins, salen, binolcomplexes[33], organocatalysts[38] and others[39].

[31] Representative review: Xia, Q. H.; Ge, H. Q.; Ye, C. P.; Liu, Z. M.; Su, K. X. *Chem. Rev.* **2005** (105), 1603.
[32]Bergmeier, S. C. *Tetrahedron* **2000** (17), 2561–2576.
[33] Pastor, I.; Yus, M. *Curr. Org. Chem.***2005** (*9),* 1.
[34]For epoxide opening with alcohols: (a) Nicotra, F.; Panza, L.; Russo, G. *Tetrahedron Lett.* **1991** (32), 4035 [ZnCl2]; (b) Moberg, C.; Rakos, L.; Tottie, L. *TetrahedronLett.* **1992** (33), 2191 [SnCl4]; (c) Chini, M.; Crotti, P.; Gardelli, C.; Macchia, F. *Synlett* **1992**, 673 [CaCl2]; (d) Iranpoor, N.; Salehi, P. *Synthesis* **1994**, 1152 [FeCl3].
[35]For epoxide opening with amines: (a) Reddy, L. R.; Reddy, M. A.; Bhanumathi, N.; Rao, K. R.; *New. J. Chem.* **2001**, 221 [InCl3]; (b) Iqbal, J.; Pandey, A. *Tetrahedron Lett.* **1990** (31), 575 [CoCl2]; (c) Chini, M.; Crotti, P.; Macchia, F.

Considering the strong Lewis acidity of some aminotriphenolate complexes, and being aware of the plethora of epoxide ring opening transformations, we designed four different projects aiming to the synthesis of to high-valuable 1,2-difunctionalized products starting from epoxides (or directly from olefins, in *Chapter 2*). The next paragraph will explain the organization of these projects inside the thesis work.

1.7 Aim and scope of the thesis

On the basis of what has been discussed in the present chapter, the aim of this thesis deals with the synthesis of new decorated aminotriphenolate ligands, using both established and new procedures for the ligand functionalization, the synthesis of the corresponding complexes and their use in catalysis for the activation of epoxides for the synthesis of aminoalcohols and cyclic carbonates.

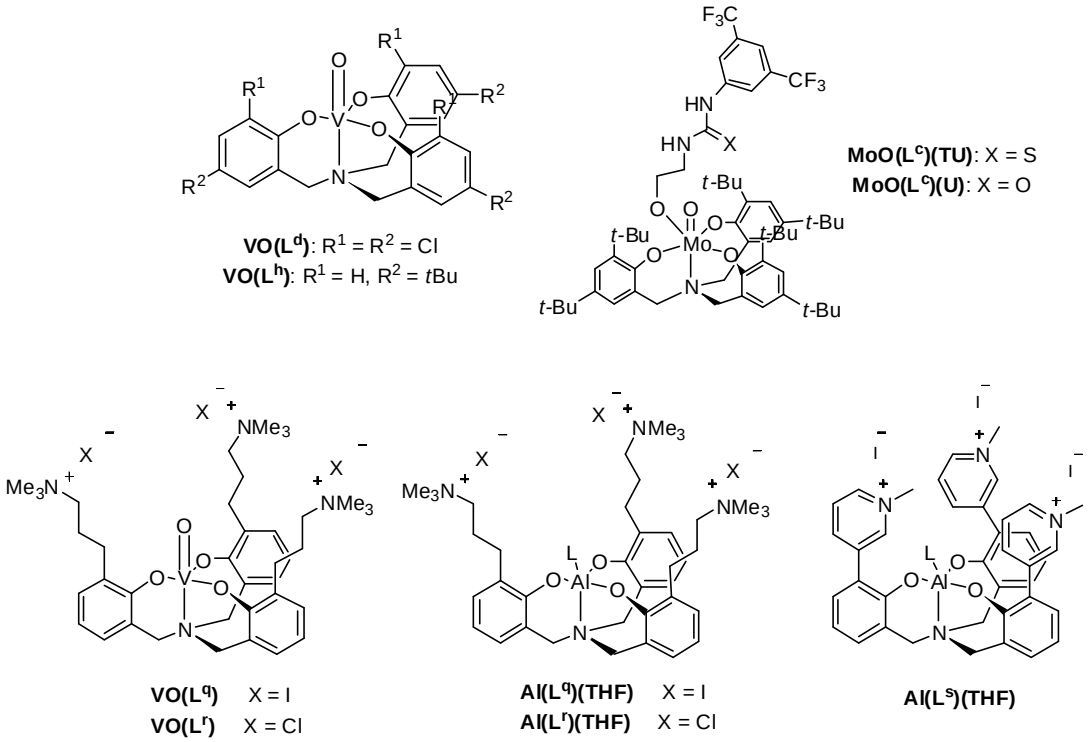

Figure 11 Aminotriphenolate complexes synthesized and tested in this thesis work.

Tetrahedron Lett. **1990** (31), 4661 [CaCl2 and ZnCl2]; (d) Chandrasekhar, S.; Ramachandar, T.; Prakash, S. J. *Synthesis* **2000,** 1817 [TaCl5]; (e) Fu, X.-L.; Wu, S.-H.*Synth Commun*. **1997** (27), 1677 [SmCl3]; (f) de Weghe, P. V.; Collin, J. *Tetrahedron Lett*. **1995** (36), 1649 [SmI2].

[36]Salehi, P.; Seddighi, B.; Irandoost, M.; Behbahani, F. K. *Synth.Commun.* **2000** (30), 2967–2973.

[37](a) China, M.; Critti, P.; Flippin, L. A.; Macchia, F.; Pineschi, M. *J. Org. Chem*. **1992** (57), 1405 [Zn(OTf)2]; (b) Sekar, G.; Singh, V. K. *J. Org. Chem*. **1999** (64), 287 [Cu(OTf)2]; (c) Auge, J.; Leroy, F. *Tetrahedron Lett*. **1996** (37), 7715 [LiOTf].

[38]Yadav, G. D.; Singh, S. *Tetrahedron Lett.* **2014** (29), 3979–3983.

[39]Chandrasekhar, S.; Raji Reddy, C.; NagendraBabu, B.; Chandrashekar, G. *Tetrahedron Lett.* **2002** (21), 3801–3803.

Complexes **MoO(L^{c})(TU)**, **MoO(L^{c})(U)**, **VO(L^{q})**, **VO(L^{r}), Al(L^{q})(THF)**, **Al(L^{r})(THF)** and **Al(L^{s})(THF)** have been therefore synthesized starting from the newly decorated ligands, and tested as catalysts in different epoxide valorization reactions. Moreover, this thesis work wants to take advantage of the possibility of different ligand *ortho*/*para* substitutions for choosing the most appropriate complex as catalysts for a given reaction. This is the case of complexes **VO(L^{d})** (R^1, R^2 = Cl) and **VO(L^{h})** (R^1 = *t*Bu, R^2 = H), in which a different ligand functionalization lead to opposite preferences concerning the catalytic activities. Finally, the activities of the synthesized complexes in catalysis must be fully explored, discussing the reasons for the specific high or low reactivity.

In *Chapter 2*, the synthesis and characterization of molybdenum(VI)aminotriphenolate complexes**MoO(L^{c})(TU)** and **MoO(L^{c})(U)** is described. These complexes have been functionalized linking a (thio)urea derivative at the metal centre, in order to build bifunctional systems able to catalyze olefines epoxidation/epoixde ring opening tandem reactions. In fact, Mo(VI) aminotriphenolate complexes have shown to be effective catalysts for olfin epoxidation reaction (see *Parahraph 1.3*), while (thio)urea derivatives are well-known organocatalysts for epoxide ring opening reactions. This complexes represent a different way of functionalize the complex after the coordination reaction between the triphenolamine and the metal. Indeed, the (thio)urea derivatives have been linked directly to the metal centre, in a straight ward and easy functionalization.

In *Chapter 3*, vanadium(V) aminotriphenolate complex **VO(L^{h})** (R^1 = *t*Bu, R^2 = H) has been investigated as catalyst for epoxide ring opening reactions. Indeed, it was found during the study of complexes**MoO(L^{c})(TU)** and **MoO(L^{c})(U)** for tandem reactions that some vanadium and molybdenum aminotriphenolate complexes are very effective catalysts for epoxide ring opening reactions. Therefore, it was worth expanding this study testing the catalytic activities of these catalysts. In particular, complex **VO(L^{h})** was found to have the highest activity.

The activity of vanadium(V) aminotriphenolate complexes **VO(L^{h})** (R^1 = *t*Bu, R^2 = H) and **VO(L^{d})** (R^1, R^2 = Cl) as catalysts for CO_2 cycloaddition to epoxides has been explored in *Chapter 4*. In this case, the *chloro*-functionalized complex **VO(L^{d})** was chosen as the leading catalyst. Using this complex a wide substrate scope has been conducted using internal epoxides - the most challenging substrates for this reaction - which is lacking in literature. Moreover, the epoxide coordination mode to the metal centre has been explored with ^{51}V-NMR and X-ray experiments, finding an interesting structure in which propylene oxide, coordinated to the metal, has been ring opened by the phenoxy moieties of the ligand itself.

The synthesis of bifunctional catalysts **VO(L^{q})**, **VO(L^{r}), Al(L^{q})(THF)**, **Al(L^{r})(THF)** and **Al(L^{s})(THF)** is described in *Chapter 5*. These have been prepared using both previously set-up

procedures (Suzuki-Miyaura cross-coupling reactions, complex **Al(L^{s})(THF)**) and a new strategy based on Sonogashira coupling reaction for the ligand functionalization. These complexes have been tested for CO_2 cycloaddition reactions and the activity of these bifunctional systems have been carefully compared to that of binary catalysts, composed by a non-functionalized V(V) or Al(III) aminotriphenolate complex and the co-catalyst added separately.

Chapter 2

Mo(VI) aminotriphenolate complex-based bifunctional catalysts for tandem reactions

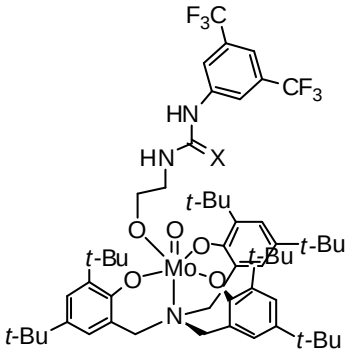

MoO(Lc)(U): X = O
MoO(Lc)(TU): X = S

In this Chapter, the synthesis, characterization and reactivity studies of bifunctional catalysts **MoO(L^c)(U)** and **MoO(L^c)(TU)** are discussed. These systems are composed by a Molybdenum centre, effective catalyst for olefin epoxidation, and a (thio)urea moiety linked directly to the metal. (Thio)urea derivatives are well-know organocatalysts able to activate epoxides via hydrogen bonds towards nucleophilic attack. These bifunctional catalysts are therefore designed with the aim of performing olefin epoxidation - epoxide ring opening reaction as a tandem sequence.

2.1 Introduction

In the search for new catalysts, bifunctional (or multifunctional) systems have been gaining much attention during the last years, owing to the attractiveness of attaching two (or more) catalytic sites with different activities on the same substrate.[1] As shown in *Figure 1*, a bifunctional catalyst can be employed for its cooperative effect, when the two catalytic moieties activate two different reactants of the same reaction (A), or it can be used for tandem reactions, if the two active sites are catalysts for two different reactions which can take place as a tandem sequence (B).[2]

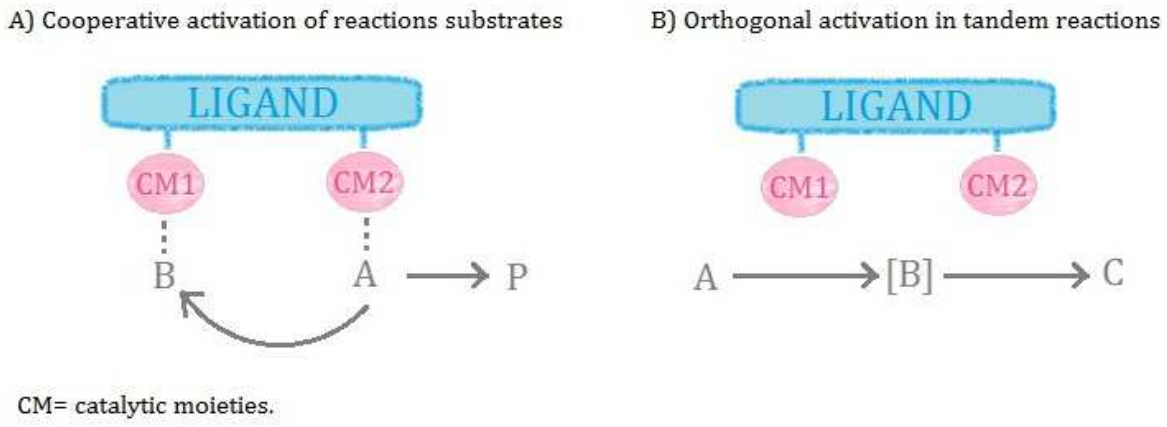

Figure 1 Two different modes of activation for bifunctional catalysts.

As an example of bifunctional catalyst for tandem reactions, Schreiner and co-workers have designed a system in which two organocatalytic moieties are strung together on a peptidic scaffold (*Scheme 1*).[3] This catalysts is reminiscent of an assembly line, in which each interconnected station performs a particular function and only their proper sequence gives the desired product. The one-pot multicatalyst approach has some operational advantages (*e.g.*, decreases solvent use, time, and enables a simpler workup) that become apparent as the number of catalyzed steps increases. Indeed, the ultimate goal with these multifunctional catalysts, according to the authors, would be the use of a library of catalytic moieties that can be assembled to serve the purpose of synthesizing a complex organic molecule in one pot by a programmed series of catalyzed reactions utilizing a retrosynthetic algorithm.

[1] a) Ikariya, T.; Murata, K.; Noyori, R.; *Org. Biomol. Chem*. **2006** (4), 393; b) Groger, H.; *Chem. Eur. J.* **2001**, 7, 5247. c) Lev, D. *J. Am. Chem. Soc*. **2004**, 126, 12232
[2] Hrdina, R.; Muller, C. E.; Wende, R. C.; Wanka, L.; Schreiner, P.R. *Chem. Comm.* **2012**, 48, 2498
[3] Müller, C. E.; Hrdina, R.; Wende, R. C.; Schreiner, P. R. *Chem. Eur. J.* **2011**, 6309.

As depicted in *Scheme 1*, in this system two orthogonal (i.e., independent) catalytic moieties are held together through a oligopeptide backbone and at the same time compartmentalized so they do not interfere one to each other, by putting an adamantane γ-amino acid in between. This lipophilic amino acid also enables the catalyst solubility in a broad variety of solvents.

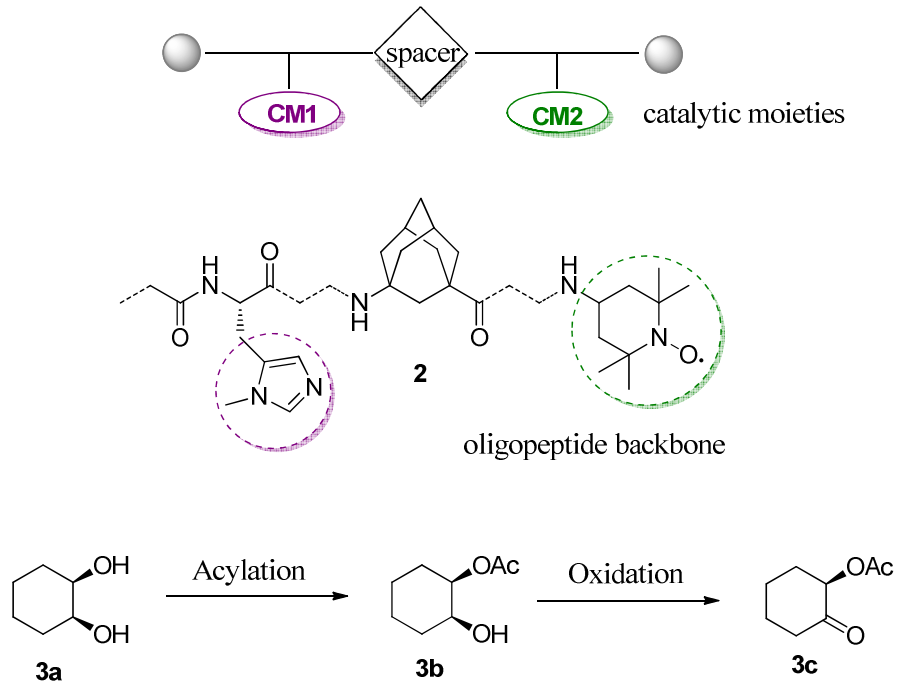

Scheme 1 Modular approach to design the bifunctional system of Schreiner and co-workers. Catalyst **2** has been depicted with a simplified backbone.[3]

Me-histidine residue and 2,2,6,6-tetramethylpiperidine N-oxide (TEMPO), the two funtional moieties chosen for this system, are able to catalyze the enantioselective acetylation and oxidation of *meso*-1,2-cycloalkane diols **3a**. In this work, the authors demonstrated not only that the two active sites are still active and perform their independent functions when placed into one catalyst structure, but also that the oxidation step occurs under milder conditions than in the separate protocols. Whereas the operational advantages of this reaction sequence are minor, this work provided proof of principles studies for a new multifunctional approach in catalysis.

Based on this concept, we designed a new bifunctional catalyst based on a Mo(VI) aminotriphenolate complex and a (thio)urea organocatalyst (*Scheme 2*) for tandem reactions. This bifunctional system has been designed considering that Mo(VI) aminotriphenolate complexes are

effective catalysts for olefin epoxidation reactions[4] (see *Chapter 1*), while (thio)urea-based organocatalysts are able to activate epoxides in ring opening reactions of these substrates by nucleophiles[5]. The goal of this project is thus to carry out these two reactions as a tandem sequence and to obtain the final product starting directly from the olefin and using only one bifunctional catalyst.

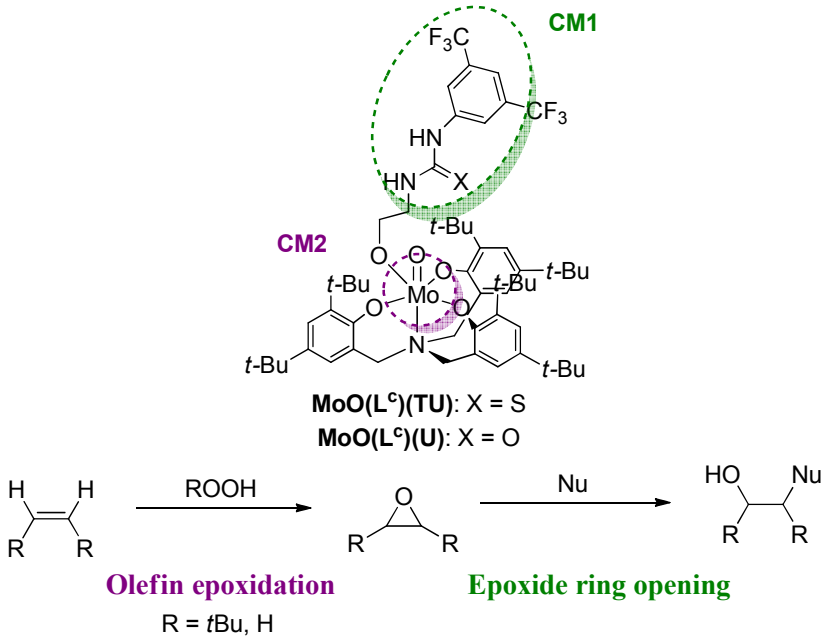

Scheme 2 Bifunctional catalysts **MoO(L^c)(TU)** and **MoO(L^c)(U)**, composed by a Mo(VI)aminotriphenolate complex (CM1) and a thiourea derivative linked to the metal centre.

Thiourea and urea derivatives, together with squeramides, diols and phosphoric acids, belong to the same class of hydrogen bond donors organocatalysts. These catalysts activate neutral functionalities such as R_2C=X, R-NO_2, epoxides and aziridines through the hydrogen bond donating ability of their acidic NH moieties.[6] Usually, one or two electron-withdrawing groups are used as substituents to enahance the pK_a of these compounds, *e.g.*1,3-bis(trifluoromethyl)phenyl or nitrophenyl groups. *Figure 2* shows the hydrogen bond donating mechanism of catalysis for epoxides ring opening reactions.[7] The hydrogen bond formed between the substrate and NH groups of organocatalyst withdraws electron density from oxygen of the epoxide, making the adjacent carbon atoms more electrophilic and thus suscettible to nucleophilic attack.

[4] Romano, F.; Linden, A.; Mba, M.; Zonta, C.; Licini, G. *Adv. Synth. Catal.* **2010** (352), 2937.
[5] a) Schreiner, P. R. *Chem. Soc. Rev.* **2003** (32), 289; b) Dove, A. P. et al, *J. Am. Chem. Soc.* **2005** (127), 13798; c) Chimni, S. S.; Bala, N.; Dixit, V. A.; Bharatam, P. V. *Tetrahedron* **2010** (66), 3042; d) Thomas, C.; Brut, S.; Bibal, B. *Tetrahedron* **2014** (70), 1646.
[6] Zhang, Z.; Schreiner, P. R. *Chem. Soc. Rev*. **2009** (38), 1187.
[7] a) Kleiner, C M.; Schreiner, P. R. *Chem. Commun*., **2006**, 4315; b) Takemoto, Y. *Org. Biomol. Chem.* **2005** (3), 4299.

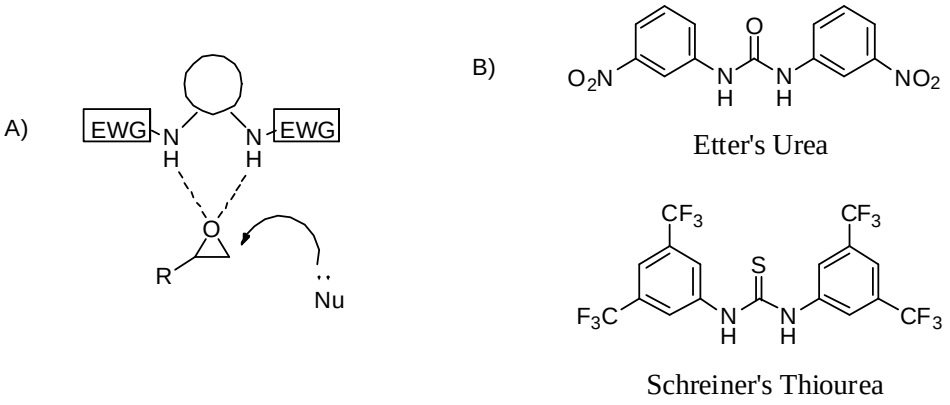

Figure 2 A) Mechanism of epoxide activation for a general NH-based hydrogen bond donating organocatalyst; B) Examples of organocatlysts from literature.[7]

For each reaction taken singularly, the catalytic activity of bifunctional catalysts **MoO(L^c)(U)** and **MoO(L^c)(TU)** have been compared to those of Mo(VI) aminotriphenolate complex **MoO(L^c)(OMe)** and organocatalysts **U** and **TU** (*Figure 3*).

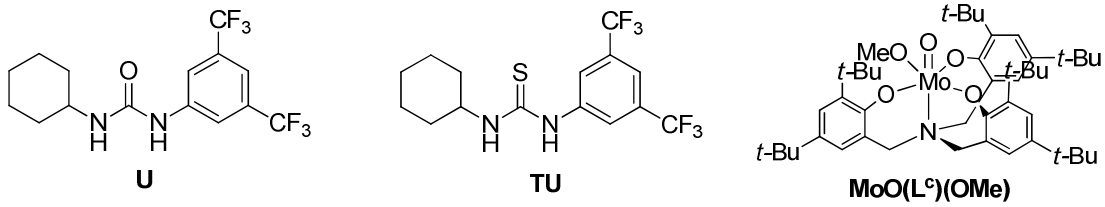

Figure 3 Chemical structures of organocatalysts **TU** and **U**, and Mo(VI)aminotriphenolate complex **MoO(L^c)(OMe)** used as comparison with bifunctional catalysts **MoO(L^c)(U)** and **MoO(L^c)(TU)** in this Chapter.

In the next paragraphs, the synthesis of bifunctional catalysts **MoO(L^c)(TU)** and **MoO(L^c)(U)** is reported, together with the characterization and reactivity studies. Moreover, a detailed speciation study will be discussed concerning the dimerization properties of these complexes.

2.2 Synthesis of bifunctional catalysts MoO(L^c)(U) and MoO(L^c)(TU)

In *Scheme 3*, the synthesis of the bifunctional catalysts **MoO(L^c)(U)** and **MoO(L^c)(TU)** is shown. Starting material **L^{c}H$_3$** has been synthesized using a well-established procedure set up by our groups.[8] Using MoO_2Cl_2 as metal source,[4] Mo(VI) aminotriphenolate complex **MoO(L^c)Cl** was prepared in 90% yield. Displacement of the chloro ligand of Mo(VI) complex **MoO(L^c)Cl** with the (thio)urea derivative to gain the final products **MoO(L^c)(U)** and **MoO(L^c)(TU)** was recognized to

[8] Licini, G.; Mba, M.; Zonta, C. *Dalton Trans.* **2009**, No. 27, 5265.

be easier if preceded by a chloro - methoxy group exchange, which leads to the synthesis intermediate **MoO(L^c)(OMe)** in 84% yield. Finally, Mo complexes **MoO(L^c)(U)** and **MoO(L^c)(TU)** was synthesized through a metoxy - (thio)urea derivative exchange. Reaction yields are in all cases satisfying (>80%).

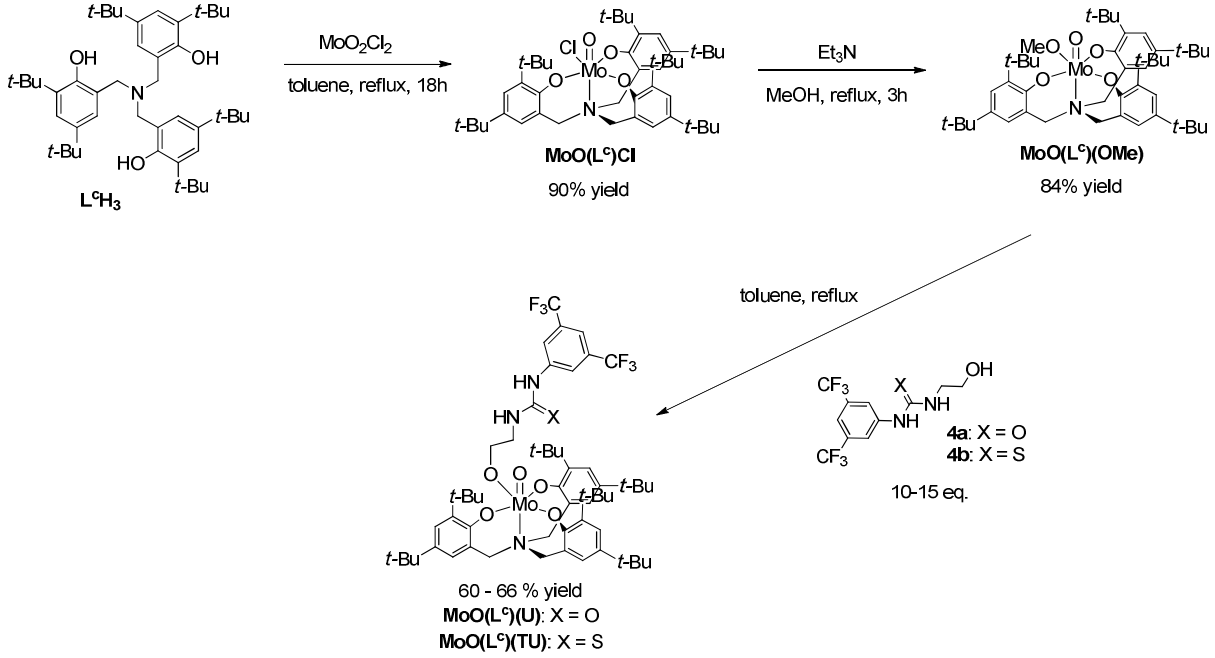

Scheme 3 Synthetic scheme for the preparation of bifunctional catalysts **MoO(L^c)(U)** and **MoO(L^c)(TU)**.

All the synthesis intermediates have been purified by flash silica gel chromatography or filtration and characterized by ESI-MS and ^{13}C- and ^{1}H-NMR spectroscopy.

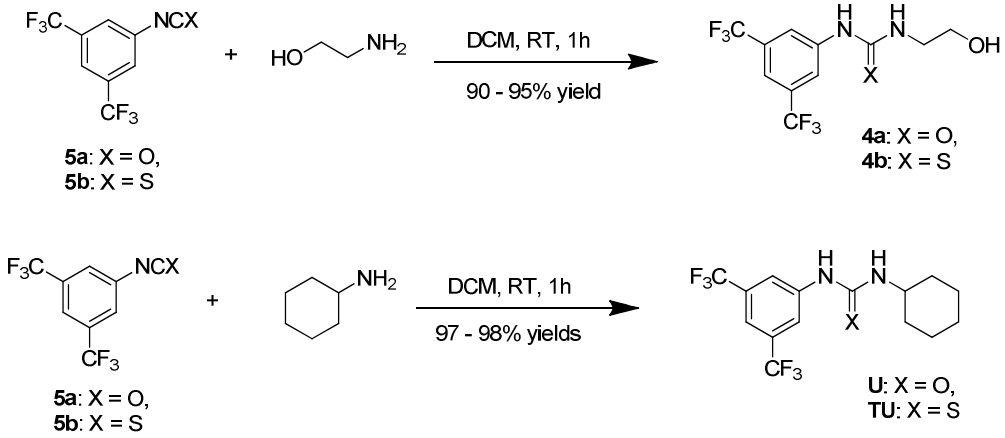

Scheme 4 Synthesis of (thio)urea derivative **4a-b**, **U** and **TU**.

Scheme 4 shows the synthetic procedures to obtain the organocatalysts used in this Chapter. Reacting the appropriate iso(thio)cyanate **5a-b** with cyclohexylamine or ethanolamine in DCM at room temperature leads to the urea-based organocatalyst **TU**, **U** and **4a-b** in high yields. Also in this case, all the synthesized compounds have been characterized via ^{1}H- and ^{13}C-NMR spectroscopy and mass spectrometry.

The characterization of **MoO(L^{c})(TU)** is discussed as a reference for the two bifunctional catalysts, using the proton assignation depicted in *Figure 4*. The formation of the different intermediates towards the synthesis of **MoO(L^{c})(TU)** can be followed conveniently via ^{1}H NMR (*Figure 5*).

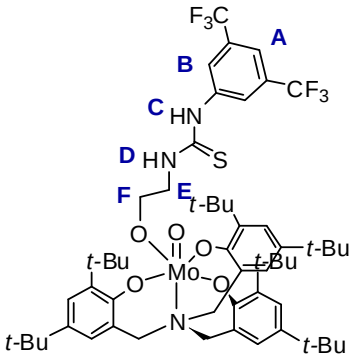

Figure 4 Structure of **MoO(L^{c})(TU)** with proton assignation determined by COSY-NMR experiments.

Starting ligand **L^{c}H$_3$** is highly symmetric and only one set of signals can be detected for the three different arms. The corresponding Mo(VI) complex presents an octahedral geometry and therefore a splitting of NMR signals is detected. Complex **MoO(L^{c})Cl**, **MoO(L^{c})(OMe)** and **MoO(L^{c})(TU)** show a ^{1}H-NMR spectrum with three characteristic sets of signals for the diasterotopic benzyl protons, one singlet and two duplets. This particular signal pattern is consistent with a C_s average symmetry of the system caused by fluxional processes, and was already observed in previous studies in the research group.[4] The effective formation of complex **MoO(L^{c})(OMe)** and **MoO(L^{c})(TU)** was confirmed by ^{1}H-NMR with the presence of the new signal of methoxy (4.1 ppm) and methylene groups (3.3 and 4.2 ppm, represented in *Figure 4* as **E** and **F**) respectively.

The effective coordination has been confirmed also by NOESY experiments, which show the interactions through space between protons of the thiourea moiety **B**, **C**, **D** and **F** and the *t*-Bu groups of the ligand (*Figure 6*). The synthesized bifunctional catalysts **MoO(L^{c})(TU)** and **MoO(L^{c})(U)** have then been tested in the tandem sequence of reactions, as discussed in the next paragraph.

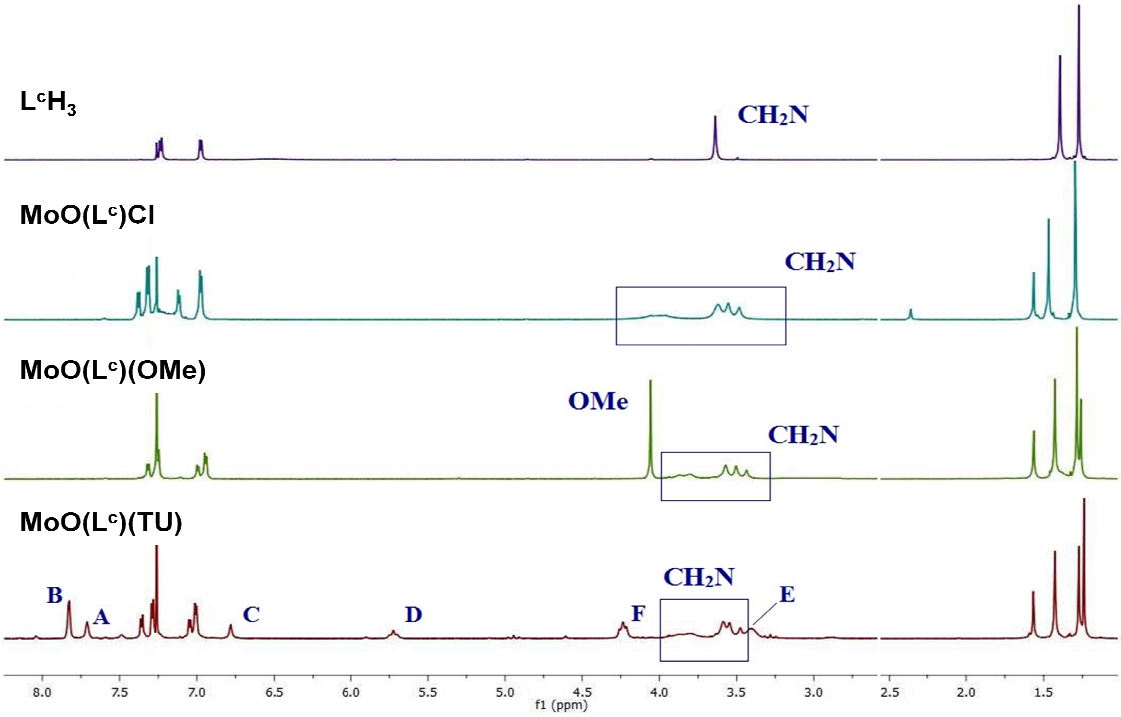

Figure 5 ^{1}H-NMR characterization of **MoO(L^{c})(TU)** and synthesis intermediates.

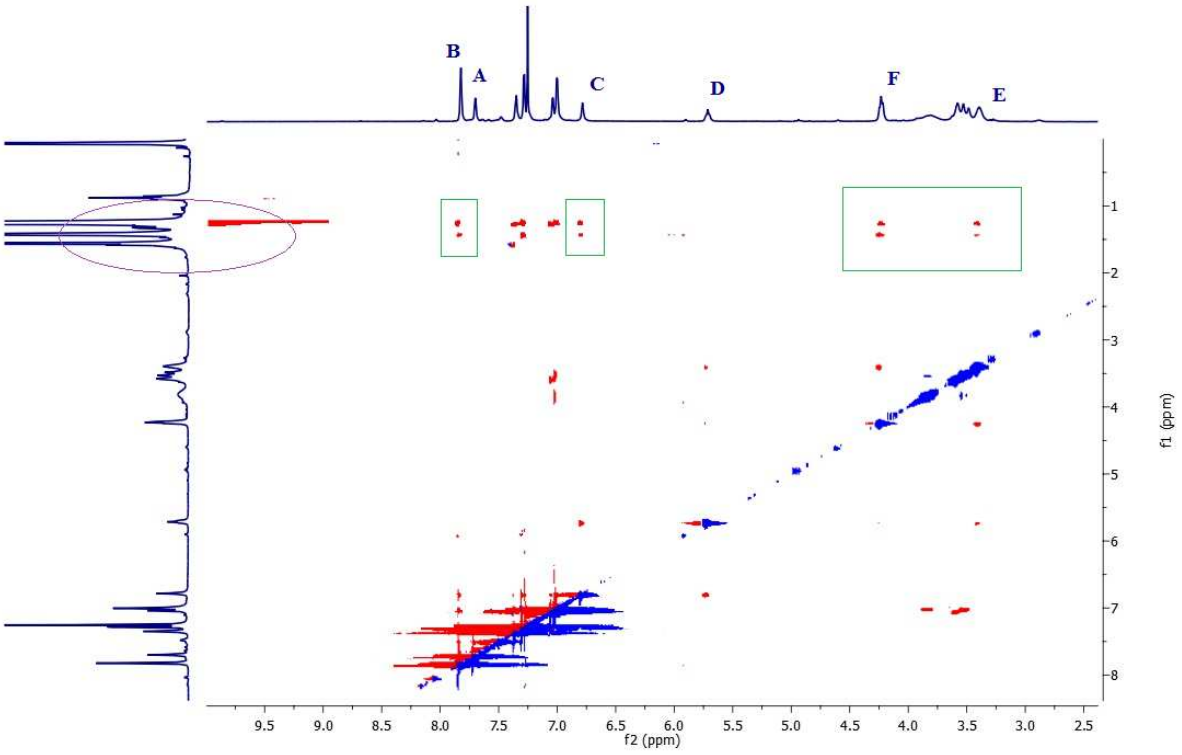

Figure 6 NOESY NMR spectrum of **MoO(L^{C})(TU)**. Interactions through space between protons of the thiourea derivative and the t-Bu protons (visible in the vertical 1D spectrum inside the violet circle) of the ligand are highlighted in green. Interactions with *t*-Bu groups are observable for protons **B**, **C**, **F** and **E**.

2.3 Catalytic activity studies of bifunctional catalysts MoO(L^c)(TU) and MoO(L^c)(U)

Before testing the bifunctional catalysts in the tandem sequence, their performance on each single reaction has to be explored. As the catalytic activity of Mo(VI) aminotriphenolate complexes in olefin epoxidation had already been studied in our research group, we focused first on testing complexes **MoO(L^c)(TU)** and **MoO(L^c)(U)** in the epoxide ring opening reaction.

Catalytic activity of MoO(L^c)(TU). The catalytic activity of bifunctional catalyst **MoO(L^c)(TU)** in the epoxide ring opening reaction was expected to be the same of the organocatalyst **TU** alone, as Molybdenum was not known to have an effect on epoxide activation. On the contrary, it was found that Mo(VI) aminotriphenolate complex **MoO(L^c)(OMe)** itself has an effect in catalyzing the reaction (*entry 3*, *Table 1*), giving 50% NMR yield in the conversion of 1,2-epoxyhexane **6** to aminoalcohol **8**. **TU** organocatalyst showed 70% NMR yield (*entry 2*) after the same time (24h), while the blank reaction gave a sensible lower conversion (*entry 1*). The effect that both the metal centre and the thiourea moiety have in catalyzing this reaction explains the good catalytic activity of bifunctional catalyst **MoO(L^c)(TU)**, higher than **TU** organocatalyst alone, with 82% NMR yield in aminoalcohol **8**.

Table 1 1,2-epoxyhexane **6** ring opening with dibutylamine **7** in ACN (0.5 M concentration), 85°C. Effect of the catalysts.

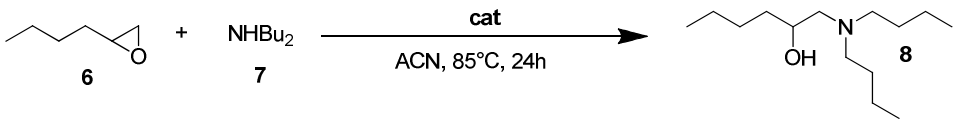

Entry	Cat	[Cat] mol%	Yield (%)[a]
1	-	-	15
2	**TU**	10	70
3	**MoO(L^c)(OMe)**	10	50
4	**MoO(L^c)(TU)**	10	82
5	**MoO(L^c)(OMe) + TU**	10 + 10	80

Reaction conditions:[9] [**6**] = 0.5 mmol, [**7**] = 0.5 mmol 24h, ACN 1mL, 24 hours, 85°C. [a]Yields calculated via ^{1}H-NMR analysis with dichloroethane as external standard. Selectivity was in all cases >99%.

[9] These are the reaction conditions optimized for the epoxide ring opening reaction only. The reaction conditions optimized for both the olefin epoxidation and epoxide ring opening consist in $CHCl_3$ as solvent and 1M substrate concentration. These results were therefore repeated in these conditions, giving very similar profiles.

These results demonstrated that molybdenum and the thiourea mioety that compose the bifunctional catalyst **MoO(L^c)(TU)** have a synergistic effect in catalyzing the epoxide ring opening reaction, acting as Lewis acid and hydrogen bond donor, respectively. The yield of the reaction catalyzed by bifunctional catalyst **MoO(L^c)(TU)** has been compared to that of reaction catalyzed by **TU** + **MoO(L^c)(OMe)** added separately (*entry 4* and *5*). Similar conversions have been obtained for the binary and bifunctional system, meaning that no cooperative effect is present between these two catalytic moieties for this reaction.

These results on the epoxide ring opening reaction seemed very promising, as an unexpected increase in the reaction yield was obtained for the bifunctional catalyst **MoO(L^c)(TU)** respect to the thiourea derivative alone. Unfortunately, when testing the system in the olefin epoxidation reaction, a catalyst decomposition was observed. We recognized that thiourea moiety is not stable in the oxidative conditions of olefin epoxidation reaction: by means of ^{1}H-NMR spectroscopy and ESI-MS analysis we could observe that in these conditions thiourea derivatives undergo a desolfurization reaction (*Scheme 5*), and some evidences were also found in literature.[10]

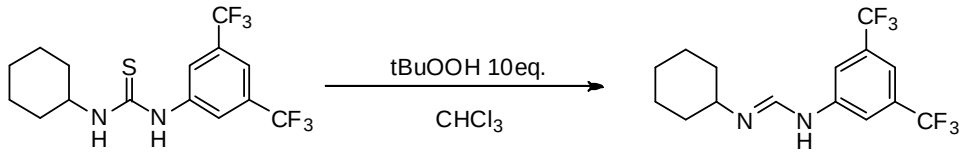

Molecular Weight: 370,36 Molecular Weight: 338,29

Scheme 5 Scheme of desolfurization side reaction occurring to thiourea derivatives in the oxidative conditions of olefin epoxidation reaction (*t*BuOOH 10 eq., in $CHCl_3$).

On the contrary, urea derivatives were found to be stable in these oxidative conditions, so we soon turned on testing bifunctional catalyst **MoO(L^c)(U)** in the tandem sequence of reactions.

Catalytic activity of MoO(L^c)(U). As done for **MoO(L^c)(TU)**, catalytic activity of bifunctional catalyst **MoO(L^c)(U)** has been tested first for epoxide ring opening reaction (*Figure 7)*. In this case, the conditions optimized for both the tandem reactions have been used ($CHCl_3$, 1M substrate concentration, 60°C, 24 hours). Again, 1,2-epoxyhexane and dibutylamine have been chosen as substrate and nucleophile. Unfortunately, bifunctional catalyst **MoO(L^c)(U)** showed to be less

[10] a) Farzaliev, V. M.; Allakhverdiev, M. A.; Magerramov, A. M.; Shirinova, N. A.; Dzhavadova, L. A.; Rzaeva, I. A.; Khalilova, A. Z.; Aliev , F. Y. *Russ. J. App. Chem*. **2001** (74), 114. b) Khurana, J. M.; Kukreja, G.; Bansal G. *J. Chem. Soc*., *Perkin Trans.* **2002** (1), 2520. c) Krivenko, L. V.; Sibgatullin, I. M.; Cherezova, E. N.; Galkin, V. I.; Mukmeneva, N. A. Russ. J. Gen. Chem. **2003** (73), 1086.

active then the organocatalyst **U** alone, giving 64% NMR yield in aminoalcohol **8** after 24 hours, respect to 90% yield of **U**. Opposite to what was found for **MoO(L^c)(TU)**, this urea-based bifunctional catalyst showed to be even less active than urea organocatalyst that is part of the molecular structure.

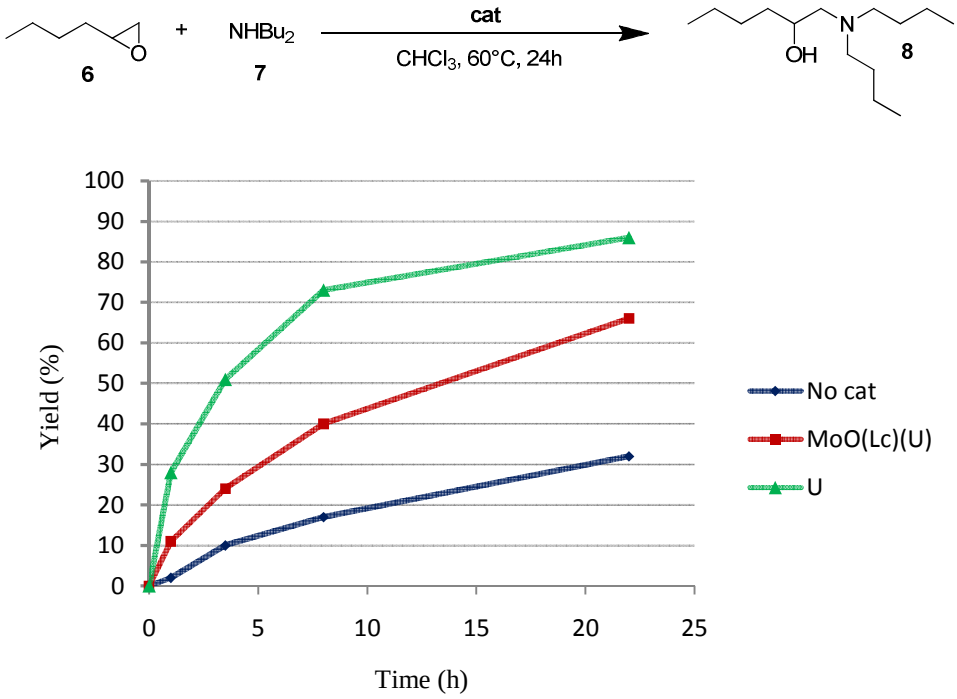

Figure 7 1,2-epoxyhexane **6** ring opening with dibutylamine **7**, effect of the catalysts. Reaction conditions:[1] [**6**] = 1 mmol, [**7**] = 1 mmol, [**cat**] = 0.1 mmol, 24h, $CHCl_3$ 1mL, 24 hours, 60°C. [a]Yields calculated via ^{1}H-NMR analysis with dichloroethane as external standard. Selectivity was in all cases >99%.

The opposite behavior of bifunctional catalysts **MoO(L^c)(TU)** and **MoO(L^c)(U)** towards epoxide ring opening reactions has been explained thanks to a series of considerations about the different hydrogen bonding mode between urea and thiourea moieties, which leads to different dimerization abilities of related bifunctional catalysts. This is fully discussed in the next paragraph.

2.4 Speciation studies of bifunctional catalysts MoO(L^c)(TU) and MoO(L^c)(U)

While performing the catalytic activities studies, we managed to grow an X-ray quality crystal of bifunctional catalyst **MoO(L^c)(TU)**. The X-ray structure, depicted in *Figure 8*, shows that the complex forms dimers at the solid state, with the two NH groups of the thiourea derivative hydrogen bonded to the Mo-oxo moiety of another molecule of catalyst. On account of this

founding, and considering the inverse reactivity of **MoO(L^c)(TU)** and **MoO(L^c)(U)** towards epoxide ring opening reaction, we tried to better understand the behavior of bifunctional catalysts also in solution, as the speciation of complexes can have an influence on catalytic activities.

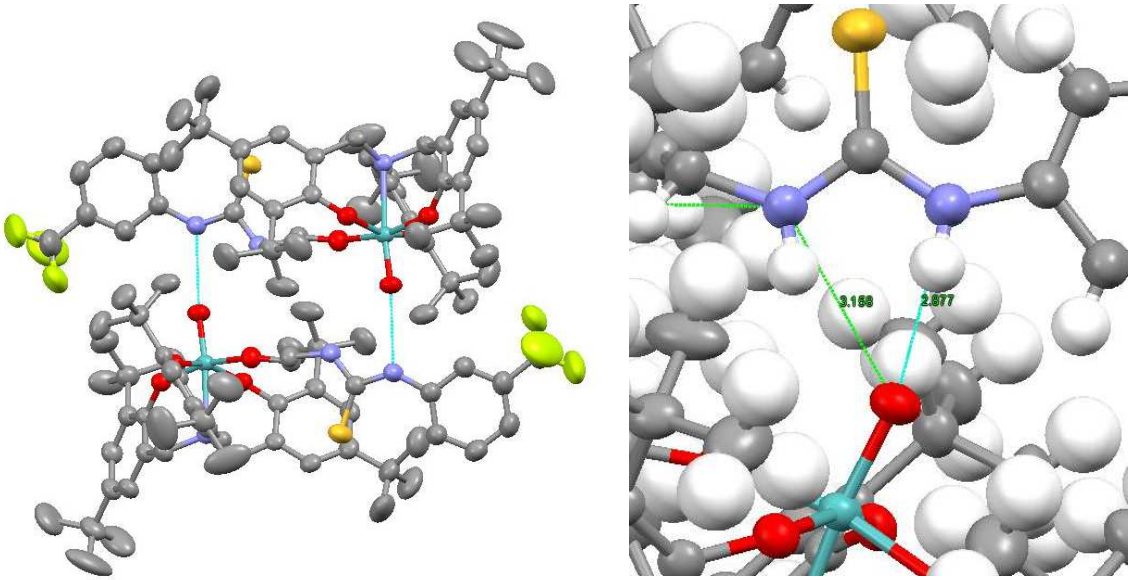

Figure 8 X-ray structure of the **MoO(L^c)(TU)** dimer formed by hydrogen bonds between the Mo-oxo group (depicted in red) and thioureas moieties (depicted in light blue).

ESI-MS spectra of complexes **MoO(L^c)(TU)** and **MoO(L^c)(U)** in acetonitrile and methanol provided a first sign of dimers persistence in solution. Indeed, signals referred to the molecular weight of dimers were detected in the MS spectra of both **MoO(L^c)(TU)** (with a very low intensity signal) and **MoO(L^c)(U)**, other than monomeric species (*Figure 9*).

Another important information about the dimerization of complexes can be obtained from IR spectrometry, considering NH stretching bands of bifunctional catalysts both in solid state and in solution (*Figure 10*). NH bands are located in the H-bonded NH region (3334 cm^{-1} for **MoO(L^c)(TU)** and 3395 cm^{-1} for **MoO(L^c)(U)**) and show the typical broad shape of H-bonded NH bond, both for spectra in solid state and in solution. This confirm the X-ray evidence that complexes self-assemble through hydrogen bonds involving urea and thiourea NH groups, and also reveals that dimers persist in solution. Three different concentration of complexes in $CDCl_3$ (10^{-4}M, 10^{-3}M, 10^{-2}M) have been used to detect IR spectra in solution, and no significant shift in NH bands is observed ranging from concentrated to dilute solutions. These results suggest that in the range of concentration used, complexes are stable in form of dimers and no disaggregation processes seem to take place.

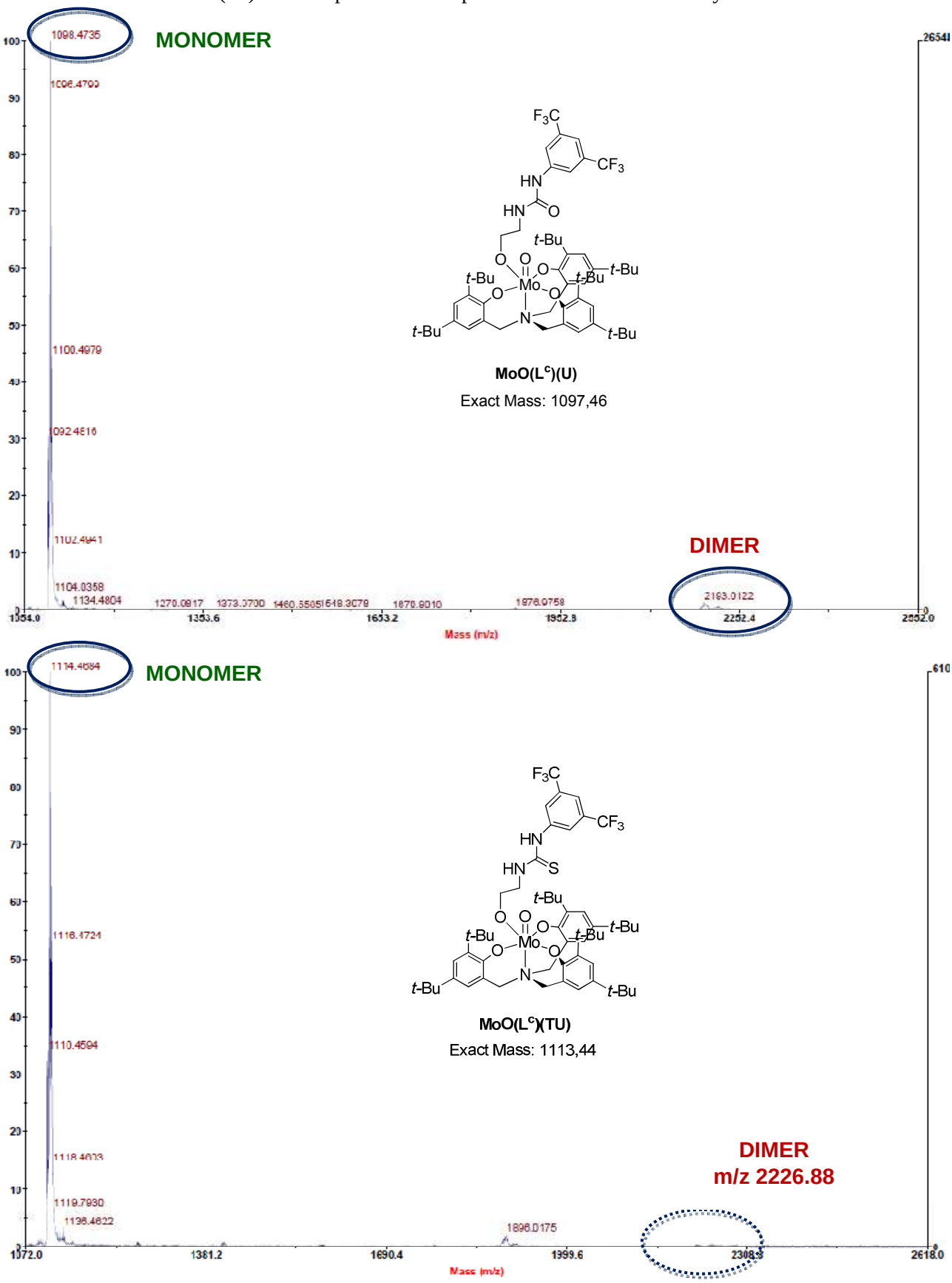

Figure 9 ESI-MS spectrum of **MoO(L^c)(U)** and **MoO(L^c)(TU)** in ACN, showing mass signals of monomers and dimers. In the case of **MoO(L^c)(TU)**, the signal of the dimer is present at a very low intensity (hardly visible). This is in line with the considerations discussed later on in this chapter, in which the H-bond generated by the urea moiety is considered stronger than the one generated by thiourea NH. **MoO(L^c)(U)** calc $[M]^+$: 1097,46; **MoO(L^c)(TU)** calc $[M]^+$: 1113,44.

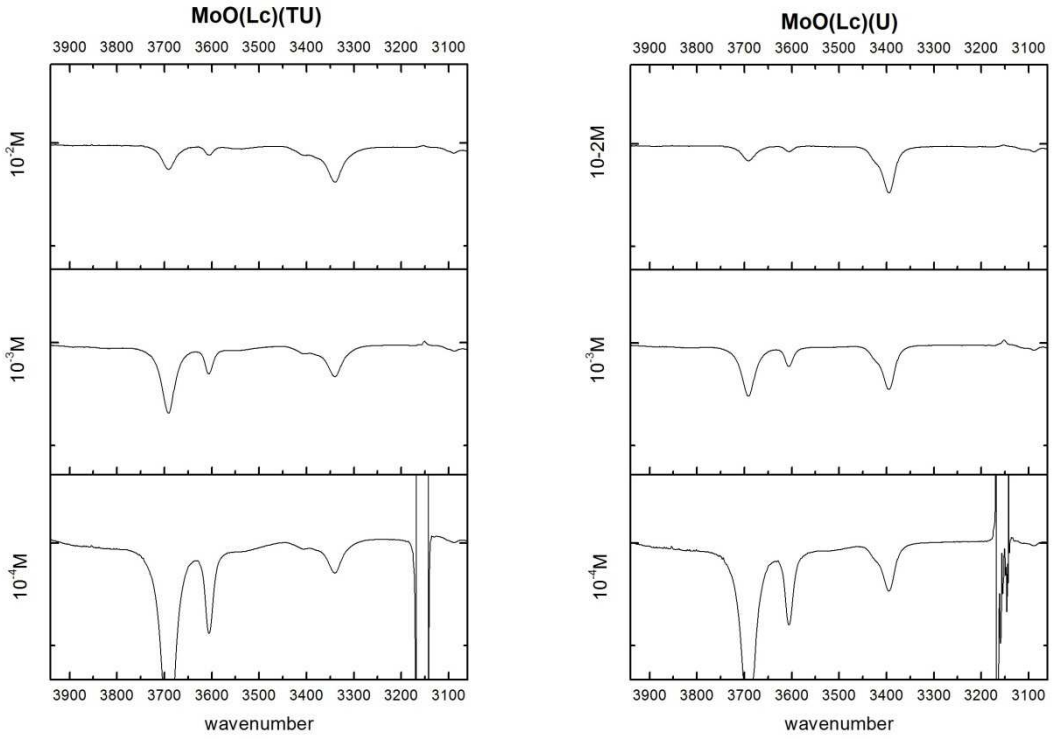

Figure 10 H-bonded NH bands of **MoO(L^c)(U)** (3395 cm^{-1}) and **MoO(L^c)(TU)** (3334 cm^{-1}) in IR spectra of complexes in $CDCl_3$ solution (10^{-4}M, 10^{-3}M, 10^{-2}M).

To get a quantitative view of speciation equilibrium of complexes we set up a 2D DOSY-NMR experiment procedure in order to calculate diffusion coefficients D of **MoO(L^c)(TU)** and **MoO(L^c)(U)** in coordinating and non-coordinating solvents and to obtain information on molecular weights of complexes in solution by using complex **MoO(L^c)(OMe)** as external standard.

^{1}H-NMR titration experiments showed that adding increasing equivalents of DMSO-d_6 to solution of **MoO(L^c)(TU)** or **MoO(L^c)(U)** complexes in $CDCl_3$ causes a shift in NH signals, indicating that the solvent is coordinating to the (thio)urea moiety of complexes. After adding 40 equivalents of DMSO-d_6 the shift of NH signals stops, and therefore we can assume that in these conditions all molecules of catalysts form hetero-dimers with DMSO-d_6.

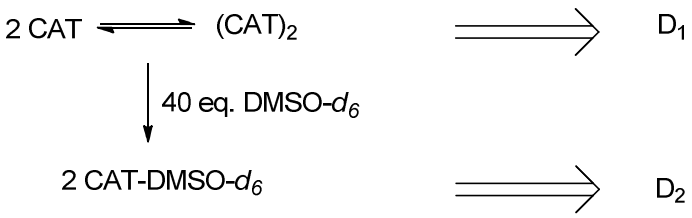

Scheme 6 Equilibrium of limit situation in $CDCl_3$ (10^{-2}M) leads to a diffusion coefficient D_1; limit situation in $CDCl_3$ (10^{-2}M) + 40 eq. of DMSO-d_6 leads to a second diffusion coefficient D_2.

On the contrary, ESI-MS and IR analysis suggest that catalysts in non-coordinating solvents such as $CDCl_3$ are present in equilibrium between monomers and dimers. These two limit situations can be depicted in *Scheme 6*.

Considering the Graham Law,[11] the ratio between diffusion coefficient D_1 and D_2 is related to the ratio between molecular weights of involved molecules by the following equation:

$$\frac{D_1}{D_2} = \sqrt{\frac{M_2}{M_1}}$$

being $M_1 = MW_{catalyst}$ in $CDCl_3$ and $M_2 = MW_{catayst} + MW_{DMSO\text{-}d6}$ in $CDCl_3$ + 40 equivalents DMSO-d_6. M_1/M_2 gives a good idea of the degree of aggregation of catalysts in solution.

To obtain absolute molecular weights, a monomeric external standard of known weight and similar structure is required. Complex **MoO(L^c)(OMe)** has therefore been chosen as external standard.

Thus, M_1 and M_2 can be found with the following equation:

$$M_{Analyte} = M_{Ref}\left(\frac{D_{Ref}}{D_{Analyte}}\right)^2 - M_{DMSO d6}$$

where $M_{Analyte} = M_1$ or M_2, and $D_{Analyte} = D_1$ or D_2.

Table 2 Diffusion coefficient ratio, M_1/M_2 and absolute molecular weight for complex **MoO(L^c)(TU)**.

D_1/D_2	M_1/M_2	M_1	M_2	$M_{theoretic}$	ε
1.483	2.20	2377.17	995.83	1112,93	-10%

Table 3 Diffusion coefficient ratio, M_1/M_2 and absolute molecular weight for complex **MoO(L^c)(U)**.

D_1/D_2	M_1/M_2	M_1	M_2	$M_{theoretic}$	ε
1.553	2.413	2395.14	908.59	1098	-16%

Table 2 and *Table 3* show M_1/M_2 values and absolute MWs for **MoO(L^c)(TU)** and **MoO(L^c)(TU)**; M_1 and M_2 are expressed in g/mol, ε is the error for absolute molecular weight calculated for

[11] a) Cohen, Y.; Avram, L.; Frish, L. *Angew. Chem. Int. Ed*., **2005** (44), 520. b) Timothy D.W. Claridge. High-Resolution NMR Techniques in Organic Chemistry. Elsevier, 2nd edition, 2009. c) Braun, S.; Berger, S- 200 and More NMR Experiments. Wiley VCH, 2nd edition, 1998

complexes as monomers referred to the theoretic molecular weight. DOSY spectra are reported in *Figure 11* and *12*.

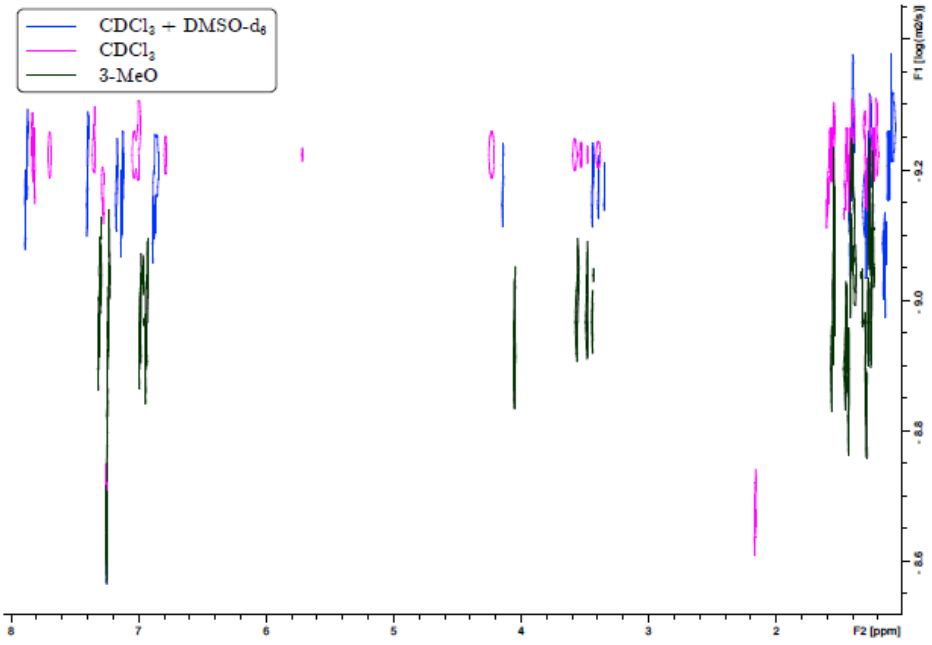

Figure 11 2D-DOSY spectrum of **MoO(L^c)(TU)** in $CDCl_3$ (violet line), **MoO(L^c)(TU)** in $CDCl_3$ + DMSO-d_6 (blue line) and **MoO(L^c)(OMe)** as external standard (green line) (300MHz).

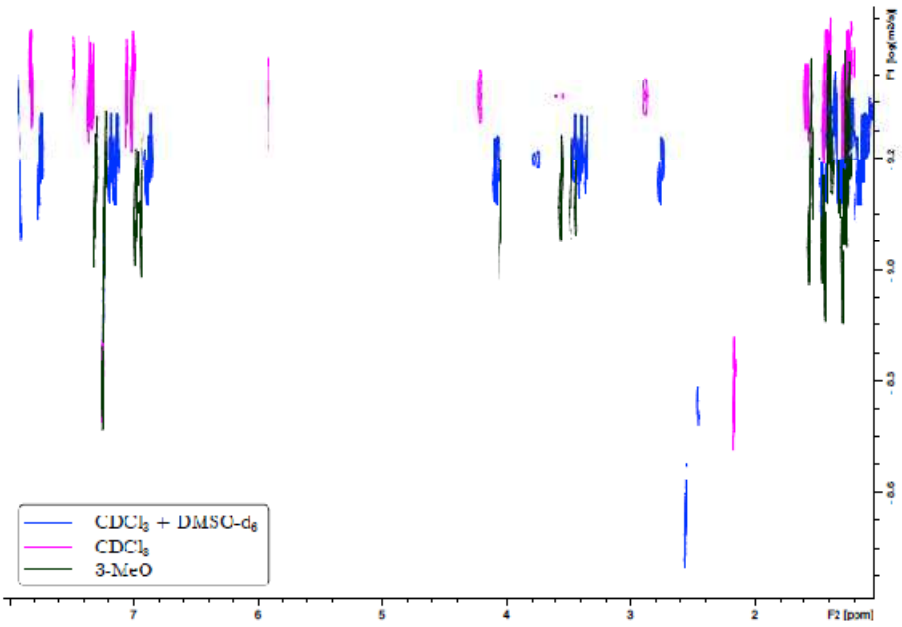

Figure 12 2D-DOSY spectrum of **MoO(L^c)(U)** in $CDCl_3$ (violet line), $CDCl_3$ + DMSO-d_6 (blue line) and **MoO(L^c)(OMe)** as external standard (green line) (300MHz).

As we can see from M_1/M_2 values, for both **MoO(L^c)(TU)** and **MoO(L^c)(U)**, molecular weights in solution have resulted to be more than twice the molecular weight of monomeric species. Equilibrium of dimerization can thus be considered shifted towards dimeric species. As **MoO(L^c)(TU)** has shown good results for epoxide ring opening reaction, we can hypothesize that, to a certain extent, dimers disassociate upon addition of epoxide, which forms hydrogen bonds with thiourea moiety. On the contrary, hydrogen bonds forming dimers of bifunctional catalyst **MoO(L^c)(U)** are probably too strong to disassociate in favor of an hydrogen bonding with the substrate, thus leading to low catalytic activity.[12]

2.5 Conclusions

In conclusion, bifunctional catalysts **MoO(L^c)(U)** and **MoO(L^c)(TU)** have been synthesized and fully characterized. Complex **MoO(L^c)(TU)** showed good catalytic activity in epoxide ring opening reaction, thanks to the synergic effect between the organocatalytic and the metal functions of the system in activating the substrate. Indeed, the yield of reactions catalyzed by the bifunctional catalyst **MoO(L^c)(TU)** is higher than using the organocatalyst **TU** alone. Unfortunately, this bifunctional catalysts showed to be not stable in oxidative conditions, and it was thus impossible to test it in the oleifn epoxidation-epoxide ring opening tandem reactions. On the other hand, bifunctional catalyst **MoO(L^c)(U)**, even if stable in oxidative conditions, is not active in the epoxide ring opening reaction, giving product yields lower then **U** organocatalyst. To explain this poor reactivity, a speciation study has been conducted, reveling that bifunctional catalysts are present as dimers in solution. In the aggregate form, NH proton of urea derivative in bifunctional system **MoO(L^c)(U)** are not free to form hydrogen bonds with the substrate to activate them.

At the end of this project, we serendipitously found that Mo(VI) aminotriphenolate complex **MoO(L^c)Cl**, bearing chloride rather then methoxo as ancillary ligand, exerts a catalytic activity for epoxide ring opening reaction much higher than the organocatalysts and bifunctional catalysts tested in this chapter. We then tested a series of aminotriphenolate complexes as Lewis acids as catalysts for epoxide ring opening reactions by amines, which is the subject of the next chapter.

[12] Within this aspect, it is important to notice that NH groups in urea-based bifunctional catalyst **MoO(L^c)(U)** can form hydrogen bonds also with the urea carbonyl group, other than with Mo-oxo moiety. There is the possibility of a different dimer assembly, which leads to a different catalytic behaviour.

2.6 Experimental

General Remarks

All chemicals and dry solvents have been purchased from Sigma-Aldrich or Fluka and used as provided, without further purification. Triphenolamine ligands were synthesized as previously reported[8]. (Thio)urea organocatalysts have been synthesized as reported in literature.[5]

Flash cromatographies and filtrations have been performed with Macherey-Nagel siliga gel 60 (0.04-0.063 mm, 230-400 mesh). TLC analyses were performed using Macherey-Nagel POLYGRAM® SIL G/UV254 silica plates, detecting by UV/VIS and by treatment with PMA staining reagent made from a solution of phosphomolibdic acid ($H_3PMo_{12}O_{40}$) 10 g in 100 mL ethanol. The NMR spectra has been recorded on a Bruker AC200 (^{1}H: 200.13 MHz; ^{13}C: 50.0 MHz) or on an Bruker AV300 (^{1}H: 300.13 MHz; ^{13}C: 75.5.0 MHz) spectrometer. Chemical shift (δ) have been reported in parts per million (ppm) relative to the residual undeuterated solvent as a internal reference ($CDCl_3$: 7.26 ppm for ^{1}H-NMR and 77.16 for ^{13}C-NMR; ACN-d_3: 1.94 ppm for ^{1}H-NMR, 1.32 and 118.26 for ^{13}C-NMR). The following abbreviations have been used to descrive multeplicities: s = singlet, d = doublet, t = triplet, dd = double duplet, q = quartet, m = multiplet, br = broad. ^{13}C-NMR have been recorded with complete proton decoupling. ESI-MS spectra have been obtained on a LC/MS Agilent series 1100 spectrometer in both positive and negative modes using acetonitrile or acetonitrile/formic acid 0.1% as mobile phase, with ESI-ion trap mass detector. IR spectra have been recorded on a Nicolet 5700 FT-IR, with range 4000-400 cm^{-1} and resolution 4 cm^{-1}, using KBr pellets or NaCl plates.

For reactivity studies, deuterated solvents used for reactions have been treated with 3Å molecular sieves (beads, 8-12 mesh purchased from Fluka) previously activated at 300°C for 8 hours, and stored in dry-box during all times.

Synthesis of Mo(VI) aminotriphenolate complex MoO(L^c)Cl

The ligand precursor **L^{c}H$_3$** (500 mg, 0.75 mmol) was dissolved in toluene 40 mL, and milled MoO_2Cl_2 (148 mg, 0.75 mmol) was added. The stirred suspension was heated to reflux. After 18 hours, ^{1}H-NMR spectra ($CDCl_3$ as solvent) of the crude product and TLC (DEE/Hex, 3:7 or DCM) was used to see if the reaction was finished. The resulting intense blue solution was filtered through silica gel and evaporated to afford complex **MoO(L^c)Cl** as a blue solid in 85% yield (520 mg). The final product was characterized by ESI-MS and ^{1}H-NMR spectroscopy. ^{1}H-NMR (200 MHz, $CDCl_3$): δ 7.38 (1H, d, J = 7 Hz ArH), 7.32 (2H, d, J = 7 Hz ArH), 7.12 (1H, d, J = 7 Hz ArH), 6.98 (2H, d, J = 7 Hz ArH), 4.01 (2H, broad, $ArCH_2N$), 3.62 (4H, s, $ArCH_2N$), 1.56 (9H, s, $C(CH_3)_3$), 1.47 (18H, s, $C(CH_3)_3$), 1.30 (27H, s, $C(CH_3)_3$). ^{13}C NMR (50MHz, $CDCl_3$): δ 157.89,

147.05,146.27, 139.69, 139.14, 128.01, 127.29, 124.34,123.61, 123.41, 61.59 60.38, 35.37, 34.65, 31.52, 30.44, 30.31, 29.67. ESI-MS: m/z= 818.39 ($M+H^+$).

Synthesis of Mo(VI) aminotriphenolate complex MoO(L^c)(OMe)

Complex **MoO(L^c)Cl** (260 mg, 0.32 mmol) was dissolved in dry methanol and triethylamine (88.4 µL, 0.64 mmol) was added. The solution was stirred for 20 hours at reflux temperature under a N_2 inert atmosphere. ^{1}H-NMR confirmed that the reaction was complete, and a change in color was observed: the solution became purple. The solution was filtered though silica gel and evaporated to afforf complex 3-OMe as a purple solid in 80% yield (206 mg). The final product was characterized by ESI-MS and ^{1}H-NMR spectroscopy. ^{1}H-NMR (200 MHz, $CDCl_3$): δ 7.32 (1H, d, J = 7 Hz ArH), 7.26 (2H, d, J = 7 Hz ArH), 7.00 (1H, d, J = 7 Hz ArH), 6.95 (2H, d, J = 7 Hz ArH), 4.06 (3H, s, OCH_3), 3.87 (2H, s, $ArCH_2N$), 3.57 (4H, d, J = 10, $ArCH_2N$), 1.56 (9H, s, $C(CH_3)_3$), 1.43 (18H, s, $C(CH_3)_3$), 1.29 (27H, s, $C(CH_3)_3$). ^{13}C NMR (50 MHz, $CDCl_3$): δ 157.00, 145.21, 144.75, 140.26, 138.39, 128.66, 126.20, 125.34, 125.12, 124.40, 123.59, 123.43, 68.79, 61.24, 60.53, 35.69, 35.47, 34.79, 31.98, 30.63, 30.35. ESI-MS: m/z= 782.40 ($M+H^+$).

Synthesis of Mo(VI) aminotriphenolate complex MoO(L^c)(TU)

Complex **MoO(L^c)(OMe)** (73 mg, 0.09 mmol) was dissolved in toluene and the thiourea derivative **4b** was added (100 mg, 0.3 mmol). The solution was stirred for 5 hours at reflux temperature under a N_2 inert atmosphere, the course of reaction being monitored via TLC (Ethyl acetate/Hexane, 3:7). The solution was then evaporated and the crude product purified through a gradient flash silica gel chromatography (Ethyl acetate/Hexane from 9:1 to 6:4). The final product was characterized by ESI-MS and ^{1}H-NMR spectroscopy. ^{1}H-NMR (200 MHz, $CDCl_3$): δ 7.83 (2H, s, ArH), 7.71 (1H, s, ArH), 7.36 (1H, d, J = 7 Hz ArH), 7.29 (2H, d, J = 7 Hz ArH), 7.05 (1H, d, J = 7 Hz ArH), 7.01 (2H, d, J = 7 Hz ArH), 6.78 (1H, s, NH), 5.72 (1H, s, NH), 4.24 (2H, J = 10 Hz $CH_2\mathbf{CH_2}O$), 3.86 (2H, s, $ArCH_2N$), 3.55 (4H, s, $ArCH_2N$), 3.40 (2H, d, J = 10 Hz, $NH\mathbf{CH_2}CH_2$). ^{13}C NMR (50 MHz, $CDCl_3$): δ 154.60, 141.99, 131.56, 126.04, 120.62, 117.35, 114.00, 53.40, 48.35, 33.41, 25.47, 24.64. ESI-MS: m/z= 1111.46 (M+).

Synthesis of Mo(VI) aminotriphenolate complex MoO(L^c)(U)

Complex **MoO(L^c)(OMe)** (73 mg, 0.09 mmol) was dissolved in toluene and the thiourea derivative **4a** was added (95 mg, 0.3 mmol). The solution was stirred for 18 hours at reflux temperature under a N_2 inert atmosphere, the course of reaction being monitored via TLC (Ethyl acetate/Hexane, 3:7).

The solution was then evaporated and the crude product purified through a gradient flash silica gel chromatography (Ethyl acetate/Hexane from 9:1 to 6:4). The final product was characterized by ESI-MS and ^{1}H-NMR spectroscopy. ^{1}H-NMR (200 MHz, $CDCl_3$): δ 7.84 (2H, s, ArH), 7.50 (1H, s, ArH), 7.37 (1H, s, J = 7 Hz ArH), 7.34 (2H, s, J = 7 Hz ArH), 7.08 (1H, s, J = 7 Hz ArH), 7.03 (2H, s, J = 7 Hz ArH), 5.91 (1H, s, NH), 4.23 (2H, m, $CH_2\mathbf{CH_2}O$), 3.91 (1H, s, NH), 3.82 (2H, broad, $ArCH_2N$), 3.55 (4H, $ArCH_2N$), 3.40 (2H, $NH\mathbf{CH_2}CH_2$). ^{13}C NMR (50 MHz, $CDCl_3$) δ 154.60, 141.99, 131.56, 126.04, 120.62, 117.35, 114.00, 53.40, 48.35, 33.41, 25.47, 24.64. ESI-MS: m/z= 1111.46 (M+).

Procedure for the screening of thiourea-based catalysts (*Table 1*)

Five screw top V-vials were charged with 0.05 mol of catalysts, internal standard dichloroethane (0.12 mmol), 1,2-epoxyhexane (0.5 mmol), dibutylamine (0.5 mmol), and ACN to get a final volume of 1 mL (0.5M solutions in substrate, 10 mol% catalysts). One screw top V-vials was charged without catalyst to get the blank reaction. Uniformity in amounts of reagents and ratio substrate/catalysts was assured by charging vials using stock solutions. Reaction mixtures were allowed to stir at 85°C for 24 hours. Concentrations of product and starting material were determined by integration of CH-O proton signals: 2.91 ppm for 1,2-hepoxyhexane and 3.56 for aminoalcohol **9**, respect to the internal standard DCE (3.78 ppm).

Procedure for the screening of urea-based catalysts (*Figure 7*)

Three screw top V-vials were charged with 0.1 mol of catalysts, internal standard dichloroethane (0.25 mmol), 1,2-epoxyhexane (1 mmol), dibutylamine (1 mmol), and $CHCl_3$ to get a final volume of 1 mL (1M solutions in substrate, 10 mol% catalysts). One screw top V-vials was charged without catalyst to get the blank reaction. Uniformity in amounts of reagents and ratio substrate/catalysts was assured by charging vials using stock solutions. Reaction mixtures were allowed to stir at 60°C for 24 hours. Concentrations of product and starting material were determined by integration of CH-O proton signals: 2.91 ppm for 1,2-hepoxyhexane and 3.56 for aminoalcohol **8**, respect to the internal standard DCE (3.78 ppm).

Chapter 3

Aminotriphenolate complexes as catalysts for epoxide ring opening reactions

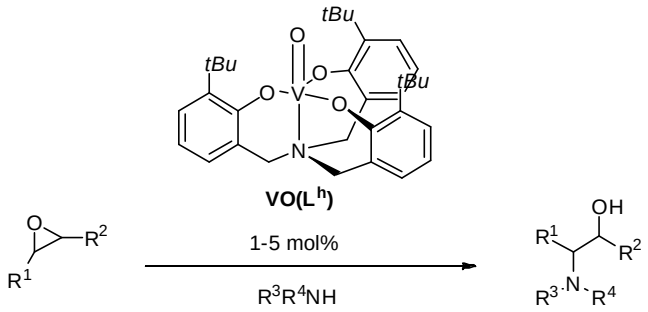

The catalytic activity of aminotriphenolate metalcomplexes in the epoxide ring opening reactions by nucleophiles has been investigated. Among all the catalysts investigated, vanadium(V) complex **VO(L^h)** has shown the best performance and therefore its reactivity has been explored in details. Effect of solvent, temperature and catalysts loading have been examined with 1,2-epoxyhexane as substrate and dibutylamine as nucleophile, to get complete conversion in 30 minutes with 1 mol% of catalyst. To test the versatility of **VO(L^h)** to different substrates and nucleophile, a wide amine and epoxide scope has been conducted, obtaining excellent conversions in most cases and satisfying selectivities.

3.1 Introduction

In *Chapter 1*, the possibility of using epoxides as versatile starting materials to obtain a wide range of value-added products has been discussed. Among all of these possible transformations, the synthesis of vicinal amino alcohols (also called 1,2-amino alcohols or β-amino alcohols) from epoxides (*Scheme 1*) plays a significant role, as this moiety is a common structural component in a vast group of naturally occurring and synthetic molecules.[1]

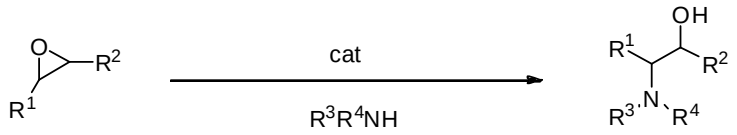

Scheme 1 Generic epoxide ring opening reaction with amines as nucleophiles. With poor nucleophilic amines, or when using unreactive epoxides, a catalyst is needed for this reaction.

Either the amino or the alcohol group can be further transformed (acylated, alkylated or be part of a cyclic structure), and most of the time the vicinal amino alcohol moiety, together with its stereochemistry, is essential for the biological activity of these molecules. Considering also that drug discovery is based largely on screening of possible pharmacophores, it is evident that the procedures for the synthesis of a pool of differently substituted vicinal amino alcohols are of particular interest.

Figure 1 shows some selected examples of relevant molecules containing vicinal amino alcohols. One of the most common class is hydroxy amino acids, e.g. the dipeptide bestatin, which contains a *syn*-α-hydroxy-β-amino acid. *Bestatin* is an aminopeptidase inhibitor that exhibits immunomodulatory activity,[2,3] and is used clinically as an adjuvant in cancer chemotherapy.[4] Lipids and lipid-like molecules make up a large class of naturally occurring molecules containing the vicinal amino alcohol moiety. Possibly, the most synthesized molecule of all amino alcohols is *sphingosine*.[5] Sphingosine is a compound which was originally considered to be solely a structural biomolecule, but has more recently been found to be important in cell signaling. Structurally sphingosine and analogues are 2-amino-1,3-diols. Frequently the amino group is acylated and the 1-

[1]Bergmeier, S. C. *Tetrahedron* **2000** (17), 2561–2576.
[2]Umezawa, H.; Aoyagi, T.; Suda, H.; Hamada, M.; Takeuchi, T. *J. Antibiot*. **1976** (29), 97.
[3]Nakamura, H.; Suda, H.; Takita, T.; Auyagi, T.; Umezawa, H.;Iitaka, Y. *J. Antibiot*. **1976**, (29), 102.
[4]Ino, K.; Goto, S.; Nomura, S.; Isobe, K.-I.; Nawa, A.; Okamoto, T.; Tomoda, Y. *Anticancer Res*. **1995** (15), 2081.
[5]Koskinen, P. M.; Koskinen, A. M. P. *Synthesis* **1998**, 1075.

hydroxyl is substituted.[6] *Swainsonine* is a cyclic amino alcohol in which the amino group is contained within a ring. It can be isolated from different natural sources or synthesized, and it is used for its effect in the inhibition of the glycoprotein processing.[7,8]

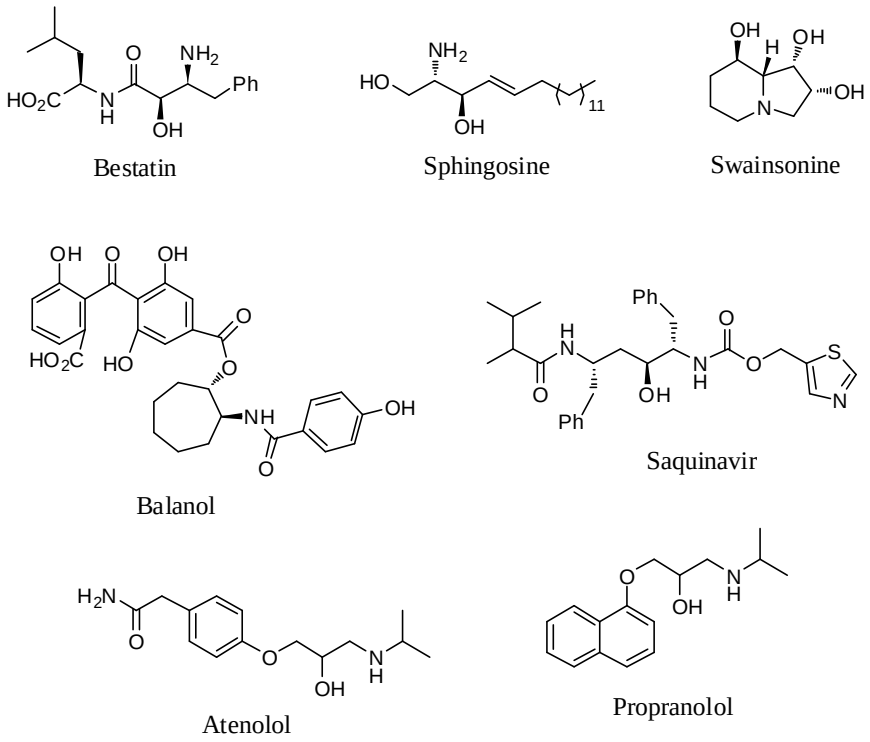

Figure 1 Natural and synthetic compounds of interest containing vicinal amino alcohols.

Another molecule that has attracts considerable synthetic interest, due to its ability to inhibit protein kinase C, is *balanol*. It is a structurally interesting azepino amino alcohols in which both the amino and the hydroxyl groups are acylated.[9]

Considering totally synthetic molecules, the hydroxyethylene isostere peptidomimetics are maybe the best known drugs containing vicinal amino alcohols.[10] This group of peptide analogues is typifed by the HIV protease inhibitor *saquinavir*,[11] and they are used as anti-HIV agents. Also β-blocking compounds, one of the most employed class of antihypertensive drugs, are vicinal amino alcohols. Atenolol and propranolol are two examples shown in *Figure 1*.

[6]Hannun, Y. A.; Linardic, C. M. *Biochem. Biophys.Acta* **1993**, 1154.
[7]Colegate, S. M.; Dorling, P. R.; Huxtable, C. R. *Aust. J. Chem.* **1979** (32), 2257.
[8]Molyneux, R. J.; James, L. F. Science **1982**, 216.
[9](a) Kulanthaivel, P.; Hallock, Y. F.; Boros, C.; Hamilton, S. M.; Janzen, W. P.; Ballas, L. M.; Loomis, C. R.; Jiang, J. B. Katz, B.; Steiner, J. R.; Clardy, J. *J. Am. Chem. Soc*. **1993** (115), 6452. (b) Hu, H.; Hollinshead, S. P.; Hall, S. E.; Kalter, K.; Ballas, L. M. *Bioorg. Med. Chem. Lett*. **1996** (6), 973.
[10]Gante, J. *Angew. Chem., Int. Ed. Engl.***1994** (33), 1699.
[11]Ohta, Y.; Shinkai, I. *Bioorg.Med. Chem*. **1997** (5), 465.

Throughout the years, researchers have introduced a variety of materials that can enhance the electrophilic character of epoxides through metallic coordination or H-bonding. In fact, few amines are nucleophilic enough to undergo this reaction, even considering the high reactivity of epoxides, without using elevated temperatures, which can easily lead to degradation of products.[12]

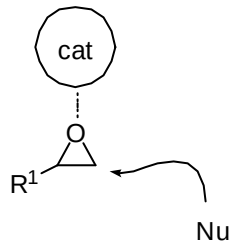

Scheme 2 Schematic representation of the catalytic activation of epoxides towards nucleophilic attack. An electron-poor group of the catalyst coordinates to the oxygen atom of the epoxide enhancing its electrophilic character.

The most employed catalysts for epoxide ring opening by amines are Lewis acids. Many examples can be found in literature, e.g. $ZnCl_2$,[13] ScOTf,[14] $MgBr_2{\cdot}OEt_2$,[15] bismuth salts,[16] $CoCl_2$,[17] $CuBF_4$,[18] DIPAT,[19] $Ti(OiPr)_4$,[20] $TaCl_5$,[21] $ZrCl_4$.[22]

Also organocatalytic approaches have been gaining a significant importance during the last years, in particular systems with H-bonding activation mode.[23] Substituted thioureas (**TU**, **9**),[24] polyphenols (**10**),[25] proline derivatives (**11**)[26] and β-amino alcohols (**12**)[27] have been used as catalysts for these reactions (*Figure 2*).

[12]Saddique, F. A.; Zahoor, A. F.; Faiz, S.; Naqvi, S. A. R.; Usman, M.; Ahmad, M. *Synth. Commun.* **2016** (*46)*, 831.
[13]Pachon, L. D.; Gamez, P.; VanBrussel, J. J.; Reedijk, J. *Tetrahedron Lett.* **2003** (44), 6025.
[14]Placzek, A. T.; Donelson, J. L.; Trivedi, R.; Gibbs, R. A.; De, S. K. *Tetrahedron Lett*. **2005** (46), 9029.
[15]Mojtahedi, M. M.; Abaee, M. S.; Hamidi, V. *Catal. Commun*. **2007** (8), 1671.
[16]Khosropour, A. R.; Khodaei, M. M.; Ghozati, K. *Tetrahedron Lett.* **2004** (33), 3525.
[17]Sundararajan, G.; Vijayakrishna, K.; Varghese, B. *Tetrahedron Lett.* **2004** (45), 8253.
[18]Kamal, A.; Ramu, R. R.; Azhar, M. A.; Khanna, G. B. R. *Tetrahedron Lett.* **2005** (46), 2675.
[19]Rampalli, S.; Chaudhari, S. S.; Akamanchi, K. G. *Synthesis* **2000**, 78.
[20]Sagawa, S.; Abe, H.; Hase, Y.; Inaba, T. *J. Org. Chem*. **1999** (64), 4962.
[21]Chandrasekhar, S.; Ramachandar, T.; Prakash, S. J. *Synthesis* **2000**, 1817.
[22]Chakraborti, A. K.; Kondaskar, A. *Tetrahedron Lett.* **2003** (44), 8315.
[23]Chawla, R. RSC Adv. **2013** (29), 11385.
[24] (a) Kleiner, C. M.; Schreiner, P. R. *Chem. Commun.* **2006** (41), 4315; (b) Thomas, C.; Brut, S.; Bibal, B. *Tetrahedron* **2014** (*70*), 1646; (c) Fleming, E. M.; Quigley, C.; Rozas, I.; Connon, S. J. *J. Org. Chem.* **2008** (*7*3), 948; (e) Chimni, S. S.; Bala, N.; Dixit, V. a.; Bharatam, P. V. *Tetrahedron* **2010**, (*66*), 3042.
[25]Braddock, D. C.; MacGilp, I. D.; Perry, B. G. *Adv. Synth.Catal.* **2004** (*346*), 1117.
[26]Wei, S.; Stingl, K. a.; Weiß, K. M.; Tsogoeva, S. B. *Synlett* **2010** (5), 707.
[27](a) Kumar, P.; Dubey, A.; Harbindu, A.*Org. Biomol. Chem.* **2012** (10), 6987; (b) Malik, G.; Ferry, A.; Guinchard, X.; Crich, D.*Synthesis* **2013** (45), 65.

Additionally to these catalytic systems, some non-conventional methods to increase the yields of these transformations have been reported, namely the use of silica under high pressure,[28] clay,[29] ionic liquids,[30] supercritical carbon dioxide ($scCO_2$),[31] microwave irradiation[32] and water as a solvent.[33]

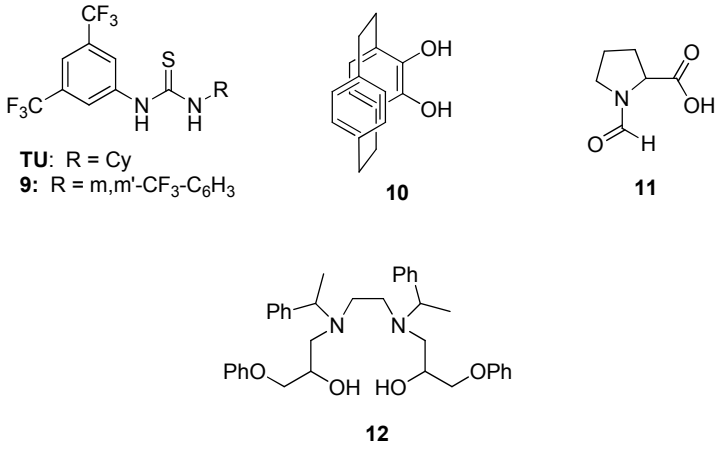

Figure 2 Organocatalysts used for epoxide ring openings by amines. For clarity, only the parent compound for each group is shown.

Concerning the stereoselective ring opening of epoxides, Yb-,[34] Ti-,[35] Pr-[36] and Sm-based[37] chiral BINOL catalysts have been reported in literature, together with scandium bipyridine complexes.[38]

Although significant advances have been made in this area, low regioselectivity, long reaction time, use of elevated temperature, high catalyst loading, toxic solvents and low substrate compatibility are still problems of significant relevance fort these transformations.[39] Moreover, the use of Lewis acidic catalysts, usually the most active compounds, is often limited by the irreversible coordination of amines to the catalyst, decreasing dramatically the yield of reactions and restricting the scope of

[28]Kotsuki, H.; Hayashida, K.; Shimanouchi, T.; Nishizawa, H. *J. Org. Chem.* **1996** (61), 984.
[29]Yadav, J. S.; Reddy, B. V.; Basak, A. K.; Narasaiah, A. V. *Tetrahedron Lett.* **2003** (44), 1047.
[30]Mojtahedi, M. M.; Saidi, M. R.; Bolrtchian, M. *J. Chem. Res.* **1999**, 128.
[31]Surendra, K.; Krishnaveni, N. S.; Rao, K. R. *Synlett* **2005**, 506.
[32]Mojtahedi, M. M.; Saidi, M. R.; Bolourtchian, M. *J. Chem. Res., Synop.* **1999**, 128.
[33]Azizi, N.; Saidi, M. R. *Org. Lett.* **2005** (17), 3649.
[34]Hou, X. L.; Wu, J.; Dai, L. X.; Xia, L. J.; Tang, M. H. *Tetrahedron: Asymmetry* **1998** (*9)*, 1747.
[35](a) Sagawa, S.; Abe, H.; Hase, Y.; Inaba, T. *J. Org. Chem.* **1999** (64), 4962; (b) Kureshy, R. I.; Singh, S.; Khan, N. H.; Abdi, S. H. R.; Suresh, E.; Jasra, R. V. *Eur. J. Org. Chem.* **2006**, 1303.
[36]Sekine, A.; Ohshima, T.; Shibasaki, M. *Tetrahedron* **2002** (58), 75.
[37]Carree, F.; Gil, R.; Collin, J. *Org. Lett.* **2005** (*7)*, 1023.
[38]Schneider, C.; Sreekanth, A. R.; Mai, E. *Angew. Chem. Int. Ed.* **2004** (43), 5691; *Angew. Chem.* **2004** (116), 5809.
[39]Bhanushali, M. J.; Nandurkar, N. S.; Bhor, M. D.; Bhanage, B. M. *Tetrahedron Lett.* **2008**, (49), 3672.

nucleophiles.**Errore. Il segnalibro non è definito.** This is particularly true for aliphatic amines; in many cases, the reactions are carried out with aromatic amines only.[40]

Aware of the strong Lewis acidity of some aminotriphenolate complexes, and based on high catalytic activity of complex **MoO(L^c)Cl** (R^1, R^2 = *t*Bu) found out as noted in *Chapter 2,* we decided to test a series of vanadium, molybdenum and aluminum aminotriphenolate complexes (*Figure 3*) in epoxide ring opening reactions by amines. In complexes **VO(L^d)** (R^1, R^2 = Cl), **VO(L^o)** (R^1= *t*Bu, R^2 = NO_2), **MoO(L^d)Cl** and **Al(L^o)(THF)** the aminotriphenolate ligand is functionalized with electron-withdrawing groups, which should increasing the Lewis acidity of catalysts, as discussed in *Chapter 1*. Reactivity of aminotriphenolate complexes reported in *Figure 3* has been compared to **TU**, among the most active H-bond donor organocatalyst employed for this reaction.[24]

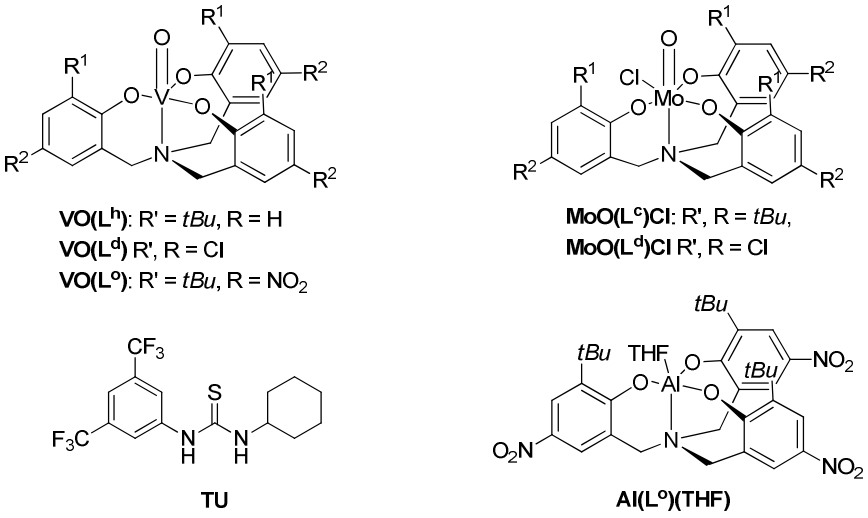

Figure 3 Aminotriphenolate complexes screened in epoxide ring opening reactions.

As standard conditions, we used 1,2-epoxyhexane **6** as substrate and dibutylamine**7** as a nuclephile (1:1 ratio) at 1M concentration in $CDCl_3$, with 5% of catalyst at 60°C (*Scheme 3*).

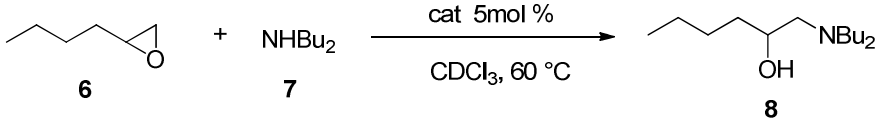

Scheme 3 Reaction conditions used for catalysts screening in epoxide ring opening reaction of 1,2-epoxyhexane **6** by dibutylamine **7**.

[40]Placzek, A. T.; Donelson, J. L.; Trivedi, R.; Gibbs, R. a.; De, S. K. *Tetrahedron Lett.* **2005** (46), 9029.

Reactivities of catalysts **VO(L^{d})** (R^1, R^2 = Cl), **VO(L^{h})** (R^1= *t*Bu, R^2 = H), **VO(L^{o})** (R^1= *t*Bu, R^2 = NO_2), **MoO(L^{d})Cl** (R^1, R^2 = Cl), **MoO(L^{c})Cl** (R^1, R^2 = *t*Bu) and **Al(L^{o})(THF)** are compared in *Figure 4*, in which the yield in amino alcohol **8**, calculated via ^{1}H-NMR analysis, is plotted versus time. The regioselectivity of the reaction showed to proceed as expected, with the nucleophile attacking the less hindered carbon atom of the epoxide. No traces of the other regioisomer have been detected. The best catalyst had shown to be complex **VO(L^{h})** (R^1= *t*Bu, R^2 = H), with 85% yield after 1 hour, followed by complex **MoO(L^{c})Cl** (R^1, R^2 = *t*Bu), with 69% yield after 1 hour. At this time in the blank reaction, carried out as a control, only traces of product are detectable.

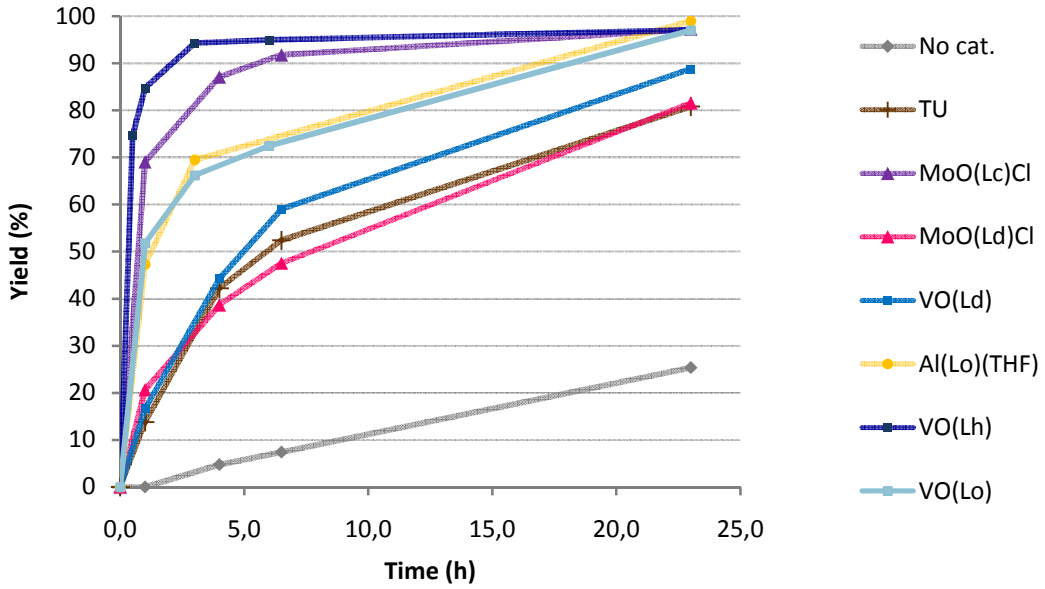

Figure 4 Screening of catalysts **VO(L^{d})** (R^1, R^2 = Cl), **VO(L^{h})** (R^1 = *t*Bu, R^2 = H), **VO(L^{o})** (R^1 = *t*Bu, R^2 = NO_2), **MoO(L^{d})Cl** (R^1, R^2 = Cl), **MoO(L^{c})Cl** (R^1, R^2 = *t*Bu) and **Al(L^{o})(THF)** in epoxide ring opening reaction of epoxide. Yields in amino alcohol **8** is plotted versus time.

Results show that complexes **VO(L^{d})** (R^1, R^2 = Cl), **Al(L^{o})(THF)** (R^1 = *t*Bu, R^2 = NO_2), **MoO(L^{d})Cl** (R^1, R^2 = Cl), **VO(L^{o})** (R^1 = *t*Bu, R^2 = NO_2), bearing ligands functionalized with electron-withdrawing groups, gave lower conversions respect to complexes **MoO(L^{c})Cl** (R^1, R^2 = *t*Bu) and **VO(L^{h})** (R^1= *t*Bu, R^2 = H). This can be explained arguing that not only electronic factors are to play a role in the effect that aminotriphenolate ligands have on catalysts' reactivity, but also the stability of complexes is of major importance. As discussed in *Chapter 1*, bulky substituents in *ortho* position respect to the phenol increase the stability of complexes preventing aggregation. Moreover, as discussed before, the coordination of the amine to the complex, rather than the epoxide, can become the main event in presence of a stronger Lewis acid, thus decreasing the catalytic performance. Notably, reactivities of complexes **Al(L^{o})(THF)** (R^1 = *t*Bu, R^2 = NO_2),

VO(L^{o}) (R^1 = *t*Bu, R^2 = NO_2), **VO(L^{h})** (R^1 = *t*Bu, R^2 = H), **MoO(L^{c})Cl** (R^1, R^2 = *t*Bu) are significantly higher than organocatalyst **TU**, which gave 14% yield after 1 hour. On the base of these results, we went on studying in more details the reactivity of vanadium(V) aminotriphenolate complex **VO(L^{h})** (R^1= *t*Bu, R^2 = H) and molybdenum(VI)aminotriphenolate complex **MoO(L^{c})Cl** (R^1, R^2 = *t*Bu), as it will be discussed in the next paragraph.

3.2 V(V) amino triphenolate complex VO(L^{h}): catalytic activity

Vanadium aminotriphenolate complex **VO(L^{h})** (R^1= *t*Bu, R^2 = H) has been tested in the epoxide ring opening reaction of 1,2-hepoxyhexane by dibutulyamine. First, a screening of different solvents and temperatures was conducted to find the best reaction conditions. Then, the yield of the reaction was evaluated with different catalyst loadings. An amine and epoxide scope have been performed in order to investigate the versatility of this catalytic system. Finally, the solution behavior of **VO(L^{h})** under turnover conditions has been explored via ^{51}V-NMR spectroscopy.

Effect of solvent. A screening of five solvents with different polarity, namely $CDCl_3$, ACN-d_3, Tol-d_8, D_2O and CD_3OD, has been performed to find the best reaction conditions for the epoxide ring opening with amines catalyzed by **VO(L^{h})** (2.5 mol% at 60°C). Deutereted solvents have been used in order to follow the reaction via ^{1}H-NMR analysis. Also, a reaction has been run under neat conditions.

Table 1 Solvent screening for the ring opening of **6** by **7** catalyzed by **VO(L^{h})**.

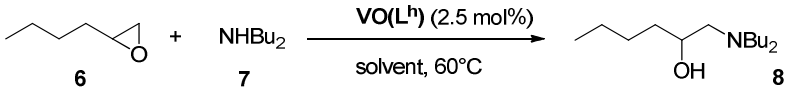

6 7 8

Entry	Solvent	Yield (%) at 30 min[a]	Yield (%) at 3.5 hr[a]
1	ACN-d_3	85.5	97.1
2	$CDCl_3$	58.8	89.2
3	CD_3OD	47.4	88.5
4	Tol-d_8	66.2	90.1
5	D_2O[b]	29.3	51.1
6	-[c]	>99	>99

Reaction conditions: [**6**] = [**7**] = 0.5 mmol, 2.5 mol% cat **VO(L^{h})**, solvent 0.5 mL, 60°C. [a]Yields calculated via ^{1}H-NMR analysis with DCE as internal standard.[b] Catalyst **VO(L^{h})** is not soluble in water. In this case the reaction has been carried out in two phases. Selectivity is in all cases >99%.[c][**6**] = [**7**] = 2 mmol, 2.5 mol% cat **VO(L^{h})**, 60°C

After 24 hours, all reactions reached yields >95%. As shown in *Table 1*, ACN-d_3 has shown to be the best solvent, with 85.5% yield in amino alcohol **8** after 30 minutes and 97.1% yield after 3.5 hours. However, the conversion of 1,2-epoxyhexane under neat conditions ([**5**] = [**6**] = 2 mmol) was completed after only 30 minutes. On the basis of this result, we decided to continue the study using neat conditions. In fact, all the amines that will be used are liquid, and can easily dissolve also solid epoxides.

Catalyst loading. Five epoxide ring opening reactions have been carried out with different substrate/catalyst ratios. Results reported in *Table 2* show the effect of decreasing the amount of catalyst **VO(L^h)** from 2.5 mol% to 1, 0.5, 0.1 and 0.01 mol%. A blank reaction has been conducted at the same time. Decreasing the catalyst loading from 2.5 to 1 mol % lead to no detectable changes in product yield. With 0.5 mol % catalyst, a slightly lower yield is observed only at early times, with a complete conversion after 2 hours. Notably, 88% yield in 1,2-aminoalcohol **8** can be reached with 0.1 mol% of catalyst after 2 hours. Very few catalytic system reported for epoxide ring opening by amines can be lower to such an amount maintaining a remarkable epoxide conversion.[41] In particular, Lewis acidic catalysts are usually employed at 1 - 10mol% concentrations.

Table 2 Ring opening of 1,2-epoxyhexane **6** by dibutylamine**7** catalyzed by **VO(L^h)**, effect of catalyst loading.

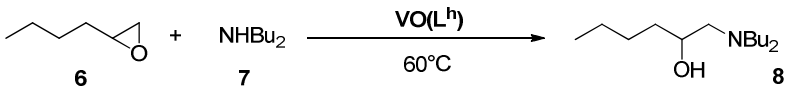

Entry	[Cat] mol %	Yield (%) at 30 min[a]	Yield (%) at 2 hours[a]	Yield (%) at 24 hours[a]
1	2.5	>99		
2	1	>99		
3	0.5	80	>99	
4	0.1	63	88	98
5	0.01	22	32	41
6	0	0	0	5

Reaction conditions: [**6**] = [**7**] = 2 mmol, 60°C. Yields calculated via ^{1}H-NMR analysis with DCE as internal standard.

Decreasing the catalyst amount to 0.01 mol%, significantly lower reaction yields were obtained: after 24 hours, only 41% of 1,2-epoxyhexane **6** was converted to 1,2-aminoalcohol **8**. However,

[41]Schneider, C.*Synthesis,* **2006**, 3919

even at such a low amount, the effect of catalyst is still quite evident, considering that the blank reaction gave only 5% yield after 24 hours.

Effect of temperature. Then, the same reaction has been performed at different temperatures, namely 25, 60 and 90°C. To better reveal the differences in reactivity, a lower amount of catalyst has to be used. For this reason, 0.5 mol% of vanadium(V) aminotriphenolate complex **VO(L^h)** has been employed. *Figure 5* shows the yields versus time profiles in 6 hours time.

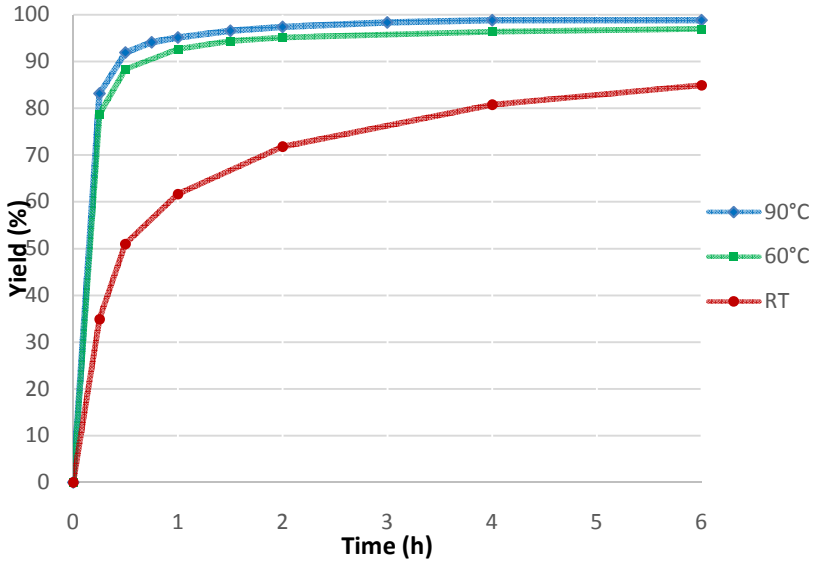

Figure 5 Ring opning of **6** by **7**, catalyzed by **VO(L^h)**; effect of temperature. Reaction conditions: [**6**] = [**7**] = 2 mmol, 0.5 mol% cat **VO(L^h)**. Yields calculated via ^{1}H-NMR analysis with DCE as internal standard.

Yields of reactions run at 60 and 90°C are significantly higher than the reaction at room temperature (25°C), giving respectively 94 and 95% yield after 30 minutes, compared to 33% yield at 25°C. On the contrary, no relevant differences have been revealed between reactions run at 60 and 90°C, as shown in *Figure 5*. We therefore decided to continue using 60°C as reaction temperature.

Amine scope. Using optimized reaction conditions (neat, 60°C, 1mol% of catalyst), the catalytic activity of vanadium(V)aminotriphenolate complex was explored using different amines. *Table 3* shows the ring opening of 1,2-epoxyhexane (taken as a reference substrate) by various primary, secondary (cyclic and non-cyclic) and aromatic amines. Reactions have been followed by ^{1}H-NMR, measuring a sample after 1, 2, 4 and 6 hours. After 6 hours, all reactions have reached from 95% to

complete conversion of the substrate, demonstrating an excellent generality for this catalytic system concerning the nucleophile scope. Pyrrolidine **13a**, morpholine **13b** and piperidine **13c**, highly reactive secondary cyclic amines, together with dibutylamine **13d**, gave total conversion after 1 hour, with complete selectivity towards product **14a-d**. Secondary aliphatic acyclic amines (**13e-f**), with bulky substituents, take longer reaction times, giving >99 and 95% conversion after 6 hours. Also in these cases, selectivity is complete towards the expected regioisomers **14e-f**.

Table 31,2-epoxyhexane **6** ring opening by amines **13a-m**, to give aminoalcohol **14a-m**, catalyzed by **VO(L^h).**

Entry	Amine	Product	Conversion (%)	Selectivity (%)	Time (h)
1	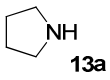 **13a**	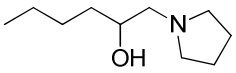 **14a**	>99	>99	1
2	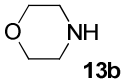 **13b**	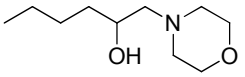 **14b**	>99	>99	1
3	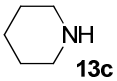 **13c**	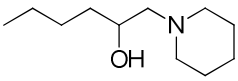 **14c**	>99	>99	1
4	Bu_2NH**13d**	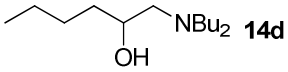 **14d**	>99	>99	1
5	iPr_2NH**13e**	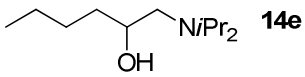 **14e**	95	>99	6
6	Bn_2NH**13f**	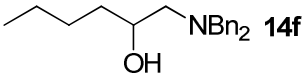 **14f**	>99	>99	6
7	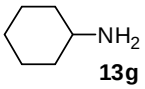 **13g**	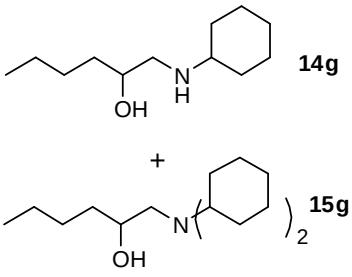 **14g** + **15g**	>99	58 42	2

		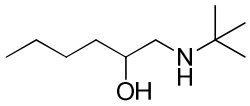 **14h**		65	
8	*t*BuNH$_2$ **13h**	+	>99		2
		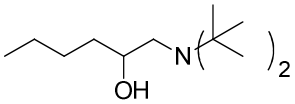 **15h**		45	
9	*n*BuNH$_2$**13i**	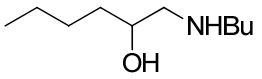 **14i**	96	>99	6
		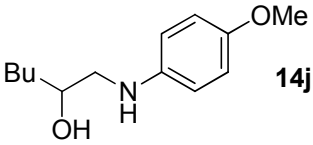 **14j**		60	
10	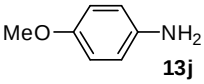 **13j**	+	>99		1
		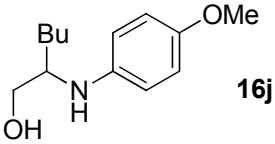 **16j**		40	
		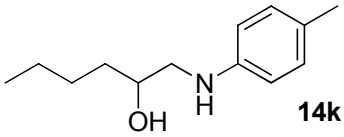 **14k**		59	
11	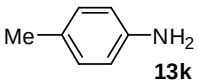 **13k**	+	>99		1
		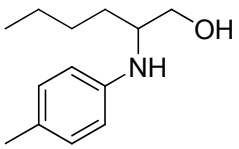 **16k**		41	
		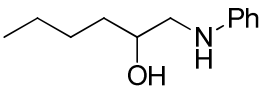 **14l**		61	
12	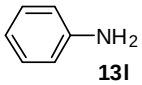 **13l**	+	>99		6
		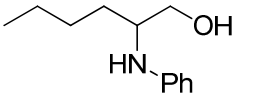 **16l**		39	
13	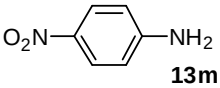 **13m**	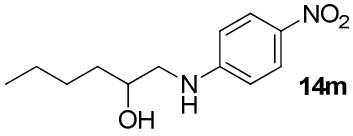 **14m**	5	-	6

Reaction conditions: [**6**] = [**13a-m**] = 2 mmol, [**VO(L^h)]** = 1mol%, 60°C. Conversions and selectivities calculated via ^{1}H-NMR analysis with DCE as internal standard.

When using primary amines (**13g-i**), the 1,2-aminoalchols produced (**14g-i**) can further react with another equivalent of epoxide, giving a bis-adduct as shown in *Scheme 4*.

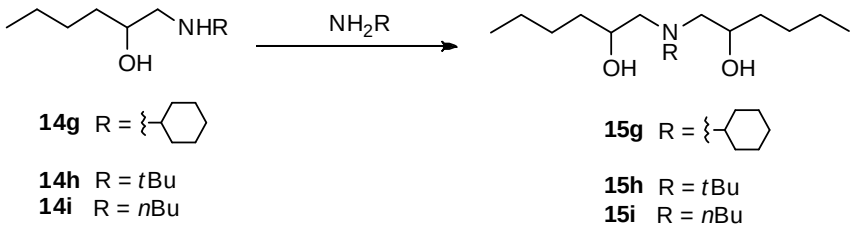

Scheme 4 By-products **15g-i** that can be formed when using primary amines **13g-i** as nucleophiles for the ring opening of 1,2-epoxyhexane. 1,2-aminoalcohols **14g-i** formed during the first ring opening can further react with a second equivalent of epoxide to give bis-adducts.

This was the case of cyclohexylamine **13g** and *tert*-butylamine **13h**, which reacted with 1,2-epoxthexane to give a mixture of mono- and bis-adduct in ratio **14g** : **15g** = 58: 42 for cyclohexylamine, and **14h** : **15h** = 65 : 35 for *tert*-butylamine.[42] *n*-Butylamine gave only the desired product **14i**.

For all the secondary and primary aliphatic amines **13a-i**, only one regioisomer (**14a-i)** is formed from the ring opening of 1,2-epoxyhexane. This is the product of the amine nucleophilic attack to the least hindered carbon atoms of the epoxide cycle (path **a**, *Scheme 5*).

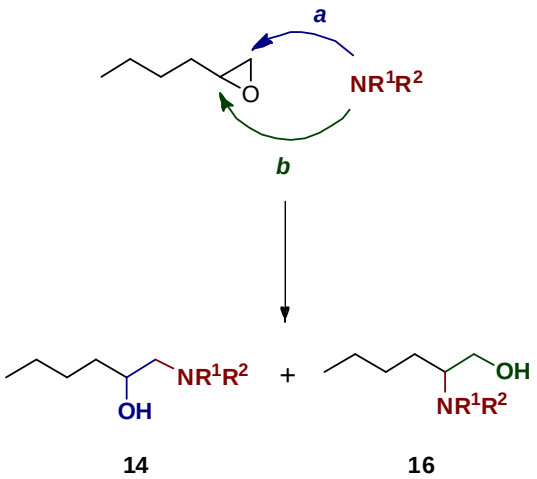

Scheme 5 Epoxide ring opening of 1,2-epoxyhexane by a generic amine NR^1R^2. Nucleophilic attack can occur to the least hindered carbon atom of epoxidic ring (pathway **a**) or to the most hindered carbon atom (pathway **b**), giving product **14** and **16**, respectively.

[42] By-products formed in ring opening of 1,2-epoxyhexane have been identified by ^{1}H-NMR spectroscopy and GC-MS analysis. In particular, bis-adducts **15g** and **15h** show twice the molecular weight of expected products **14g-h**, being thus easily detectable using GC-MS. Discrimination between two regioisomer with the same molecular weight is possible by GC-MS thanks the presence of characteristic ion peaks: regioisomers product of amine attack to the most hindered carbon atom of the epoxide cycle present the typical ion peak [M^+ - 31] resulted from the loss of CH_2OH.

In general, amines can attack the epoxidic ring at the least hindered carbon atom giving 1,2-aminoalcohol **14**, or to the most hindered carbon atom following path **b** (*Scheme 5*), to give product **16**. The ratio between these two regioisomers depends on electronic and steric factors, being thus strongly influenced by the epoxide and amine employed. In the case of 1,2-epoxyhexane, an aliphatic epoxide, the nucleophilic character of the amine has to be taken in account to explain which regioisomer is produced mostly. With primary and secondary aliphatic amines, steric factors give the major contribution, producing only regioisomer **14**, with complete selectivity. On the contrary, less nucleophilic aromatic amines **13j-l** gave a mixture of **14** and **16** (ratios: **14j** : **16j** = 60 : 40 for *p*-anisylamine **13j**; **14k** : **16k** = 59 : 41 for *p*-toluidine **13k**; **14l** : **16l** = 61 : 39 for aniline**13l**). This was already observed in literature and explained arguing that, when using poorly nucleophilic amines with less-hindered substituents (*e.g.* aromatic amines), electronic factors become equally important.[43] For this reason, the product of the nucleophilic attack to the most hindered epoxidic carbon atom (that is, the most stable carbocation) is present as well. In conclusion, excellent yields in the desired 1,2-aminoalcohol **14** was obtained when using secondary amines **13a-f**, with 95% to complete conversion of 1,2-epoxyhexane after 6 hours or less. In these cases, a complete regioselectivity is observed. With primary amines **13g-m** (aliphatic and aromatic) the reaction loses its regioselectivity, thus maintaining excellent conversions of the starting material.

Epoxide scope. After a wide amine scope, we wanted to test our catalytic method also with different substrates. Dibenzylamine **13f** was chosen as reference amine (it does not give problems of regioselectivity and it is not very reactive), and reacted with a series of terminal and internal epoxides **17a-g** (*Table 4*). Satisfying results were obtain for epoxides **17a-e**, which were completely converted in 1-24 hours under optimized reaction conditions (neat, 60°C, 1 mol% of catalyst).
Terminal epoxides **17a-b** were totally converted to 1,2-aminoalcohols **18a-b** after 1 hour, with complete regioselectivity. Ring opening of styrene oxide, which was complete in 2 hours, led to the formation of a mixture of regioisomers **18c** and **19c** with a 51 : 49 ratio (*Scheme 6*).

[43] Shivani; Pujala, B.; Chakraborti, A. K. *J. Org. Chem.***2007** (72), 3713.

Table 4 Epoxides ring opening by dibutylamine **13f**, to give aminoalcohol **18a-g**, catalyzed by **VO(L^h).**

Entry	Epoxide	Product	Selectivity (%)	Conversion (%)	Time (h)
1	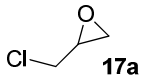 **17a**	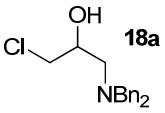 **18a**	>99	>99	1
2	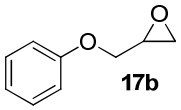 **17b**	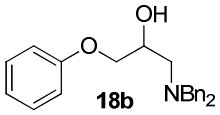 **18b**	>99	>99	1
3	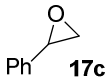 **17c**	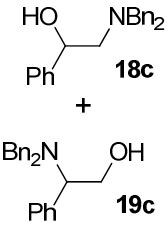 **18c** + **19c**	51 49	>99	2
4	 **17d**	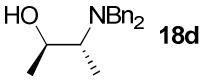 **18d**	>99	97 (>99)	8 (24)
5	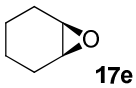 **17e**	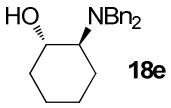 **18e**	>99	97 (>99)	8 (24)
6	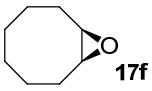 **17f**	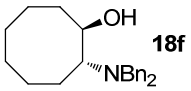 **18f**	traces	-	24
7	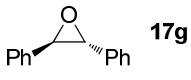 **17g**	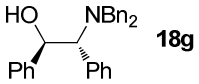 **18g**	traces	-	24

Reaction conditions: [**epoxide**] = [**13f**] = 2 mmol, [**VO(L^h)] =** 1mol%, 60°C. Conversions and selectivities calculated via ^{1}H-NMR analysis with DCE as internal standard.

In this case, electronic and steric factors have similar importance for the regioselectivity of the epoxide ring opening reaction, as benzylic carbocation is highly stabilized, resulting in about 1 : 1 formation of regioisomer **18c** and **19c**.

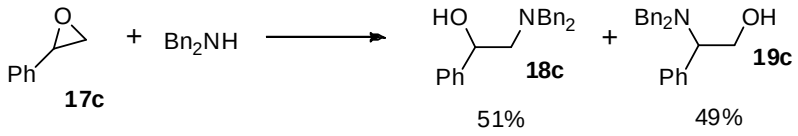

Scheme 6 Aminolysis of styrene oxide **17c** by dibenzylamine which afforded regioisomers **18c** and **19c** in 51 : 49 ratio.

Also *cis*-2,3-epoxybutane **17d** and cyclohexene oxide **17e** gave excellent conversions and selectivities, forming products **18d-e** almost quantitatively in 8 hours, with the predicted stereochemistry.[44] Given the good results obtained with internal epoxides **17d-e**, we tested vanadium(V)aminotriphenolate complex **VO(L^h)** with more challenging cyclooctene oxide **17f** and *trans*-stilbene oxide **17g**, but no conversion were observed after 24 hours, due to the strong unreactive character of **17f** and the high steric hindrance of **17g**.

The substrate and amine scope clearly indicated the wide applicability of the tested catalytic system to different amines and epoxides, together with the effectiveness of the optimized reaction conditions.

Catalyst stability. To have a preliminary idea of the solution behavior of complex **VO(L^h)** under turnover conditions, six ^{51}V-NMR spectra have been recorded at different times during ring opening reaction of 1,2-epoxyhexane **6** with dibutylamine **7** (*Figure 7*). Spectrum **1** shows the ^{51}V-NMR signal of complex **VO(L^h)** at time 0, when only the catalyst and the epoxide are present in solution (ratio 1/100). Then, after the addition of the nucleophile, spectra **2 - 6** have been recorded at increasing times and thus increasing yields of amino alcohol **8**, within two hours. Two main considerations can be reported: a small shift of the signal at -389ppm (of about 2 ppm) and the appearance of another species at -576 ppm, which disappeared when the reaction is finished. This experiment proves that the complex is stable under turnover conditions. Indeed, a part from the new species forming and disappearing during the reaction, the ^{51}V-NMR signal of complex **VO(L^h)** has not changed.

[44] Cyclohexene oxide: Miyano, S.; Lu, L. D.; Viti, S. M.; Sharpless, K. B. *J. Org. Chem.***1985** (5), 4350; cis-2,3-epoxybutane: Bernad, P. L.; Solar, V. *J. Org. Chem.* **2006** (4), 6420.

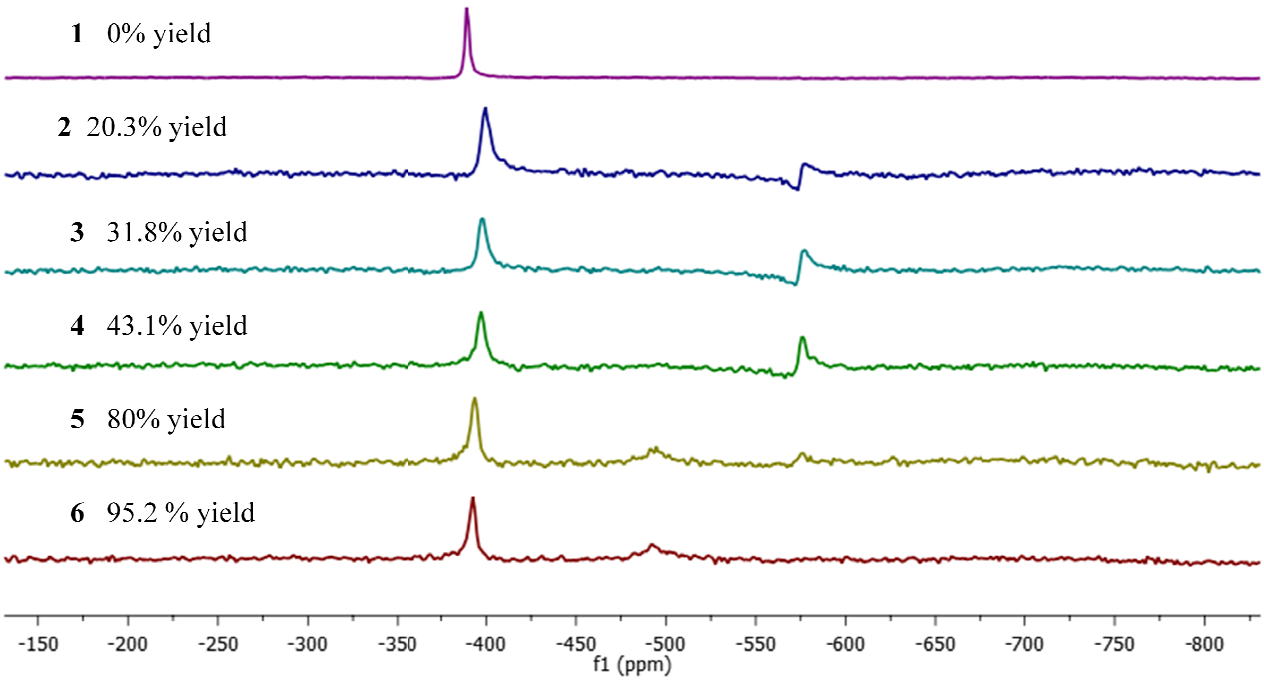

Figure 6 ^{51}V-NMR spectra of samples taken at increasing times - thus increasing yields - of epoxide ring opening reaction of 1,2-epoxyhexane **6** with dibutylamine **7** under neat conditions. Spectrum **1** displays the ^{51}V-NMR signal of complex **VO(L^{h})** at time 0, when only the catalyst and 1,2-epoxyhexane are present in solution. Spectra *2-6* are recorded while following the reaction during time. For each spectrum, the yield in aminoalcohol **8** is reported. These spectra have been recorded in $CDCl_3$.

3.3 Mo(VI) amino triphenolate complex MoO(L^{c})Cl: tandem reactions

As discussed before in this chapter, also Mo(VI) aminotriphenolate complex **MoO(L^{c})Cl** (R^1, R^2 = *t*Bu) has demonstrated a good catalytic activity towards epoxide ring opening reaction by amines (see *Figure 4*), with 92 % yield in amino alcohol **7** after 6.5 hours. Being this catalyst highly active in epoxidation reactions of olefins to give epoxides, few attempts of catalyzing olefin epoxidation - epoxide ring opening tandem reactions have been conducted (7).

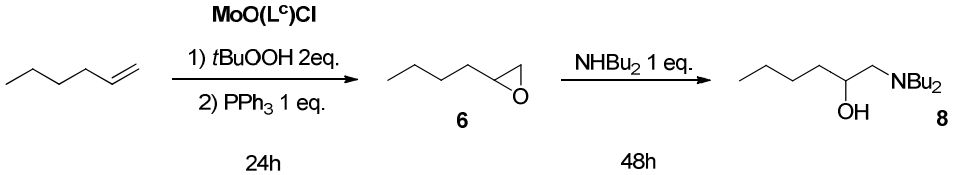

Scheme 7 Epoxidation reaction of 1-hexene 8 to 1,2-epoxyhexane, followed by epoxide ring opening by dibutylamine, catalyzed by **MoO(L^{c})Cl**. Reaction conditions: [**20**] = 0.5 mmol, [*t*BuOOH] = 1 mmol, 5 mol % cat **MoO(L^{c})Cl**, 0.5 mL $CDCl_3$, 60°C, 72h.

1-hexene was first converted to 1,2-epoxyhexane using *t*BuOOH as oxidant and **MoO(L^{c})Cl** as catalyst. Two equivalents of tBuOOH are needed to have quantitative yield of 1,2-epoxyhexane **6** (> 98%). After the complete conversion of the substrate, monitored via ^{1}H-NMR spectroscopy, one equivalent of PPh_3 was added to quench the residual oxidant.[45] The reaction mixture was allowed to stir at room temperature for 30 minutes, then 1 equivalent of Bu_2NH was added, and the reaction was stirred again at 60°C for 48 hours and monitored with ^{1}H-NMR. As shown in *Figure 7*, the ^{1}H-NMR signal of amino alcohol **8** (C**H**OH), a broad multiplet at 3.6 ppm, is visible after 24 and 48 hours, increasing in integration. At the same time, the ^{1}H-NMR signal of 1,2-epoxyhexane **6** (C**H**O), a multiplet at 2.9 ppm, is decreasing in intensity till the complete disappearance after 48 hours. Integration of signals are made impractical by the lost in the baseline definition, making ^{1}H-NMR not the best analytic method to follow these tandem sequence of reactions. However, we can conclude that amino alcohol **8** is formed, and after 48 hours, the epoxide is completed converted.
Although being a very preliminary study (and not the aim of this chapter), this experiment showed the potential for **MoO(L^{c})Cl** to be extensively studied for tandem reactions.

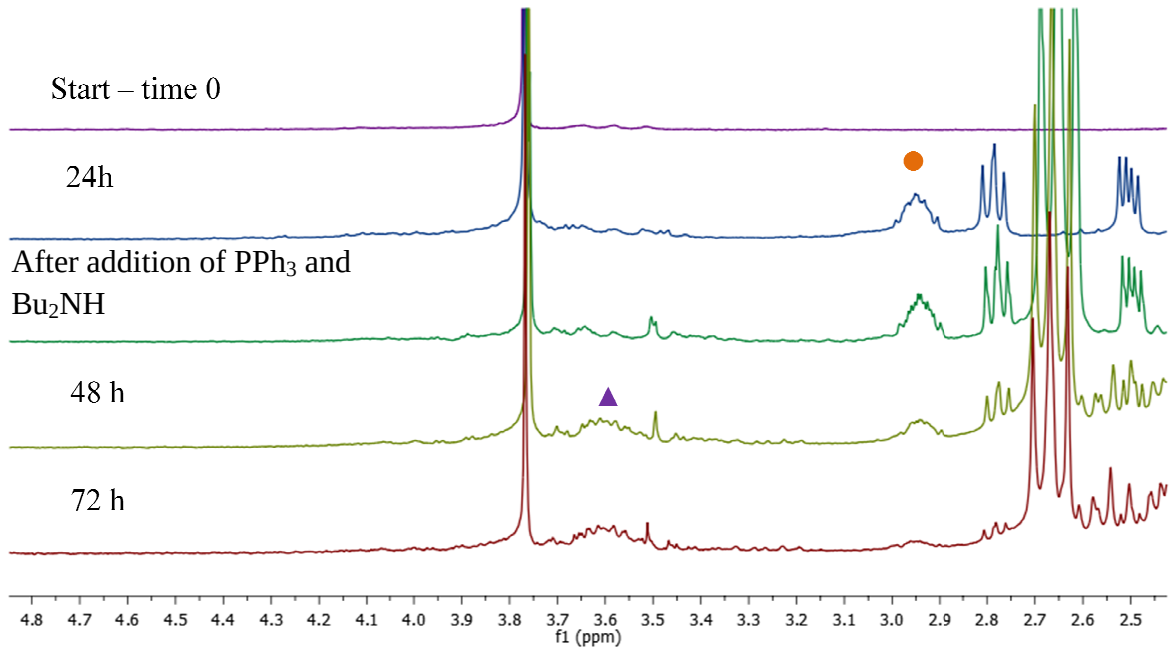

Figure 7 ^{1}H-NMR spectra (recorded in $CDCl_3$) of 1-hexene epoxidation followed by epoxide ring opening by dibutylamine **7**, catalyzed by complex **MoO(L^{c})Cl**. The circle indicates the signal of 1,2-epoxyhexane **6** (C**H**O) while the triangle indicates the signal of amino alcohol **7** (C**H**OH).

[45]Four oxidant quenchers have been tested for this reactions: PPh_3, polystyrene-supported PPh_3 resin, Bu_2S and $Na_2S_2O_3$aq., with PPh_3 giving the best results. Dibutylamine was tried to be added to the reaction mixture also without a quencher, but no product was formed. Finally, 1-hexene epoxidation has been tried with 1 equivalent of *t*BuOOH, in order not to use any quenchers, but only 50 - 60% substrate conversion has been in reached in 24 - 48 hours. After this screening, the use of PPh_3 has been chosen as a quencher.

3.4 Conclusions

Vanadium(V) aminotriphenolate complex **VO(L^h)** has shown to be highly active in the ring opening reaction of epoxides by amines, with high catalytic activities and wide applicability.

The effect of solvent and temperature has been evaluated, indicating that neat conditions at 60°C are the most favorable reaction conditions, reaching complete conversion of 1,2-epoxyhexane **6** in 30 minutes, using dibutylamine **7** as nucleophile, with 1mol% of catalyst. Notably, the catalyst loading can be lowered to 0.1mol% maintaining satisfactory yields. A wide amine and substrate scope, covering all the principal classes of amines and epoxides, indicated the quality and limitations of the tested catalytic system. In summary, even if a complete regioselectivity has been achieved only with a part of reaction tested, the epoxide conversions were excellent in almost all cases. Finally, a prelimiary study concerning epoxidation/epoxide ring opening tandem reactions using **MoO(L^c)Cl** as catalyst has been discussed, revealing potential for a subsequent extending of this project.

3.5 Experimental

General Remarks

All chemicals and dry solvents have been purchased from Sigma-Aldrich or Fluka and used as provided, without further purification. Triphenolamines ligands were synthesized as previously reported[46].

Flash cromatographies and filtrations have been performed with Macherey-Nagel siliga gel 60 (0.04-0.063 mm, 230-400 mesh). TLC analyses were performed using Macherey-Nagel POLYGRAM® SIL G/UV254 silica plates, detecting by UV/VIS and by treatment with PMA staining reagent made from a solution of phosphomolibdic acid ($H_3PMo_{12}O_{40}$) 10 g in 100 mL ethanol. The NMR spectra has been recorded on a Bruker AC200 (^{1}H: 200.13 MHz; ^{13}C: 50.0 MHz) or on an Bruker AV300 (^{1}H: 300.13 MHz; ^{13}C: 75.5.0 MHz) spectrometer. Chemical shift (δ) have been reported in parts per million (ppm) relative to the residual undeuterated solvent as a internal reference ($CDCl_3$: 7.26 ppm for ^{1}H-NMR and 77.16 for ^{13}C-NMR; ACN-d_3: 1.94 ppm for ^{1}H-NMR, 1.32 and 118.26 for ^{13}C-NMR). The following abbreviations have been used to descrive multeplicities: s = singlet, d = doublet, t = triplet, dd = double duplet, q = quartet, m = multiplet, br = broad. ^{13}C-NMR have been recorded with complete proton decoupling. 51V-NMR spectra have

[46]Licini, G.; Mba, M.; Zonta, C. *Dalton Trans.***2009** (27), 5265.

been recorded at 301K with 1000 scans at 78.28 MHz on a AV300 spectrometer. ESI-MS spectra have been obtained on a LC/MS Agilent series 1100 spectrometer in both positive and negative modes using acetonitrile or acetonitrile/formic acid 0.1% as mobile phase, with ESI-ion trap mass detector.IR spectra have been recorded on a Nicolet 5700 FT-IR, with range 4000-400 cm^{-1} and resolution 4 cm^{-1}, using KBr pellets or NaCl plates. All vanadatrane complexes were prepared under nitrogen atmosphere in a MBraun MB 200MD dry-box, equipped with a MB 150 G-I gas recycling system (nitrogen working pressure: 6 bar). Oxygen and water levels inside the box were real-time monitored by MBraun oxygen and moisture analyzers.

For reactivity studies, deuterated solvents used for reactions have been treated with 3Å molecular sieves (beads, 8-12 mesh purchased from Fluka) previously activated at 300°C for 8 hours, and stored in dry-box during all times.

Synthesis of N-cyclohexyl-N′-(3,5-bis(trifluoromethyl)phenyl)thiourea TU

In a 50mL two-neck round-bottom flask 3,5-Bis(trifluoromethyl)phenyl isothiocyanate (5.47 mmol, 1.48 g) was dissolved in dry DCM (2.5 mL). Then cyclohexylamine (5.47 mmol, 0.543 g), previously dissolved in 2.5 ml of dry DCM, was added dropwise under stirring. The reaction mixture was stirred under a N_2 atmosphere at room temperature, and after 10 minutes a white precipitate was formed. The precipitate was filtered, washed four times with DCM and dried with a vacuum pump. The final product was obtained as a white fuzzy solid (1.82 g, 90% yield).

IR (KBr): ν 3235, 3084, 2945, 2859, 1556, 1479, 1380, 1278, 1176, 1135, 710 cm^{-1}.^{1}H-NMR (200 MHz, $CDCl_3$): δ 8.26 (1H, s, broad), 7.76 (2H, s), 7.70 (1H, s), 4.18 (1H, s, broad), 2.09 (2H, m), 1.45 (9H, m). ^{13}C-NMR (50 MHz, $CDCl_3$) 179.36 (C=S), 139.09 (C), 133.25 (C-CF_3, q, J=33 Hz), 123.98 (CH), 122.91 (CF_3, q, J=271) 119.45 (CH, m), 54.16 (CH), 32.50 (CH_2), 25,41 (CH_2), 24.69 (CH_2). MS (ESI): m/z calc. 393.08 $[M+Na]^+$, found 393.1.

Synthesis of Mo(VI) complex MoO(L^c)Cl

In a two-neck round-bottom flask, ligand precursor $\mathbf{L^cH_3}$ (0.745 mmol, 500 mg) was dissolved in toluene (35 mL) and MoO_2Cl_2 (0.745 mmol, 148 mg) was added. The reaction mixture was stirred under reflux overnight. The resulting deep-blue solution was dried with a rotary evaporator and the crude product was filtered through a short pad of silica (ethyl acetate/hexane 3/7). The final product was obtained as a deep-blue solid (600 mg, 98% yield).

IR (KBr): ν 1366, 1262, 1240, 1204, 1171, 1126, 1070, 954, 931, 914, 874, 849, 806, 760, 735, 694, 601, 578, 553 cm^{-1} .^{1}H-NMR (200 MHz, $CDCl_3$): δ 7.37 (1H, d, J=2.4 Hz), 7.31 (2H, d, J=2.4 Hz), 7.11 (1H, d, J=2.2 Hz), 6.97 (2H, d, J=2.2Hz), 4.02 (2H, broad), 3.61 (2H, s), 3.51 (2H, d, J=14),

1.56 (9H, s), 1.56 (18H, s), 1.29 (27H, s). ^{13}C-NMR (50 MHz, $CDCl_3$): δ 147.21, 146.43, 139.85, 139.29, 128.17, 127.45, 124.5, 123.77, 123.57, 61.75, 60.54, 35.53, 34.81, 31.68, 30.60, 30.47. MS (ESI): m/z calc. 818.38 $[M+H]^+$, found 818.4.

Synthesis of Mo(VI) complex MoO(L^d)Cl

Inside a dry-box, ligand precursor **L^dH_3**(0.369 mmol, 200 mg) was dissolved in dry toluene (20 mL) in a 50 mL two-neck round-bottom flask, then MoO_2Cl_2 (0.369 mmol, 73.36 mg) was added. The flask was taken out from the glove-box, and the reaction mixture was stirred at reflux under a N_2 atmosphere. The end of the reaction was checked via TLC (ethyl acetate/hexane 2/8) and ^{1}H-NMR spectroscopy. After 18 hours the reaction mixture was cooled down and the solvent was evaporated with a rotary evaporator. The crude product was dissolved in DCM and filtered through a short pad of silica, to get a deep-blue solid (215 mg, 85% yield).

^{1}H-NMR (200 MHz, $CDCl_3$): δ 7.42 (2H, d, J=2.2 Hz), 7.36 (1H, d, J=2.4 Hz), 7.08 (2H, d, J=2.2 Hz), 6.83 (1H, d, J=2.4 Hz), 4.33 (2H, d, J=14.2), 3.50 (2H, s), 3.42 (2H, d, J=14.2).^{13}C-NMR (50 MHz, $CDCl_3$): δ 150.21, 148.48, 138.03, 135.27, 127.18, 127.58, 124.57, 123.77, 123.57, 61.75, 60.54, 35.53, 34.81, 31.68, 30.60, 30.47. MS (ESI): m/z calc. 687.77 $[M+H]^+$, found 687.9.

Synthesis of V(V) complex VO(L^d)

Inside a dry-box, ligand precursor **L^dH_3** (1.693 mmol, 918 mg) was dissolved in dry DCM (25 mL) in a 50 mL round-bottom flask, and VO(*i-Pr*O)$_3$ (1.693 mmol, 400 μL), previously dissolved in dry DCM (5mL), was added dropwise. The deep-blue reaction mixture was allowed to stir inside the dry-box at room temperature for 2 hours. The end of the reaction was checked via ^{1}H-NMR spectroscopy in ACN-d_3. The solvent was evaporated using a vacuum pump, and the deep-blue solid was extracted several times with dry DEE and dry DCM. The solid that could not be dissolved in these solvents was discarded, while the remaining fraction was purified through crystallization via slow evaporation of the solvents. All the operations described has been conducted inside the dry-box. The product was obtained as a deep-blue solid (400 mg, 39% yield).

^{1}H-NMR (200 MHz, ACN-d_3): δ 7.30 (1H, d, J=2.6 Hz), 7.02 (1H, d, J=2.6 Hz), 3.53 (2H, s). ^{13}C-NMR (50 MHz, $CDCl_3$): δ 156.71, 145.80, 137.52, 133.72, 128.11, 126.43, 124.88, 123.25, 123.00, 62.75, 61.22, 35.53, 35.01, 31.68, 30.60, 30.47.51V-NMR (78.28MHz, ACN-d_3): δ -429.76.

Synthesis of V(V) complex VO(L^h)

Inside a dry-box, precursor ligand **L^hH_3** (1.271 mmol, 639.9 mg) was dissolved in dry THF (12 mL) in a 50 mL round-bottom flask, and VO(*i-Pr*O)$_3$ (1.271 mmol, 300 μL), previously dissolved in dry THF (3mL), was added dropwise. The deep-red reaction mixture was allowed to stir inside the dry-box at room temperature for 2 hours. The end of the reaction was checked via ^{1}H-NMR spectroscopy in $CDCl_3$. The solvent was evaporated using a rotary evaporator, and the crude product was purified through crystallization in DCM/DEE. The product was obtained as deep-red crystals (660 mg, 92% yield).

IR (KBr): ν 3081, 2952, 1426, 1236, 1188, 1080, 945, 891, 752 cm^{-1}. ^{1}H-NMR (200 MHz, ACN-*d*$_3$): δ 7.25 (1H, dd, J=7 and 1 Hz), 7.02 (1H, dd, J=7.4 and 1,6 Hz), 6.88 (1H, t, J=7.6 Hz), 3.80 (1H, broad), 2.88 (1H, broad), 1.56 (9H, s). ^{51}V-NMR (78.28MHz, ACN-*d*$_3$): δ -389.20. MS (ESI): m/z calc. 568.26 $[M+H]^+$, found 568.25.

Procedure for monitoring the epoxide ring opening reaction of 1,2-epoxyhexane with dibutylamine catalyzed by a series of catalysts (Figure 4)

Ten screw top V-vials were charged with 0.025 mol of catalysts, internal standard dichloroethane (0.12 mmol), 1,2-epoxyhexane (0.5 mmol), dibutylamine (0.5 mmol), and $CDCl_3$ to get a final volume of 0.5 mL (1M solutions in substrate, 5 mol% catalysts). One screw top V-vials was charged without catalyst to get the blank reaction. Uniformity in amounts of reagents and ratio substrate/catalysts was assured by charging vials using stock solutions. Reaction mixtures were allowed to stir at 60°C for 23 hours, and samples of 20 μL were taken at intermediate times to monitor reactions via ^{1}H-NMR spectroscopy. Concentrations of product and starting material were determined by integration of CH-O proton signals: 2.91 ppm for 1,2-hepoxyhexane and 3.56 for aminoalcohol x, respect to the internal standard DCE (3.78 ppm). Before taking samples, reaction mixture were allowed to cool by putting them in an ice bath for 5 minutes.

Procedure for monitoring the epoxide ring opening reaction of 1,2-epoxyhexane with dibutylamine catalyzed by catalyst VO(L^h) in different solvents. (Table 1)

Five screw top V-vials were charged with 0.0125 mol of catalyst **VO(L^h)**, internal standard dichloroethane (0.12 mmol), 1,2-epoxyhexane (0.5 mmol), dibutylamine (0.5 mmol), and five different deuterated solvents ($CDCl_3$, ACN-*d*$_3$, CD_3OD, Tol-*d*$_8$, D_2O) to get a final volume of 0.5 mL (1M solutions in substrate, 2.5 mol% catalyst). Reaction mixtures were allowed to stir at 60°C for 24 hours, and samples of 20 μL were taken at intermediate times to monitor reactions via ^{1}H-

NMR spectroscopy in $CDCl_3$. Concentrations of product and starting material were determined by integration of CH-O proton signals: 2.91 ppm for 1,2-hepoxyhexane and 3.56 for aminoalcohol x, respect to the internal standard DCE (3.78 ppm). Before taking samples, reaction mixture were allowed to cool by putting them in an ice bath for 5 minutes.

Procedure for monitoring the epoxide ring opening reaction of 1,2-epoxyhexane with dibutylamine catalyzed by catalyst VO(L^h) at different temperatures (Figure 5)

Four screw top V-vials were charged with 0.005 mol of catalyst **VO(L^h)**, internal standard dichloroethane (0.12 mmol), 1,2-epoxyhexane (0.5 mmol), dibutylamine (0.5 mmol), and ACN-d_3 to get a final volume of 0.5 mL (1M solutions in substrate, 1 mol% catalysts). Uniformity in amounts of reagents and ratio substrate/catalysts was assured by charging vials using stock solutions. Reaction mixtures were allowed to stir at different temperatures (room temperature, 40°C, 60°C, 80°C) for 24 hours, and samples of 20 μL were taken at intermediate times to monitor reactions via ^{1}H-NMR spectroscopy. Concentrations of product and starting material were determined by integration of CH-O proton signals: 2.91 ppm for 1,2-hepoxyhexane and 3.56 for aminoalcohol x, respect to the internal standard DCE (3.78 ppm). Before taking samples, reaction mixture were allowed to cool by putting them in an ice bath for 5 minutes.

Procedure for monitoring the epoxide ring opening reaction of 1,2-epoxyhexane with dibutylamine catalyzed by catalyst VO(L^h) at different catalyst loadings (Table 2)

Four screw top V-vials were charged with different mol of catalyst **VO(L^h)**, internal standard dichloroethane (0.5 mmol), 1,2-epoxyhexane (2 mmol), dibutylamine (2 mmol). Uniformity in amounts of reagents and ratio substrate/catalysts was assured by charging vials using stock solutions. Reaction mixtures were allowed to stir at different temperatures (room temperature, 40°C, 60°C, 80°C) for 24 hours, and samples of 20 μL were taken at intermediate times to monitor reactions via ^{1}H-NMR spectroscopy. Concentrations of product and starting material were determined by integration of CH-O proton signals: 2.91 ppm for 1,2-hepoxyhexane and 3.56 for aminoalcohol x, respect to the internal standard DCE (3.78 ppm). Before taking samples, reaction mixture were allowed to cool by putting them in an ice bath for 5 minutes.

Titration of catalyst VO(L^h) with 1,2-epoxyhexane

Two stock solutions were prepared, one with catalyst **VO(L^h)** (0.01 mmol) in 1 mL ACN-d_3 (stock solution 1, *ST1*), another one with catalyst **VO(L^h)** (0.01 mmol) and 1,2-epoxyhexane (1mmol, 100 equivlents) in 1 mL ACN-d_3 (*ST2*). Titration of catalyst **VO(L^h)** with increasing equivalents of

epoxide has been performed adding increasing amounts of *ST2* to *ST1*, in order to maintain the same concentration of catalyst. Every sample was analyzed via ^{1}H- and ^{51}V-NMR spectroscopy.

Chapter 4

Internal epoxides coupling with CO_2 catalyzed by vanadium(V) aminotriphenolate complexes

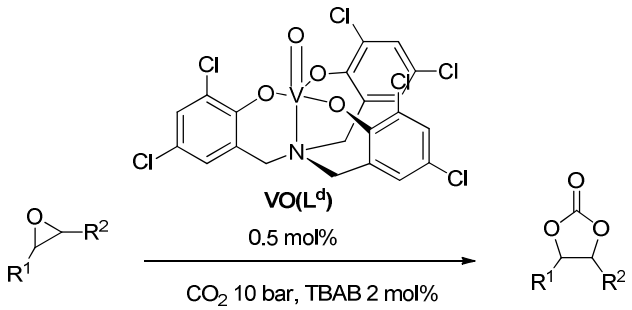

Converting internal epoxides is still a major challenge in the synthesis of cyclic carbonates from CO_2 and epoxides, despite the growing progress in the field of CO_2 fixation. In this chapter, the catalytic performance of vanadium(V) aminotriphenolate complexes **VO(L^h)** and **VO(L^d)** will be discussed concerning these transformations. In particular, complex **VO(L^d)** was extremely active in converting differently substituted internal epoxides, affording high yields of cyclic carbonates using 0.5 mol% of catalyst at 85°C in 16 hours, with a CO_2 pressure of 10 bar. The catalyst loading could be decreased down to 0.025 mol%. The X-ray structure of propylene oxide coordinated to vanadium complex **VO(L^d)**, together with ^{51}V-NMR complex titration with the substrate, give some interesting insights into the nature of the active species involved in the catalytic cycle.

4.1 Introduction

Carbon dioxide fixation has become a topic of primary importance among chemistry research fields, due to two main aspects that affect both the economical and environmental sphere of society. The first deals with the depletion of fossil fuels reserves, which are still the most important source of energy and chemical feedstock of our times, furnishing the suppliant for carbon-containing molecules used in chemical synthesis.[1,2] It is now clear that in the near future crude oil will be not enough to fulfill the increasing global demand for energy, and contemporary scientific interest is thus focusing more and more efforts in developing sustainable alternatives for chemical production.[3,4] Carbon dioxide represents a potential and alternative carbon feedstock, and some examples of CO_2 industrial applications in chemical synthesis are already widely employed, such as the large-scale production of methanol,[5] urea,[6] salicylic acid[7] and several carbonate-based materials.[8,9]

The second aspect is connected to another major problem of these times, which is the increasing pollution of the Earth. CO_2 is released in many combustion processes and is considered - together with methane - as a main contributor to the so-called Greenhouse Effect.[10,11] One long considered strategy to reduce atmospheric CO_2 content is CCS (carbon capture and storage),[12] which is assumed to considerably diminish the carbon dioxide concentration via storage in underground sites. Intense research activities in this area indicate promising results in the near future, however the thought of retaining huge CO_2 reservoirs is not very appealing.[13] Another strategy is the so-called CCU (carbon capture and utilization), which is defined as a process in which CO_2 molecules end up in a new molecule, that is - carbon dioxide fixation.[14] The use of carbon dioxide as a chemical feedstock will never be able to compensate emission-based CO_2, however this strategy

[1] Klaus, S.; Lehenmeier, M. W.; Anderson, C. E.; Rieger, B. *Coord. Chem. Rev.* **2011** (255), 1460.
[2] Gross, R. A.; Kalra, B. *Science* **2002** (297), 803.
[3] Fiorani, G.; Guo, W.; Kleij, A. W. *Green Chem.* **2014** (17), 1375.
[4] Okada, M. *Prog. Polym. Sci.* **2001** (27), 87.
[5] Saito, A. *Kagaku* **2010** (65), 12.
[6] Heffer, P.; Prud'homme, M. IFA Production and International Trade Committee International Fertilizer Industry Association, 36th IFA Enlarged Council Meeting New Delhi (India), 2-4 December 2010.
[7] Federsel, C.; Jackstell, R.; Beller, M. *Angerw. Chem. Int. Ed.* **2010** (49), 6254.
[8] Kakakugyokai no Wadai, Knak database, January 29, **2011** p. 7.
[9] Ando, K.; *Kagaku Keizai*, **2011**, 124.
[10] Santer, B.D.; Taylor, K.E.; Wigley, T.M.L.; Johns, T.C.; Jones, P.D.; Karoly, D.J.; Mitchell, J.F.B.; Oort, A.H.; Penner, J.E.; Ramaswamy, V.; Schwarzkopf, M.D.; Stouffer, R.J.; Tett, S. *Nature* **1996** (382), 39.
[11] Broecker, W.S. *Science* **1997** (278), 1582.
[12] Wissenschaftlicher Beirat der Bundesregierung Globale Umweltveranderungen, Sequestrierung von CO2: Technologien, Potenziale, Kosten und Umweltauswirkungen, **2003**.
[13] Paul, J.; Pradier, C.M. Carbon Dioxide Chemistry: Environmental Issues, *R. Soc. Chem.*, **1994**.
[14] Keim, W.; Behr, A.; Schmitt, G. Principles of Industrial Chemistry. Industrial Products and Processes, Sale und Sauerlander, Frankfurt, **1986**.

potentially provides access to high-value products from a non-toxic, renewable and low-cost resource.[15,16]

Considering the benefits of using carbon dioxide as a C1-feedstock for chemical reactions, few industrial processes utilize CO_2 as a starting material, exploiting only a small fraction of its potential. Being carbon dioxide the most oxidized state of carbon, its high kinetic and thermodynamic stability is the principal obstacle to its industrial usage as a starting material. Four methodologies are used to face the large energy input that is required to transform CO_2 (*Figure 1*):[17]

I. To use high energy starting materials such as hydrogen, unsaturated compounds, small-membered ring compounds and organometallics;[18]
II. To choose oxidized low-energy synthetic targets such as organic carbonates;[19]
III. To lower the activation energy of the specific transformation by means of a catalyst, and/or supply physical energy with light or electricity;
IV. To shift the equilibrium to the product side by removing a particular compound.

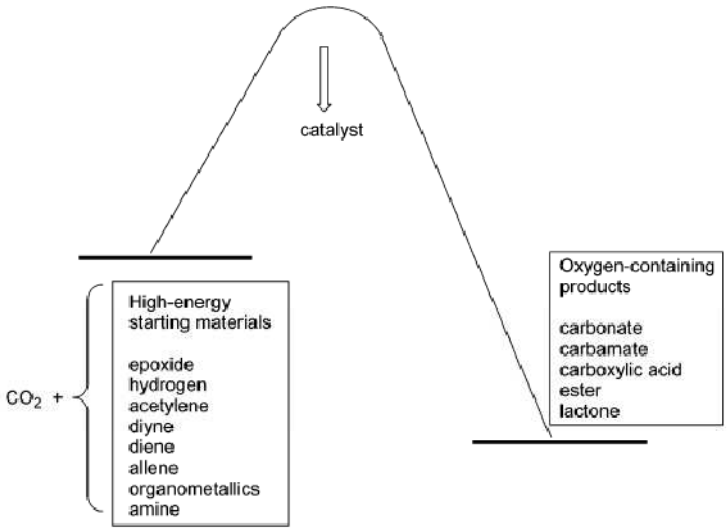

Figure 1 Organic synthesis using CO_2. Adapted with permission from Sakakura, T.; Choi, J. C.; Yasuda, H. *Chem. Rev.* **2007** (107), 2365. Copyright 2007 American Chemical Society [17]

Carbon dioxide transformation reactions can be divided into two main groups, namely reductive and non-reductive conversions.[20,21] Reductive conversion of CO_2 leads to compounds such as

[15] Aresta, M.; Dibenedetto, A.; Angelini, A. *Chem. Rev.*, **2014** (114), 1709.
[16] *Energy Production and Storage: Inorganic Chemical Strategies for a Warming World,* ed. R. H. Crabtree, John Wiley & Sons Ltd., Chichester, **2010**.
[17] Sakakura, T.; Choi, J. C.; Yasuda, H. *Chem. Rev.* **2007** (107), 2365.
[18] Bruckmeier, C.; Lehenmeier, M. W.; Reichardt, R.; Vagin, S.; Rieger, B. *Organometallics* **2010**, (29), 2199.
[19] Comerford, J. W.; Ingram, I. D. V.; North, M.; Wu, X. *Green Chem.* **2015**, 1966.

methanol[22,23] and formic acid,[24,25] requiring high energies and powerful reducing agents like H_2. Non-reductive transformations maintain the +4 oxidation state of the carbon atom and are moderately endo- or exothermic.[26] The target compounds of non-reductive CO_2 transformations include carbonates, carbamates, urea, carboxylates, polycarbonates, polyurethanes and others. *Scheme 1* summarizes examples of organic synthesis starting from carbon dioxide.

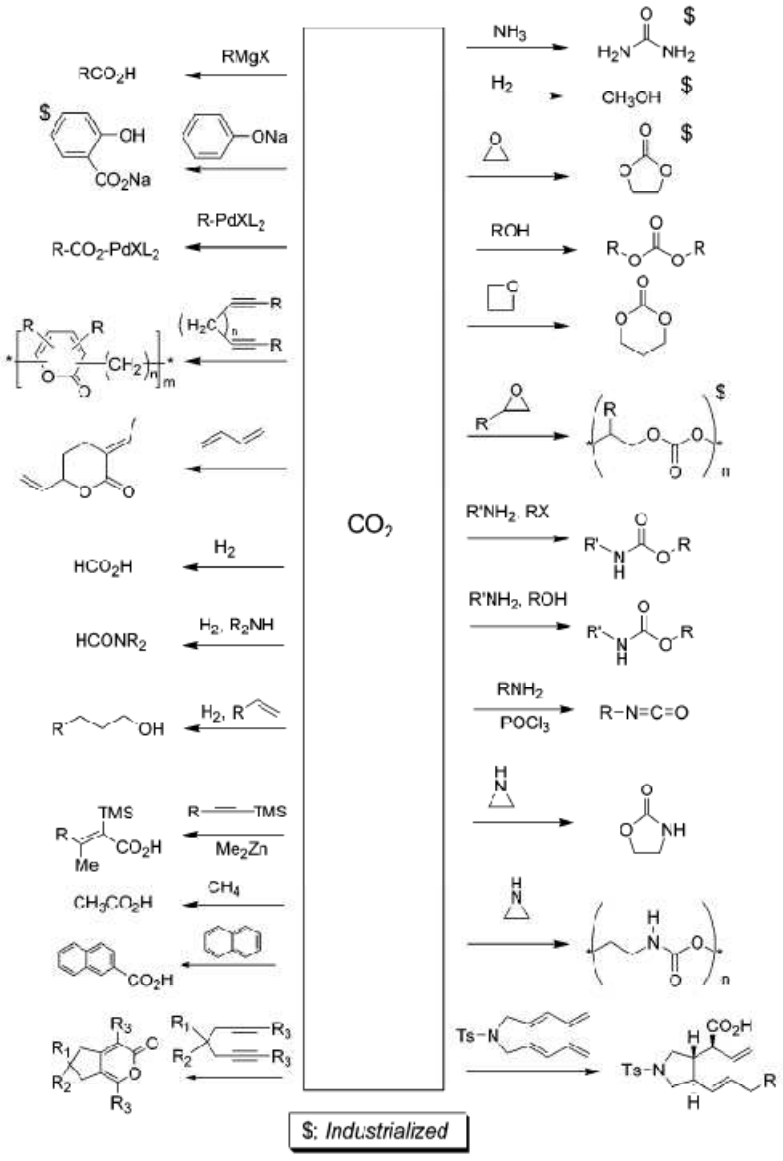

Scheme 1 Examples of possible CO_2 transformations as a starting material. Adapted with permission from Sakakura, T.; Choi, J. C.; Yasuda, H. *Chem. Rev.* **2007** (107), 2365. Copyright 2007 American Chemical Society [17]

[20] Gomes, C. D. N.; Jacquet, O.; Villiers, C.; Thuéry, P.; Ephritikhine, M.; Cantat, T. *Angew. Chem. Int. Ed.* **2012** (51), 187.
[21] Aresta M, Carbon Dioxide as Chemical Feedstock. *Wiley-VCH* **2010**.
[22] Arena, F.; Barbera, K.; Italiano, G.; Bonura, G.; Spadaro, L.; Frusteri F. *J. Catal.* **2007** (249), 185.
[23] Toyir, J.; de la Piscina, P. R.; Fierro, J. L. G.; Homs, N. *App. Catal. B* **2001** (34), 255.
[24] Tanaka, R.; Yamashita, M.; Nozaki, K. *J. Am. Chem. Soc.* **2009** (131), 14168.
[25] Jessop, P. G.; Ikariya, T.; Noyori, R. *Chem. Rev.* **1999** (99), 475.
[26] Aresta, M.; Dibenedetto, A. *Dalton Trans.* **2007**, 2975.

One of the most studied CO_2 transformations is the synthesis of cyclic carbonates,[27] along with their related analogs linear carbonates[28] and polycarbonates,[29] starting from oxiranes, oxiethanes and alcohols. Cyclic organic carbonates (COCs) have been associated with numerous applications including their usage as non-protic solvents, precursors for polycarbonate synthesis,[30] intermediates for the synthesis of fine chemicals and pharmaceutics,[31] solvents or electrolytes in lithium ion batteries.[32] The production of five-membered cyclic carbonates has been industrialized since the 1950s,[33] as in the case of propylene and ethylene carbonates, but many other COCs are still synthesized using phosgene and diols as precursors.[34] Phosgene is a quite reactive and easily available reagent for producing cyclic carbonates and isocyantes, but its high toxicity makes the search for synthetic substitutes a primary issue for the industrial production of these chemicals. Among the starting materials for the synthesis of COCs from CO_2, oxiranes are probably the most employed, [27a] giving access to transformations producing both cyclic carbonates and polycarbonates (*Scheme 2*).

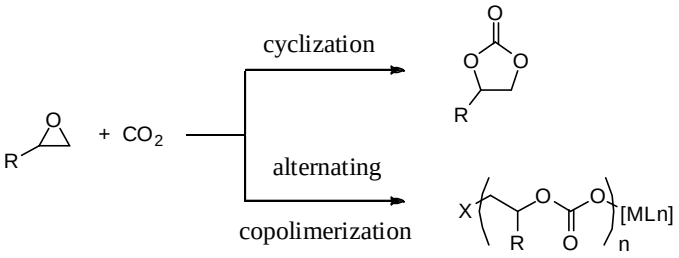

Scheme 2 Synthesis of cyclic carbonates from epoxides and carbon dioxide. According to the catalyst (a transition metal catalyst in this picture) and reaction conditions employed, alternating copolymerization can occur at different ratios.

This 100% atom-economical transformation takes advantage of three of the four methodologies described before, including the use of a high energy low-membered ring compound as the starting material and the choice of an oxidized low energy product. Moreover, an appropriate catalytic system is required for these reactions, as the catalyst-free direct coupling of CO_2 and oxiranes is

[27] a) Sakakura, T.; Kohno, K. *Chem. Commun*. **2009**, 1312; b) Pescarmona, P. P.; Taherimehr, M. *Catal. Sci. Technol*. **2012** (2) , 2169; c) North, M.; Pasquale, R.; Young, C. *Green Chem*. **2010** (12), 1514; d) Decortes, A.; Castilla, A. M.; Kleij, A. W. *Angew. Chem., Int. Ed*. **2010** (49), 9822.
[28] Tundo, P.; Selva, M. *Acc. Chem. Res*. **2002** (35), 706.
[29] a) Coates, G. W.; Moore, D. R. *Angew. Chem., Int. Ed*. **2004** (43), 6618; b) Lu, X.-B.; Darensbourg, D. *J. Chem. Soc. Rev*. **2012** (41), 1462; c) Darensbourg, D. *J. Chem. Rev*. **2007** (107), 2388.
[30] Martín, C.; Fiorani, G.; Kleij, A. W. *ACS Catal*. **2015** (5), 1353.
[31] a) Zhang, Y. J.; Yang, J. H.; Kim, S. H.; Krische, M. J. *J. Am. Chem. Soc*. **2010** (132), 4562; b) Khan, A.; Yang, L.; Xu, J.; Jin, L. Y.; Zhang, Y. J. *Angew. Chem. Int. Ed*. **2014** (53), 11257.
[32] Aresta, M.; Dibenedetto, A.; Pastore, C. *Inorg. Chem*. **2003** (42), 3256.
[33] Darensbourg, D. J.; Holtcamp, M. W. *Coord. Chem. Rev*. **1996** (153),155.
[34] Cokoja, M.; Bruckmeier, C.; Rieger, B.; Herrmann, W. a.; Kühn, F. E. *Angew. Chem. Int. Ed*. **2011** (50), 8510.

extremely unfavorable as the result of the high energy barriers associated with these transformations.[30] As an example, the free energy barriers for the non-catalyzed reaction between propylene oxide and carbon dioxide was calculated by DFT and found to be 53 and 58 kcal·mol^{-1} for the two possible isomeric transition states, respectively (in the gas phase).[35,36]

The current industrial process for cyclic carbonate synthesis is typically catalyzed by halide salts such as Et_4NBr and KI, which are cheap and soluble in oxiranes or cyclic carbonates, also used as solvents.[27a] Halide salts are employed as catalysts for these transformations because a nucleophile is needed to open up the epoxide ring thus permitting the CO_2 insertion, as depicted in *Scheme 3*. Although the nucleophile itself can be employed as catalyst for these transformations, harsh reaction conditions are needed, and only few substrates can be converted. Improved catalytic performances are obtained when halide salts are used as co-catalyst in the presence of a metal catalyst acting as a Lewis acid to activate the epoxide. The general accepted mechanism[30,37] is described in *Scheme 3*.

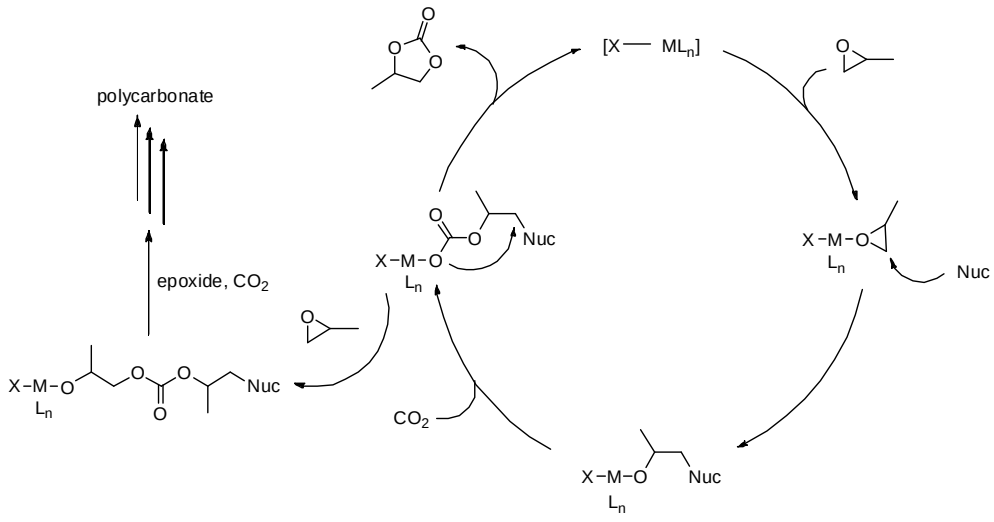

Scheme 3 Catalytic cycle for the synthesis of cyclic carbonates starting with CO_2 and epoxides. In these scheme, propylene oxide is taken as a reference compound.[34]

In the first step, the epoxide coordinates to the metal center through the oxygen atom, and is thus activated. Then, the nucleophile, which can be a co-catalyst used in combination with the catalyst or a ligand of the metal complex itself, attacks and opens the epoxide ring to yield a metal bound alkoxide. In the case of terminal epoxides, the nucleophilic attack occurs at the least hindered

[35] Sun, H.; Zhang, D. *J. Phys. Chem. A* **2007** (111), 8036.
[36] Guo, C.-H.; Wu, H.-S.; Zhang, X.-M.; Song, J.-Y.; Zhang, X. *J. Phys. Chem. A* **2009** (113), 6710.
[37] a) Pescarmona, P. P.; Taherimehr, M. *Catal. Sci. Technol*. **2012** (2), 2169; b) North, M.; Pasquale, R.; Young, C. *Green Chem.* **2010** (12), 1514; c) Shen, Y. M.; Duan, W. L.; Shi, M. *J. Org. Chem.* **2003** (68), 1559.

carbon atom. The alkoxide can in turn act as a nucleophile leading to CO_2 insertion into the metal alkoxide bond, generating a metal carbonate intermediate. Then, a following ring closure can lead to the release of the cyclic carbonates, or another epoxide molecule can insert afterwards. This latter case leads to the synthesis of polycarbonates after a number of CO_2/epoxide alternating insertions. Selectivity toward the formation of COCs arises from a specific balance between the components of the catalytic mixture, including the choice of substrate, metal catalyst, co-catalyst, type of solvent and temperature. In particular, the nature of the co-catalyst and its ratio with respect to the metal catalyst can have a strong influence on the outcome of these coupling reactions.[30]

The exact reaction mechanism is, however, so far not clearly understood. Bimetallic pathways[29a,38] or monometallic mechanisms involving two nucleophiles[39] have been proposed for reaction catalyzed by salen metal complexes. The predominance of a specific reaction path depends on the nature of the catalytic system, but also on the substrate and reaction conditions.[40] Concerning the stereochemistry of the process, a formal retention of configuration for cyclic carbonates products is the result of two subsequent S_N2 reactions - the nucleophilic attack and the ring closure. In the case of polycarbonates formation, the cycle ends with an overall inversion of configuration, lacking the S_N2-guided ring closure. Other parallel mechanisms can lead to a partial lost of stereoselectivity, as it will be fully discussed in the next section.

The most widely employed catalysts for these transformations are homogeneous metal-based complexes, employed as binary systems together with halide salts as co-catalysts .[30] Many homogeneous metal complexes have been reported in the literature in the last 30 years,[34] with substantial improvements of the catalytic performance and reaction conditions. The first report on this topic concerned aluminum porphyrin catalysts described by Takeda and Inoue for the synthesis of polycarbonates from epoxides and CO_2.[41] Although reaction yields were quantitative, long reaction times (two weeks) were required. Since then, different metal complexes (Al(III), Co(III) and Cr(III) being the most prevalent metals) active in cyclocarbonates synthesis from epoxides and CO_2 have been published, reaching high catalytic activities. Today, two are the challenges to deal with for these kind of transformations, namely the use of mild reaction conditions and the conversion of difficult substrates, like internal epoxides. A truly substainable process for the preparation of cyclic carbonates should employ a catalyst showing high activity under mild reaction conditions - at low temperature (below 100°C) and low CO_2 pressures (below 1 MPa). To date, only few catalytic systems have shown these eligible performances. The other target for the development

[38] Darensbourg, D. J.; Yarbrough, J. C. *J. Am. Chem. Soc.* **2002** (124), 6335.
[39] Kember, M. R.; Buchard, A.; Williams, C. K. *Chem. Comm.* **2011** (47), 141.
[40] Klaus, S.; Lehenmeier, M. W.; Anderson, C. E.; Rieger, B. *Coord. Chem. Rev.* **2011** (255), 1460.
[41] Takeda, N.; Inoue, S. *Makromol. Chem.* **1978** (179), 1377.

of CO_2 based protocols is the preparation of COCs starting from synthetically challenging di- and tri-substituted internal epoxides. In fact, if the synthesis of cyclic carbonates from terminal epoxides has been extensively covered over the past ten years, the use of internal epoxides as starting material for this transformation is seldom reported in literature.[30]

Figures 2, *3* and *4* present some selected examples of the most active catalysts reported to date, including catalytic systems that brought significant progress in the targets discussed previously. Among them, salen and salphen metal complexes have been extensively studied for the synthesis of cyclic carbonates starting from CO_2 and epoxides. Salen and salphen ligands provide complexes with a rather planar geometry exerting a tetradentate coordination around the metal center. Depending on the nature of the metal, these complexes can also accommodate two labile ligands in the two axial positions. Therefore, the nucleophile can be embedded or weakly coordinated to the catalyst, resulting in a dual effect: it can act as a nucleophile in the ring-opening of the epoxide or favor the coordination of the oxirane to the metal center by a trans ligand effect.[42] One of the most active catalyst under mild reaction conditions is the dinuclear μ-oxo-bridged Al(salen) complex **20** (*Figure 2)* reported by North and co-workers.[43]

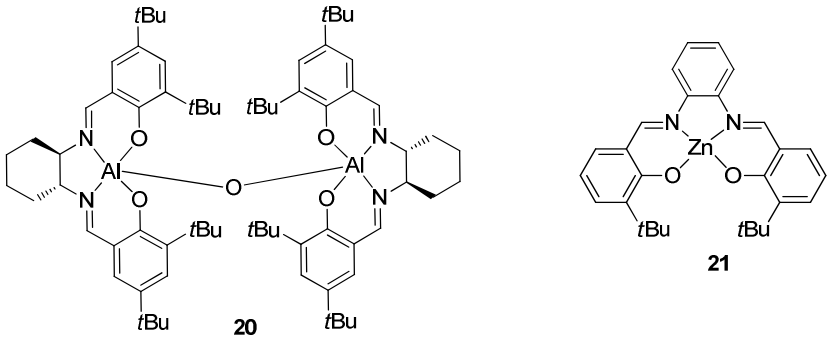

Figure 2 Salen and salphen metal complexes reported by North and Kleij.

This catalyst has shown to be active at room temperature and atmospheric pressure of CO_2 for the synthesis of COCs starting from internal aliphatic and aromatic epoxides. The high activity has been ascribed to the presence of two neighboring metal centers capable of simultaneous activation of both oxirane and carbon dioxide.[44]

[42] Decortes, A.; Castilla, A. M.; Kleij, A. W. *Angew. Chem., Int. Ed*. **2010** (49), 9822.
[43] Meléndez, J.; North, M.; Pasquale, R. Eur. *J. Inorg. Chem*. **2007**, 3323.
[44] a) North, M.; Pasquale, R. *Angew. Chem., Int. Ed*. **2009** (48), 2946; b) Clegg, W.; Harrington, R. W.; North, M.; Pasquale, R. *Chem. Eur. J*. **2010** (16), 6828.

The monometallic Zn(salphen) complex **21** (*Figure 2*) reported by Kleij and co-workers[45] has shown as well high catalytic activity toward CO_2 coupling with terminal epoxides under moderate CO_2 pressures (0.2-1MPa) and mild temperatures (25-45°C). In this case the high activity under mild reaction conditions was ascribed to the constrained geometry imposed by the ligand scaffold, which increases the Lewis acidity of the metal. Although efficient, these catalysts suffer from some limitations, with a narrow substrate scope and requiring high catalyst loading (2.5 mol%).

Another class of homogeneous catalysts giving important contributions to the recent improvements in the field of synthesis of COCs from epoxides and carbon dioxide is aminotriphenolate metal complexes (*Figure 3*).

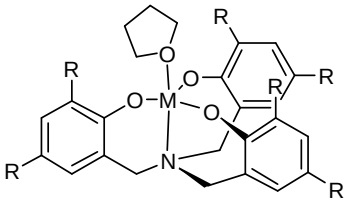

Fe(L^b)(THF): M = Fe, R = CH_3
Fe(L^c)(THF): M = Fe, R = *t*Bu
Al(L^b)(THF): M = Al, R = CH_3
Al(L^c)(THF): M = Al, R = *t*Bu
Al(L^d)(THF): M = Al, R = Cl

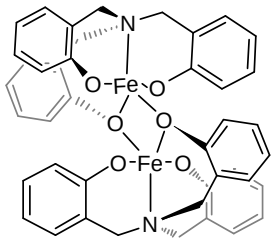

22

Figure 3 Fe(III) and Al(III) aminotriphenolate complexes highly active in CO_2 copuling to epoxides.

The different coordination geometry of these complexes - trigonal bipiramidal rather than the planar coordination geometry of salen and salphen complexes - allow for more sterically congested substrates to be activated/coordinated. In fact, Kleij's group reported the conversion of some internal epoxides using catalysts **Fe(L^b)(THF)** and **22**,[46] obtaining moderate to good yields[47] (yield: 39-69%, cat = co-cat = 0.5%, T = 85°C, $p(CO_2)$=0.2 MPa, 18h).[48] In the case of congested substrates, tetrabutylammonium bromide (TBAB) is used as a co-catalyst, while with terminal epoxides usually tetrabutylammonium iodide (TBAI) gives the best results. This is due to the fact that iodide anion is a stronger nucleophile, while bride is smaller and more suitable for internal

[45] a) Decortes, A.; Martinez Belmonte, M.; Benet-Buchholz, J.; Kleij, A. W. *Chem. Commun*. **2010** (46), 4580; b) Decortes, A.; Kleij, A. W. *ChemCatChem* **2011** (3), 831; c) Salassa, G.; Coenen, M. J. J.; Wezenberg, S. J.; Hendriksen, B. L. M.; Speller, S.; Elemans, J. A. A. W.; Kleij, A. W. *J. Am. Chem. Soc*. **2012** (134), 7186.
[46] Whiteoak, C. J.; Gjoka, B.; Martin, E.; Belmonte, M. M.; Escudero-Adán, E. C.; Zonta, C.; Licini, G.; Kleij, A. W. *Inorg. Chem*.**2012** (51), 10639.
[47] Whiteoak, C. J.; Martin, E.; Belmonte, M. M.; Benet-Buchholz, J.; Kleij, A. W. *Adv. Synth. Catal*. **2012** (354), 469.
[48] Details of the yields or reaction conditions are reported when a connection with results discussed within this chapter is present.

epoxides. Catalyst **Al(L^{d})(THF)** also showed a high activity converting cyclic epoxides.[49] Among the aluminum-based aminotriphenolate complexes **Al(L^{b,c,d})(THF)**, catalyst **Al(L^{d})(THF)** turned to be the most active, reaching very high TONs and TOFs converting terminal epoxides.[50] This is a relevant example of the effect that ring substituents have in the catalytic activity of the complex. As discussed before in this thesis, the electron-withdrawing effect of the chloro substituent increases the Lewis donor ability of the metal, allowing higher activities.

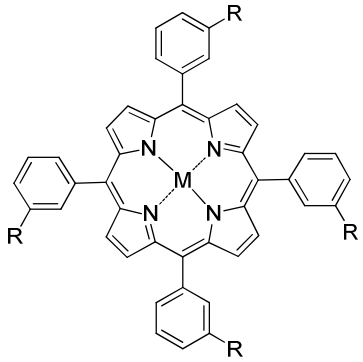

23a: R = H, M = Al(OMe)
23b: R = $O(CH_2)_6NBuBr$, M = Mg
23c: R = $O(CH_2)_6NBuBr$, M = Zn

Figure 4 Porphyrin-based catalyst reported by Inoue (**23a**) and Ema (**23b-c**).

Porphyrin-based catalysts are another class of powerful catalytic systems toward CO_2 coupling with oxiranes. These catalysts are characterized by a planar geometry, which is beneficial for the coordination of terminal epoxides.[30] The first homogeneous metal catalyst for the synthesis of poly- and cyclocarbonates was an aluminium porphyrin complex **23a** (*Figure 4*) reported by Inoue's group in the late 70s, with N-methylimidazole used as a co-catalyst.[41] Low to moderate yields (8–40%) and poor TOFs (0.03 h-1), mainly due to the long reaction time required, were obtained. It is noteworthy, however, that the process was carried out at room temperature, and atmospheric pressure in a dichloromethane solution. In the following years, many other cobalt,[51] chromium,[52] zinc and magnesium[53] based porphyrin catalysts have been reported.

[49] Laserna, V.; Fiorani, G.; Whiteoak, C. J.; Martin, E.; Escudero-Adán, E.; Kleij, A. W. *Angew. Chemie Int. Ed.* **2014** (53), 10416.
[50] a) Whiteoak, C. J.; Kielland, N.; Laserna, V.; Escudero-Adán, E. C.;Martin, E.; Kleij, A. W. *J. Am. Chem. Soc*. **2013** (135), 1228; b) Whiteoak, C. J.; Kielland, N.; Laserna, V.; Castro-Gómez, F.; Martin, E.; Escudero-Adán, E. C.; Bo, C.; Kleij, A. W. *Chem. Eur. J*. **2014** (20), 2264.
[51] a) Paddock, L. R.; Hiyama, Y.; McKay J. M.; Nguyen, S. T. *Tetrahedron Lett.* **2004** (45), 2023; b) Jin, L.; Jing, H.; Chang, T.; Bu, X.; Wang, L.; Liu, Z. *J. Mol. Catal. A: Chem.*, **2007** (261), 262.
[52] Kruper W. J.; Dellar, D. V. *J. Org. Chem.*, **1995** (60), 725.
[53] a) Hasegawa, J.; Miyazaki, R.; Maeda, C.; Ema, T. **2016**, *Chem. Rec*., DOI**:** 10.1002/tcr.201600053. b) Maeda, C.; Taniguchi, T.; Ogawa, K.; Ema, T. *Angew. Chemie - Int. Ed.* **2015** (*54*), 134; c) Ema, T.; Miyazaki, Y.; Koyama, S.; Yano, Y.; Sakai, T. *Chem. Commun.* **2012** (48), 4489.

The most noticeable example is the work reported by Ema and co-workers. In particular, using Mg-based bifunctional catalyst **23b**, in which the nucleophile is linked directly to the ligand scaffold through an alkylic chain, Ema's group have measured one of the highest TONs for homogeneous metal-based catalysis (TON = 103000 after 24 hours).[53c] The recent development of bifunctional catalysts for the synthesis of cyclic and polycarbonates starting from epoxides and CO_2 will be widely discussed in the next chapter. Besides these selected examples of homogeneous metal catalysts, chosen on the basis of the focus of this thesis, many others have been reported in the literature, showing high catalytic performances.[30,54]

In the next section, the catalytic activity of V(V) aminotriphenolate complexes **VO(L^{d})** (R^1, R^2 = Cl) and **VO(L^{h})** (R^1= *t*Bu, R^2 = H) (*Figure 5*) will be discussed, concerning the synthesis of cyclic carbonates starting from epoxides and carbon dioxide. After a preliminary investigation regarding reaction conditions and suitable substrates, the work focused on internal epoxides conversions. As explained before, aminotriphenolate complexes posses a coordination geometry which is likely more suitable for congested substrates activation respect to salen/salphen or porphyrin complexes.

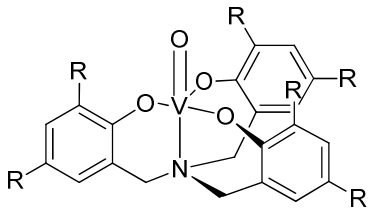

VO(L^{d}): R = Cl
VO(L^{h}): R = *t*Bu

Figure 5 Vanadium(V) aminotriphenolate complexes as catalysts for CO_2 cycloaddition to epoxides discussed in the next section.

Also with these complexes it turned to be case, and a full substrate scope has been conducted using cyclic and acyclic internal epoxides. Then, experiments have been conducted to investigate the active species involved in the catalytic mechanism and disclose the substrate coordination mode to the catalysts, which is not known for these complexes.

[54] North, M.; Pasquale, R.; Young, C.; North, M. Green Chem. **2010** (12), 1514.

4.2 Cataytic activity studies and substrate scope

Vanadium(V) aminotriphenolate complexes **VO(L^{d})** and **VO(L^{h})** have been synthesized in the University of Padova, while the catalytic activity studies for the CO_2 cycloaddition to epoxides have been conducted in the Istitut Català de Investigació Química (ICIQ) of Tarragona, Spain, in the laboratory of Prof. Arjan Kleij, in which I spent three months in the framework of CARISMA COST Action CM1205. Reactions have been carried out under CO_2 pressure $p(CO_2)$ = 10 MPa in single pressurized reactors, as explained in the experimental section of this chapter.

Terminal Epoxides As a first thing we explored the reactivity of V(V) aminotriphenolate complexes **VO(L^{d})** (R^1, R^2 = Cl) and **VO(L^{h})** (R^1= *t*Bu, R^2 = H) using terminal epoxides as substrates. Reaction conditions required for these transformations are quite known, therefore no optimization was necessary. The best co-catalysts for converting terminal epoxides are usually iodide ammonium or phosphonium salts, as a result of both nucleophilicity and leaving ability of this anion.[27] It was pointed out in previous studies that tetrabutylamminium iodide (TBAI) gave the best results when Al(III) aminotriphenolate complexes were employed as catalysts.[50] For this reason, TBAI was used as the co-catalyst for the conversion of internal epoxides.

Table 1 Cycloaddition of CO_2 to 1,2-hepoxyhexane **6** using complex **VO(L^{h})** as catalyst - effect of catalyst loading.

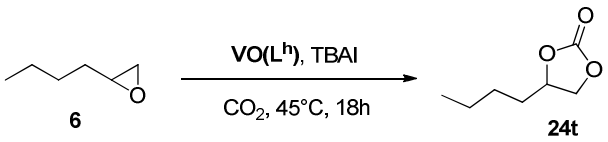

Entry	[2d] mol%	[TBAI] mol%	Yield (%)[a]
1	0.5	1.25	>99
2	0.5	-	0
3	-	1.25	64
4	0.2	0.5	94
5	0.1	0.25	58
6	0.1	-	0
7	-	0.25	23

Reaction conditions: [**6**] = 2 mmol, $p(CO_2)$ = 10 MPa, 45°C, 18h, neat conditions. [a]Yields calculated via ^{1}H-NMR analysis with mesitylene as external standard. Selectivity was in all cases >99%.

A catalyst loading screening was performed using **VO(L^h)** (R^1= *t*Bu, R^2 = H) as catalyst and 1,2-epoxyhexane as a substrate under mild reaction conditions (45°C, *p*(CO2) = 10 MPa, neat), as reported in *Table 1* .

Catalyst loading can be decreased to 0.2 mol% without affecting the yield of the reaction, while a sensible drop in substrate conversion was detected when using 0.1 mmol% of catalyst. It is clear from this table that the metal catalyst alone is not enough to enable this reaction, being the contribution of the nucleophile necessary to the catalysis by ring opening the epoxide. The alkoxide resulting from this first step of the catalytic mechanism (see *Scheme 3*) attacks carbon dioxide which then acts both as a nucleophile and electrophile, as depicted in *Scheme 4*.

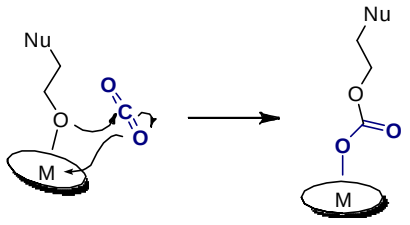

Scheme 4 A detail of catalytic mechanism showing the alkoxide attacking carbon dioxide. The presence of the nucleophile is necessary to have the reactive alkoxide intermediate.

Co-catalyst/catalyst ratio is an important aspect having a deep influence on the cyclic carbonate yield for these transformation. It has been demonstrated before that a high co-catalyst/catalyst ratio leads to the preferential formation of cyclic carbonates over poly-carbonates, by facilitating the displacement of the metal-bound carbonate intermediate by a new nucleophilic anion. In this way, the ring closure reaction is favored over the chain elongation (see *Scheme 3*).[37a,55] For this reason, 1/2.5 cat/co-cat ratio has been employed for these screenings.

Afterwords, catalytic activity of V(V) aminotriphenolate complexes **VO(L^d)** and **VO(L^h)** has been compared in the conversion of three different terminal epoxides, using a catalyst concentration of 0.1 mol% (*Table 2*).

[55] a) Taherimehr, M.; Sertã, J. P. C. C.; Kleij, A. W.; Whiteoak, C. J.; Pescarmona, P. P. *ChemSusChem* **2015** (8), 1034; b) Taherimehr, M.; Al-Amsyar, S. M.; Whiteoak, C. J.; Kleij, A. W.; Pescarmona, P. P. *Green Chem.* **2013** (15), 3083.

Table 2 Comparison of V(V) aminotriphenolate complexes **VO(L^{d})** and **VO(L^{h})** in cycloaddition of CO_2 to 1,2-epoxyhexane **6**, styrene oxide **17c** and epichlorohydrin **17a**.

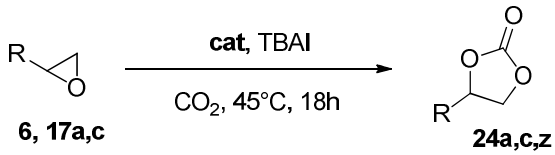

6, 17a,c **24a,c,z**

Entry	R	Cat	Yield (%)[a]
1	*n*-Bu (**6**)	**VO(L^{d})** (R^1, R^2 = Cl)	73
2		**VO(L^{h})** (R^1= *t*Bu, R^2 = H)	58
3		**Al(L^{d})(THF)**	99
4		-[b]	23
5	Ph (**17c**)	**VO(L^{d})** (R^1, R^2 = Cl)	19
6		**VO(L^{h})** (R^1= *t*Bu, R^2 = H)	70
7		**Al(L^{d})(THF)**	74
8		-[b]	7
9	Cl(CH_2)- (**17a**)	**VO(L^{d})** (R^1, R^2 = Cl)	18
10		**VO(L^{h})** (R^1= *t*Bu, R^2 = H)	67
11		**Al(L^{d})(THF)**	60
12		-[b]	26

Reaction conditions: [**epoxide**] = 2 mmol, [**cat**] = 0.1 mol%, TBAI = 0.25 mol%, $p(CO_2)$ = 10 MPa, 45°C, 18h, neat conditions. [a]Yields calculated via ^{1}H-NMR analysis with mesitylene as external standard. [b]Only co-catalyst was employed. Selectivity was in all cases >99%.

Aminotriphenolate complex **VO(L^{h})**, in which the ligand is functionalized with *t*Bu groups, gave higher conversions respect to complex **VO(L^{d})** (R^1, R^2 = Cl) in the case of styrene oxide and epichlorohydrin, while the contrary can be said for 1,2-epoxyhexane, although with lower difference in cyclic carbonate yields. With the results reported in *Table 2*, vanadium has shown to be a suitable metal as a Lewis acid catalyst for these transformations. Catalytic activity of vanadium(V) complexes **VO(L^{h})** and **VO(L^{d})** has been compared to aluminum(III) aminotriphenolate complex **Al(L^{d})(THF)** (R^1, R^2 = Cl), reported by Kleij's group as one of the most active catalyst for the synthesis of cyclic carbonates from terminal epoxides (cfr infra). Conversions was comparable in most cases, confirming triphenolamines excellent ligands for CO_2 cycloaddition reactions.

Internal epoxides. After having shaped a general idea about the catalytic activity of V(V) aminotriphenolate complexes in CO_2 cycloaddition to epoxides, we turned our attention to the more challenging internal epoxides. As discussed before, aminotriphenolate complexes with trigonal bipyramidal coordination geometry should be in principle optimal catalysts for bulky substrates. In

addition to this, a real substrate scope for internal epoxides is lacking in literature for homogeneous metal based-catalyzed synthesis of cyclic carbonate starting from carbon dioxide and oxiranes. For these reasons, most effort has been dedicated to the use of vanadium triphenolate complexes as catalysts for CO_2 cycloaddition to internal epoxides. *Table 3* reports catalytic activities of complex **VO(L^{d})** (R^1, R^2 = Cl) and **VO(L^{h})** (R^1= *t*Bu, R^2 = H) in the conversion of 2-methyl-2-phenyloxirane **17h** to the corresponding cyclic carbonate **24h**.

Table 3 CO_2 cycloaddition to phenyl-methyl-oxirane **17h** catalytzed by V(V) aminotriphenolate complexes **VO(L^{d})** and **VO(L^{h})**.

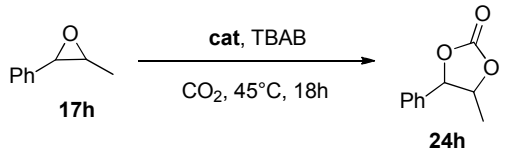

Entry	Cat	[Cat] mol%	Yield (%)[a]
1	**VO(L^{h})** (R^1= *t*Bu, R^2 = H)	0.5	93
2	**VO(L^{d})** (R^1, R^2 = Cl)	0.5	>99
3	**VO(L^{d})** (R^1, R^2 = Cl)	0.25	>99
4	-[b]	-[b]	26

Reaction conditions: [**17h**] = 2 mmol, [TBAB] = 5 mol%, $p(CO_2)$ = 10 MPa, 45°C, 18h, neat conditions. [a]Yields calculated via ^{1}H-NMR analysis with mesitylene as external standard. [b]Only co-catalyst was employed. Selectivity was in all cases >99%.

With internal epoxides tetrabutylammonium bromide (TBAB) is used instead of the corresponding chloride salt, because the minor radius of bromide respect to iodide anion allow a better approach of the ion to hindered substrates. In some cases, even chloride anions are preferred, as in the case of 1-methyl-1,2-cyclohexeneoxide **17k** (*vide infra*). Also with **17h**, complexes **VO(L^{h})** and **VO(L^{d})** showed excellent catalytic activities, with complex **VO(L^{d})** (R^1, R^2 = Cl) giving a higher yield in cyclic carbonate **24h** respect to complex **VO(L^{h})** (R^1= *t*Bu, R^2 = H). Thus, V(V) aminotriphenolate complex **VO(L^{h})** was employed as catalyst to investigate a wide scope of internal epoxides to give the corresponding cyclic carbonates **17d-s** as depicted in *Figure 6*.

Substrate scope. To examine a large set of di-substitutes epoxides, standard reactions conditions were defined at 85°C and 18 hours with $p(CO_2)$ = 10 MPa. Cyclohexene and cyclopentene oxides derivatives **17e,l-n** and **17i,j** have been converted to cyclic carbonates **24e,l-n** and **24i,j** with excellent isolated yields, using **VO(L^{d})** (R^1, R^2 = Cl) as catalyst in 0.5 mol% concentration. Starting from *cis*-epoxides, only *cis*-products were formed. Also cyclic carbonates **24d,h,g,r,s** were obtained with mostly quantitative conversions and high isolated yields. It is interesting to notice that for cyclic carbonates **17d** and **17s**, a mixture of *cis*/*trans* products was obtained starting from the pure *cis*-epoxide. In particular, the *cis*-stilbene oxide **17s** was converted into the corresponding cyclic carbonate with a 2:98 *cis*/*trans* ratio.[56] Moreover, a small amount of *cis*-cyclic carbonate was obtained starting from the pure *trans*-2,3-butylene oxide **17r**. This behavior suggests a S_N1 pathway at some point in the catalytic mechanism, which eventually leads to the formation of the two *cis*/*trans* diasteroisomers. *Scheme 5* illustrates the two generic pathways A and B giving an overall retention of configuration or a mixture of the two diasteroisomers.[57] The initial nucleophilic attack of the X^- nucleophile leads to a firs inversion of substrate configuration (intermediate II and III). In general, after the CO_2 insertion, the ring closure can be driven by a S_N2 (pathway A) or S_N1 (pathway B) mechanism. Pathway A is usually the one described in the general review about this field,[27] though the type of the mechanism involved in the cycle is probably depending on reaction conditions and substrate. For example, a low co-catalyst/catalyst ratio could promote the elimination of the X^- leaving group by coordination to another metal centre, thus favoring the S_N1 pathway (intermediate V). Concerning the substrates, di-substituted epoxides are surely more prone to an S_N1 ring closure mechanism, as secondary carbocations are more stable than primary ones. An overall inversion of configuration is also observed when cyclic carbonates are the result of back-biting, a side reaction in polycarbonate synthesis (see *Chapter 5*). When a S_N1 mechanism is involved, a mixture of the two diasteroisomers is obtained, with a ratio shifted towards the most thermodynamically stable product. This is the case of cyclic carbonates **24r**, **24d** and **24s**. For cyclic carbonates obtained from cyclohexene and cyclopentene oxide derivatives **17e,l-n** and **17i,j**, the *trans* configuration is highly unfavourable, thus only *cis*-cyclic carbonates have been formed, even if pathway B is driving the mechanism.

[56] This was already reported in literature. See for example: Büttner, H.; Steinbauer, J.; Werner, T. *ChemSusChem* **2015** (8), 2669.
[57] Whiteoak, C. J.; Martin, E.; Escudero-Adán, E.; Kleij, A. W. *Adv. Synth. Catal.* **2013** (335), 2239.

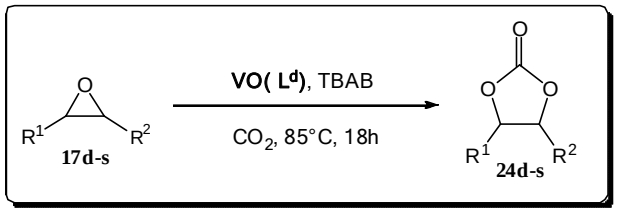

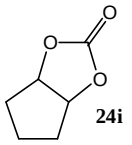

Conv. >99%; Sel. >99%
Cis>99%; Yield = 79%

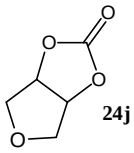

Conv. >99%; Sel. >99%
Cis>99%; Yield = 89%

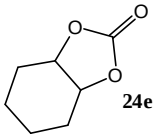

Conv. >99%; Sel. >99%
Cis>99%; Yield = 71%

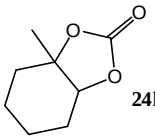

Conv. 22%; Sel. 38%[a]
PPNCl used as co-cat

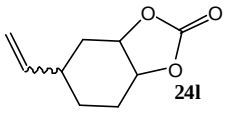

Conv. 88%; Sel. >99%
Cis>99%; Yield = 82% *dr* 56:44

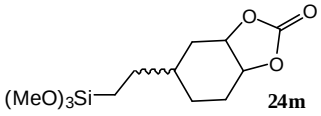

Conv. >99%; Sel. >99%
Cis>99%; Yield = 65% *dr* 60:40

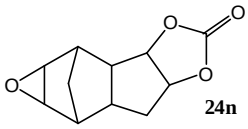

Conv. 51%; Sel. >99%
Cis>99%; Yield = 32%

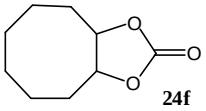

Conv. 5%; Sel. >99%
Cis>99%;

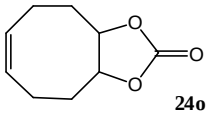

Conv. 37%; Sel. 99%
Cis/Trans 61/39; Yield = 19%

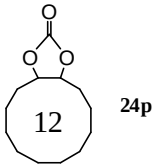

No conversion

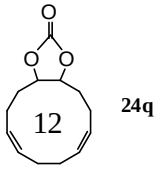

Conv. 9%; Sel. > 99%
Cis > 99%

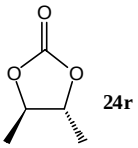

Conv. >99%; Sel. 99%[b]
Cis/Trans 8/92; Yield = 79%

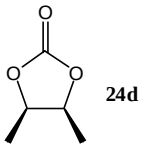

Conv. >99%; Sel. >99%
Cis/Trans 54/46; Yield = 75%

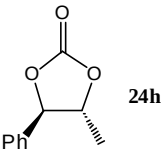

Conv. >99%; Sel. 95%[b]
Trans >99% Yield = 85%

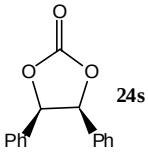

Conv. >99%; Sel. 72%[b]
Cis/Trans 2/98 Yield 61 %

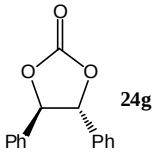

Conv. 78%; Sel. 92%[b]
Trans >99% Yield = 59%

Figure 6 Substrate scope for the formation of cyclic carbonates **24d-s**. Reaction conditions, unless otherwise noted: [substrate] = 4mmol, [**VO(L^d)**] = 0.5 mol%, [TBAB] = 5 mol%, neat conditions, 85°C, p(CO2) = 10MPa, 18h. Reported *dr* values were determined by ^{13}C-NMR spectroscopy and relate to the relative configuration of carbonate unit and R substituent. Yields: isolated yields. [a]Unidentified by-product. [b]Aldehydic by-product. Wedge -dash configuration of chemical structures are referred to the substrate configuration (and thus the expected product), while the obtained cis/trans ratio of products is given below each structure.

Having ten internal epoxides converted with excellent yields, the vanadium(V) aminotriphenolate complex **VO(L^{d})** was tried with even more challenging substrates.

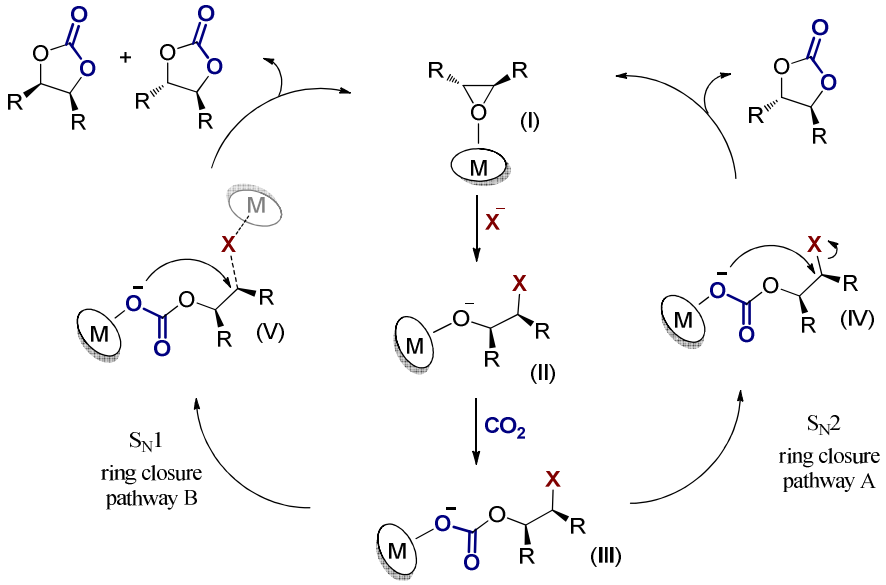

Scheme 5 Two possible pathway leading to an overall retention of configuration or a mixture of two diasteroisomers.

The tri-substituted epoxide **17k** required bis(triphenylphosphine)iminium chloride (PPNCl) instead of TBAI, as nucleophiles with a minor steric hindrance facilitates the attack to a such bulky substrate. With PPNCl as nucleophile, a reasonable 22% conversion was reached. The bis-epoxide **17n** was converted only at one epoxidic ring, as reported in literature,[58] forming cyclic carbonate **24n** with 51% conversion and 32% isolated yields. These two substrates usually require longer reaction times to get higher conversions,[59] but in our case, increasing the reaction time to 66 hours did not lead to higher yields, not even using 1% mol of catalyst. This is probably due to catalyst stability problem at these temperatures. Cyclooptene and cyclododecene oxides **17f,p** provided very low conversions, revealing to be the most tricky substrates for the synthesis of cyclic carbonates starting from epoxides and CO_2. Increasing the rigidity of the ring with one (**17o**) or two (**17q**) double bonds, somewhat higher yields were obtained: epoxide **17o** was converted to the corresponding cyclic carbonate with 19% isolated yield, while substrate **17q** gave 9% conversion. These substrates, which can be converted with higher yields only by a small number of catalysts,[58] define the limitations of this system. In general, a large number of internal epoxides have been

[58] Laserna, V.; Fiorani, G.; Whiteoak, C. J.; Martin, E.; Escudero-Adán, E.; Kleij, A. W. *Angew. Chem. Int. Ed.* **2014** (53), 10416.
[59] Fiorani, G.; Stuck, M.; Martín, C.; Belmonte, M. M.; Martin, E.; Escudero-Adán, E. C.; Kleij, A. W. *ChemSusChem* **2016**, 1304.

converted to the corresponding cyclic carbonates with high isolated yields, demonstrating the high versatility of vanadium(V) aminotriphenolate complex **VO(L^{d})**.

4.3 Epoxide coordination to the complex

To be activated towards the nucleophilic attack, the epoxide must be coordinated to the metal catalyst. In the case of aluminum(III) aminotriphenolate complex **Al(L^{d})(THF)** (see *Introduction*), the substrate coordinates to the metal in the axial position, which is usually occupied by a THF molecule or another ancillary ligand.[50b] *Figure 7* shows the X-ray structure of Al(III) complex **Al(L^{d})** with oxetane coordinated in the axial position.

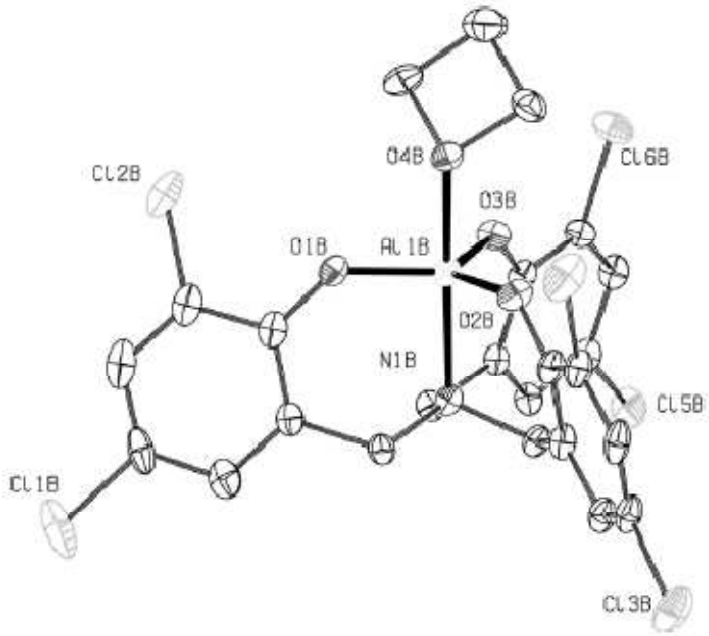

Figure 7 X-ray structure of **Al(L^{d})** · oxetane. The substrate is coordinated in the axial position, trans to the ligand nitrogen.

In the case of vanadium(V) aminotriphenolate complex **VO(L^{d})**, the coordination of an epoxide is likely to occur in the equatorial position, changing the coordination geometry from trigonal bipyramidal to octahedral. Indeed, C_6D_6 solutions of complex **VO(L^{d})** present clearly a ^{1}H-NMR signals pattern of a mixture of TBP and octahedral complexes in equilibrium (*Scheme 6*).[60]

[60] Groysman, S.; Goldberg, I.; Goldschmidt, Z.; Kol, M. *Inorg. Chem.* **2005** (44), 5073.

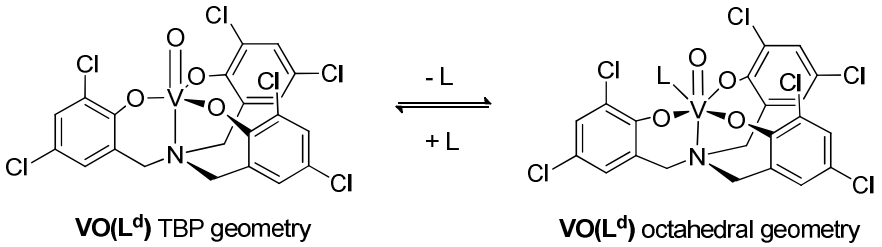

Scheme 6 Equilibrium between TBP and octahedral 2b vanadium(V) aminotriphenolate complexes in C_6D_6 solution.

An X-ray structure of complex **VO(L^d)** revealed a mononuclear hexacoordinated oxo complex, the sixth coordination site being occupied by an aqua ligand to which two THF molecules were H-bonded (*Figure 8*).

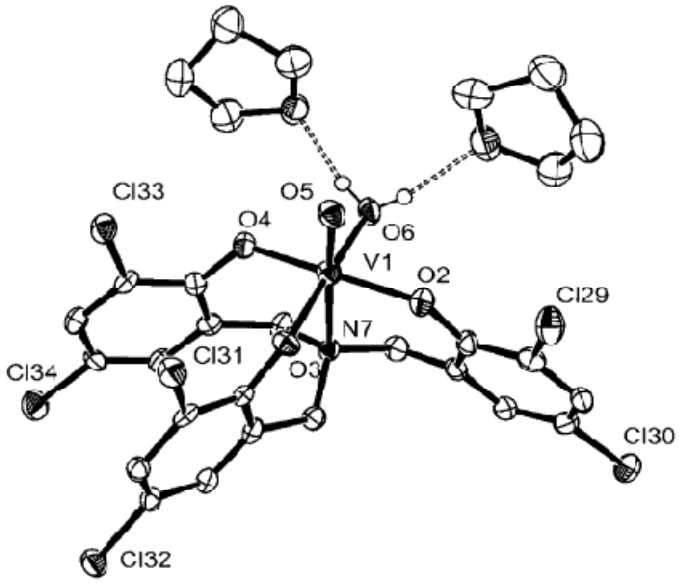

Figure 8 X-ray structure of **VO(L^d)** reported by Kol and co-workers.[60]

To investigate epoxides coordination mode, some ^{51}V-NMR experiments were performed in order to detect any formation of different complex species when an epoxide is added to a solution of **VO(L^d)**. In particular, adding increasing amounts of propylene oxide **PO** to a solution of **VO(L^d)** in ACNd_3, maintaining the complex concentration constant, a new pattern of signals is observed, which changes according to the number of equivalents of epoxide added. The overall experiment is depicted in *Figure 9*. In the first ^{51}V-NMR spectrum, only one resonance is present, which

corresponds to the TBP **VO(L^d)** complex.[61] Adding 10 equivalents of propylene oxide **PO**,[62] the ^{51}V-NMR spectrum revealed that many other complex species are formed, generating other signals both downfield and upfield respect to the initial resonance at -426 ppm. Increasing the amount of propylene oxide added to the complex, the system becomes simpler until it shows only two major species at -451 and -465 ppm in the spectrum, when 100 equivalents are added.

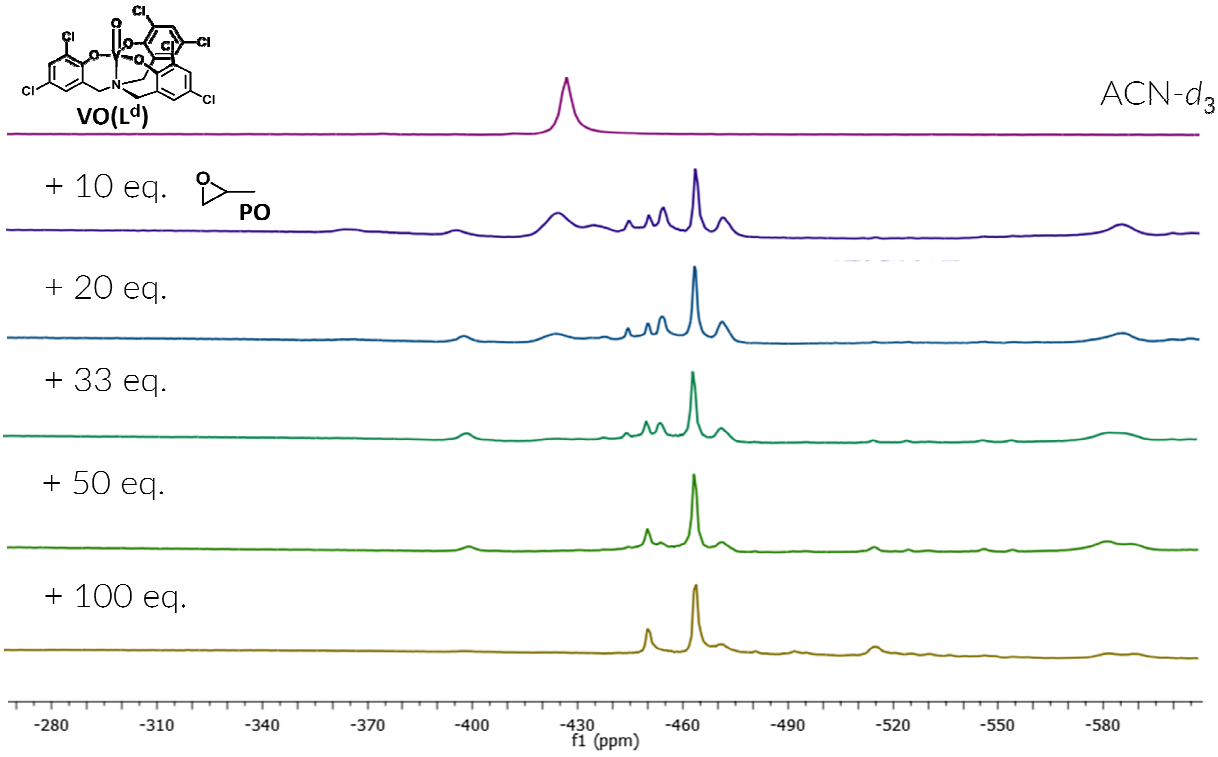

Figure 9 51V-NMR experiments showing the formation of new vanadium species when propylene oxide is added to a 0.01M solution of **VO(L^d)** in ACNd_3.

The initial resonance at -426 ppm decreases in intensity while increasing the amount of propylene oxide, and it is completely absent in the final spectra with 100 equivalents of epoxide. All these spectra have been recorded 5 hours after the addition of the propylene oxide to the **VO(L^d)** solution in ACNd_3. The same spectra evolution can be obtained also adding an intermediate amount of propylene oxide (33 equivalents, for example) to complex **VO(L^d)** in ACNd_3, and recording ^{51}V-NMR spectra during two days.

[61] Unlike for C_6D_6, $CDCl_3$ and other deuterated solvents, ^{51}V- , ^{1}H- and ^{13}C-NMR of complex **VO(L^d)** dissolved in ACNd_3 show clean spectra where only the TBP species is present. For this reason, ACNd_3 have been used as deuterated solvent for the complex characterization and for this ^{51}V-NMR experiment.
[62] Note that the concentration of complex **VO(L^d)** is constant in all the spectra.

We managed to grow crystals from the ACNd_3 solution of **VO(L^d)** with propylene oxide **PO**, the X-ray analysis showing a completely unexpected structure **VO(L^d)(PO)** (*Figure 10*).

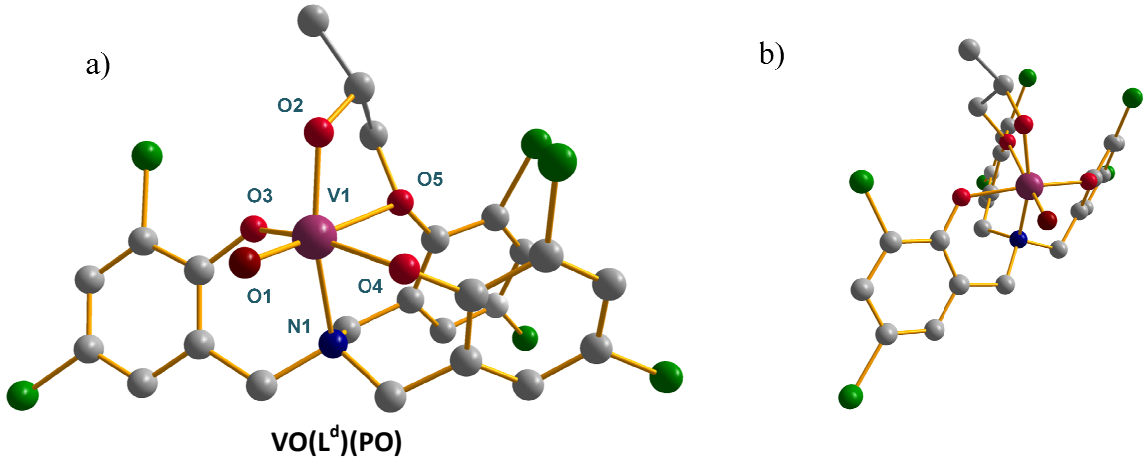

Figure 10 X-ray structure of complex **VO(L^d)(PO)**, obtained by crystallization of **VO(L^d)** in ACNd_3 (0.01M) with 33 equivalents of propylene oxide, from two different side views a) and b). Selected bond distances (Å) and angles (deg): V1 - O1 1.5879, V1 - O2 1.7875, V1 - O3 1.8914, V1 - O4 1.8700, V1 - O5 2.34, V1 - N1 2.2438, O1 - V1 - O5 178.71, O1 - V1 - O3 97.37, O1 - V1 - O4 96.62, O1 - V1 - O2 102.54, O1 - V1 - N1 100.49, O2 - V1 - N1 155.90, O2 - V1 - O5 76.18, O2 - V1 - O4 100.44, O2 - V1 - O3 91.77, O3 - V1 - O4 158.96, O3 - V1 - O5 82.83, O5 - V1 - O4 83.54, O3 - V1 - N178.25, O4 - V1 - N1 83.81.

The crystallized complex presents a distorted octahedral geometry, with the oxo function occupying an equatorial position, *cis* to the central nitrogen. The axial position, *trans* to the central nitrogen, is occupied by the oxygen of the propylene oxide (depicted in *Figure 10* with grey bonds for clarity), which has been opened by one of the three phenoxo moiety of the aminotriphenolate ligand. The *b)* side view shows that the branches of the ligand have twisted to accommodate the substrate. We were searching for the propylene oxide coordination to the complex, and we found it not only coordinated to the vanadium atom, but also already ring-opened by the ligand itself, the phenoxo moiety acting as the nucleophile. As a first thing, we therefore wanted to understand if complex **VO(L^d)** is able to catalyze the CO_2 cycloaddition to propylene oxide without the nucleophilic co-catalyst, considering its ability to coordinate and open the substrate. Even trying the CO_2 cycloaddition reaction in different reaction conditions, this was not the case. Complex **VO(L^d)** needs a nucleophilic co-catalyst for the cyclic carbonate to be produced, meaning that the complex alone is able to open the propylene oxide but not to further react with CO_2. The characterization of complex **VO(L^d)(PO)** have been completed with MALDI-TOF mass spectrometry (*Figure 11*) analysis and ^{1}H- and ^{51}V-NMR spectroscopy.

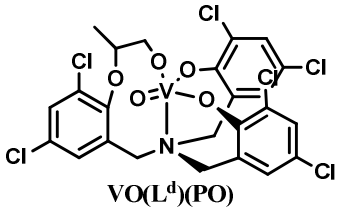

VO(L^{d})(PO)

Exact Mass: 660,88

Calculated isotopic pattern:

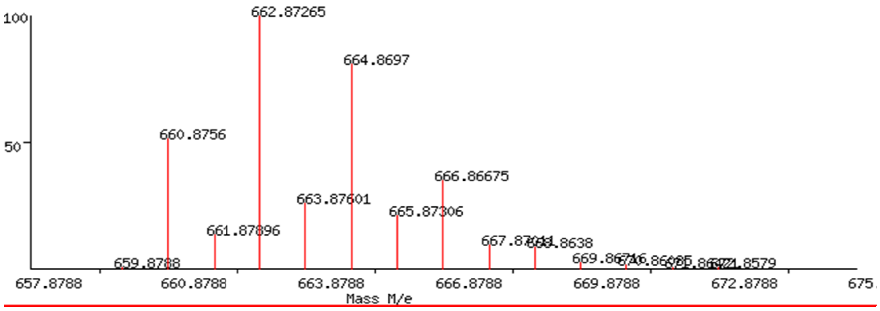

MALDI analysis:

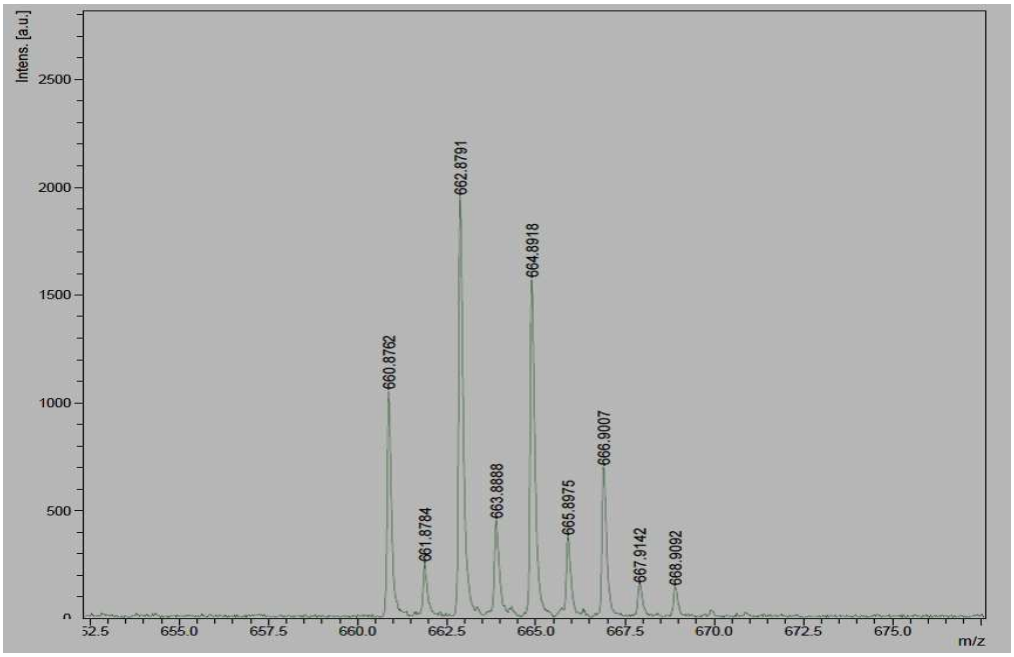

Figure 11 MALDI-TOF mass spectrometry analysis of complex **VO(L^{d})(PO)**. The calculated and found isotopic patterns are shown.

The ^{51}V-NMR analysis showed that this complex corresponds to the signal at -465 ppm (*Figure 12*).

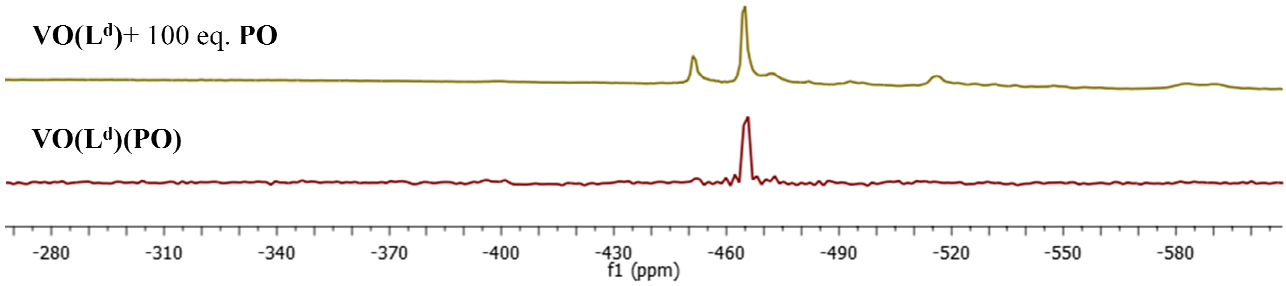

Figure 12 ^{51}V-NMR spectra of complex **VO(L^{d})** + 100 equivalents of propylene oxide (green) and complex **VO(L^{d})(PO)** (red).

The minor signal at -451 ppm was not identified. Anyway, it could be assessed to a complex similar to **VO(L^{d})(PO)**, with the oxo function in the axial rather than equatorial position. Indeed, similar species can be found in literature, which present in the ^{51}V-NMR spectrum a major signal referred to the complex with the oxo moiety in the equatorial position, and another minor downfielded signal for the species with oxo in axial position.[63]

In summary, species **VO(L^{d})(PO)** demonstrates that vanadium(V) aminotriphenolate complex **VO(L^{d})** is able to coordinate propylene oxide activating it towards the nucleophilic ring opening. In the conditions used for the crystallization, with no other nucleophiles present in solution, propylene oxide is ring-opened by the ligand itself. When running the reaction, it is the co-catalysts which opens the substrate, permitting the cyclic carbonates formation.

4.4 Conclusions

In conclusion, vanadium(V) aminotriphenolate complexes **VO(L^{d})** and **VO(L^{h})** have shown to be effective catalysts for the synthesis of cyclic carbonates starting from epoxides and CO_2, with reactivities comparable to those of aluminum(III) aminotriphenolate complex **Al(L^{d})(THF)**, one of the most active catalysts for this reaction. Complex **VO(L^{d})** has been chosen as catalyst to collect a wide substrate scope using internal epoxides, which cannot be found in literature. Among these, ten epoxides have been converted with excellent yields, while the remaining substrates, even more challenging to react with, define the limitation of this catalytic system giving lower yields. Finally, the coordination mode of propylene oxide, taken as a reference substrate, to complex **VO(L^{d})** was investigated. ^{51}V-NMR spectroscopy experiments together with crystallographic analysis, revealed

[63] a) Wolff, F.; Lorber, C.; Choukroun, R.; Donnadieu, B. *Inorg. Chem.* **2003** (42), 7839. b) Barroso, S.; Adão, P.; Madeira, F.; Duarte, M. T.; Pessoa, J. C.; Martins, A. M. *Inorg. Chem.* **2010** (49), 7452.

a species in which propylene oxide has been ring-opened by one of the phenoxo moiety of the aminotriphenolate ligand. Complex **VO(L^d)(PO)** was characterized with ^{1}H- and ^{51}V-NMR spectroscopy, MALDI-TOF mass spectrometry and X-ray analysis, demonstrating that complex **VO(L^d)** is able to coordinate propylene oxide activating it towards nucleophilic ring opening reactions.

4.5 Experimental

Vanadium(V)aminotriphenolate complexes **VO(L^d)** and **VO(L^h)** were synthesized as reported in *Chapter 3*.^{1}H-NMR,^{13}C-NMR and ^{51}V-NMR spectra were recorded at r.t. on Bruker AV-300, AV-400 or AV-500 spectrometers and referenced to the residual deuterated solvent signals. Diastereo-isomeric ratios (*dr´*s) were calculated from the corresponding ^{1}H NMR spectra using signal integration where possible; alternatively, integrable ^{13}C NMR spectra were recorded with a 500 MHz AV-500 spectrometer equipped with a cryoprobeusing at least 2048 scans. All reported NMR values are given in parts per million (ppm). FT-IR measurements were carried out on a Bruker Optics FTIR Alpha spectrometer equipped with a DTGS detector, KBr beam splitter at 4 cm^{-1} resolution. Mass spectrometric analyses and X-ray diffraction studies were performed by the Research Support Group at ICIQ, Tarragona. Commercially available epoxides, solvents, co-catalysts were purchased from various commercial sources (Acros, Aldrich and TCI) and used without further purification. Carbon dioxide (purchased from PRAXAIR) was used without further purification or drying *prior to* its use.

All reactions of the substrate scope (synthesis of cyclic carbonates **24d-s**) were performed in a 30 mL stainless steel reactor. As a typical experiment, cyclopentene oxide **17i** (336.5 mg, 4.0 mmol) was introduced in the inner Teflon vessel (30 mL) of an autoclave along with **VO(L^d)** (12 mg 0.005 mmol) and TBAB (64.8 mg, 0.05 mmol). Then, the reactor was purged with $CO_2$and the pressure was stabilized at 1.0 MPa. The reactor was heated to the required temperature (T = 85°C), and the mixture was then stirred for 18 hours. The autoclave was allowed to cool down by immersion in an ice bath for 1 hour before venting. The reaction mixture was diluted in $CDCl_3$ (2.0 mL) and a weighed quantity of mesitylene (typically around 0.5mol with respect to the epoxide substrate) was added. A quantitative ^{1}H-NMR determination was performed on samples consisting of 100 mL of this solution diluted with 0.5 mL of $CDCl_3$. After concentration of the crude reaction mixture in vacuo, the cyclic carbonate product **24i** (tetrahydro-4H-cyclopenta[d][1,3]dioxol-2-one) was

isolated upon purification through a silica gel flash-cromatography with etylacetate hexane 6 4 as eluents.

Characterization of cyclic carbonates 24d-s:

Tetrahydro-4H-cyclopenta[d][1,3]dioxol-2-one (24i): ^{1}H-NMR (300 MHz, 298 K, $CDCl_3$): δ = 5.13-5.05 (m, 2H), 2.19-20.07 (m, 2H), 1.85-1.57 (m, 4H); ^{13}C-NMR (75MHz, 298 K, $CDCl_3$): δ = 155.58 (C), 81.95 (CH), 33.28 (CH_2), 21.67 (CH_2); FTIR (neat): ν (cm^{-1}) =2973, 1781 (CO), 1371, 1334, 1217, 1165, 1145, 1108, 1042, 771.

Tetrahydrofuro[3,4-d][1,3]dioxol-2-one (24j): ^{1}H-NMR (400 MHz, 298 K, $CDCl_3$): δ=5.20 (dd, *J* = 2.2, 1.2 Hz, 2H), 4.26 (d, *J* = 12.4 Hz, 2H), 3.61-3.51 (m, 1H); ^{13}C-NMR (101 MHz, $CDCl_3$) δ 154.45 (C), 80.11 (CH), 73.16 (CH_2); FTIR (neat): ν (cm^{-1}) = 2935, 2876, 1778 (CO), 1463, 1369, 1272, 1238, 1169, 1115, 1091, 1052, 909, 768, 689.

Hexahydrobenzo[d][1,3]dioxol-2-one (24e): ^{1}H-NMR (400 MHz, 298 K, $CDCl_3$): δ = 4.73-4.66 (m, 2H), 1.96-1.86 (m, 4H), 1.70-1.59 (m, 2H), 1.49-1.38 (m, 2H).^{13}C NMR (101 MHz, $CDCl_3$) δ 155.32 (CO), 75.72 (CH), 26.77 (CH_2), 19.15 (CH_2); FTIR (neat): ν (cm^{-1}) = 2942, 2868, 1784 (CO), 1352, 1206, 1165, 1137, 1027, 995.

5-vinylhexahydrobenzo[d][1,3]dioxol-2-one (24l): ^{1}H-NMR (300 MHz, 298 K, $CDCl_3$): δ = 5.80-5.64 (m, 2H), 5.08-4.93 (m, 4H), 4.81-4.58 (m, 4H), 2.40-2.07 (m, 5H), 1.88-1.49 (m, 6H), 1.43-1.07 (m, 3H); ^{13}C NMR (75 MHz, $CDCl_3$) δ 155.19 (CO), 155.16 (CO), 141.05 (=CH), 140.96 (=CH), 114.29 (=CH_2), 114.00 (=CH_2), 76.03 (CH), 75.66 (CH), 75.17 (CH), 36.38 (CH), 33.91 (CH), 33.58 (CH_2), 31.70 (CH_2), 26.70 (CH_2), 25.81 (CH_2), 25.73 (CH_2), 25.08 (CH_2). FTIR (neat): ν (cm^{-1}) = 3080, 2938, 2866, 1790 (CO), 1640, 1356, 1144, 1028, 916, 779, 700.

5-(2-(trimethoxysilyl)ethyl)hexahydrobenzo[d][1,3]dioxol-2-one (24m): ^{1}H-NMR (400 MHz, 298 K, $CDCl_3$): δ = 4.79-4.73 (m, 1H), 4.72-4.58 (m, 3H), 3.55 (s, 9H), 3.54 (s, 9H), 2.35-2.03 (m, 4H), 1.47-1.87 (m, 6H), 1.46-1.08 (m, 7H), 1.01-0.88 (m, 1H), 0.68-0.53 (m, 4H); ^{13}C NMR (101 MHz, $CDCl_3$) δ 155.22 (CO), 155.18 (CO), 76.36 (CH), 75.99(CH), 75.51 (CH), 50.57 (CH_3), 35.25 (CH), 33.90 (CH_2), 32.34 (CH), 32.04 (CH_2), 29.05 (CH_2), 28.77 (CH_2), 26.81 (CH_2), 25.97 (CH_2), 25.57 (CH_2), 24.97 (CH_2). FTIR (neat): ν (cm^{-1}) =2928, 2841, 1794 (CO), 1451, 1354, 1189, 1140, 1066, 1028, 781.

Octahydro-2H-2,7-methanooxireno[2',3':5,6]indeno[1,2-d][1,3]dioxol-4-one (24n): ^{1}H NMR (400 MHz, $CDCl_3$) δ 5.05 (dd, *J* = 13.8, 6.1 Hz, 1H), 4.95 (d, *J* = 6.3 Hz, 1H), 3.17 (d, *J* = 3.0 Hz, 1H), 3.11 (d, *J* = 3.0 Hz, 1H), 2.75 (d, *J* = 2.5 Hz, 1H), 2.54 (s, 1H), 2.33 (ddd, *J* = 16.1, 7.9, 2.8 Hz, 1H), 2.33 (ddd, *J* = 16.1, 7.9, 2.8 Hz, 1H), 1.46 (dt, *J* = 10.1, 1.8 Hz, 1H), 0.91 (d, *J* = 10.1 Hz, 1H).^{13}C NMR (101 MHz, $CDCl_3$) δ 154.48 (CO), 84.60 (CH), 82.86 (CH), 50.62 (CH), 49.06 (CH), 48.53 (CH), 43.85 (CH), 40.03 (CH), 39.38 (CH), 32.53 (CH_2), 28.86 (CH_2); FTIR (neat): ν (cm^{-1}) = 2969, 1780 (CO), 1159, 1050, 846.

(Z)-3a,4,5,8,9,9a-hexahydrocycloocta[d][1,3]dioxol-2-one (24o): ^{1}H NMR (400 MHz, $CDCl_3$) δ 5.71-5.62 (m, 4H), 4.79-4.73 (m, 2H), 4.51-4.45 (m, 2H), 2.60-2.47 (m, 3H), 2.35-2.11 (m, 12H), 1.74-1.63 (m, 1H); ^{13}C NMR (101 MHz, $CDCl_3$) δ 154.31 (CO), 129.51 (CH), 129.43 (CH), 82.55 (CH), 80.27 (CH), 30.14 (CH_2), 27.87 (CH_2), 22.57 (CH_2), 20.71 (CH_2); FTIR (neat): ν (cm^{-1}) = 3019, 2928, 1793 (CO), 1452, 1378, 1346, 1216, 1175, 1138, 1045, 776, 715.

4,5-dimethyl-1,3-dioxolan-2-one (24r): ^{1}H NMR (400 MHz, $CDCl_3$) δ 4.83-4.75 (m, 2H, cis), 4.33-4.24 (m, 2H, trans), 1.41-1.35 (m, 6H, cis), 1.31-1.28 (m, 6H, trans); ^{13}C NMR (126 MHz, $CDCl_3$) δ 154.51 (CO), 79.91 (CH, trans), 76.05 (CH, cis), 18.25 (CH_3, trans), 14.26 (CH_3, cis); FTIR (neat): ν (cm^{-1}) = 2985, 1786 (CO), 1458, 1367, 1316, 1193, 1068, 998, 776, 700.

4,5-dimethyl-1,3-dioxolan-2-one (24d): ^{1}H NMR (400 MHz, $CDCl_3$) δ 4.83-4.75 (m, 2H, cis), 4.33-4.24 (m, 2H, trans), 1.41-1.35 (m, 6H, cis), 1.31-1.28 (m, 6H, trans); ^{13}C NMR (126 MHz, $CDCl_3$) δ 154.51 (CO), 79.91 (CH, trans), 76.05 (CH, cis), 18.25 (CH_3, trans), 14.26 (CH_3, cis); FTIR (neat): ν (cm^{-1}) = 2988, 1785 (CO), 1460, 1367, 1317, 1195, 1155, 1067, 998, 777.

4-methyl-5-phenyl-1,3-dioxolan-2-one (24h): ^{1}H NMR (400 MHz, $CDCl_3$) δ 7.46-7.40 (m, 3H), 7.38-7.33 (m, 2H), 5.13 (d, *J* = 8.0 Hz, 1H), 4.65-4.55 (m, 1H), 1.55 (d, *J* = 6.2 Hz, 3H); ^{13}C NMR (101 MHz, $CDCl_3$) δ 154.38 (CO), 135.16 (C), 129.84 (CH), 129.30 (CH), 126.09 (CH), 84.99 (CH), 80.85 (CH), 18.42 (CH_3); FTIR (neat): ν (cm^{-1}) = 2983, 2934, 1792 (CO), 1457, 1366, 1302, 1185, 1065, 1023, 764, 699.

4,5-diphenyl-1,3-dioxolan-2-one (24s): ^{1}H NMR (300 MHz, $CDCl_3$) δ 7.49-7.40 (m, 6H), 7.37-7.29 (m, 4H), 5.44 (s, 2H); ^{13}C-NMR (75MHz, 298 K, $CDCl_3$): δ = ^{13}C NMR (75 MHz, $CDCl_3$) δ

154.17 (CO), 134.83 (C), 129.88 (CH), 129.30 (CH), 126.17 (CH), 85.43 (CH); FTIR (neat): ν (cm^{-1}) = 3045, 3023, 2941, 1809 (CO), 1457, 1384, 1273, 1164, 1022, 907, 772, 724, 697, 628.

4,5-diphenyl-1,3-dioxolan-2-one (24g) Using the *cis* substrate, only the trans product has been purified. The characterization of this product is thus the same as **24g**.

Chapter 5

Bifunctional catalysts for CO_2 fixation into epoxides

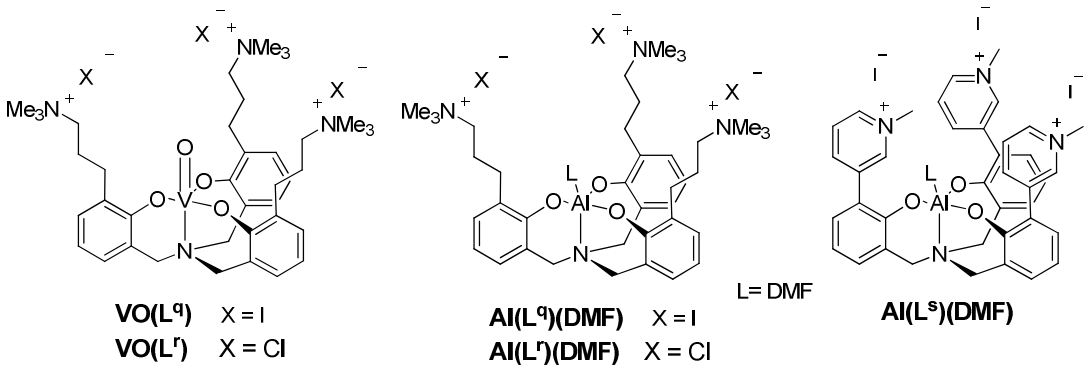

In recent years, the major advances in the field of cyclic and poly-carbonates synthesis starting from epoxides and CO_2 have been achieved using bifunctional catalysts. In these systems, the metal catalyst and the halide salts used as co-catalysts are linked together, exploiting the proximity effect to get higher catalytic activities respect to the binary systems. We have designed and synthesized five different bifunctional catalysts based on vanadium(V) and aluminum(III) aminotriphenolate complexes **VO(L^{q,r})** and **Al(L^{q,r,s})(DMF)** in which three ammonium or pyridinium salts - with halide anions as the nucleophiles - are linked to the ligand scaffold. This chapter reports the synthesis and characterization of these complexes, together with preliminary studies of catalytic activity studies for the synthesis of cyclic carbonates starting from epoxides and CO_2.

5.1 Introduction

Bifunctional catalysts represent the most recent advances to circumvent the problems that have been uncovered with traditional catalysts for the synthesis of cyclic and poly-carbonates starting from epoxides and CO_2.[1] Reviews concerning recent progress in the field discuss mostly about bifunctional complexes, especially when considering poly-carbonates synthesis.[1,2] In these systems, the nucleophile acting as co-catalyst is linked to the catalyst - usually is it part of the ligand scaffold - rather than being a separate molecule. A general representation of a bifunctional catalyst is depicted in *Figure 1*.

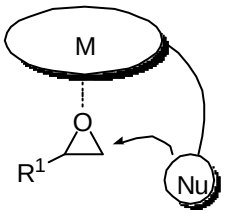

Figure 1 General representation of bifunctional catalysts for CO_2 fixation into epoxides: the nucleophile linked to the metal complex is in the appropriate position to attack the epoxide coordinated to the metal. A generic terminal epoxide has been employed in this picture.

The increase in the activity of these systems respect to traditional catalysts has to be ascribed to the proximity effect that the two catalytic entities have on catalysis when they are linked together. Homogeneous catalysts are considered to follow a cooperative mechanism (bimetallic or binary), as discussed in *Chapter 4*.[3] This explains the loss in activity at high dilutions (needed to overcome diffusion limitations and enhance TON and TOF values), which are often observed with these systems.[4] Mechanism considerations lead to the conclusion that the two interacting catalytic moieties need to be in spatial proximity to achieve high catalytic activity.[5] At high dilutions, the probability of formation of an active species by interaction of two catalyst molecules or a catalyst and a co-catalyst is therefore decreased and activities tend to drop. Therefore new strategies for the synthesis of cyclic and poly-carbonates starting from epoxides and CO_2 increasingly focus on dinuclear or binary linked systems.

[1] Klaus, S.; Lehenmeier, M. W.; Anderson, C. E.; Rieger, B. *Coord. Chem. Rev.* **2011** (255), 1460.
[2] Darensbourg, D. J.; Wilson, S. J. *Green Chem.* **2012** (14), 2665.
[3] a) Inoue, S. *CHEMTECH 6* **1976**, 588. b) Kuran, W. *Prog. Polym. Sci*. **1998** (23), 919. c) Kuran, W.; Listos, T. *Macromol. Chem. Phys.* **1994** (195), 977.
[4] Hino, Y.; Yoshida, Y.; Inoue, S. *Polym. J*. **1984** (16), 159.
[5] a) Tsuruta, T. *Makromol. Chem.* **1986** (6), 23. b) Kuran, W. *Appl. Organomet. Chem.* **1991** (5), 191. c) Kuran, W.; Listos, T. *Pol. J. Chem*. **1994** (68), 1071.

Concerning poly-carbonate synthesis, bifunctional systems have found to prevent back-biting side reactions and de-metallation processes that lead to low molecular weight polymers.[6] When talking about CO_2/epoxide co-polymerization, the formation of cyclic carbonates (which are more thermodinamically stable than polycarbonates, and thus easily formed) is considered a side reaction.[7] In general, a catalytic system is expected to give selectivity for one of the two transformations, in order to be competitive and industrially attracting. Selectivity for poly-carbonates over cyclic carbonates synthesis can be also enhanced by optimizing the reaction conditions, e.g. decreasing the reaction temperature or co-catalyst loading. The back-biting side reaction leading to cyclic carbonate and shorter polymers is represented in *Scheme 1*.[8]

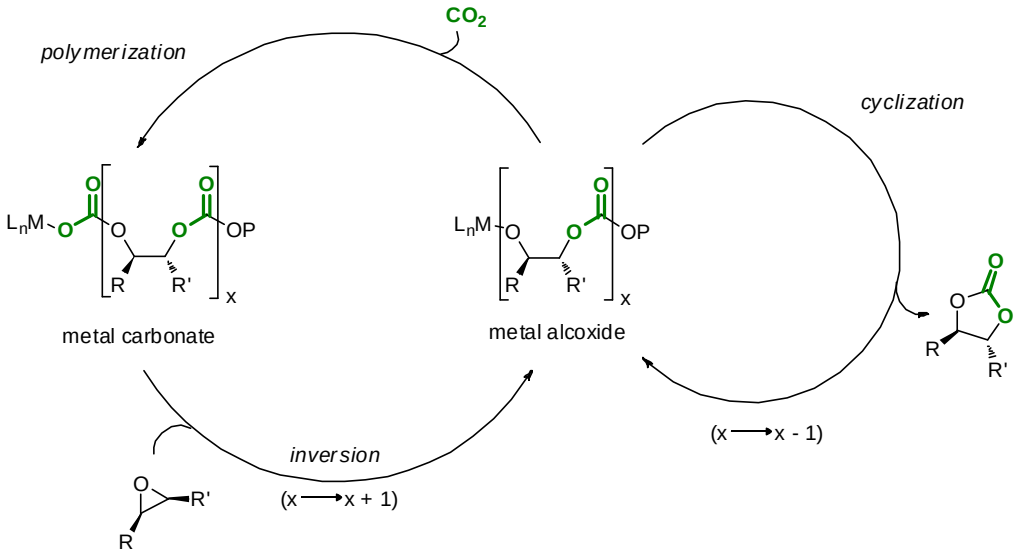

Scheme 1 Basic mechanism of epoxide/CO_2 copolymerization and the formation of cyclic carbonates via back-biting side reaction. From the metal alkoxide species a cyclic carbonate and the (x - 1) polymer is formed through an internal cyclization. (M = metal; L_n = ligand; P = polymer chain).

In most cases, cyclic carbonates are thought to be generated by the backbiting of the metal alkoxide into an adjacent carbonate linkage.[9] The thus formed (x-1) polymer enters again the polymerization cycle,[10] but this side pathway will lead to polymers with low molecular weight.[11]

[6] a) Nakano, K.; Kamada, T.; Nozaki, K. *Angew. Chem. Int. Ed.* **2006** (45), 7274. b) Sugimoto, H.; Ohtsuka, H.; Inoue, S. *J. Polym. Sci. Part A: Polym. Chem.* **2005** (43), 4172. c) Gao, L. G.; Xiao, M.; Wang, S. J.; Du, F. G.; Meng, Y. Z.; *J. Appl. Polym. Sci.* **2007** (104), 15.
[7] Luinstra, G. A.; Haas, G. R.; Molnar, F.; Bernhart, V.; Eberhardt, R.; Rieger, B. *Chem. Eur. J.* **2005** (11), 6298.
[8] Coates, G. W.; Moore, D. R. *Angew. Chemie - Int. Ed.* **2004** (43), 6618.
[9] Gorecki, P.; Kuran, W. *J. Polym. Sci. Part C* **1985** (23), 299.
[10] It is worth to note that in the case of epoxide/CO_2 copolymerization, the epoxide C - O bond cleavage tipically occurs with inversion of configuration at the site of attack (S_N2-type mechanism) to give the trans ring-opened product. Cyclic carbonates deriving from this side reaction pathway can be easily recognize from the *trans* configuration.
[11] Kuran, W.; Listos,T. *Macromol. Chem. Phys*. **1994** (195), 1011.

As these back-biting side reactions are thought to occur easier with the de-metalated metal alkoxide, a positively charged group anchored to the ligand scaffold, hanging in proximity of the catalytic center, should prevent back-biting by forming an ionic couple with the alkoxide, thus decreasing its reactivity.[2]

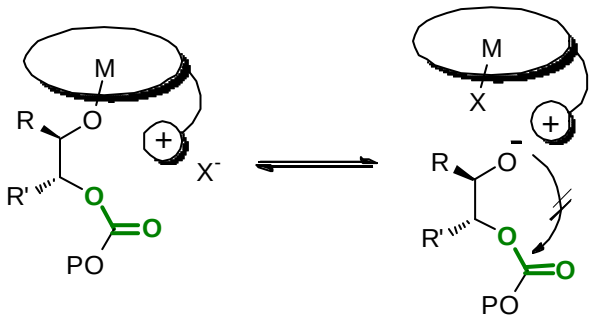

Scheme 2 Effect of a positively charged group anchored to the metal catalyst on back-biting side reactions. The alcoxide forms an ionic couple with the cationic group decreasing its reactivity through nucleophilic attack.

Scheme 2 shows a generic bifunctional catalyst in which the ligand scaffold is functionalized with a pending positively charged group. In such decorated complexes, the positively charged group is used both as a counterion for the nucleophilic co-catalyst (usually a halide anion) and to prevent back-biting reactions. In an event of metal alkoxide decomplexation, the formation of an ionic couple with the positively charged moiety will prevent the nucleophilic attack to form the cyclic carbonate. Moreover, the growing polymer will not diffuse away from the complex thus interrupting the chain growth. Eventually, it will coordinate back to the metal, to continue the CO_2/epoxide copolymerization. In this way, the formation of back-biting side products is prevented, and the polymer molecular weight is increased.[6a]

For all these reasons, it is easy to understand why new advances in this area concern mostly the development of bifunctional catalysts, as can be found in the most recent reviews.[1,2] The first example of bifunctional catalysts for CO_2/epoxide coupling was a cobalt catalyst functionalized with a piperidinyl and a piperidinium arms, reported by Nozaki and co-workers in 2006[6a] (*Scheme 3*). The key feature is the piperidinium arm which controls the nucleophilicity of the growing polymer chain by protonating the alkoxide moiety in case it is released from the cobaltate centre. The protonated propagating species is not nucleophilic enough to form cyclic carbonate through

back-biting, but it can react with carbon dioxide[12] or activated epoxide[13] once it is deprotonated by one of the piperidinyl groups.

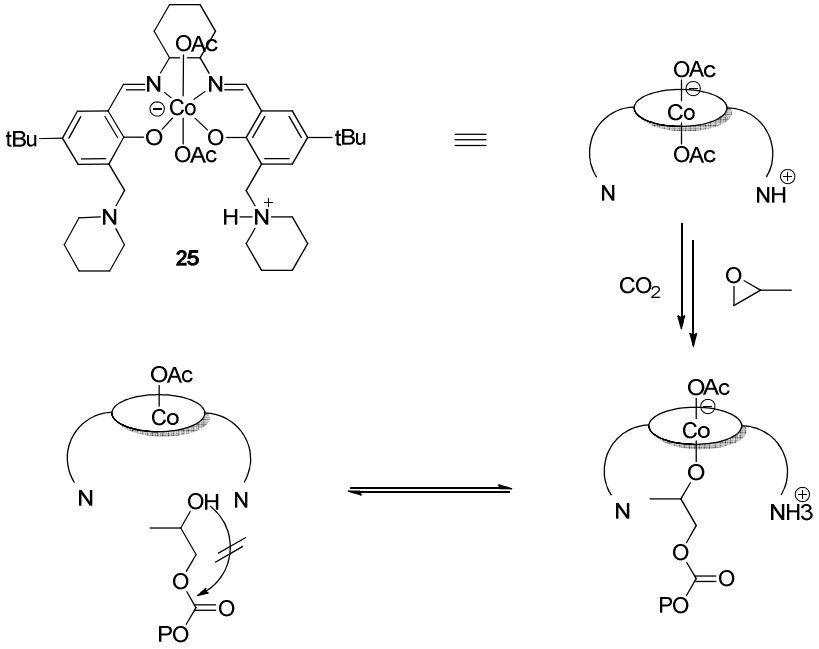

Scheme 3 Co-based bifunctional catalyst reported by Nozaki ad co-workers, designed to suppress the production of cyclic carbonate. P = growing polymer chain.

At high (80%) conversions, Co-based byfunctional catalyst **25** was able to maintain 96% selectivity for copolymer production when reactions were run in neat propylene oxide. Even at the comparatively high temperature of 60 °C, where most contemporary catalysts would only produce cyclic propylene carbonate, this catalyst was able to maintain 90% selectivity for polycarbonate production, though with low yields. The ability of bifunctional catalyst **25** to reduce the cyclic carbonate formation by protonating the alkoxide moiety opened up an entirely new branch of ligand design, whereby a single complex serves the combined purposes of both the catalyst and the co-catalyst. After this first work, more and more bifunctional catalysts started to appear in literature.

The following year, the second example of bifunctional systems in the field of polycarbonates synthesis was reported by Lee and co-workers.[14] The authors designed a cobalt salen complex bearing quaternary ammonium salts bound at the 5-position of each phenyl rings of the salen ligand

[12] Kuran, W.; Listos, T. *Macromol. Chem. Phys.* **1994** (195), 1011. c) Gorecki, P.; Kuran, W. *J. Polym. Sci. Polym. Lett.* **1985** (23), 299 .
[13] Luinstra, G. A.; Haas, G. R.; Molnar, F.; Bernhart, V.; Eberhardt, R.; Rieger, B. *Chem. Eur. J.* **2005** (11), 6298.
[14] Noh, E. K.; Na, S. J.; Sujith, S.; Kim, S.; Lee, B. Y. J. Am. Chem. Soc. **2007** (129), 8082.

(*Figure 2*, compound **26a**). This catalyst is able to operate at temperature of up to 90°C, achieving TOF values up to 3500 h^{-1}.

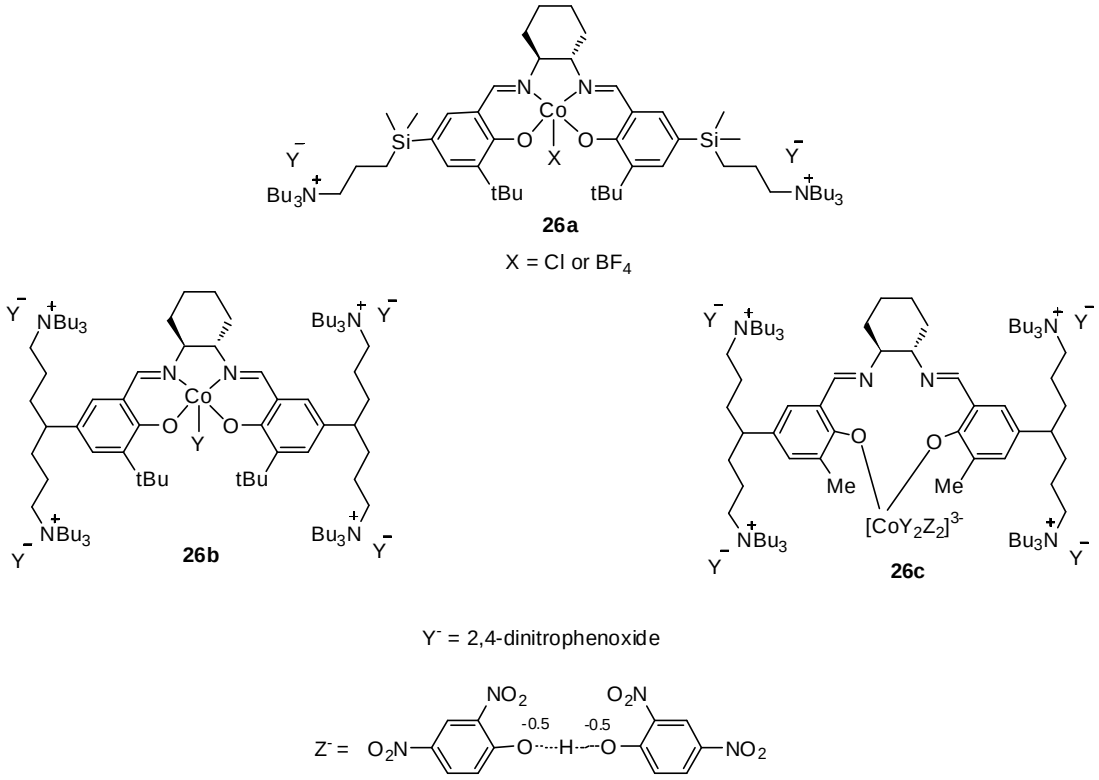

Figure 2 The highly active bifunctional catalysts synthesized by Lee and co-workers.

By combining the catalyst and the co-catalyst into one single molecule, the loading of catalyst could be decreased down to 0.05 mol%, which is more than ten times greater than that of traditional catalyst/co-catalyst systems. Complex **26b** and **26c**, functionalized with four quaternary ammonium salts, have shown to be even more active, among the most performing catalysts for this reaction.[15] Interestingly, the structure and activity of the complex rely strongly on the nature of the substituent at the 3-position of the phenyl rings. With a tert-butyl group (complex **26b**) the cobalt remains locked in the typical salen tetradentate pocket and the catalytic activity is high (TOF ≈ 1300 h^{-1}), though in the same realm of other catalysts.[15a] If a methyl group is placed at the 3-position (complex **5c**), the cobalt sits outside the salen pocket, coordinating to the four 2,4-dinitrophenoxide moieties.[15b] This unusual binding mode allows for the greatly increased activity and stability, with a TOF of >20 000 h^{-1} at 80 °C. Later improvements involved exchanging the 2,4-dinitrophenoxides for 2,4-dichlorophenoxides or 4-nitrophenoxides for increased laboratory safety.[16]

[15] a) Sujith, S.; Min, J. K.; Seong, J. E.; Na S. J.; and Lee, B. Y. *Angew. Chem., Int. Ed*. **2008** (47), 7306. b) Na, S. J.; Sujith, S.; Cyriac, A.; Kim, B. E.; Yoo, J.; Kang, Y. K.; Han, S. J.; Lee C.; Lee, B. Y. *Inorg. Chem*. **2009** (48), 10455.
[16] Yoo, J.; Na, S. J.; Park, H. C.; Cyriac A.; Lee, B. Y. *Dalton Trans*. **2010** (39), 2622.

Bifunctional catalysts similar to those reported in *Figure 2* have been employed recently to synthesize some novel high-valuable polycarbonates. A cobalt salen catalysts functionalized with ammonium salts was used by Grinstaff and co-workers for the synthesis of polyglyceric acid carbonate, a degradable analogue of polyacrilic acid.[17] High carbonate linkage selectivity (>99%) and high polymer/cyclic carbonate selectivity (90%) were achieved.

Another biocompatible polymer, poly(*tert*-butyl 3,4-dihydroxybutanoate carbonate), was synthesized by Darensbourg's research group in 2016 starting from *tert*-butyl 3,4-epoxybutanoate (a fatty acid derivative) and CO_2.[18] A bifunctional system based on cobalt or chromium salen complexes functionalized with quaternary ammonium salts was used as catalyst, reaching very high selectivities.

Other than ammonium salts, also neutral amines have been used as nucleophiles to design a bifunctional catalyst. *Figure 3* shows two examples of bifunctional catalysts with neutral functionalizations.

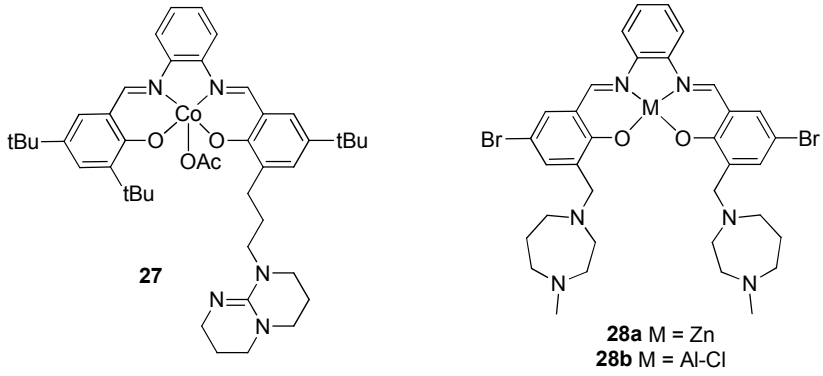

Figure 3 Bifunctional catalysts reported by Lu (complex **27**) and Jiang and co-workers (complex **28a-b**). In these case the ligand scaffold is functionalized with neutral nucleophilic arms that act as co-catalysts in epoxide/CO_2 copolymerization or cycloaddition reactions.

Complex **27**, featuring an appended 1,5,7-triabicyclo[4,4,0] dec-5-ene (TBD) sterically hindered base, was able to catalyze epoxide/CO_2 copolymerization reactions operating at temperatures as high as 100 °C, reaching a TOF of 10 900 h^{-1}, while maintaining 97% selectivity for the polymer.[19]

Complexes **28a-b** have been synthesized by Jiang and co-workers very recently[20] and were used as catalysts for CO_2 cycloaddition reactions to epoxides. The authors demonstrated the cooperative

[17] Zhang, H.; Lin, X.; Chin, S.; Grinstaff, M. W. *J. Am. Chem. Soc.* **2015** (137), 12660.
[18] Tsai, F. Te; Wang, Y.; Darensbourg, D. J. *J. Am. Chem. Soc.* **2016** (138), 4626.
[19] a) Ren, W.; Liu, Z.; Wen, Y.; Zhang, R.; Lu, X. *J. Am. Chem. Soc.* **2009** (131), 11509. b) Ren, W. M.; Liu, Y.; Xin, A. X.; Fu, S.; Lu, X. B. *Macromolecules* **2015** (48), 8445.
[20] a) Ren, Y.; Jiang, O.; Zeng, H.; Mao, Q.; Jiang, H. *RSC Adv.* **2016** (6), 3243. b) Ren, Y.; Chen, J.; Qi, C.; Jiang, H. *ChemCatChem* **2015** (7), 1535.

role of the couple catalyst/nucleophile and the effect of spatial proximity on catalysis reporting higher yields for the bifunctional catalysts respect to binary systems, even thought the differences binary/bifunctional catalysts are modest most of the times. The most significative case was achieved with complex **28a**: using propylene oxide as starting material, 100°C, 2MPa CO_2 pressure and 1 mol% catalysts, the bifunctional systems gave 90% yield in carbonate respect to 65% yield with the binary system.

A very systematic study concerning cycloaddition of CO_2 and epoxides with bifunctional catalysts has been addressed by Ema and co-workers, using functionalized metalloporphyrins. A fist set of zinc and magnesium porphyrins was synthesized, in which the ligand is functionalized with four chains ending with phosphonium, pyridinium or ammonium salts, as shown in *Figure 4*.[21,22]

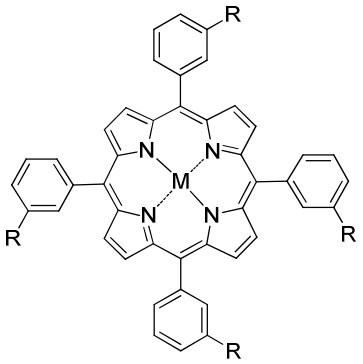

29a: M= Zn, R = $O(CH_2)_6P^+Ph_3Br^-$
29b: M= Mg, R = $O(CH_2)_6P^+Ph_3Br^-$
29c: M= Zn, R = $O(CH_2)_6N^+Bu_3Br^-$
29d: M= Mg, R = $O(CH_2)_6N^+Bu_3Br^-$
29e: M= Mg, R = $O(CH_2)_8N^+Bu_3Br^-$
29f: M= Mg, R = $O(CH_2)_4N^+Bu_3Br^-$
29g: M= Mg, R = $O(CH_2)_6N^+$ X^-
29h: M= Mg, R = $O(CH_2)_6N^+Bu_3Cl^-$
29i: M= Mg, R = $O(CH_2)_6N^+Bu_3I^-$
29k: M= Mg, R = $O(CH_2)_6N^+Pr_3Br^-$
29l: M= Mg, R = $O(CH_2)_6N^+Hex_3Br^-$
29m: M= Mg, R = $O(CH_2)_6N^+Oct_3Br^-$
29m: M= Mg, R = $O(CH_2)_6NEt_2$

Figure 4 First set of Mg(II) and Zn(II) porphyrins synthesized by Ema and co-workers.

With this set of catalysts the authors could investigate the effect that different metals (Mg and Zn), nucleophiles (iodide, bromide and chloride anions), chain lengths and substituents of the ammonium groups have on catalytic activities. This eventually led to a reasoned optimization of the catalyst, together with a deeper understanding of the system. In particular, the observations concerning the effect of different halides is of relevant interest for this thesis work. The authors found that the catalytic activity increases in the order **29i** < **29h** < **29d** (I^- < Cl^- < Br^-), which was explained considering that Cl^- has the higher nucleophilicity in aprotic solvents, while I^- has the highest leaving ability.[23] These results indicate that both the nucleophilicity and the leaving ability of halides are important for the catalytic activity of these complexes, although the former seems to be the more relevant as **29h** and **29d** are more active than **29i**.[21]

[21] Ema, T.; Miyazaki, Y.; Koyama, S.; Yano, Y.; Sakai, T. *Chem. Commun.* **2012** (48), 4489.
[22] Ema, T.; Miyazaki, Y.; Shimonishi, J.; Maeda, C.; Hasegawa, J. *J. Am. Chem. Soc*. **2014** (136), 15270.
[23] Smith, J. G. *Organic* Chemistry, 3rd ed.; McGraw-Hill: Singapore, **2011**.

The effect on catalytic activity of different substituents of ammonium groups were negligible, while considering the chain lengths, metal centre and the nature of counterions (ammonium or phosphonium salts), the best bifunctional system was found to be complex **29d**. Using 1,2-epoxyhexane as substrate, neat conditions and 120°C as reaction temperature, this catalyst showed a TON of 103000. The respective binary system, composed of (5,10,15,20-tetraphenylporphyrinato) magnesium(II) (Mg(TPP)) and tetrabutylammonium bromide (TBAB) showed much lower catalytic activity (TON = 5,000) under otherwise identical reaction conditions. These results clearly indicate the cooperation of the two functional groups within the same molecule.

Shortly after this work, the same group reported some highly active bifunctional diporphyrins and triporphyrins (*Figure 5*), which showed improved catalytic activities compared to the monomers (**29c** and **29d**).[24] Very high turnover numbers were obtained: 220000 for magnesium catalyst **30b** and 310000 for zinc catalyst **30a**. These systems are among the most active catalysts reported for cyclic carbonate synthesis starting from CO_2 and epoxide.

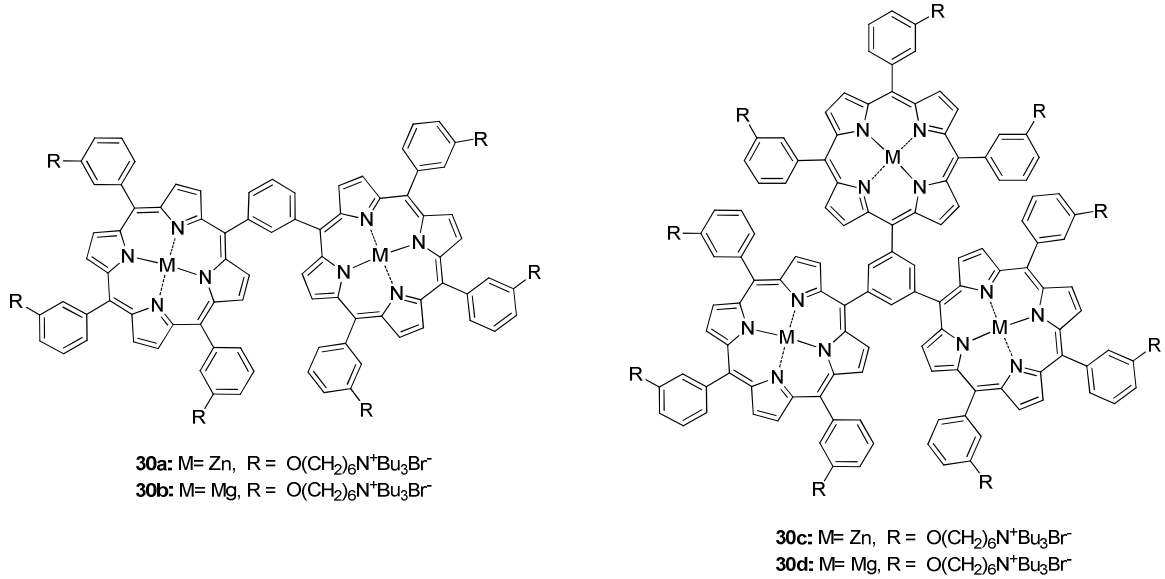

Figure 5 Structures of bifunctional diporphyrins and triporphyrins reported by Ema and co-workers.

To date, the number of publications concerning bifunctional catalysts for CO_2 valorization is rapidly increasing,[25] yet only salen (or salphen) ligands and porphyrines have been used as scaffolds for the catalyst functionalization.

[24] Maeda, C.; Taniguchi, T.; Ogawa, K.; Ema, T. *Angew. Chem. Int. Ed.* **2015** (54), 134.

[25] Some selected examples from the last two years: a) Duan, S.; Jing, X.; Li, D.; Jing, H. *J. Mol. Catal. A Chem.* **2016**, (411*)*, 34. b) Lang, X. D.; Yu, Y. C.; He, L. N. *J. Mol. Catal. A Chem.* **2016** (420), 208. c) Leng, Y.; Lu, D.; Zhang, C.; Jiang, P.; Zhang, W.; Wang, J. *Chem. - A Eur. J.* **2016** (22), 8368. d) Liu, M.; Li, X.; Lin, X.; Liang, L.; Gao, X.; Sun, J. **2016** (412), 20. e) Maeda, C.; Shimonishi, J.; Miyazaki, R.; Hasegawa, J. Y.; Ema, T. *Chem. - A Eur. J.* **201** (22), 6556. f) Ren, Y.; Jiang, O.; Zeng, H.; Mao, Q.; Jiang, H. *RSC Adv.* **2016** (6), 3243. g) Yue, T. J.; Ren, W. M.; Liu, Y.; Wan,

Based on the expanding interest for bifunctional systems, and considering the rooted expertise of our research group in aminotriphenolate ligands functionalization, a project was set for the present PhD thesis concerning the design and synthesis of aminotriphenolate-based bifunctional catalysts for CO_2 fixation.

As a first approach, using an established synthetic procedure developed previously in our group, the 3-(trimethylammonium)phenyl functionalized aminotriphenolate ligand $\mathbf{L^pH_3}$ was prepared (*Figure 6*), in order to prepare vanadium(V) and aluminum(III) functionalized catalysts.

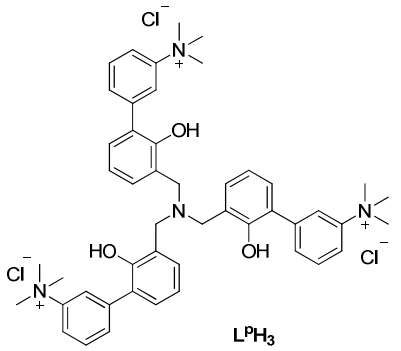

Figure 6 Aminotriphenolate ligand functionalized with N,N,N-trimethylaniline.

Unfortunately, this ligand was found to be highly unstable in air: only few days after the synthesis, ^{1}H-NMR analysis clearly indicated significant decomposition. Aromatic ammonium salts are not stable enough to be used as pending moieties for ligand functionalization. Thus, we designed ligand $\mathbf{L^qH_3}$, in which aliphatic rather than aromatic ammonium salts have been chosen as pendant groups, as shown in *Figure 7*.

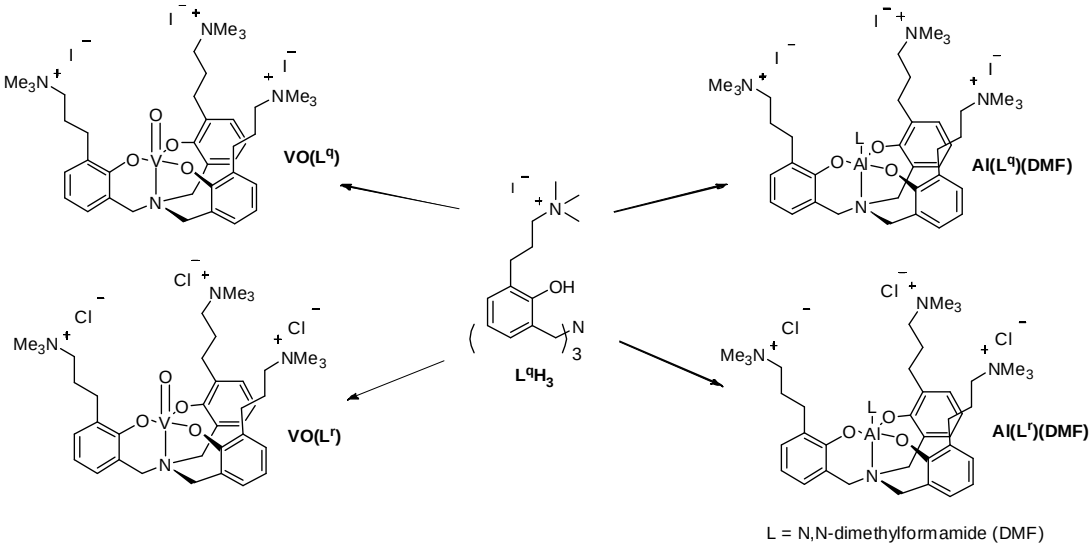

Figure 7 Aminotriphenolate ligand $\mathbf{L^qH_3}$ and vanadium(V) and aluminum(III) bifunctional catalysts synthesized within this thesis project.

Z. Q.; Lu, X. B. *Macromolecules* **2016** (49), 2971. h) Büttner, H.; Lau, K.; Spannenberg, A.; Werner, T. *ChemCatChem* **2015** (7), 459. i) Kohrt, C.; Werner, T. *ChemSusChem* **2015** (8), 2031.

Aminotriphenolate ligand $\mathbf{L^qH_3}$, functionalized with three C3 alkylic chains ending with ammonium salts, has been synthesized and successfully employed for the synthesis of vanadium(V) and aluminum(III) bifunctional catalysts $\mathbf{VO(L^{q,r})}$ and $\mathbf{Al(L^{q,r})(DMF)}$. Iodide (complexes $\mathbf{VO(L^q)}$ and $\mathbf{Al(L^q)(DMF)}$) and chloride (complexes $\mathbf{VO(L^r)}$ and $\mathbf{Al(L^r)(DMF)}$) anions have been chosen as nucleophiles for these systems, considering both nucleophilicity and synthetic convenience.
Moreover, aminotriphenolate ligand $\mathbf{L^sH_3}$ has been designed and synthesized, in which the ligand scaffold is functionalized with three pyridinium salts. This compound has been used as substrate for the synthesis of aluminum(III) and vanadium(V) complexes $\mathbf{VO(L^s)}$ and $\mathbf{Al(L^s)(DMF)}$, but only catalyst $\mathbf{Al(L^s)(DMF)}$ was isolated with a good yield and has been characterized. ^{1}H-NMR and mass spectrometry analysis of complex $\mathbf{VO(L^s)}$ revealed only a complex mixture of unknown species.

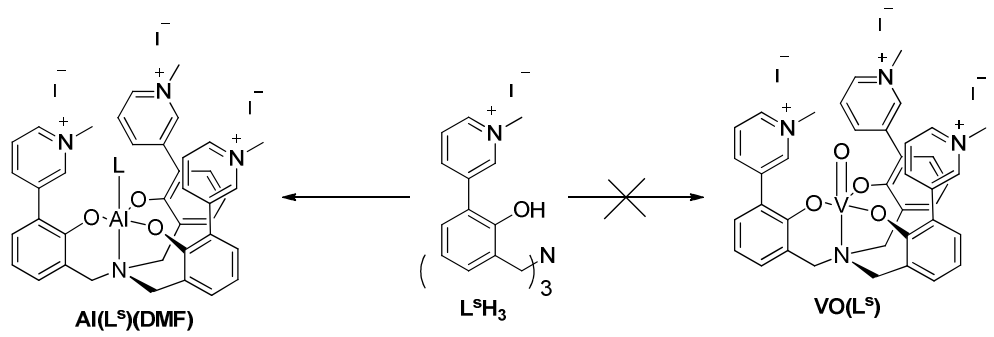

Figure 8 Synthesis of Al(III) aminotriphenolate complex $\mathbf{Al(L^s)(DMF)}$ from ligand $\mathbf{L^sH_3}$.

In summary, bifunctional catalysts $\mathbf{VO(L^{q,r})}$ and $\mathbf{Al(L^{q,r,s})(DMF)}$ have been synthesized and characterized. These complexes have been tested as catalysts for the synthesis of cyclic and poly-carbonates starting from CO_2 and epoxides in the laboratory of Prof. Arjan Kleij in which I spent three months in the frame of CARISMA COST Action CM1205. We devoted particular attention in comparing the activity of these bifunctional catalysts to the most similar binary systems, in order to get a clear understanding of the importance of spatial proximity in this binary catalytic mechanism.
Synthesis of the ligands and corresponding metal complexes, characterization and catalytic activity studies of these complexes will be thoroughly discussed in the following sections.

5.2 Synthesis of bifunctional catalysts

A first entry in the synthesis of bifunctional catalysts has been attempted with aminotriphenolate ligand $\mathbf{L^pH_3}$. The idea was to make use of a synthetic procedure set up previously in our group,[26] in which the Suzuki-Miyaura coupling reaction is the key step to decorate the aminotriphenolate scaffold with a functionalized aromatic group (step *d* in *Scheme 4*), as discussed in *Chapter 1*.

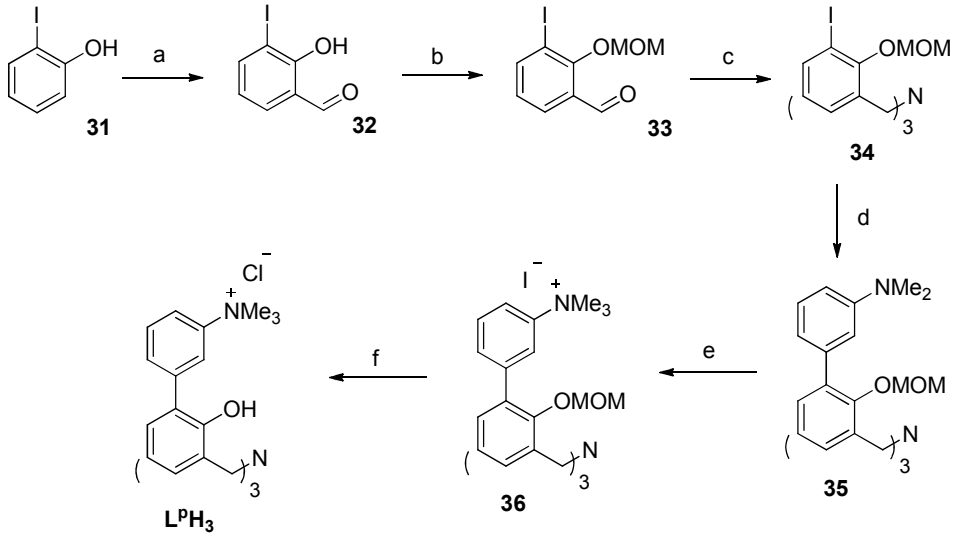

Scheme 4 Synthetic procedure for the preparation of aminotriphenolate ligand $\mathbf{L^pH_3}$. MOM: methoxymethyl. a: $MgCl_2$, Et_3N, $(CH_2O)n$, dry THF, RT, overnight, 70% yield; b: MOMCl, Et_3N, dry THF, RT, overnight, 95% yield; c: NH_4OAc, $NaBH(OAc)_3$, dry DMF, reflux, 10h, 60% yield; d: N,N-dimethyl-3-aminoboronic acid, $Pd(PPh_3)_4$, K_2CO_3, dioxane, reflux 10h, 82% yield; e: MeI, DCM, reflux, 18h, 37% yield; f: HCl 1M in MeOH, reflux, 5h, 92% yield;

Steps a-c of *Scheme 4* represent the synthetic procedure for the preparation of aminotriphenolate ligands established by our research group,[27] therefore no optimization of reaction conditions was required. *Ortho*-iodo phenol **31** is used as starting material, which is first formylated in the *ortho* position. The phenolic group on salicylic aldehyde **32** is protected as methoxymethylether by reaction with MOMCl and then, intermediate **33** undergoes a three-fold reductive amination to give the three-iodo protected aminotriphenolate ligand **34**. This is an ideal substrate for the Suzuki-Miyaura coupling reaction, which was found to be an excellent functionalization method as well in this case. Compound **34** was treated with the commercially-available *N*,*N*-dimehtyl-3-aminoboronic acid using $Pd(PPh_3)_4$ as catalyst, to give the decorated ligand **35** in 70% yield after flash-cromatography purification. Then, the methylation of *N*,*N*-dimethylaniline moiety using

[26] Badetti, E.; Wurst, K.; Licini, G.; Zonta, C. *Chem. - A Eur. J.* **2016** (22), 6515.
[27] Licini, G.; Mba, M.; Zonta, C. *Dalton Trans.* **2009** (27), 5265–5277.

methyliodide provided intermediate **36**, which contains the three ammonium salts needed as co-catalysts for CO_2 coupling reactions with epoxides. The MOM group on **36** was then removed under acidic conditions, to give the final triphenoamine $\mathbf{L^pH_3}$, which was successfully characterized. Unfortunately, as reported before, this compound was found to be not stable in air, even as a solid: ^{1}H-NMR analysis showed clearly significant decomposition of the ligand few days after the synthesis and characterization (*Figure 9*).

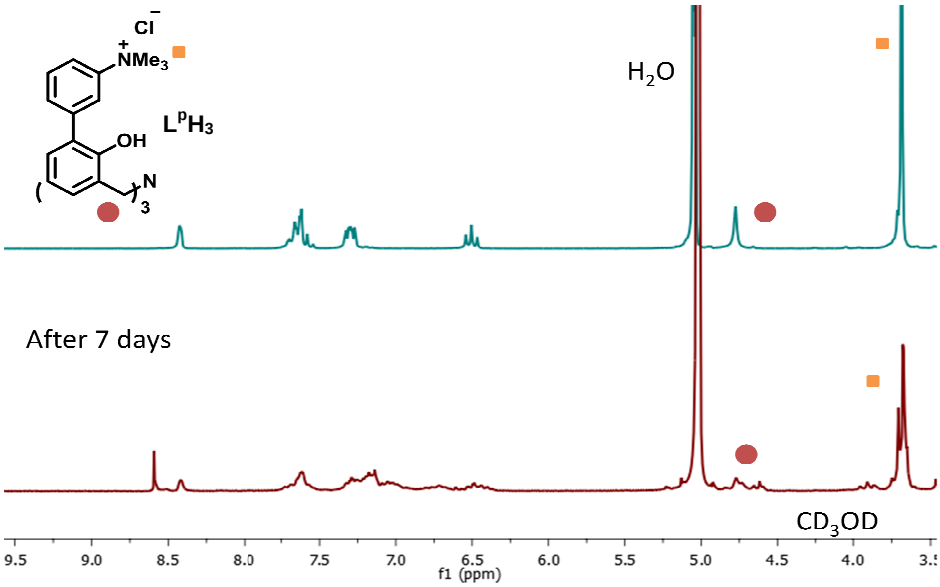

Figure 9 ^{1}H-NMR spectra of ligand $\mathbf{L^pH_3}$ that show the decomposition: after 7 days, signals of aromatic protons, methylene (red circle) and methyl (orange square) groups have definitely become broad and split.

Aromatic ammonium salts are then not stable enough, probably because of the good ability of trimethylamine as a leaving group, to be used for ligand functionalization. To overcome the instability problem, we designed aminotriphenolate ligand $\mathbf{L^qH_3}$, functionalized with aliphatic ammonium salts.

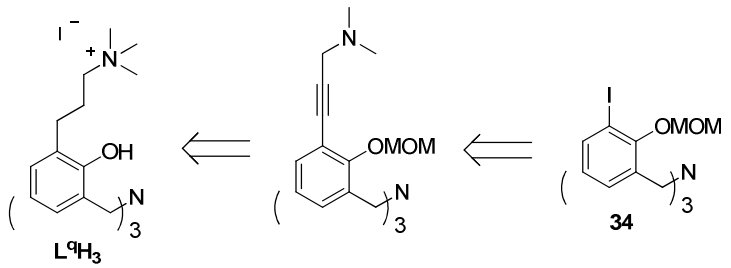

Scheme 5 Design of functionalized aminotriphenolate ligand $\mathbf{L^qH_3}$.

The choice of a C3 alkyl chain was due to synthetic reasons, as an easy way to prepare this ligand can be the use of Sonogashira coupling reaction starting from the three-iodo aminotriphenolate ligand **34** and the commercially available N,N-dimethylaminopropyne, a C3 functionalized alkyne (*Scheme 5)*. The flexible nature of the resulting alkylic chain would lead to a bifunctional system able to adapt to the substrate, adopting the most favorable conformation.

The three-fold Sonogashira coupling using $Pd(PPh_3)_4$ and CuI as catalysts between the three-iodo substituted triphenolamine **34** and *N,N*-dimethylaminopropyne provided functionalized ligand **37** (*Scheme 6*). An optimization of reaction conditions and purification procedures was required in order to obtain good yields and minimize the by-product deriving from the homo-coupling reaction between two alkynes. A yield of 60% has been reached after purification via silica gel flash-chromatography and precipitation of the product with cold hexane.

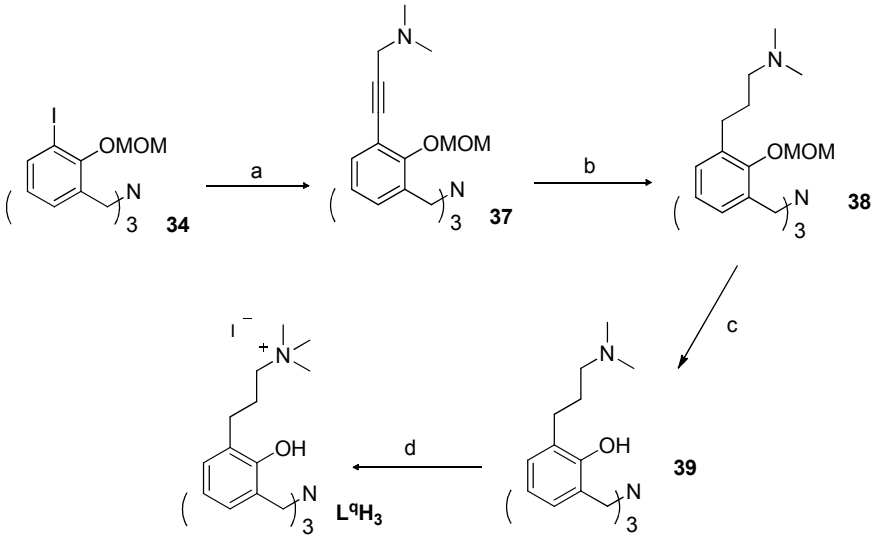

Scheme 6 Synthetic procedure for the preparation of aminotriphenolate ligand $\mathbf{L^qH_3}$. MOM: methoxymethyl. a: N,N-dimethylaminopropyne 6eq, $Pd(PPh_3)_4$, CuI, triethylamine, dry THF, reflux 24h, 60% yield; b: H_2 1 atm, Pd/C, EtAcO RT, 2 days, 70% yield; c: HCl in MeOH, reflux 5h, 85% yield; d: MeI, DCM, 56% yield;

The subsequent step is a Pd/C catalyzed hydrogenation to reduce the alkynyl substituent to a flexyble alkylic chain. Ligand **38**, bearing three (*N,N*-dimethylamino)-propyl chains, was synthesized in good yields after the optimization of reaction conditions. The phenolic protecting group was removed using an HCl solution in methanol as in the previous synthetic pathway, leading to deprotected triphenolamine **39** in 85% yield. Finally, the three amino groups have been methylated using methyl iodide in DCM at room temperature, providing the wanted compound $\mathbf{L^qH_3}$, in which the aminotriphenolate scaffold is functionalized with three ammonium salts, bearing iodide as counterions. Aminotriphenolate ligand $\mathbf{L^qH_3}$, together with all synthesis intermediates, has

been characterized through ^{1}H- and ^{13}C-NMR spectroscopy, IR spectroscopy and mass spectrometry. *Figure 10* shows the ^{1}H-NMR spectrum of the ligand in DMSO-d_6.

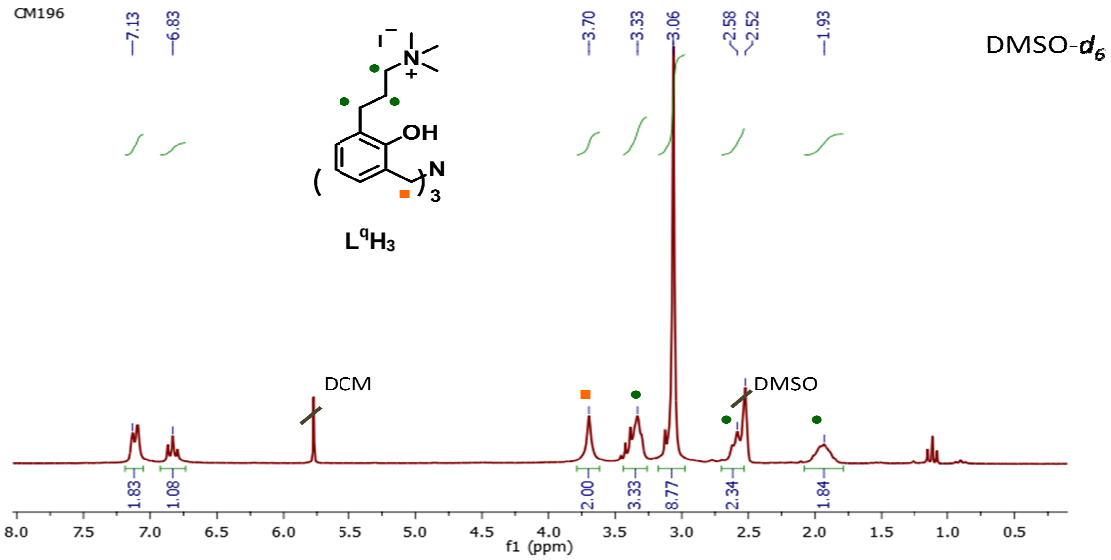

Figure 10 ^{1}H-NMR spectrum of aminotriphenolate ligand $\mathbf{L^qH_3}$ in DMSO-d_6. Integrations refers to one branch of the triphenolate ligand. The simmetry of the signal pattern reveal that the three branches of the ligand are identical.

To make sure of the stability of the ligand functionalized with alkyl ammonium salts, ^{1}H-NMR control analysis have been performed one week, one and three months after the synthesis, revealing no changes in the product signals.

From the works present in literature about bifunctional catalysts for CO_2/epoxide coupling reactions, it is evident that different nucleophiles can lead to dramatic changes in the catalytic activity of these systems. For this reason, in order to build up two sets of bifunctional systems with different nucleophiles, we searched for a valid method to exchange iodide counterions of ligand $\mathbf{L^qH_3}$ with chloride anions.

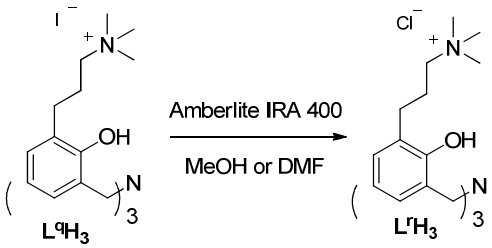

Scheme 7 Anion exchange on ligand $\mathbf{L^qH_3}$ using the anion exchange resin Amberlite IRA 400.

The best method was found to be the anion exchange resin Amberlite IRA 400, a trimethylammonium functionalized resin with chloride as counterions. Dissolving ligand $\mathbf{L^qH_3}$ in dry methanol or DMF, and stirring it with an excess of the resin for 3 hours, the anion exchange could be detected using mass-spectrometry (*Figure 11*) and NMR spectroscopy analysis. ^{1}H-NMR spectroscopy cannot reveal if there are iodide or chloride counterions in the lignad, but it gives precious information about the symmetry of the molecule (see *Figure 10*). ^{1}H-NMR spectrum of $\mathbf{L^rH_3}$ presents small changes in chemical shifts of resonances respect to $\mathbf{L^qH_3}$ (see *Experimental part*) maintaining the same set of signals, indicating that the symmetry of the ligand is retained. This reveals that something has changed in the molecule, and that this change has taken place at all three branches symmetrically.

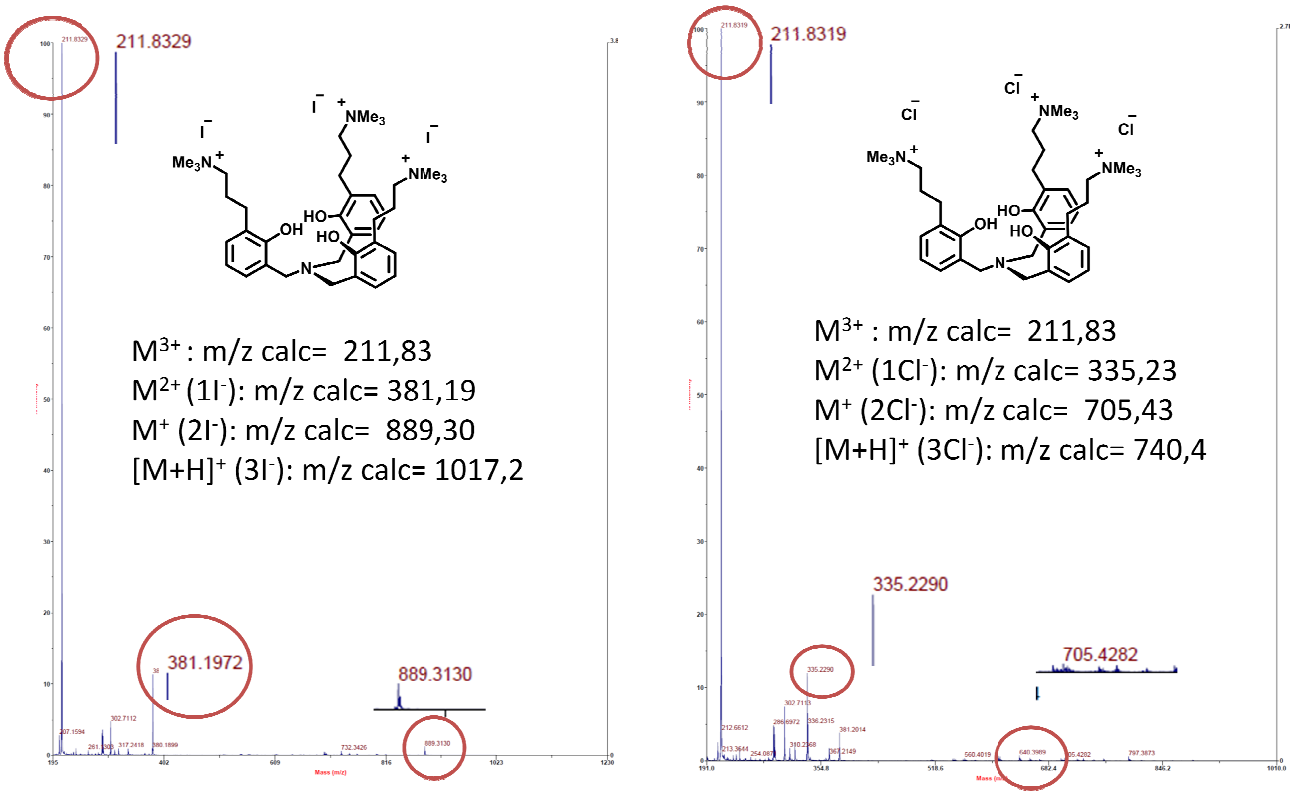

Figure 11 Mass spectrometry spectra of ligand $\mathbf{L^qH_3}$ (on the left), and $\mathbf{L^rH_3}$ after the treatment with the anion exchange resin (on the right). The chemical structure of ligands is reported, together with the calculated m/z values for the species detectable in the mass spectrometry analysis. Highlighted with red circles, the found m/z values are reported for each ligand. Zooms of signals have been placed in this figure because of the poor visibility of the image.

ESI-MS analysis allowed to detect the peak relative to M^{3+} major species at m/z = 211.83, which was expected for both the ligands. Furthermore, M^{2+} and M^+ species with 1 ore 2 iodides or chlorides have been detected. These species originate from the complete or partial disassociation of the ionic couples during the electron-spray process. According to these observations, we can assume that ligand $\mathbf{L^qH_3}$ and $\mathbf{L^rH_3}$ have been successfully prepared. Together, NMR and MS

techniques demonstrated that chloride anions have been exchanged with iodides of ligand **LqH3**, and that this exchange took place at all the three pending groups.

Aminotriphenolate ligand $\mathbf{L^qH_3}$ has been successfully employed as the starting material for the synthesis of vanadium(V) and aluminum(III) complexes $\mathbf{VO(L^{q,r})}$ and $\mathbf{Al(L^{q,r})(DMF)}$ shown in *Scheme 8*.

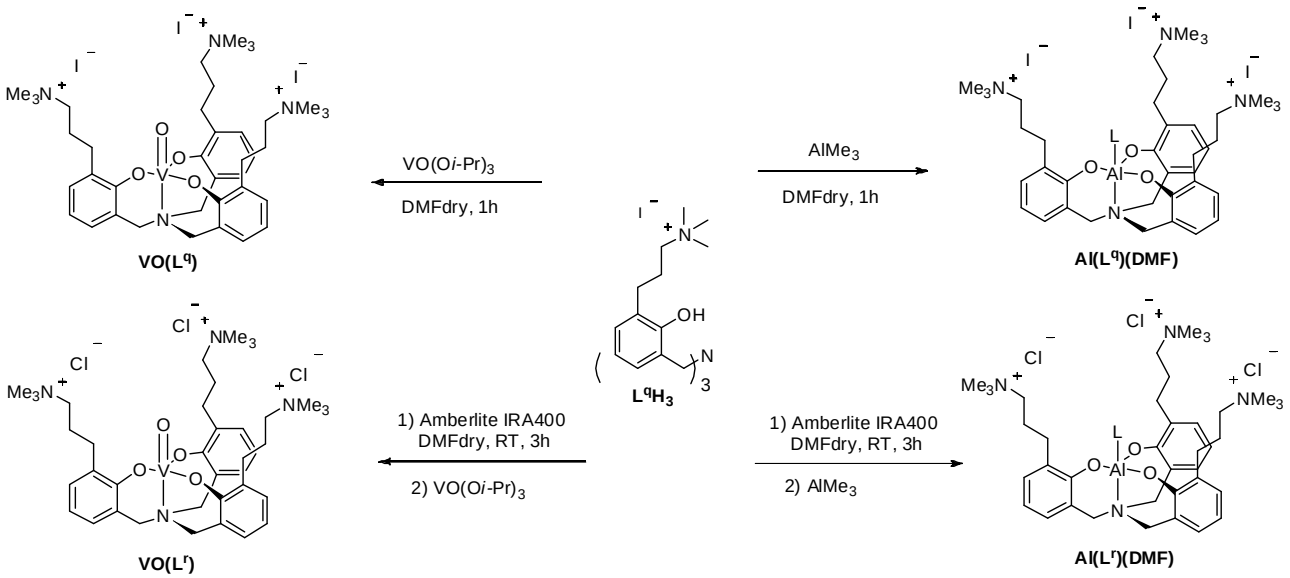

Scheme 8 Synthesis of vanadium(V) and aluminum(III) aminotriphenolate complexes $\mathbf{VO(L^{q,r})}$ and $\mathbf{Al(L^{q,r})(DMF)}$ starting from ligand $\mathbf{L^qH_3}$. L = DMF.

To prepare complexes $\mathbf{VO(L^q)}$ and $\mathbf{Al(L^q)(DMF)}$, bearing iodide as counterions, ligand $\mathbf{L^qH_3}$ was stirred at room temperature with one equivalent of VO(O*i*-Pr)$_3$ and $AlMe_3$, respectively. After one hour, ^{1}H-NMR analysis showed quantitative conversions. Complexes $\mathbf{VO(L^q)}$ and $\mathbf{Al(L^q)(DMF)}$ have been characterized with IR spectroscopy, ^{1}H- and ^{13}C-NMR spectroscopy and mass spectrometry. For the synthesis of complexes $\mathbf{VO(L^r)}$ and $\mathbf{Al(L^r)(DMF)}$, bearing chloride as counterions, ligand $\mathbf{L^qH_3}$ was first treated with Amberlite IRA 400 anion exchange resin as explained before. After three hours, the metal precursors were added. Also in this case, one hour was enough to get complete conversions. Complexes $\mathbf{VO(L^r)}$ and $\mathbf{Al(L^r)(DMF)}$ have been characterized with IR spectroscopy, ^{1}H- and ^{13}C-NMR spectroscopy. Mass spectrometry furnished a clear identification only of complex $\mathbf{VO(L^r)}$.

Finally, the synthesis of ligand **LsH3** has been set up (*Scheme 9*). Starting with the three-iodo substituted aminotriphenolate ligand **34**, this synthesis takes advantage of the well-known Suzuki-Miyaura coupling reaction, which has been previously described. Using an excess of 3-pyridinyl boronic acid and Pd(PPh$_3$)$_4$ as the palladium catalyst, intermediate **40** was obtained in 78% yield.

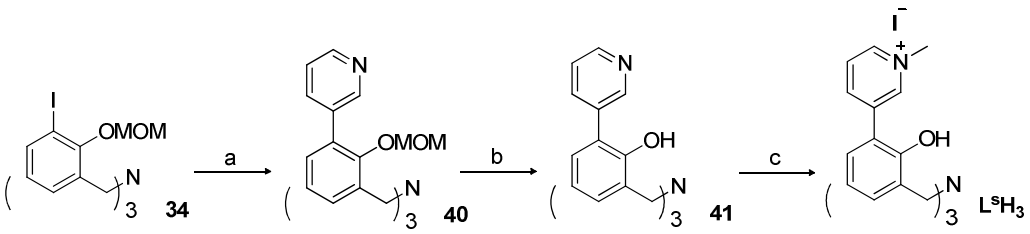

Scheme 9 Synthesis of ligand aminotriphenolate ligand $\mathbf{L^sH_3}$ functionalized with pyridinium units. a: 3-pyridinyl boronic acid, $Pd(PPh_3)_4$, Na_2CO_3, dioxane, reflux 10h, 78% yield; b: HCl 1M in MeOH, reflux, 5h, 65% yield; c: MeI, ACN, reflux, 18h, 46% yield;

The hydrolysis of methoxymethyl with HCl in MeOH gave aminotriphenolate ligand **41** (65% yield), which was then methylated using methyliodide. Harsher reaction conditions (ACN at reflux) were used respect those employed for the synthesis of ligand $\mathbf{L^qH_3}$, due to the lower nucleophilicity of pyridinyl substituents. Eventually, aminotriphenolate ligand $\mathbf{L^sH_3}$, substituted with three methylated pyridinium moieties has been obtained in 46% yields and characterized via ^{1}H- and ^{13}-C NMR spectroscopy and IR spectroscopy.

Ligand $\mathbf{L^sH_3}$ was then used as starting material for the synthesis of vanadium(V) and aluminum(III) complexes (*Scheme 10*).

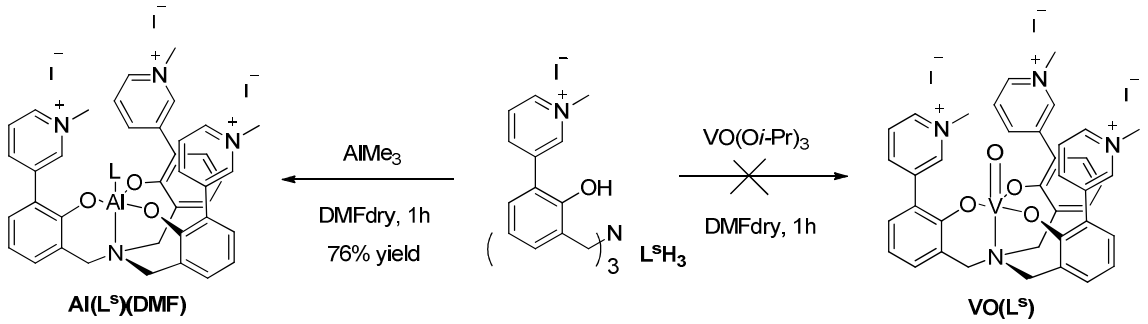

Scheme 10 Synthesis of aluminum(III) aminotriphenolate complex **Al(L^s)(DMF).** Preparation of vanadium(V) aminotriphenolate complexes **VO(L^s)** was not successful. L = DMF.

Using the reaction conditions optimized for complexes **VO(L^q)** and **Al(L^q)(DMF)**, aluminum(III) aminotriphenolate complex **Al(L^s)(DMF)** was synthesized using one equivalent of $AlMe_3$ and characterized through ^{1}H- and ^{13}C-NMR spectroscopy and IR spectroscopy. On the contrary, the synthesis of vanadium(V) complex **VO(L^s)** under the standard reaction conditions was not successfully. Changes in color while manipulating the complex anticipated the difficulties in the characterization of this complex, which gave unclear NMR spectra. The synthesis was not studied in further details and the complex was not used in the following catalytic studies.

5.3 Catalytic activity studies of bifunctional catalysts

Vanadium(V) and aluminum(III) aminotriphenolate complexes **VO(L^{q,r})** and **Al(L^{q,r,s})(DMF)** have been tested as catalysts in the synthesis of cyclic and poly-carbonates starting from epoxides and CO_2. Particular attention has been devoted to the comparison between bifunctional and binary systems (*Figure 12*), in order to evaluate the importance of having the two catalytic sites linked together. Especially for the synthesis of cyclic carbonates from CO_2 and epoxides, very few examples of comparison between similar bifunctional and binary systems are present in literature.

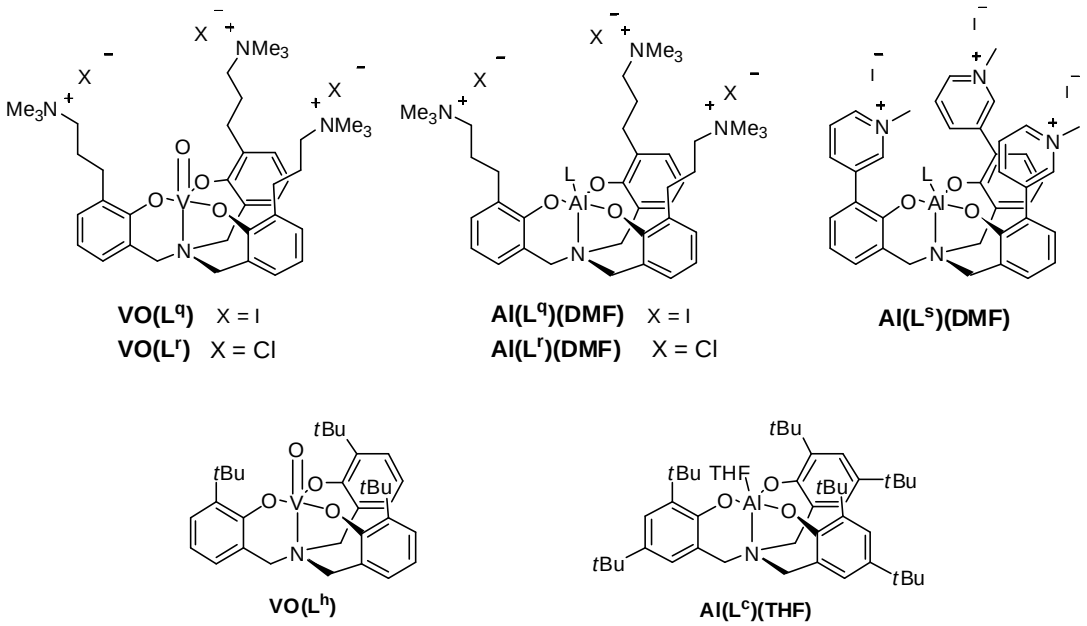

Figure 12 Bifunctional catalysts **VO(L^{q,r}) and Al(L^{q,r,s})(DMF)** tested in CO_2/epoxide coupling reactions and non-functionalized vanadium(V) and aluminum(III) aminotriphenolate complexes **VO(L^{h})** and **Al(L^{c})(THF)** used as comparison. L = DMF.

Vanadium(V) and aluminum(III) aminotriphenolate complexes **VO(L^{h})** and **Al(L^{c})(THF)**, together with three equivalents of tetrabutylammonium iodide (TBAI) and bis(triphenylphosphyne)iminium chloride (PPNCl)[28] have been chosen as comparative binary systems.

Preliminary results, conducted under neat conditions at 45°C with 1,2-epoxyhexane as substrate using bifunctional complexes **VO(L^{q})** and **Al(L^{q})(DMF)** (X = I), showed that the two complex are active but they gave low conversions (

[28] PPNCl has been chosen as chloride nucleophile for the binary systems as tetrabutylammonium chloride (TBAC) starts melting at room temperature, rendering the weighing difficult.

Table 1). We assigned the scarce activity to the low solubility of bifunctional catalysts (bearing three ammonium salts) in the epoxide.

Table 1 Cycloaddition of CO_2 to 1,2-hepoxyhexane **6** using complex **VO(L^q) and Al(L^q)(DMF)** as catalysts, in neat conditions at 45°C. Catalytic activities of bifunctional catalysts have been compared to the binary system composed by **VO(L^h)** and TBAI.

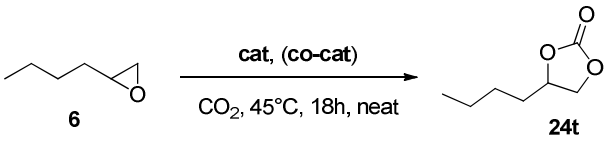

Entry	cat	co-cat	Yield (%)[a]
1	**VO(L^h)** (R^1 = *t*Bu, R^2 = H)	TBAI	58
2	**VO(L^q)** (X = I)	-	10
3	**Al(L^q)(DMF)** (X = I)	-	6

Reaction conditions: [**6**] = 2 mmol, [**cat**] = 0.1 mol%, [**co-cat**] = 0.3mol%, $p(CO_2)$ = 10 MPa, 45°C, 18h, neat conditions. [a]Yields calculated via ^{1}H-NMR analysis with mesytelene as external standard. Selectivity was in all cases >99%.

To make sure that bifunctional catalysts fully dissolve in the reaction mixture, the cycloaddition of CO_2 to 1,2-epoxyhexane was performed using acetonitrile (*Table 2*) and *N*,*N*-dimethylformammide (*Table 3*) as solvents.

In *Table 2*, a comparison of the catalytic activity of bifunctional and binary systems is reported using ACN as solvent at 70°C and compared to reactions catalyzed by co-catalysts only or metal complexes only are reported. Firstly, it can be noticed that co-catalysts TBAI and TBAC are active even without using the metal complex, even if for a minor extent (12 and 35%, *entry 1* and *2*). This is known and already reported in literature:[29] the nucleophiles can act as catalysts even without the Lewis acidic counterpart when using certain reaction conditions such as high co-catalyst loading or high temperatures. The chloride nucleophile PPNCl gave a three times higher yield than the iodide nucleophile TBAI, and this is in line with the higher nucleophilicity of chloride respect to iodide anions in polar aprotic solvents. On the other hand, metal complexes alone do not show any conversion at all (*entry 3* and *8*), as the epoxide ring opening by a nucleophile is a necessary step in the reaction mechanism. As far as the reactivity of bifunctional catalysts **VO(L^q)** (X = I), **Al(L^{q,r})(DMF)** and **Al(L^s)(DMF)** is concerned, (*entry 5*, 10, 11, 13), we were pleased to see that they are highly active in catalyzing the cycloaddition reaction of CO_2 to 1,2-epoxyhexane, giving

[29] North, M.; Pasquale, R.; Young, C. *Green Chem.* **2010** (12), 1514.

quantitative conversions after 18h using 0.5 mol% of catalyst loading. Bifunctional catalyst **VO(L^r)** (X = Cl), on the contrary, gave only 56% NMR yield (*entry 7*). This is again due to the low solubility of this complex in the reaction medium, as it was found partially non-dissolved at the end of the reaction. However, a real comparison between bifunctional and binary systems could not be obtained with this reaction conditions, as both these systems gave quantitative conversion in 18 hours (*entry 4-5*, 6-7, 9-10-11, 12-13). Attempt to analyze reaction performances at shorter reaction times were not significative due to limited catalyst solubility.[30] Therefore we decided to use a different solvent in order to assure complete solubility of all the reaction components.

Table 2 Cycloaddition of CO_2 to 1,2-hepoxyhexane **6** using bifunctional and binary systems as catalysts, in ACN at 70°C.

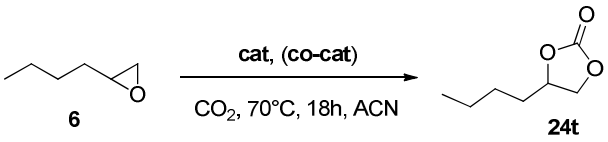

Entry	cat	co-cat	Yield (%)[a]
1	-	TBAI	12
2	-	PPNCl	35
3	**VO(L^h)**	-	0
4	**VO(L^h)**	TBAI	>99
5	**VO(L^q)** (X = I)	-	>99
6	**VO(L^h)**	PPNCl	>99
7	**VO(L^r)** (X = Cl)	-	56
8	**Al(L^c)(THF)**	-	0
9	**Al(L^c)(THF)**	TBAI	>99
10	**Al(L^q)(DMF)** (X = I)	-	>99
11	**Al(L^s)(DMF)** (X = I)	-	>99
12	**Al(L^c)(THF)**	PPNCl	>99
13	**Al(L^r)(DMF)** (X = Cl)	-	>99

Reaction conditions: [**6**] = 1 mmol, [**cat**] = 0.5 mol%, [**co-cat**] = 1.5 mol%, $p(CO_2)$ = 10 MPa, 70°C, 18h, ACN 0.5 mL. [a]Yields calculated via ^{1}H-NMR analysis with mesytelene as external standard. Selectivity was in all cases >99%.

[30] Using pressurized autoclaves or reactors, it's not possible to withdraw samples at different times of a reaction. Therefore, when different times are reported, the yields refer to different reactions performed using exactly the same conditions.

In DMF at 90°C (*Table 3*), bifunctional catalysts **VO(L^{q})** (X = I), **Al(L^{q,r})(DMF)** and **Al(L^{s})(DMF)** (X = I) gave complete conversions of the substrate after 3 hours (*entry 5,10,11* and *13*), while a slightly lower yield was obtained using complex **VO(L^{r})** (X = Cl) (*entry 7*). This again highlights the high activity of bifunctional catalysts **VO(L^{q})** (X = I), **Al(L^{q,r})(DMF)** and **Al(L^{s})(DMF)** (X = I) in CO_2/epoxide cycloaddition reactions. As reported in ACN, yields of reactions catalyzed by co-catalysts alone were much lower than those obtained with binary or bifunctional systems (*entry 1* and *2*), and no conversions were detected using non-functionalized metal complexes alone (*entry 3* and *8*). The poor conversion obtained with **Al(L^{c})(THF)** as catalyst is probably due to the decomposition of the catalyst in DMF under the reaction conditions (*entry 9*).

Table 3 Cycloaddition of CO_2 to 1,2-hepoxyhexane **6** using bifunctional and binary systems as catalysts, in DMF at 90°C.

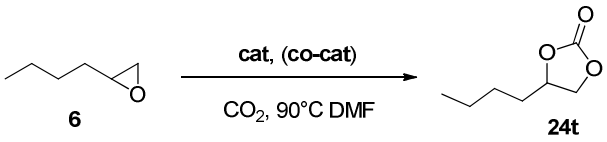

Entry	cat	co-cat	Yield(%)[a] after 1h	Yield(%)[a] after 3h
1	-	TBAI	0	5
2	-	PPNCl	12	33
3	**VO(L^{h})**	-	0	0
4	**VO(L^{h})**	TBAI	7	91
5	**VO(L^{q})** (X = I)	-	57	>99
6	**VO(L^{h})**	PPNCl	90	>99
7	**VO(L^{r})** (X = Cl)	-	31	86
8	**Al(L^{c})(THF)**	-	0	0
9	**Al(L^{c})(THF)**	TBAI	tr	13
10	**Al(L^{q})(DMF)** (X = I)	-	51	>99
11	**Al(L^{s})(DMF)** (X = I)	-	73	>99
12	**Al(L^{c})(THF)**	PPNCl	61	>99
13	**Al(L^{r})(DMF)** (X = Cl)	-	89	>99

Reaction conditions: [**6**] = 1 mmol, [**cat**] = 0.5 mol%, [**co-cat**] = 1.5 mol%, $p(CO_2)$ = 10 MPa, 90°C, DMF 0.5 mL. [a]Yields calculated via ^{1}H-NMR analysis with mesytelene as external standard. Selectivity was in all cases >99%.

The reaction course was also monitored after one hour. In the case of aluminum(III) complexes (*entry 9-13*), all bifunctional catalysts provided higher yields respect to the relative binary system. Vanadium(V) bifunctional catalyst **VO(L^q)** (X = I) with iodides as nucleophiles gave a five-fold higher yield respect to the binary system composed by complex **VO(L^h)** and 3 equivalents of TBAI (*entry 4-5*). Only bifunctional catalyst **VO(L^r)** (X = Cl) gave lower conversions than with the binary system (*entry 6-7*).

Bifunctional catalysts **VO(L^q)** (X = I) and **VO(L^r)** (X = Cl) were tested for the cycloaddition reactions of CO_2 to five different epoxides (*Table 4*), using optimized reaction conditions (DMF, 90°C, CO_2 10 bar, 3h).

Table 4 Cycloaddition reactions using substrates **6**, **17c,u,e,d** with **VO(L^q)** (X = I) and **VO(L^r)** (X = Cl**)** as catalyst.

Entry	substrate	product	Cat	Yield (%)[a]
1	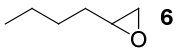 **6**	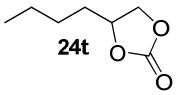 **24t**	**VO(L^q)** (X = I)	>99
2	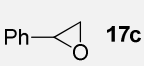 **17c**	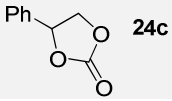 **24c**	**VO(L^q)** (X = I)	>99
3	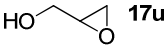 **17u**	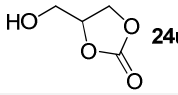 **24u**	**VO(L^q)** (X = I)	>99
4	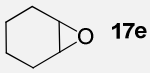 **17e**	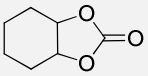 **24e**	**VO(L^q)** (X = I) **VO(L^r)** (X = Cl)	3 11
5	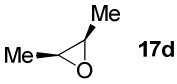 **17d**	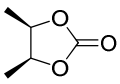 **24d**	**VO(L^q)** (X = I) **VO(L^r)** (X = Cl)	2 (*cis* >99%) 60 (*cis* >99%)

Reaction conditions: [substrate] = 1 mmol, [**cat**] = 0.5 mol%, $p(CO_2)$ = 10 MPa, 90°C, DMF 0.5 mL. [a]Yields calculated via ^{1}H-NMR analysis with mesytelene as external standard.

Even though the results obtained are very preliminary and we cannot draw no real conclusions at this stage, we can certainly say that they are very promising.

More in details:

1. All the three different terminal epoxides tested (**6**, **17c** and **17u**) have been converted quantitatively into the cyclic carbonate in only 3 hours (*entries 1*, *2* and *3*), demonstrating the effectiveness of bifunctional catalyst **VO(L^q)** (X = I).

2. The intrinsically slower reaction of internal epoxides **17e** and **17d** did not led to complete conversions in 3 hours time. In this case, we observed a better reactivity of catalyst **VO(L^{r})** (X = Cl), bearing a smaller chloride conterion, compared to **VO(L^{q})** (X = I) (entries 4 and 5). Particularly interesting and promising are the results obtained with *cis*-2,3-butene oxide (entry 5): catalyst **VO(L^{r})** (X = Cl) gave 60% substrate conversion instead of 2% (**VO(L^{q})** (X = I)), in only 3 hours. Very noticeably, a complete *cis*-selectivity in the corresponding carbonate was obtained. This selectivity is in contrast with the standard reactivity of this substrate where significant amount of *trans* carbonates are obtained. Also with our systems we observed that when using a TPA-based binary system (see *Chapter 4*, substrate scope), we obtained the formation of the cyclic carbonate in a 54:46 *cis*/*trans* ratio.

   For cyclohexene epoxide the yields after 3 hours were too low for a significant product formation. However, also in this case catalyst bifunctional catalyst **VO(L^{r})** (X = Cl) is more active of **VO(L^{q})** (X = I) (11 vs 3% conversion). In the very near future we will explore these systems more in detail.

5.4 Conclusions

In conclusion, five new bifunctional catalysts based on vanadium(V) and aluminum(III) aminotriphenolate complexes **VO(L^{q,r})** and **Al(L^{q,r,s})(DMF)** have been synthesized and characterized with ^{1}H- and ^{13}C-NMR spectroscopy, IR spectroscopy and mass spectrometry. In these bifunctional systems, the ligand is decorated with alkyl ammonium or pyridinium salts with chloride or iodide acting as nucleophilic co-catalysts. First, it has been demonstrated that these catalysts are quite active in the synthesis of cyclic carbonates from epoxides and CO_2, gaining full conversion of 1,2-epoxyhexane after 3 hours in DMF at 90°C. Only for vanadium complex **VO(L^{r})** (X = Cl) a slight lower yield has been reported (86%). Then, a comparison with binary systems has been conducted. Two similar vanadium(V) and aluminum(III) aminotriphenolate complexes have been chosen for comparison, in which the ligand is functionalized with *t*Bu groups. These catalysts used together with TBAI or PPNCl as co-cataysts as binary systems showed to be less effective than the corresponding bifunctional systems, leading to lower yields in cyclic carbonate. The only exception is again complex **VO(L^{r})** (X = Cl), which presents a lower solubility under turnover conditions. The yields of the reactions catalyzed by bifunctional catalysts have been compared also to that of vanadium and aluminum aminotriphenolate complexes without co-catalysts (for which no conversion was observed) and to that of co-catalysts alone, which showed much lower conversions. These results together demonstrated that the proximity effect of the two catalytic moieties have a

strong influence on the catalytic activity of the catalyst. The reactivity of these bifunctional catalysts have also tested using five different epoxides, showing that the catalyst with iodide as nucleophiles is able to effectively convert only terminal epoxides, while using the system with chloride as counterions, also 2,3-epoxy butane has been converted in 60% yield. This work will continued next year in the frame of CARISMA COST Action CM1205 in the laboratory of Prof. Arjan Kleij at ICIQ in Tarragona, Spain.

5.5 Experimental

General Remarks

All chemicals and dry solvents have been purchased from Sigma-Aldrich or Fluka and used as provided, without further purification. Vanadium(V) and aluminum(III) aminotriphenolate complexes **VO(L^h)** and **Al(L^c)(THF)** were synthesized as previously reported.[31]

Flash cromatographies and filtrations have been performed with Macherey-Nagel siliga gel 60 (0.04-0.063 mm, 230-400 mesh). TLC analyses were performed using Macherey-Nagel POLYGRAM® SIL G/UV254 silica plates, detecting by UV/VIS and by treatment with PMA staining reagent made from a solution of phosphomolibdic acid ($H_3PMo_{12}O_{40}$) 10 g in 100 mL ethanol. The NMR spectra has been recorded on a Bruker AC200 (^{1}H: 200.13 MHz; ^{13}C: 50.03 MHz) or on a Bruker AV300 (^{1}H: 300.13 MHz; ^{13}C: 75.5.0 MHz) spectrometer. Chemical shift (δ) have been reported in parts per million (ppm) relative to the residual undeuterated solvent as a internal reference ($CDCl_3$: 7.26 ppm for ^{1}H-NMR and 77.16 for ^{13}C-NMR; ACN-d_3: 1.94 ppm for ^{1}H-NMR, 1.32 and 118.26 for ^{13}C-NMR; DMSO-d_6: 2.50 ppm for ^{1}H-NMR, and 39.52 for ^{13}C-NMR, DMF-d_7: 8.03, 2.95 and 2.75 ppm for ^{1}H-NMR, 163.15, 34.89 and 29.76 ppm for ^{13}C-NMR). The following abbreviations have been used to descrive multeplicities: s = singlet, d = doublet, t = triplet, dd = double duplet, td = triplet of douplets, q = quartet, m = multiplet, br = broad. ^{13}C-NMR have been recorded with complete proton decoupling. 51V-NMR spectra have been recorded at 301K with 1000 scans at 78.28 MHz on a AV300 spectrometer. ESI-MS spectra have been obtained on a LC/MS Agilent series 1100 spectrometer in both positive and negative modes using acetonitrile or acetonitrile/formic acid 0.1% as mobile phase, with ESI-ion trap mass detector. In

[31] a) Licini, G.; Mba, M.; Zonta, C. Dalton Trans. **2009** (27), 5265. b) Whiteoak, C. J.; Kielland, N.; Laserna, V.; Escudero-, E. C. **2013**.

some cases, an ESI-TOF MarinerTM BiospectrometryTM Workstation of Applied Biosystems by flow injection, using acetonitrile or methanol/formic acid 0.1% as mobile phase, was used. IR spectra have been recorded on a Nicolet 5700 FT-IR, with range 4000-400 cm^{-1} and resolution 4 cm^{-1}, using KBr pellets or NaCl plates. Analytical gas chromatography with mass spectrometry detector (GC-MS) has been carried out on a Agilent 6850 spectrometer equipped with a split mode capillary injector and electron impact mass detector. Injector temperature has been set to 250 °C, detector temperature has been set to 280 °C and the carrier gas is He (1 mL/min) with a HP-5MS column. All vanadatrane complexes were prepared under nitrogen atmosphere in a MBraun MB 200MD dry-box, equipped with a MB 150 G-I gas recycling system (nitrogen working pressure: 6 bar). Oxygen and water levels inside the box were real-time monitored by MBraun oxygen and moisture analyzers.

2-hydroxy-3-iodo-benzaldehyde (32)

2-iodophenol **31** (55.56 mmol, 12.224 g) was dissolved in dry THF (100 mL) and magnesium chloride (72.23 mmol, 6.878 g) and triethylamine (111.12 mmol, 15.55 mL) were added. After 30 min, paraformaldehyde (8.334 g) was added and the reaction mixture was refluxed for 22 h. The end of the reaction was checked via ^{1}H-NMR spectroscopy and GC-MS. Then HCl 1N (100 mL) was added and the residue was extracted three times with ethyl acetate. The organic phases were washed with NaClaq, dried over anhydrous Na_2SO_4 and concentrated under vacuum. The final product was obtained as yellow crystals after recrystallization in hexane (9.7 g, 70% yield).

IR (KBr): ν 711, 773, 892, 1070, 1118, 1215, 1265, 1298, 1385, 1434, 1468, 1560, 1604, 1705, 1886, 2851, 3063, 3422 cm^{-1}. ^{1}H-NMR: (200 MHz, $CDCl_3$) δ 11.82 (1H, s), 9.77 (1H, s), 8.00 (1H, dd, J = 1.6, J = 7.8 Hz), 7.58 (1H, dd, J = 1.5, J = 7.6 Hz), 6.84 (1H, t, J = 7.6 Hz). ^{13}C-NMR (50 MHz, $CDCl_3$): δ 195.9 (CHO), 160.3 (CH), 146.0 (CH), 133.9 (CH), 121.6 (CH), 120.4 (C), 85.4 (C). MS (ESI): *m/z* calc. 249.02; found 248.9 $[M+H]^+$.

3-Iodo-2-(methoxymethoxy)benzaldehyde (33)

2-hydroxy-3-iodo-benzaldehyde **32** (25 mmol, 6.2 g) was dissolved in dry DMF (20 mL) under a N_2 atmosphere. K_2CO_3 (30 mmol, 4.14 g) and MOMCl (30 mmol, 2.3 mL) were slowly added and the mixture was stirred for 15 hours. The reaction mixture was diluted with water and extracted three times with ethyl acetate. The organic phase was washed with a NaClaq solution, dried over anhydrous Na_2SO_4, filtered and concentrated under vacuum. The product was obtained as a yellow oil (7 g, 95% yield) and used in the next reaction without further purification.

IR (NaCl): ν 754, 844, 923, 984, 1108, 1159, 1228, 1244, 1312, 1400, 1429, 1521, 1558, 1616, 1695, 1844, 1897, 1982, 2075, 2340, 2358, 2739, 2829, 2951, 3006, 3060, 3337 cm^{-1}. ^{1}H-NMR

(200 MHz, $CDCl_3$): δ 10.28 (1H, d, J=0.8 Hz), 8.05 (1H, dd, J = 1.8, J = 7.8 Hz), 7.82 (1H, dd, J = 1.6, J = 7.6 Hz), 7.04 (1H, td, J= 7.8 Hz, J=1), 5.16 (2H, s), 3.62 (3H, s). ^{13}C-NMR (50 MHz, CDCl3): δ 190.1 (CHO), 160.1 (C), 146.3 (C), 145.5(CH), 128.9 (CH), 126.8 (CH), 101.6 (CH2), 93.5 (C), 58.6 (CH3). MS (GC-MS): *m/z* calc. 292.07; found 292 $[M]^+$.

***Tris*-(2-(methoxymethoxy)-3-iodobenzyl)amine (34)**

Inside a dry-box, 3-iodo-2-(methoxymethoxy)benzaldehyde **33** (23.9 mmol, 7 g) was dissolved in dry THF (35 mL), then ammonium acetate (7.6 mmol, 585 mg) was added. After 60 min under stirring, sodium triacetoxy borohydride (34.25 mmol, 7.26 g) was added and the mixture was stirred for 24 h at room temperature in the dry-box. The end of the reaction was checked through ESI-MS analysis, and then the solvent was evaporated with a rotary evaporator. The residue was dissolved in ethyle acetate and washed with $NaHCO_3$aq solution and brine. The residue was dried over anhydrous Na_2SO_4 and concentrated under reduced pressure. The crude product was purified by crystallization in acetonitrile, affording light-yellow crystals (3.8 g, 60% yield).

IR (KBr): ν 733, 770, 797, 945, 1079, 1160, 1290, 1363, 1397, 1444, 1466, 1580, 2340, 2359, 2824, 2887, 2928, 2949, 2979, 3065 cm^{-1}. ^{1}H-NMR (200 MHz, $CDCl_3$): δ 7.65 (6H, td, J = 8 Hz, J = 1.4 Hz), 6.87 (3H, t, J = 7.8 Hz), 4.98 (6H, s), 3.73 (6H, s), 3.58 (9H, s). ^{13}C-NMR (50 MHz, $CDCl_3$): δ 155.9 (C), 138.4 (CH), 134.7 (C), 130.1 (CH), 126.7 (CH), 100.5 (CH_2), 92.7 (C), 58.3 (CH_3), 53.0 (CH_2). MS (ESI): *m/z* calc. 845.24; found 846.0 $[M + H]^+$.

***Tris*-(2-(methoxymethoxy)-3-(3'-(N,N-dimethylamino)phenyl)-benzyl)amine (35)**

In a two-neck round-bottom flask, *tris*-(2-(methoxymethoxy)-3-iodobenzyl)amine **34** (1.18 mmol, 1 g) was dissolved in dioxane, and K_2CO_3aq 2M (18 mL) was added. The suspension was degassed for 30 min by bubbling N_2 in the reaction mixture, then 3-(*N*,*N*-dimethylamino)phenylboronic acid (5.92 mmol, 1.189 g) and Pd(dppf)Cl_2 · DCM (0.059 mmol, 49 mg) were added. The suspension was heated at reflux overnight under stirring. After checking the end of the reaction via ESI-MS spectrometry, the solvent was evaporated under reduced pressure. The crude product was suspended in $NaHCO_3$aq and extracted three times with chloroform, then the organic phase was washed with brine, filtered twice over a short pad of celite and activated charcoal, and evaporated under reduced pressure. The product was purified via silica gel flash-chromatography (ethyl acetate/hexane, 3/7) to obtain a yellow oil (800 mg, 82% yield).

^{1}H-NMR (200 MHz, $CDCl_3$): δ 7.84 (3H, dd, J = 6.6 Hz, J = 2,8 Hz), 7.33-7.16 (9H, m), 6.95-6.84 (6H, m), 6.72 (3H, m), 4.58 (6H, s), 3.94 (6H, s), 3.20 (9H, s), 2.97 (18H, s). ^{13}C-NMR (50 MHz, $CDCl_3$): δ 152.94 (C), 150.57 (C), 139.96 (C), 135.74 (C), 133.65 (C), 129.57 (CH), 128.87 (CH),

128.47 (CH), 124.33 (CH), 118.04 (CH), 113.88 (CH), 111.39 (CH), 99.14 (CH_3), 57.33 (CH_2), 52.93 (CH_2), 40.74 (CH_3). MS (ESI): *m/z* calc. 824.45, found 825.6 $[M + H]^+$.

Tris-(2-(methoxymethoxy)-3-(3'-(N,N,N-trimethylammonium)phenyl)-benzyl)amine triiodide (36)

Tris-(2-(methoxymethoxy)-3-(3'-(N,N-dimethylamino)phenyl)-benzyl)amine **35** (0.12 mmol, 100 mg) was dissolved in DCM (1mL) and methyl iodide (1.28 mmol, 80 μL) was added. The reaction mixture was stirred at 40°C overnight. A precipitate was formed, which was filtered and washed three times with cold dichloromethane and dried undere reduced pressure. The product was obtained as a white powder and was used in the following reaction without any further purification (55mg, 37% yield).

^{1}H-NMR (200 MHz, DMSO-d_6): δ 8.12-7.86 (9H, m), 7.80-7.63 (9H, m), 7.51 (3H, t, J = 7.8 Hz), 4.87 (6H, s), 4.46 (6H, m), 3.66 (27H, s), 2.82 (9H, s). ^{13}C-NMR (50 MHz, DMSO-d_6): δ 155.68 (C), 148.12 (C), 139.65 (C), 136.05 (CH), 134.92 (CH), 134.42 (C), 131.21 (CH), 130.54 (CH), 125.70 (CH), 122.44 (C), 121.40 (CH), 120.13 (CH), 100.37 (CH_2), 61.02 (CH_2), 57.40 (CH_3), 56.98 (CH_3).

Tris-(2-hdroxy-3-(3'-(N,N,N-trimethylammonium)phenyl)-benzyl)amine trichloride (L^pH_3)

Tris-(2-(methoxymethoxy)-3-(3'-(N,N,N-trimethylammonium)phenyl)-benzyl)amine triiodide **36** (340 mg, 0.41 mmol) was dissolved in HCl solution 1.25M in methanol (25 mL) and the solution was stirred at reflux overnight. The reaction mixture was then was evaporated under reduced pressure, and the crude product was dissolved in methanol (15 mL) and stirred with K_2CO_3 for 10 minutes. K_2CO_3 was then filtered and the solvent evaporated under reduced pressure (470 mg, 92% yield).

^{1}H-NMR (200 MHz, DMSO-d_6): δ 8.17 (3H, s), 8.01-7.89 (3H, m), 7.77-7.59 (9H, m), 7.51 (3H, d, J = 7.2 Hz), 7.15 (3H, t, J = 7.4 Hz), 4.93 (6H, s), 3.60 (27H, s). ^{13}C-NMR (50 MHz, DMSO-d_6): δ 154.18 (C), 147.22 (C), 139.77 (C), 135.40 (CH), 133.36 (CH), 131.01 (CH), 130.36 (C), 129.85 (CH), 121.51 (CH), 120.91 (CH), 119.08 (CH), 118.16 (C), 60.44 (CH_2), 56.45 (CH_3).

Tris-(2-(methoxymethoxy)-3-(3'-(N,N-dimethylamino)-1'-propynyl)-benzyl)amine (37)

Inside a dry-box, *tris*-(2-(methoxymethoxy)-3-iodobenzyl)amine **34** (1.18 mmol, 1g), 3-dimethylamino-1-propyne (7.1 mmol, 765 μL) and triethylamine (11.8 mmol, 1.7 mL) were dissolved in dry THF (3 mL). Then, $Pd(PPh_3)_4$ (0.012 mmol, 14 mg) and CuI (0.024 mmol, 4.5 mg)

were added, and a change in color was observed from colorless to yellow-orange and finally a precipitate was formed. The suspension was allowed to stir at reflux overnight under a N_2 atmosphere, and the end of the reaction was checked via ESI-MS analysis. The solution was filtered through a pad of celite, while the dark precipitate of the reaction mixture was extracted three times with THF and filtered as well on celite. The liquid phases were then combined and the solvent was evaporated under reduced pressure. The crude product was dissolved in $CHCl_3$ and washed three times with $NaHCO_3$aq. The solvent was then evaporated under reduce pressure to obtain a dark oil which was purified via silica gel flash-chromatography ($CHCl_3$/MeOH 8/2 + 0.25% triethylamine). To get rid of the byproduct of the alkyne homo-coupling reaction, the product was precipitated several times in hexane (500 mg, 60% yield).

^{1}H-NMR (200 MHz,$CDCl_3$): δ 7.62 (3H, dd, J = 7.6 Hz, J = 1.4 Hz), 7.31 (3H, dd, J = 7.6 Hz, J = 1.6 Hz), 7.04 (3H, t, J = 7.8 Hz), 5.17 (6H, s), 3.71 (6H, s), 3.49 (15H, s), 2.35 (18H, s). ^{13}C-NMR (50 MHz,$CDCl_3$): δ 157.0 (C), 133.35 (C), 132.61 (CH), 129.88 (CH), 124.13 (CH), 116.75 (C), 99.69 (CH_2), 88.94 (C), 82.22 (C), 57.75 (CH_3), 52.30 (CH_2), 48.46 (CH_2), 44.21 (CH_3). MS (ESI): *m/z* calc. 710.40, found 711.4 $[M + H]^+$.

***Tris*-(2-(methoxymethoxy)-3-(3'-(N,N-dimethylamino)-propyl)-benzyl)amine (38)**

Tris-(2-(methoxymethoxy)-3-(3'-(N,N-dimethylamino)-1'-propynyl)-benzyl)amine **37** (0.14 mmol, 100 mg) was dissolved in ethyl acetate and Pd/C 10% (0.014 mmol, 15 mg) was added. The reaction mixture was allowed to stir at room temperature under a H_2 atmosphere (1 atm, baloon) for 24 hours. The end of the reaction was checked via ESI-MS analysis and the reaction mixture was filtered through a pad of celite, dried over anhydrous Na_2SO_4, filtered and concentrated under vacuum. The product was obtained as a yellow oil and was used in the following step without further purification (70 mg, 70% yield).

^{1}H-NMR (200 MHz,$CDCl_3$): δ 7.60-7.47 (3H, m), 7.14-7.01 (6H, m), 4.82 (6H, s), 3.64 (6H, s), 3.53 (9H, s), 2.65 (6H, t, J = 7.4 Hz), 2.31 (6H, t, J = 7.2 Hz), 2.22 (18H, s), 1.87-1.66 (6H, m). ^{13}C-NMR (50 MHz,$CDCl_3$): δ 154.76 (C), 135.40 (C), 132.99 (C), 128.62 (CH), 127.98 (CH), 124.61 (CH), 100.11 (CH_2), 59.81 (CH_2), 57.45 (CH_3), 52.99 (CH_2), 45.60 (CH_3), 28.77 (CH_2), 28.29 (CH_2). MS (ESI): *m/z* calc. 722.50, found 723.5 $[M + H]^+$.

***Tris*-(2-hydroxy-3-(3'-(N,N-dimethylamino)-propyl)-benzyl)amine (39)**

Tris-(2-(methoxymethoxy)-3-(3'-(N,N-dimethylamino)-propyl)-benzyl)amine **38** (0.19 mmol, 140 mg) was dissolved in HCl 1.25M in MeOH (2 mL) and stirred at reflux for 2 hours. A change in color was observed from yellow to red. After having checked the end of the reaction via ESI-MS

analysis, the solvent was evaporated under reduced pressure and the crude product was dissolved in HClaq. 1M. The solution was basified to pH = 8-9 with NaOHaq. 1M leading to the formation of a white precipitate. The precipitate was extracted three times with ethyl acetate, and the organic phase was washed with $NaHCO_{3aq}$, dried over anhydrous Na_2SO_4, filtered and concentrated under vacuum to get a pale yellow solid (95 mg, 85% yield).

^{1}H-NMR (200 MHz,$CDCl_3$): δ 7.09 (3H, dd, J = 7.4 Hz, J = 1.6 Hz), 6.96 (3H, dd, J = 7.6, J = 1.6 Hz), 6.73 (3H, t, J = 7.4 Hz), 3.77 (6H, s), 2.65 (6H, t, J = 6.4 Hz), 2.34-2.15 (24H, m), 1.94-1.68 (6H, m). ^{13}C-NMR (50 MHz,$CDCl_3$): δ 155.94 (C), 129.40 (CH), 128.81 (CH), 127.80 (C), 124.64 (C), 119.09 (CH), 56.44 (CH_2), 53.82 (CH_2), 44.67 (CH_3), 22.87 (CH_2), 26.73 (CH_2). MS (ESI): *m/z* calc. 590.42, found 590.4 $[M + H]^+$.

***Tris*-(2-hydroxy-3-(3'-(N,N,N-trimethylammonium)-propyl)-benzyl)amine triiodide (L^qH_3)**

Tris-(2-hydroxy-3-(3'-(N,N-dimethylamino)-propyl)-benzyl)amine **39** (0.71 mmol, 420 mg) was dissolved in dry dichloromethane (8 mL), and methyl iodide was added (2.35 mmol, 150 μL). The reaction mixture was stirred at room temperature overnight, and then a white precipitate was formed. The precipitate was filtered, washed three times with cold dichloromethane and milled with diethylether to get a pale yellow solid (400 mg, 56% yield).

^{1}H-NMR (200 MHz,DMF-d_7): δ 7.26-7.07 (6H, m), 6.85 (3H, t, J = 7.4 Hz), 3.80 (6H, s), 3.72-3.55 (6H, m), 3.33 (27H, s), 2.81-2.67 (6H, m), 2.29-2.05 (6H, m). ^{13}C-NMR (50 MHz,$CDCl_3$): δ 155.94 (C), 132.62 (CH), 129.31 (CH), 127.80 (C), 124.64 (C), 124.07 (CH), 68.59 (CH_2), 59.88 (CH_3), 57.34 (CH_2), 32.97 (CH_2), 28.83 (CH_2). MS (ESI): *m/z* calc. 211.83 (M^{3+}); found 211.8329 M^{3+}, 381.1972 $[M+I]^{2+}$, 889.3130 $[M+2I]^+$.

***Tris*-(2-hydroxy-3-(3'-(N,N,N-trimethylammonium)-propyl)-benzyl)amine trichloride (L^rH_3)**

Tris-(2-hydroxy-3-(3'-(N,N,N-trimethylammonium)-propyl)-benzyl)amine triiodide **L^qH_3** (0.02 mmol, 20 mg) was dissolved in dry DMF (2 mL) and stirred for three hours with Amberlite IRA400 anion exchange resin (200 mg) at room temperature. Then, the reaction mixture was filtered and the resin was washed with DMF three times. The liquid phases were combined and the solvent evaporated under reduced pressure.

^{1}H-NMR (200 MHz, ACN-d_3): δ 7.16-6.99 (6H, m), 6.80 (3H, t, J = 7.4), 3.69 (6H, s), 3.44-3.22 (6H, m), 3.05 (27H, s), 2.02-1.80 (6H, m). ^{13}C-NMR (50 MHz,$CDCl_3$): δ 156.31 (C), 132.23 (CH), 129.45 (CH), 130.78 (C), 124.51 (C), 123.32 (CH), 68.74 (CH_2), 60.03 (CH_3), 57.01 (CH_2), 33.23 (CH_2), 28.74 (CH_2). MS (ESI): *m/z* calc. 211.83 (M^{3+}); found 211.8329 M^{3+}, 335.2290 $[M+Cl]^{2+}$, 705.4283 $[M+2Cl]^+$.

Vanadium(V) aminotriphenolate complex VO(L^q)

In a dry-box, *Tris*-(2-hydroxy-3-(3'-(N,N,N-trimethylammonium)-propyl)-benzyl)amine triiodide **L^qH_3** (0.169 mmol, 172 mg) was dissolved in dry DMF (4 mL), then a solution of VO(O*i-Pr*)$_3$ (0.169 mmol, 40 μL) in dry DMF (2 mL) was added dropwise. An immediate change in colour was observed from colourless to dark blue. The reaction mixture was stirred at room temperature inside the dry-box for three hours, then the solvent was evaporated heating under reduced pressure. The crude product was purified by precipitation in dry DMF/DEE/Hexane to obtain a dark-blue solid (130 mg, 72% yield).

^{1}H-NMR (200 MHz, ACN-d_3): δ 7.16-6.94 (6H, m), 6.75 (3H, t, J = 7.4 Hz), 3.63-3.42 (12H, m), 3.15 (27H, s), 2.76 (6H, t, J = 7.6 Hz), 2.33-2.09 (6H, m). ^{13}C-NMR (50 MHz, ACN-d_3): δ 129.45 (CH), 129.17 (CH), 128.19 (C), 127.59 (C), 122.05 (CH), 67.52 (CH2), 59.86 (CH_2), 54.02 (CH_3), 28.54 (CH_2), 23.58 (CH_2). ^{51}V-NMR (78.28MHz, ACN-d_3): δ -431.64. MS (ESI): *m/z* calc. 1080.12; found 233.1360 M^{3+}, 413.1514 $[M+I]^{2+}$, 953.2258 $[M+2I]^+$.

Aluminum(III) aminotriphenolate complex Al(L^q)(DMF)

In a dry-box, *Tris*-(2-hydroxy-3-(3'-(N,N,N-trimethylammonium)-propyl)-benzyl)amine triiodide **L^qH_3** (0.05 mmol, 50.8 mg) was dissolved in dry DMF (1 mL), then 25 μL of $AlMe_3$ 2M in toluene (0.05 mmol) were dissolved in dry DMF (0.5 mL) and added to the ligand solution. The reaction mixture was stirred at room temperature inside the dry-box for three hours, then the solvent was evaporated heating under reduced pressure. The crude product was purified by precipitation in dry DMF/DEE to obtain a white powder (30 mg, 57.7% yield).

^{1}H-NMR (200 MHz, ACN-d_3): δ 7.14-6.86 (6H, m), 6.66 (3H, t, J = 7.4 Hz), 3.53-3.29 (6H, m), 2.96 (27H, s), 2.82-2.50 (6H, m), 2.15-1.96 (6H, m). ^{13}C-NMR (50 MHz, DMF-d_7): δ 157.81 (C), 130.42 (C), 129.90 (C), 128.79 (CH), 123.41 (CH), 118.41 (CH), 67.22 (CH_2), 58.67 (CH_2), 53.54 (CH_3), 27.80 (CH_2), 23.46 (CH_2). MS (ESI): *m/z* calc. 1040.16; found 219.8207 M^{3+}, 393.1788 $[M+I]^{2+}$, 913.2653 $[M+2I]^+$.

Vanadium(V) aminotriphenolate complex VO(L^r)

In a dry-box, *Tris*-(2-hydroxy-3-(3'-(N,N,N-trimethylammonium)-propyl)-benzyl)amine triiodide **L^qH_3** (0.169 mmol, 172 mg) was dissolved in dry DMF (3 mL) and 3g of Amberlite IRA-400 anion exchange resin was added. The mixture was stirred at room temperature for three hours, then the

resin was filtered and washed with dry DMF (1 mL) six times. The liquid phases were combined, and a solution of VO(O*i-Pr*)$_3$ (0.169 mmol, 40 μL) in dry DMF (1 mL) was added dropwise. An immediate change in colour was observed from colourless to dark blue. The reaction mixture was stirred at room temperature inside the dry-box for three hours, then the solvent was evaporated heating under reduced pressure. The crude product was purified by precipitation in dry DMF/DEE/Hexane to obtain a dark-blue solid (120 mg, 68.6% yield).
^{1}H-NMR (200 MHz, ACN-d_3): δ 7.14-6.82 (6H, m), 6.64 (3H, t, J = 7.4 Hz), 3.67-3.43 (12H, m), 3.13 (27H, s), 2.85-2.64 (6H, m), 2.40-2.24 (6H, m). ^{13}C-NMR (50 MHz, ACN-d_3): δ 129.15 (CH), 128.97 (C), 127.54 (C), 121.01 (CH), 67.46 (CH_2), 60.88 (CH_2), 53.69 (CH_3), 29.13 (CH_2), 23.84 (CH_2). ^{51}V-NMR (78.28MHz, ACN-d_3): δ -376.31.

Aluminum(III) aminotriphenolate complex Al(L^r)(DMF)

In a dry-box, *Tris*-(2-hydroxy-3-(3'-(N,N,N-trimethylammonium)-propyl)-benzyl)amine triiodide **L$_q$H^3** (0.14 mmol, 142 mg) was dissolved in dry DMF (3 mL) and 3g of Amberlite IRA-400 anion exchange resin was added. The mixture was stirred at room temperature for three hours, then the resin was filtered, washed with dry DMF (1 mL) six times and the liquid phases were combined. 70 μL of $AlMe_3$ 2M in toluene (0.14 mmol) were dissolved in dry DMF (0.5 mL) and added to the ligand solution. The reaction mixture was stirred at room temperature inside the dry-box for three hours, then the solvent was evaporated heating under reduced pressure. The crude product was purified by precipitation in dry DMF/DEE/Hexane to obtain a white powder (64 mg, 60% yield).
^{1}H-NMR (200 MHz, ACN-d_3): δ 7.11-6.83 (12H, m), 6.62 (3H, t, J = 7.2 Hz), 3.59 (6H, br), 2.98 (27H, s), 2.77-2.56 (6H, m), 2.49-2.20 (6H, m), 2.07-1.981 (6H, m). ^{13}C-NMR (50 MHz, ACN-d_3): δ 130.23 (CH), 129.07 (C), 127.11 (C), 121.83 (CH), 69.51 (CH_2), 61.74 (CH_2), 54.85 (CH_3), 29.21 (CH_2), 23.50 (CH_2).

***Tris*-(2-(methoxymethoxy)-3-(pyridin-3'-yl)-benzyl)amine (40)**

Tris-(2-(methoxymethoxy)-3-iodobenzyl)amine **34** (0.95, 800 mg) was dissolved in dioxane (7 mL) and an aqueous solution of Na_2CO_3 (2M, 4 mL) was added. The suspension was degassed for 30 min by bubbling N_2 in the reaction mixture, then 3-pyridinyl boronic acid (5.68 mmol, 700 mg) and $Pd(PPh_3)_4$ (0.14 mmol, 161 mg) were added. The reaction mixture was allowed to stir at reflux under a N2 atmosphere overnight, then was cooled, filtered through a pad of celite and the solvent was evaporated under reduced pressure. The crude product was dissolved in DCM and extracted three times with HClaq. 1M. The aqueous solution was then basified to pH = 8-9 and the precipitate formed was extracted three times with ethyl acetate. The organic layer was then dried over

anhydrous Na_2SO_4 and the solvent evaporated under reduced pressure. The crude product was purified via silica gel flash-chromatography ($CHCl_3$/MeOH/TEA, 9.5/0.5/0.02) to obtain a pale yellow powder (520 mg, 78% yield).

^{1}H-NMR (200 MHz, $CDCl_3$): δ 8.78 (1H, *s*), 8.50 (1H, *d*, *J* = 3.4 Hz),7.80 (2H, *dd*, *J* = 7.2, *J* = 2.4 Hz), 7.17-7.23 (3H, *m*), 4.44 (2H, *s*), 3.82 (2H, *s*) 3.00 (3H, *s*). ^{13}C-NMR (50 MHz, ACN-d_3): δ 153.45 (C), 150.31 (CH), 148.14 (CH), 136.77 (CH), 135.10 (C), 133.64 (C), 131.92 (C), 130.50 (CH), 129.54 (CH), 124.94 (CH), 123.23 (CH), 99.83 (CH), 57.33 (CH_3), 52.73 (CH_2). MS (ESI): *m/z* calc. 698.31; found 699.3 $[M+H]^+$.

***Tris*-(2-hydroxy-3-(pyridin-3'-yl)-benzyl)amine (41)**

Tris-(2-(methoxymethoxy)-3-(pyridin-3'-yl)-benzyl)amine **40** (0.902 mmol, 630 mg) was dissolved in HCl 1.25M in MeOH (10 mL) and stirred at reflux overnight. The solvent was evaporated under reduced pressure and the crude product was dissolved in HClaq. 1M. The solution was basified to pH = 8-9 with NaOHaq. 1M leading to the formation of a white precipitate. The precipitate was extracted three times with ethyl acetate, and the organic phase was washed with $NaHCO_{3aq}$, dried over anhydrous Na_2SO_4, filtered and concentrated under vacuum to get a pale yellow solid (330 mg, 65% yield).

^{1}H-NMR (200 MHz, $CDCl_3$): δ 8.34 (3H, s), 8.14 (3H, s), 7.63 (3H, br), 7.15-6.91 (9H, m), 6.83 (3H, t, J = 5 Hz), 3.93 (6H, s). ^{13}C-NMR (50 MHz, ACN-d_3): δ 153.80 (C), 149.30 (CH), 147.03 (CH), 137.31 (CH), 134.59 (CH), 130.34 (CH), 125.88 (C), 123.14 (CH), 120.05 (CH), 58.41 (CH_2). MS (ESI): *m/z* calc. 566.23; found 567.2 $[M+H]^+$.

***Tris*-(2-hydroxy-3-(N-methyl-pyridinium-3'-yl)-benzyl)amine tri-iodide (L^sH_3)**

Tris-(2-hydroxy-3-(pyridin-3'-yl)-benzyl)amine **41** (0.26 mmol, 150 mg) was suspended in dry ACN (30 mL), and methyl iodide was added (2.35 mmol, 150 μL). The reaction mixture was stirred under a N_2 atmosphere at reflux overnight, and then a white precipitate was formed. The precipitate was filtered, washed three times with cold acenonitrile and milled with diethylether to get a pale yellow solid (120 mg, 46% yield).

^{1}H-NMR (200 MHz, ACN-d_3): δ 8.88 (3H, s), 8.55 (6H, d, J = 6.8 Hz), 8.00 (3H, t, J = 7.0 Hz), 7.32 (6H, t, J = 8.2 Hz), 7.08-6.87 (3H, m), 4.34 (9H, s), 4.03 (6H, s). ^{13}C-NMR (50 MHz, ACN-d_3): δ 160.32 (C), 154.45 (CH), 151.32 (CH), 141.01 (CH), 138.78 (CH), 132.25 (CH), 126.33 (C), 125.15 (CH), 121.22 (CH), 78.96 (CH_3), 58.41 (CH_2).

Aluminum(III) aminotriphenolate complex Al(L^s)(DMF)

In a dry-box, *tris*-(2-hydroxy-3-(N-methyl-pyridin-3'-yl)-benzyl)amine $\mathbf{L^sH_3}$ (0.05 mmol, 50.8 mg) was dissolved in dry DMF (1 mL), then 25 μL of $AlMe_3$ 2M in toluene (0.05 mmol) were dissolved in dry DMF (0.5 mL) and added to the ligand solution. The reaction mixture was stirred at room temperature inside the dry-box for three hours, then the solvent was evaporated heating under reduced pressure. The crude product was purified by precipitation in dry DMF/DEE to obtain a white powder (90 mg, 74% yield). ^{1}H-NMR (200 MHz, ACN-d_3): δ 9.01 (3H, s), 8.80 (6H, d, J = 6.8 Hz), 8.32 (3H, t, J = 7.0 Hz), 7.44 (6H, t, J = 8.2 Hz), 7.51-7.01 (3H, m), 5.21 (9H, s), 4.65 (6H, s). ^{13}C-NMR (50 MHz, ACN-d_3): δ 165.72 (C), 155.77 (CH), 152.51 (CH), 140.78 (CH), 138.11 (CH), 131.89 (CH), 127.38 (C), 125.44 (CH), 121.70 (CH), 79.12 (CH_3), 58.03 (CH_2).

Catalytic activity studies

For the catalytic activity studies (*Table 1*, *2*, *3* and *4*), an HEL CAT-*24* multi-sample autoclave have been used, in which the desired number of vials (from 3 to 9) has been charged with the reaction mixture. Carbon dioxide (purchased from PRAXAIR) was used without further purification or drying *prior to* its use. As a typical experiment, the catalyst screening in DMF at 90°C (*Table 3*) is described as follow. Fourteen 8 mL vials have been charged with catalyst and/or co-catalyst, and then the epoxide (0.1 mL, 1mmol) and 0.5 mL of DMF have been added. Then, the reactor was purged with $CO_2$and the pressure was stabilized at 1.0 MPa. The reactor was heated to the required temperature (T = 90°C), and the mixture was then stirred for 1 or 3 hours. The autoclave was allowed to cool down by immersion in an ice bath for 1 hour before venting. The reaction mixture was diluted in $CDCl_3$ (1.0 mL) and a weighed quantity of mesitylene (typically around 0.5 mol with respect to the epoxide substrate) was added. A quantitative ^{1}H-NMR determination was performed on samples consisting of 100 mL of this solution diluted with 0.5 mL of $CDCl_3$.

Conclusions

This thesis work presented the synthesis and application of nine aminotriphenolate complexes as catalysts for epoxide activation in ring opening reactions by amines and CO_2 cycloadditions. The design of the ligand have been carefully adapted to the type of reaction considered, taking advantage of the versatility of triphenolamines in terms of scaffold functionalizations. *Tert*-butyl substituted vanadium(V)aminotriphenolate complex **VO(L^{h})** has been used as catalysts for epoxide ring opening reactions by amines, giving high conversions for a wide range of epoxides and amines tested. On the other hand, chloro-substituted vanadium(V) aminotriphenolate complex **VO(L^{d})** is the catalyst of choice for CO_2 cycloaddition reactions to epoxides. A full substrate scope has been conducted with a variety of challenging internal epoxides, highlighting the high catalytic activity and versatility of this catalyst. Epoxide ring opening reactions and CO_2 cycloaddition are quite unexplored reactivities for vanadium(V) aminotriphenolate complexes. More elaborated functionalizations of aminotriphenolate complexes led to the synthesis of some bifunctional catalysts, which have been tested for tandem reaction or cooperative catalysis. **MoO(L^{c})(TU)**, **MoO(L^{c})(U)**, composed by a Molybdenum centre and a (thio)urea moiety have been synthesized and tested as bifunctional catalysts for olefin epoxidation - epoxide ring opening tandem reactions. **VO(L^{q,r})** and **Al(L^{q,r,s})(DMF)**, in which the ligand is decorated with three ammonium or pyridinium salts, have shown to be active catalysts for the synthesis of cyclic carbonates starting from epoxides and CO_2. The yields of the reactions catalyzed by bifunctional catalysts have been compared also to those of vanadium and aluminum aminotriphenolate complexes and co-catalysts as binary systems, demonstrating that the proximity effect of the two catalytic moieties has a strong influence on the catalytic activity of the catalyst.